Investigation of the mechanism of translation and contribution to pathogenesis of Kaposi's sarcoma associated herpesvirus FLICE Inhibitory Protein (vFLIP)

Clemence Elizabeth Hindley

Thesis submitted for the degree of Doctor of Philosophy

University of Edinburgh

2005

Declaration

I declare that all work included in this thesis is my own except where otherwise stated. No part of this work has been, or will be, submitted for any other degree or professional qualification.

Clemence Hindley
April 2005

Laboratory for Clinical and Molecular Virology
University of Edinburgh
Summerhall
Edinburgh
EH9 1QH

Acknowledgments

I would like to thank my supervisors Dr. Simon Talbot and Dr. Bernadette Dutia for their encouragement and input throughout the course of my work. I'd particularly like to thank Simon for always being approachable and full of ideas. I must thank my fellow KSHV group members, Amanda, Lara, Jill and Maurice for all of the help they have provided with numerous techniques and endless questions. Also, Billy and Christine in the EPU for their invaluable assistance.

A big thankyou to everyone, past and present, in the second floor lab who has made the last three years, for the most part, a lot of fun. Also to the PhD students in the department who have provided support and laughter throughout. I'd particularly like to thank Anna who, over the past year in particular, has listened, advised and entertained! Finally, the support of my family and friends through all of my ups and downs and ditherings has been invaluable to me; a huge thankyou to you all.

Contents

List of figures

List of tables

List of Abbreviations

AlHV	Alcelaphine herpesvirus
AP	Alkaline phosphatase
ATP	Adenosine triphosphate
BCBL	Body cavitity based lymphoma
BCP	A PEL derived cell line
BHK	Baby hamster kidney
BHV	Bovine herpesvirus
BL	Burkitt's lymphoma
bp	Base pair
BSA	Bovine serum albumin
carb	Carbenicillin
cdk	Cyclin dependent kinase
CHO	Chinese hamster ovary
C.P.E.	Cytopathic effect
CrPV	Cricket paralysis virus
CSFV	Classical swine fever virus
CTL	Cytotoxic T lymphocyte
CTP	Cytosine triphosphate
DD	Death domain
DED	Death effector domain
DISC	Death inducing signalling complex
DMEM	Dulbecco'c modified Eagle's medium
DNA	Deoxyribonucleic acid
DTT	dithiothreitol
E.*coli*	Escherichia coli
EBV	Epstein Barr virus
EDTA	ethylenediaminetetraacetic acid
EGFP	Enhanced green fluorescent protein
EGTA	Ethyleneglycol-*bis*(β-aminoethyl)-N,N,N′,N′-tetraacetic Acid
EHV	Equine herpesvirus
EMCV	Encephalomyocarditis virus
EMSA	Electrophoretic mobility shift assay
EST	Expressed sequence tag
FADD	Fas-associated death domain
FBS	Foetal bovine serum
FF	Firefly
FITC	Fluruorescein isothiocyanate
FLIP	FLICE inhibitory protein
FMDV	Foot and mouth disease virus
GTP	Guanine triphosphate
GPCR	G protein coupled receptor
GST	Glutathione S-transferase
HAV	Hepatitis A virus
HCl	Hydrogen chloride
HCV	Hepatitis C virus
HCMV	Human cytomegalovirus virus

H&E	Haematoxylin and eosin
HEK	Human embryonic kidney
HHV	Human herpesvirus
HIV	Human immunodeficiency virus
HLA	Human leukocyte antigen
HRP	Horse radish peroxidase
HSV	Herpes simplex virus
HVS	Herpesvirus saimiri
IE	Immediate early
IFN	Interferon
IKK	IκB Kinase
IM	Infectious mononucleosis
IPTG	isopropyl-beta-D-thiogalactopyranoside
IRES	Internal ribosome entry site
ITAF	IRES transactivating factor
ITAM	Immunoreceptors tyrosine activation motif
IVS	Intervening sequence
Kb	Kilobase
KCl	Potassium chloride
KS	Kaposi's sarcoma
KSHV	Kaposi's sarcoma associated herpesvirus
LANA	Latancy associated nuclear antigen
LB	Luria-Bertani
LCV	*Lymphocryptoviruses*
LHE	Left hand end
MCD	Multicentric castleman's disease
MCMV	Murine cytomegalovirus
MHC	Major histocompatability complex
MHV	Murine herpesvirus
MOI	Multiplicity of infection
NK	Natural killer
NPC	Nasopharyngeal carcinoma
dNTP	Deoxy nucleotide triphosphate
NS0	Murine myeloma derived cell line
OD	Optical density
ORF	Open reading frame
PAGE	Polyacrylamide gel electrophoresis
PCR	Polymerase chain reaction
PEL	Primary effusion lymphoma
Pfu	Plaque forming unit
PGK	phosphoglycerate kinase
p.i.	post infection
PKR	protein kinase R
PNK	Polynucleotide kinase
PPT	Polypyrimidine tract
PRV	Pseudorabiesvirus
PTLD	Post transplant lymphoproliferative disease
pRB	Retinoblastoma protein

RDV	*Rhadinoviruses*
RL	Renilla luciferase
RNA	Ribonucleic acid
mRNA	Messenger RNA
tRNA	Transfer RNA
RPMI	Roswell Park Memorial Institute
RRL	Rabbit reticulocyte lystae
RT	Reverse transcriptase
S.A.P	Shrimp alkaline phosphatase
SDS	Sodium dodecyl sulphate
S.E.M.	Standard error of the mean
SIV	Simian immunodeficiency virus
S/N	Supernatant
SPBS	Sterile phosphate buffered saline
SSC	Saline sodium citrate
Taq	*Thermus aquaticus*
TBE	Tris borate EDTA
TE	Tris EDTA
TNF	Tumour necrosis factor
TPA	12-O-tetradecanoylphorbol-13-acetate
U	Unit
UTP	Uracil triphosphate
UTR	Untranslated region
UV	Ultraviolet
VEGF	Vascular endothelial growth factor
VZV	Varicella zoster virus

Abstract

Kaposi's sarcoma-associated herpesvirus (KSHV) is the most recently identified human herpesvirus and is the causative agent of not only Kaposi's sarcoma but also B-cell primary effusion lymphomas and some forms of multicentric Castleman's disease. During latency, translation of viral open reading frames is tightly regulated. Only two transcripts, encoding ORFs 71-73 (LANA, vCyclin and vFLIP), are truly type 1; that is, there is no increase in the rate of their transcription after the induction of lytic replication. Both transcripts are transcribed from a common start point and are subsequently spliced to produce a tricistronic transcript, encoding ORFs 71-73, and a bicistronic transcript encoding ORFs 71 and 72 (vFLIP and vCyclin). Translation of ORF 71, vFLIP, has been shown to be mediated via an internal ribosome entry site (IRES) contained within the upstream vCyclin coding sequence. This is the first example of cap-independent translation in a DNA virus. vFLIP has been demonstrated to have anti-apoptotic activity and is also capable of activating the cellular transcription factor NF-κB.

In this thesis the contribution of vFLIP toward viral pathogenesis has been investigated through the construction and use of recombinant murine gammaherpesviruses (MHV-76). KSHV vFLIP under the control of either the Cytomegalovirus immediate early (CMV-IE) or the murine phosphoglycerol kinase (PGK) promoter, together with enhanced green fluorescent protein (EGFP) and a hygromycin resistance marker, has been inserted into the left-hand end of the MHV-76 genome to produce recombinant viruses that have been used for *in vivo* and *in vitro* studies. All recombinant viruses display similar *in vitro* growth kinetics to wild-type MHV-76 during infection of BHK cells. Intranasal infection of Balb/c

mice with the CMV vFLIP viruses resulted in a 2 fold greater infectious virus titre in the lungs, at day 5, compared with the control and wild-type MHV-76 viruses. However, this enhanced viral replication was not observed following infection with the PGK vFLIP viruses. In all cases the vFLIP expressing and control viruses displayed a decreased establishment of splenic latency. The influence of vFLIP on viral replication in an *in vitro* system has been investigated through the infection of NS0 cells, a murine myeloma cell line. These data indicate that the expression of vFLIP, in the context of a herpesvirus infection, increases the initial establishment of a latently infected pool of cells, by up to 3-fold at day 8 post infection. The correlation of this process with the activation of NF-κB has been investigated.

A number of techniques have been applied to investigate the nature of any IRES interacting factors (ITAFs) necessary for translation of vFLIP from the KSHV IRES. Through the use of an *in vitro* pull-down assay it has been possible to demonstrate that a known ITAF, poly-pyrimidine tract binding protein (PTB), can associate with the KSHV IRES. Electrophoretic mobility shift assays indicate that additional cellular proteins interact with the IRES sequence and investigations indicate that one of these may be the translation initiation factor eIF4G.

Chapter 1 Introduction

1.1 Herpesviruses

It is likely that the majority of animal species harbour one or more herpesvirus. To date more than 130 different herpesviruses have been identified from organisms as diverse as oysters and humans. They are responsible for a range of diseases of medical and veterinary importance including infectious mononucleosis of humans and malignant catarrhal fever of cattle. Inclusion in the family *Herpesviridae* is dependent upon the architecture of the virion; it is currently under debate as to whether DNA sequence conservation should also be taken into account.

All known herpesviruses share four significant properties;

1. They encode a large number of enzymes required for metabolic processes including nucleic acid metabolism and protein modification.
2. The viral DNA and capsid is synthesised within the host cell nucleus.
3. Production of progeny virions results in death of the host cells.
4. They are able to become latent; the viral genome becomes circularised and only a small subset of viral genes are expressed. The viral genome retains the capacity to reactivate and cause disease.

Despite these similarities herpesviruses can differ greatly in their biological properties. The host-cell range, length of replication cycle and site and mechanisms of latency can all vary (Roizman and Pellet, 2001).

1.1.1 Classification

Members of the family *Herpesviridae* have been classified into three subfamilies, the alpha-, beta- and gammaherpesvirinae, on the basis of their biological properties and

genomic analysis (Roizman and Pellet, 2001). A phylogenetic tree showing the relationships between all eight human herpesviruses, and selected others, can be seen in figure 1.1. A table providing examples of each sub-family and detailing selected disease associations is also provided (table 1.1). A brief description of the major characteristics of each sub-family follows;

Alphaherpesvirinae: Members of this subfamily are characterised as having a generally broad host range, a relatively short reproductive cycle, rapid spread in culture, efficient destruction of the infected host cell and the ability to establish latency in the sensory ganglia. Examples of alphaherpesviruses include Herpes Simplex virus 1 (HSV-1) and Varicella Zoster virus (VZV).

Betaherpesviruses: The majority of members of this subfamily exhibit a restricted host range, a long replication cycle *in vitro* and a slow progression of infection in culture. Despite the long *in vitro* replication cycle of human CMV there is strong evidence that the virus replicates much more rapidly *in vivo* (Emery et al., 1999). Through investigation of the viral load in patients subject to antiviral therapy, or in whom immunodeficiency resulted in active viral infection, the doubling time of the virus was estimated to be between 1 and 2 days (Emery et al., 1999). Latency can be maintained in a variety of cell types and tissues including secretory glands and the kidneys. Examples include members of the genera *Cytomegalovirus*.

Gammaherpesviruses: Viruses belonging to this subfamily have a restricted host range, being confined to the family or order of the natural host. They replicate in lymphoblastoid cells, though some can lytically infect epithelial and fibroblastic cells, and establish latency in lymphoid tissue. The gammaherpesviruses are divided

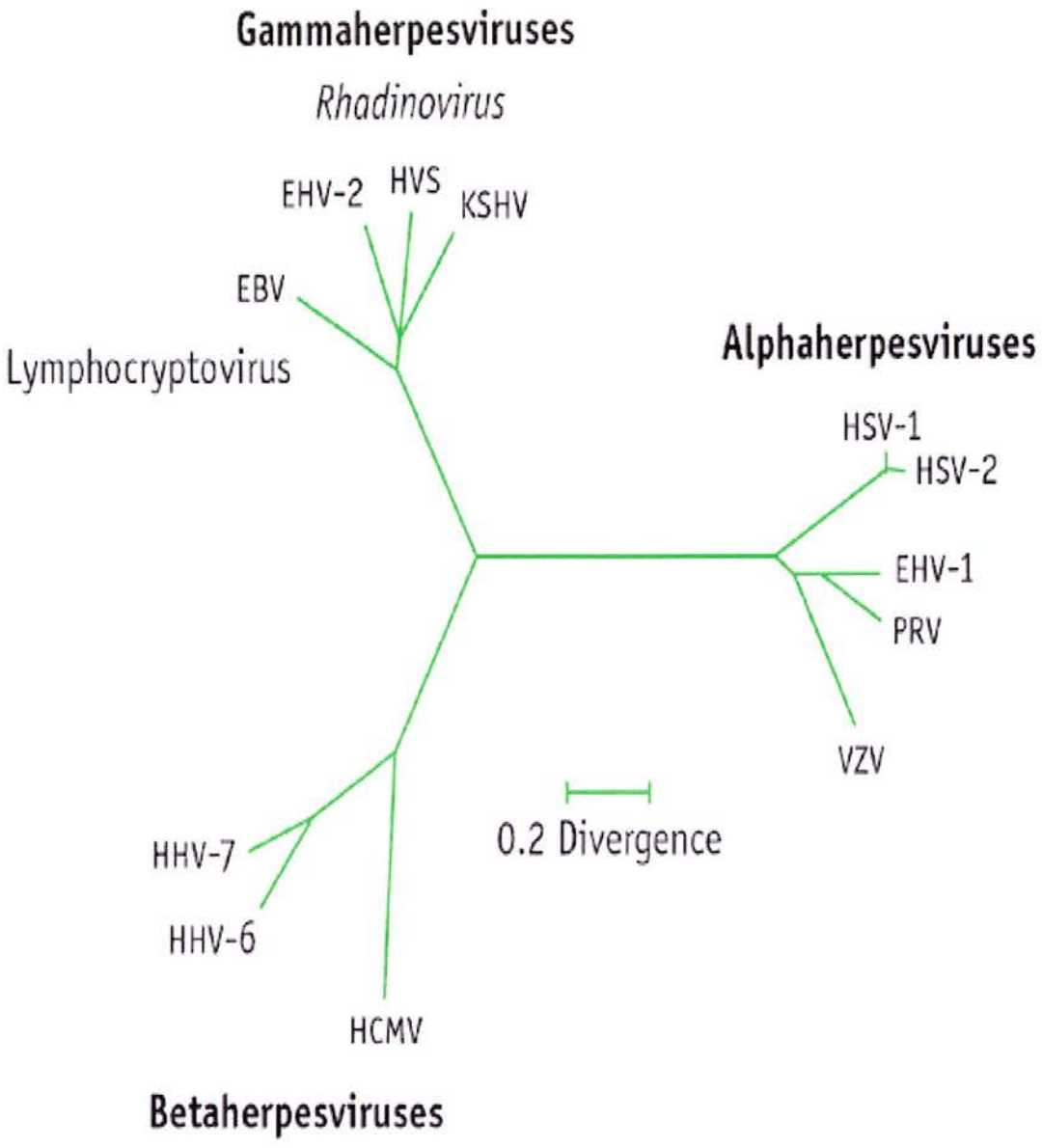

Figure 1.1 Phylogenetic tree illustrating the relationship between selected herpesviruses. Taken from Talbot and Whitby, 1999.

Subfamily	Genera	Virus	Disease Association
Alphaherpesvirinae	*Simplexvirus*	HSV-1 HSV-2	Oropharyngeal Herpes Genital Herpes Encephalitis
	Varicellovirus	VZV	Varicella (chicken pox) Herpes Zoster (shingles)
Betaherpesvirinae	*Cytomegalovirus*	HCMV	CMV mononucleosis Congenital CMV infection
	Roseolovirus	HHV-6	Liver dysfunction Exanthem Subitum (ES)
		HHV-7	ES
	Muromegalovirus	MCMV	
Gammaherpesvirinae	*Lymphocryptovirus*	EBV	Burkitt's lymphoma Post transplant lymphoproliferative disease Infectious mononucleosis Hodgkin's disease
	Rhadinovirus	KSHV	Kaposi's sarcoma Primary effusion lymphoma Multicentric Castleman's Disease
		HVS	Lymphoma
		MHV-68	Lymphoma
		AlHV-1	Malignant Catarrhal Fever

Table 1.1 Table of selected herpesviruses and disease associations. Compiled from information in Fields Virology 4th edition (ed. Knipe and Howley).

into two genera, the *lymphocryptoviruses* and the *rhadinoviruses* on the basis of genome structure and content.

1.1.2 Virion structure

A typical virion consists of a core, containing the viral DNA, which is surrounded by a capsid approximately 100nm in diameter and consisting of 162 capsomeres. Between the capsid and the envelope is the tegument the distribution and thickness of which may vary but which appears to be an ordered structure. Herpesvirus envelopes have a trilaminar appearance and are apparently derived from different cellular membranes. All herpesviruses have glycoproteins protruding from their envelopes although the number of different glycoproteins encoded and their copy number varies between different viruses. A complete, mature virion may range in size from 120nm to 300nm in diameter depending on, amongst other factors, the thickness of the tegument (Roizman and Pellet, 2001). A diagrammatic representation of the KSHV virion is shown in figure 1.2.

1.1.3 Herpesvirus genomes

Herpesvirus genomes consist of linear, double-stranded DNA, within the virion, which is immediately circularised once in the nucleus of a host cell. Genomes range in size from 120 to 250kbp and in composition from 31-75% G-C. Herpesvirus genomes have been divided into six groups, A-F, based upon their genome organisation, figure 1.3.

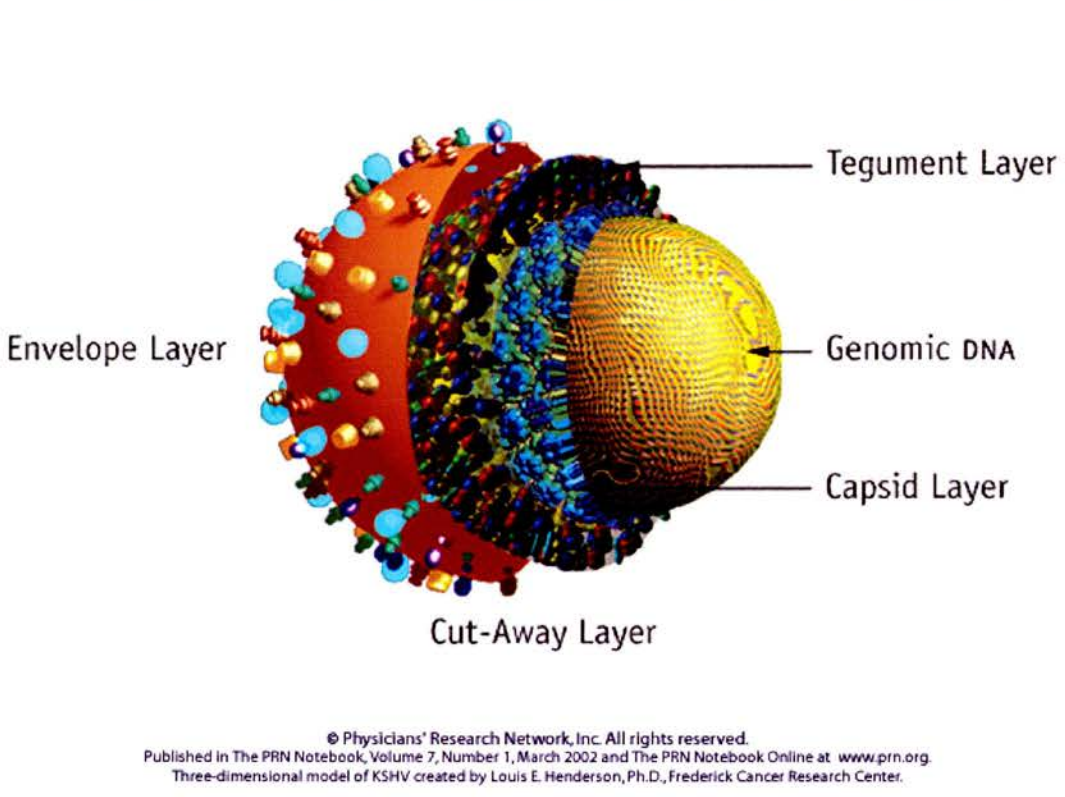

Figure 1.2 Schematic representation of the KSHV virion. Taken from PRN Notebook online, www.prn.org

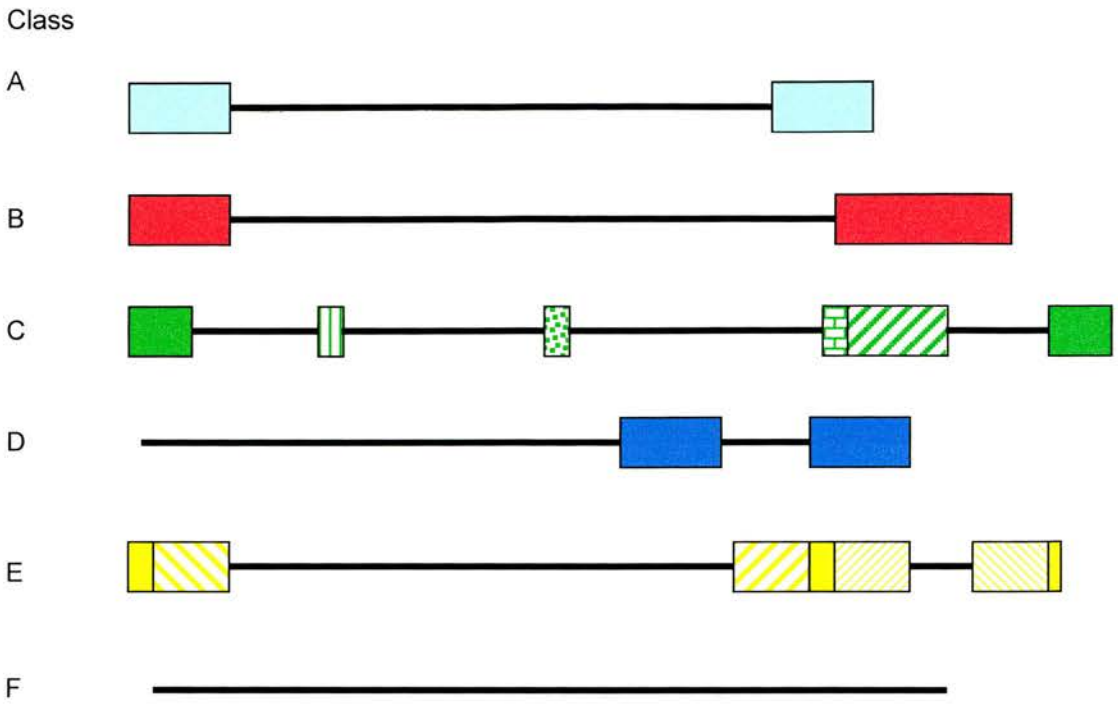

Figure 1.3 Diagram of the six classes of herpesvirus genomic arrangements, A-F. Unique regions are shown as horizontal lines whilst the coloured blocks represent repeat regions. The KSHV genome is of type B, having a central coding region flanked by large terminal repeats, whilst EBV is type C, having smaller terminal repeats than type B but also other smaller repeat sequences dividing the genome. In all six classes the signals for packaging of the genome into capsids are located at the termini. Figure adapted from Roizman and Pellet in Fields Virology 4th ed.

Herpesvirus genomes range in size from 70 to 200 genes, though these figures may prove to be underestimates as the potential for alternative splicing, frameshifting and identification of further ORFs is large (Roizman and Pellet, 2001). Most herpesvirus genes consist of a single ORF flanked by 5' and 3' untranslated regions, of 30 to 300bp and 10 to 30bp respectively, a promoter sequence upstream of a TATA box and a 3' polyadenylation signal. It is common for genes to overlap which results in the regulatory sequences of some genes being located within the coding sequence of others. The vast majority of genes are transcribed by RNA polymerase II and most are unspliced. Some instances where splicing does occur allow the differential regulation of transcription; it enables the same ORF to be transcribed from different promoters depending upon the stage of the viral replication cycle. Some herpesviruses additionally encode noncoding RNAs, for example the EBERs of EBV and the tRNAs of MHV-68.

Aside from those genes responsible for viral replication, herpesvirus gene products act to manipulate the host resulting in an environment best suited for viral replication or the establishment of latency. Furthermore herpesviruses encode proteins designed to inhibit the host immune defence. In the case of HSV more than half of the viral genes are dispensable for growth in tissue culture; however, the majority are absolutely required for replication within an animal model. The regulatory proteins encoded by herpesviruses are adapted to the cell types which the virus infects *in vivo*; much remains to be determined concerning their function.

Whilst the establishment of latency is common to all herpesviruses the mechanisms by which it is achieved and maintained differ greatly between different viruses.

There is no apparent consensus on factors necessary for establishment, maintenance or termination of latency. Some viruses, including EBV and KSHV, encode latently expressed proteins whereas others, for example HSV, have no requirement to express viral genes during latency.

The regulation of herpesvirus genes goes beyond merely lytic or latent expression. During productive infection viral genes differ in the order of their expression and the factors necessary to drive it. During a productive infection of HSV at least four different groups of viral genes can be identified. These are the immediate early (IE) genes, which require no viral protein synthesis; the early (E) genes which are expressed independently of viral DNA synthesis; partial late genes, whose expression is enhanced by viral DNA synthesis; and the late (L) genes the expression of which has an absolute requirement for viral DNA synthesis.

Sequencing of entire viral genomes or smaller sections has shown that approximately 26 genes, the core genes, are conserved across all of the herpesvirus subfamilies. They are found in seven core gene blocks each encoding 2 to 12 genes. In general block and gene order is conserved within subfamilies. Other genes are conserved at subfamily level; gammaherpesviruses, for example, encode more cell homologous genes than do alpha- and betaherpesviruses, though all herpesviruses seem to encode at least one protein of cellular origin (Roizman and Pellet, 2001).

1.1.4 Herpesvirus life cycle

The general principles of herpesvirus replication can be outlined through a description of HSV replication, the system about which most is known; though it must be remembered that the details for individual viruses can vary substantially.

HSV-1 and HSV-2 express at least a dozen envelope glycoproteins, however, only five have been shown to have a role in viral entry (reviewed in Spear and Longnecker, 2003). Glycoproteins gC and/or gB mediate binding of the virus to the cell through interactions with heparan sulphate. Fusion of the viral envelope with the cell membrane is then induced by the glycoproteins gB, gD, gH and gL; all four of which have been demonstrated to be essential for viral entry. Binding of virus to heparan sulphate does not necessarily result in viral entry, generally there is a requirement for at least one co-receptor. At least three different classes of co-receptor have been identified (Spear et al., 2000) all of which appear to be receptors for gD. The proteins shown to act as co-receptors are a TNF receptor, several members of the immunoglobulin superfamily and a product of sulphotransferase activity on heparan sulphate. The presence and localisation of viral receptors determines, at least in part, the cellular tropism of herpesviruses.

Having entered a host cell either through fusion with the plasma membrane or, in some cases, the endocytic membrane, the capsid is transported to the nuclear pore via the microtubule network (Roizman and Knipe, 2001). The viral DNA is released into the nucleus at the nuclear pore, leaving the capsid complex at the cytoplasmic side, apparently after a conformational change in the capsid proteins induced by association with components of the nuclear pore (Ojala et al., 2000).

Transcription, by host cell RNA polymerase II, occurs in the nucleus in a highly regulated manner (Honess and Roizman, 1974). First to be transcribed are the six immediate early (IE) genes. Their transcription is mediated by the tegument protein VP16, which interacts with cellular proteins to recognise IE promoter elements, and requires no prior viral protein synthesis (Campbell et al., 1984; reviewed in Roizman

and Knipe, 2001). Next to be transcribed are the early (E) genes. ICP4, one of the IE proteins, is required for all post-IE gene expression and is thought to mediate transcription through association with cellular proteins. The expression of the E genes requires only the production of ICP4 and not the onset of viral DNA replication. The early gene products promote viral DNA replication, and thus the expression of late genes, and down-regulate the expression of IE genes. The expression of the final set of genes, the late genes, is enhanced by viral DNA synthesis. The late genes are loosely divided into two categories; those whose expression does occur under early conditions but which are markedly increased by viral DNA synthesis, and those that are utterly dependent on viral DNA synthesis. In general the early gene products are involved in viral DNA replication and the late gene products are structural. HSV DNA is replicated in the nucleus in a process requiring several viral proteins. Replication occurs by the rolling-circle mechanism resulting in head-to-tail concatamers of the genome. The DNA is then packaged into pre-formed capsid complexes, empty shells containing internal scaffolding which are assembled initially in the cytoplasm and subsequently completed in the nucleus. Entry of the DNA displaces the scaffold from the capsid. Once the capsid is filled the DNA is cleaved at specific sites, by a packaging complex, and fully encapsidated (reviewed in Roizman and Knipe, 2001). Following assembly the capsid leaves the nucleus by budding through the inner nuclear membrane whereby it acquires an envelope consisting of the inner leaflet of the membrane (reviewed in Mettenleiter, 2002). Current opinion supports a de-envelopment/ re-envelopment model for subsequent steps in maturation. In this model the primary envelope is lost through fusion with the endoplasmic reticulum membrane. The capsid then gains its final

tegument and envelope in cytoplasmic compartments. Tegumentation appears to involve a complex series of protein-protein interactions resulting in a first layer with some icosohedral structure, due to interactions with the capsid, and further less structured layers. The tegument acts, amongst other roles, to link the capsid with the envelope glycoproteins. Final envelopment is still not fully understood but is believed to take place in the trans-Golgi compartment where the cytoplasmic tails of viral glycoproteins associate with the tegument. Mature virions then bud from the plasma membrane into the intracellular space.

1.2 Gammaherpesviruses

As previously mentioned the gammaherpesvirus subfamily contains two genera the *lymphocryptoviruses* (LCV), of which Epstein-Barr virus (EBV) is the prototype, and the *rhadinoviruses* (RDV), which include KSHV and MHV-68. The LCV so far identified infect only primates, in contrast RDV are endemic in a broader range of host species.

1.2.1 *Lymphocryptoviruses*

1.2.1.1 Epstein-Barr Virus

Suggestions that an infectious agent may be the causative agent of Burkitt's lymphoma (BL), a common childhood cancer throughout equatorial Africa, led to a search for the etiological agent. Epstein-Barr virus was discovered in 1964 by electron microscopy which was carried out on cell lines derived from a BL biopsy (Epstein et al., 1965). EBV is endemic globally; over 90% of the adult population

are seropositive for EBV infection. EBV is the only human LCV so far identified and is the prototype gammaherpesvirus.

Disease associations

EBV has been associated with a range of diseases including:

Infectious mononucleosis: In developed countries primary infection with EBV is often delayed until adolescence. In this circumstance the result can be infectious mononucleosis (IM), also known as glandular fever, in around 50% of infections. It is likely that the disease symptoms (fever, lymphadenopathy, sore throat, hepatosplenomegaly, fatigue) are the result of the immune response rather than a direct result of viral replication (Crawford, 2001).

Burkitt's Lymphoma: Burkitt's Lymphoma (BL) is a tumour of the jaw, and other sites, that occurs most commonly in children in equatorial Africa and Papua New Guinea but also arises sporadically throughout the world. BL consists of rapidly proliferating non-cleaved B cells infiltrated with histiocytes. A common feature of BL is chromosomal translocations that result in deregulation of expression of the c-myc oncogene. EBV DNA is found in around 96% of African BL cases; however, the association with sporadic BL is much weaker. The mechanisms by which EBV contributes to BL pathogenesis are unclear; it is hypothesised that EBV infection may play an initiating role, driving the proliferation of infected B cells or increasing the survival of a clone in which translocation has occurred (Rickinson and Kieff, 2001; Crawford, 2001; Young and Murray, 2003).

Hodgkin's disease: Hodgkins lymphoma accounts for 20% of lymphomas in the developed world. It consists of 1-2% malignant Reed-Sternberg (RS) and Hodgkin's

cells, which are derived from B lymphocytes, and a cellular infiltrate of mixed characteristics. Differences in the cellularity of the infiltrate between EBV positive and negative cases indicate underlying etiological differences. Within EBV positive lymphomas the malignant component has been shown to harbour latent EBV (Latency II). EBV is proposed to contribute to the pathogenesis by preventing apoptosis of B cells with hypermutated Ig genes which go on to form RS and Hodgkin's cells (Rickinson and Kieff, 2001; Crawford, 2001; Young and Murray, 2003).

Post-transplant lymphoproliferative disease (PTLD): Individuals who are immunosuppressed exhibit decreased EBV-specific cytotoxic T lymphocyte (CTL) activity and consequently there is an increase in virus replication and an expansion of latently infected B lymphocytes (Haque et al., 1997). PTLD tumour cells generally express all of the latency-associated genes of EBV which are presumed to be able to induce proliferation. Tumours are initially polyclonal but progress to become monoclonal lymphomas. PTLD has been successfully treated with infusions of EBV-specific CTLs (Haque et al., 2002; Rooney et al., 1998).

Nasopharyngeal carcinoma (NPC): EBV is associated with 100% of undifferentiated NPC; a tumour characterised by the presence of undifferentiated carcinoma cells with a prominent lymphocytic infiltrate. NPC shows distinct geographical localisation; it is very common in southern China and occurs at high frequency in the Inuit, Malaysians, Dyaks, Indonesians, Filipinos and Vietnamese. This distribution suggests that there is a genetic component to its development and there are indications that environmental factors, such as diet, can also influence disease development. EBV is implicated as NPC tumours are found to be

monoclonal for EBV, suggesting infection prior to expansion. Additionally the EBV genes EBNA1 and EBERs are expressed in all EBV associated cases and LMP-1 is expressed in 65% of cases (Crawford, 2001; Young and Murray, 2003).

EBV structure and genome

The general architecture of EBV is the same as other herpesviruses. The virion contains a range of envelope glycoproteins some of which are homologous to the HSV glycoproteins. The most abundant glycoprotein and tegument protein of EBV, however, do not have HSV homologues. The genome, which is type C, is approximately 184kbp in length with 0.5kb terminal and 3kb internal repeats (Kieff and Rickinson, 2001).

EBV infection and replication

EBV is transmitted via oral secretions and possibly also via sexual intercourse. It is believed that EBV may be able to directly access tonsillar B lymphocytes. Unlike many other herpesviruses the initial interaction of EBV with its target cell involves complement receptor 2 (CD21), rather than heparan sulphate. This interaction is mediated by the major envelope glycoprotein gp350/220 deletion mutants of which can still infect cells but at reduced efficiency. Following this initial interaction gp42 binds to HLA class II molecules, which are abundantly expressed on B lymphocytes, and membrane fusion then occurs due to the actions of gB, gH and gL. Besides B lymphocytes EBV is also able to enter some epithelial cell types in a gp350/220, gp42 independent manner. Infectious virus produced in epithelial cells has greater tropism for B lymphocytes, and vice versa, as gp42 is not sequestered by cellular

HLA class II (Spear and Longnecker, 2003). Following entry into B lymphocytes the expression of EBV latent genes drives cellular proliferation thus amplifying the number of latently infected cells in the body. In order to complete its replicative cycle EBV must reactivate from latency and produce infectious virions with which to infect a new host; the switch from latent to lytic replication is as yet uncharacterised but may be physiological (Macsween and Crawford, 2003). Following induction of lytic replication the immediate-early genes expressed are principally BZLF1 and BRLF1. These proteins are transactivators of lytic gene expression; BZLF1 expression activates lytic infection (Grogan et al., 1987) and both proteins up-regulate expression from early gene promoters (Chevallier-Greco et al., 1986). There are more than 30 early genes whose products have activities ranging from transcriptional activation (e.g. BMRF1; Oguro et al., 1987), DNA replication (e.g. the DNA polymerase BALF5; Kallin et al., 1985) and prevention of apoptosis (a Bcl-2 homologue BHRF1; Henderson et al., 1993b). The EBV late genes encode the viral glycoproteins and some non-glycoproteins including the nucleocapsid protein BcLF1 and the predicted tegument protein BNRF1 (Kieff and Rickinson, 2001).

EBV latency

During latent infection the viral genome is maintained as an episome in infected lymphocytes. EBV latency is more complex than that of other herpesviruses; three different forms have been identified. These are designated "latency I, II or III" and are distinguished by the pattern of gene expression (Young et al., 2000):

- Latency I has been identified in BL biopsies and early passage BL-derived cell lines. During this form of latency the EBERs and EBNA1 are the only EBV transcripts produced.
- Latency II involves transcription of the EBERs, EBNA1, LMP1, LMP2A and LMP2B. This form was identified in NPC and is also seen in EBV-associated Hodgkin's disease and some EBV-positive T cell lymphomas.
- Latency III has the most extensive expression of viral genes; the EBERs, EBNA1, EBNA2, EBNA3A, EBNA3B, EBNA3C, EBNA-LP, LMP1, LMP2A and LMP2B. Lymphoblastoid cell lines (LCLs) generated by infecting resting B lymphocytes with EBV *in vitro* display latency III, as do immunoblastic lymphomas in transplant recipients. Latency III is accompanied by a distinct cellular phenotype *in vivo* and *in vitro* with high expression of B cell activation markers and cellular adhesion molecules.

Following infection of a resting B lymphocyte the first latent transcripts produced are EBNA-LP and EBNA-2 both of which act to up-regulate transcription from viral and cellular promoters. They reach their final level within 24-32 hours of infection. As well as some cellular genes EBNA2 up-regulates transcription of the EBNAs, LMP1 and LMP2. Levels of these transcripts reach those that are maintained throughout infection by 48 hours post infection. By 70 hours post infection EBER expression has reached substantial levels. The EBERs constitute the most abundant EBV RNAs within latently infected B lymphocytes, estimated at approximately 50,000 copies per cell (Rickinson and Kieff, 2001).

A model for EBV latency which includes a fourth type of latency, latency 0, during which no viral genes are expressed has been proposed (Thorley-Lawson and Gross,

2004). The premise of this model is that following infection of a naïve B cell EBV forces the differentiation of the cell into a memory B cell, which has exited the cell cycle, in which the virus can persist silently. This arrangement is beneficial to both the virus and the host as there is no immune response directed against the infected cell and, as the cell is resting, there is no threat to the host because no viral growth-promoting genes are expressed. It is proposed that in the newly infected naïve cell the growth programme (latency III) is entered, in which all latent transcripts are expressed, and the B cell becomes activated. Having differentiated to a germinal centre cell the viral programme switches to the default programme (latency II) which enables differentiation into a memory B cell where latency 0 is established. When the memory B cell does divide, following a host stimulus, the virus enters latency I which allows the viral DNA to replicate. According to this model disease results when there is a blockage to this sequence of events resulting in constitutive expression of the EBV latent genes. An example would be Hodgkin's disease resulting from a blockage following differentiation into a germinal centre cell and subsequent expression of the latency II programme.

Roles of the EBV latent genes

EBNA-LP: EBNA-LP is encoded by the leader sequence of each EBNA mRNA and is of variable size depending on the number of *BamHI*W repeats present. It has been shown to be required for efficient growth of LCLs (Allan et al., 1992). Its proposed role is enhancement of EBNA2 mediated transcription (Rickinson and Kieff, 2001).

EBNA1: EBNA1 is a DNA-binding nuclear phosphoprotein; it binds to the plasmid origin of viral replication and consequently aids replication and maintenance of the

episome. Additionally it has been demonstrated to act as a negative regulator of its own expression (Nonkwelo et al., 1996) and a transcriptional transactivator of the Cp and LMP1 promoters (Rickinson and Kieff, 2001). *In vivo* experiments in which EBNA1 is expressed in B lymphocytes in transgenic mice suggest a possible role in oncogenesis as B cell lymphomas developed (Wilson et al., 1996).

EBNA2: EBNA2 is required for cellular transformation. An EBV strain, P3HR-1, in which EBNA2 is deleted is unable to induce transformation *in vitro.* The gene product is an acidic phosphoprotein which activates transcription of cellular and viral genes including the c-myc oncogene (Kaiser et al., 1999).

EBNA3A, B, C: All three genes are transcribed from a common origin and encode hydrophilic nuclear proteins containing potential dimerisation domains. EBNA3A and 3C are essential for transformation *in vitro* (Tomkinson et al., 1993). The EBNA3 proteins act as transcriptional regulators; they can up and down-regulate both cellular and viral genes and can work together with EBNA2 to control activity of the RBP-Jκ transcription factor (Young and Murray, 2003).

LMP1: LMP1 is essential for EBV-induced transformation *in vitro* (Kaye et al., 1993). It has six transmembrane helices, a short cytoplasmic N-terminal and a longer cytoplasmic C-terminus which is important for cell transformation. Functionally, LMP1 has been demonstrated to resemble CD40, a member of the tumour necrosis factor receptor (TNFR) superfamily; LMP1 can partially replace CD40 function in CD40 knockout mice (Uchida et al., 1999). It is able to activate the transcription factor NF-κB, via domains in its C-terminus (Huen et al., 1995), resulting in expression of various antiapoptotic and cytokine genes. Additionally LMP1 can

activate the MAP kinase cascade and phosphatidylinositol 3-kinase (Dawson et al., 2003).

LMP2A, B: These proteins are essentially identical to one another consisting of twelve transmembrane domains and a small cytoplasmic C-terminus, the only difference is the additional 119 amino acid cytoplasmic N-terminus of LMP2A. Neither protein is essential for transformation *in vitro* (Longnecker, 2000). LMP2A appears to negatively regulate protein tyrosine kinase (PTK) activity, via its N-terminus, resulting in an abrogation of normal B lymphocyte development in favour of maintenance of EBV latency (Young and Murray, 2003). LMP2B is suggested to aid regulation of LMP2A function (Longnecker, 2000).

EBERs: EBV encodes two non-coding RNAs, EBER 1 which is transcribed by RNA polymerases II and III, and EBER 2 which is transcribed by RNA polymerase III (Kieff and Rickinson, 2001). The EBERs localise to the nucleus where they are found in complex with the La autoantigen (Lerner et al., 1981) and the ribosomal protein L22 (Toczyski et al., 1994). The EBER complex is able to bind to PKR which in involved in mediating the effects of interferons; it has been proposed that inhibition of PKR by EBERs may be involved in viral persistence (Clemens et al., 1994). More recently there has been some evidence to suggest that the EBERs may increase the tumourigenicity of BL (Komano et al., 1999; Kitagawa et al., 2000).

Immune evasion

EBV encodes a number of potentially immunomodulatory proteins. The glycoprotein gp42 may interfere with HLA class II maturation or epitope presentation (Rickinson and Kieff, 2001). BARF1 acts as a soluble colony-

stimulating factor-1 receptor and interferes with interferon-α release (Cohen and Lekstrom, 1999). A viral homologue of cellular interleukin-10 (BCRF1) augments B lymphocyte growth and differentiation and inhibits antigen presentation by monocytes and dendritic cells. Unlike cIL-10, BCRF1 cannot directly impair T lymphocyte function, however, inhibition of priming of T-cell responses has been observed (Bejarano and Masucci, 1998).

1.2.2 *Rhadinoviruses*

1.2.2.1 Kaposi's sarcoma-associated herpesvirus

Discovery, epidemiology and pathogenesis

Despite suspicions of a viral aetiology for Kaposi's sarcoma (KS) (Beral, 1991) it was not until 1994 that herpesvirus-like sequences were identified in samples of AIDS-associated KS lesions using representational difference analysis (Chang et al., 1994). Subsequently numerous epidemiological studies have shown that KSHV is the causative agent of not only KS but also B-cell primary effusion lymphomas (PEL) and some forms of multicentric Castleman's disease.

KSHV strains, transmission and world-wide prevalence

Unlike other herpesviruses which tend to be wide spread within a host population KSHV seropositivity shows a more complex distribution. The prevalence of seropositivity in the USA, and central, northern and western Europe is low, up to 10% with regional variation. In some Mediterranean countries the frequency is

increased and can be as high as 35% in some areas, again there is regional variation. In sub-Saharan Africa KSHV infection is much more widespread (reviewed in (Boshoff and Weiss, 2001).

Subtyping of KSHV is based on ORFK1 which encodes a glycoprotein related to the immunoglobulin superfamily and is the most variable part of the genome. To date five different subtypes have been identified, designated A-E. Within subtypes A-D there are more than fifteen different clades (Hayward, 1999). Subtype B is found almost exclusively in patients from Africa, subtype C in those from the Mediterranean and Middle East, subtype A in western Europe and North America and subtype D in areas of the Pacific (Hayward, 1999; Zong et al., 1999). Subtype E is the most recently described and was found in South American indigenous people (Biggar et al., 2000). The view of the majority of researchers is that KSHV is an ancient pathogen of humans with a particularly low rate of horizontal transmission (Hayward, 1999). Others, however, suggest that KSHV may have entered the human population more recently as a result of interspecies transfer from another primate host (McGeoch and Davison, 1999).

Disease associations

Kaposi's sarcoma: Kaposi's sarcoma was first described by the dermatologist Moritz Kaposi in 1872 (Kaposi, 1872). It is a mesenchymal tumour, involving blood and lymphatic vessels, which usually presents as brownish-purple lesions at the extremities but that can progress to internal organs. KS lesions contain a number of cell types but are characterised by the presence of spindle cells the origin of which is disputed (Talbot and Whitby, 1999). KS spindle cells have been shown to express

markers for smooth muscle, macrophage and dendritic cells (Sturzl et al., 1992). More recently it has been shown that all spindle cells express vascular endothelial growth factor receptor 3 (Jussila et al., 1998). As this is a marker for lymphatic endothelium and neoangiogenic vessels, but not mature vascular endothelial cells, it indicates that KS spindle cells are probably of endothelial lineage and can differentiate into lymphatic cells (Boshoff and Weiss, 2001). Most recently two groups have shown that KSHV infection of blood vascular endothelial cells leads to a shift in the gene expression profile of the infected cell towards that of lymphatic endothelial cells (Wang et al., 2004; Hong et al., 2004). These data raise the possibility that KS spindle cells do not represent a particular cell lineage but, instead, the virus is able to infect cells of both the blood and lymphatic lineage and drive their gene expression profiles towards one another. Tumour development is dependent on viral oncogenesis, cytokine mediated growth and some immunological compromise in the host (Hengge et al., 2002).

KSHV has been causally linked to KS by four different observations which individually do not prove a link but taken together show KSHV to be the etiological agent of KS (reviewed in Boshoff and Weiss, 2001);

1. KSHV DNA can be detected by PCR in all forms of KS, however, it is rarely detected in other mesenchymal tumours.
2. HIV positive patients carrying a higher viral load of KSHV, assessed by PCR, are at greater risk of developing KS.
3. The incidence of classic and AIDS-KS correlates broadly with the level of KSHV within a population.

4. Latent KS transcripts can be found in nearly all spindle cells of advanced KS lesions.

Prior to the onset of the AIDS pandemic KS had a low profile being mainly endemic in areas around the Mediterranean and in sub-Saharan Africa. The incidence of classic and endemic KS is more common in men than women despite similar levels of seropositivity suggesting that there may be sex-specific co-factors involved in disease development (Serraino et al., 2001). In the early 1980's KS appeared, in an aggressive form, in young homosexual men in the USA (CDC, 2004), one of the first signs of the AIDS epidemic. KS is now amongst the most common forms of cancer in several African countries (Wabinga et al., 1993; Wabinga et al., 2000), in some areas there has been a twenty-fold increase in the number of cases since 1988, and the previous bias towards male patients has rescinded (Sitas and Newton, 2001), reviewed in (Dedicoat and Newton, 2003).

There are four, clinically distinguishable, manifestations of KS;

1. **Classic KS**

   The form of KS described by Kaposi affects mainly elderly males of Mediterranean, east European or Jewish descent and generally presents as plaques and nodules on the lower extremities. Classic KS rarely metastasises and patients survive for a mean of 10- 15 years and die of an independent cause (Hengge et al., 2002; Wahman et al., 1991).

2. **Endemic KS**

In the 1960's an unusually high prevalence of KS in some sub-Saharan African countries was noticed. The high incidence of KS was confined to distinct geographical locations. Endemic KS is generally more aggressive than classic KS and occurs in younger individuals, particularly children, in whom the lymph node is often involved and the disease often proves fatal (Hengge et al., 2002; Talbot and Whitby, 1999).

3. **Iatrogenic KS**

Iatrogenic, or post-transplant, KS develops in solid organ transplant recipients as a result of either primary infection with KSHV or reactivation of latent virus. The course of the disease can be rapid but withdrawal of immuno-suppression usually results in spontaneous remission. Recent work has shown that not only the virus but also KS progenitor cells can originate from the organ donor (Barozzi et al., 2003).

4. **AIDS-associated KS**

The risk of KS is greatly increased in AIDS patients, estimated to be 20,000 times that of the general population and 300 times that of other immunosuppressed individuals (Hengge et al., 2002). Additionally the means of HIV transmission seems to influence the likelihood of developing KS. The incidence of KSHV in Africa as tested by seropositivity has not altered since the onset of the AIDS pandemic; however, prior to AIDS, development of KS was much more common in some geographical locations than others and in males than females. Concurrent infection with HIV seems to abrogate these effects suggesting that development of KS is dependent on co-factors, other than immunodeficiency, which are overcome by HIV infection (Dedicoat and Newton,

2003). The introduction of HAART (highly active anti-retroviral therapy) has seen a huge decrease in incidence of AIDS-KS in the West, however, in the developing world it remains a common disease.

Primary Effusion Lymphoma (PEL): PEL typically presents as malignant effusions in the visceral cavities usually without significant tumour mass or lymphodenopathy. Such lymphomas are mostly seen in HIV positive patients in the advanced stages of AIDS, but they are occasionally seen in HIV negative individuals. PEL was specifically associated with KSHV by PCR and Southern blotting analysis; KSHV sequences were not identified in any other lymphomas (Cesarman et al., 1995). Analysis of the cells shows that they lack many lineage markers; a B cell origin was indicated by clonal rearrangement of Ig genes. The presence of CD138, a molecule associated with the late stages of B cell differentiation, and frequent mutations in the 5' non-coding region of BCL-6 define PEL cells as pre-terminally differentiated, post-germinal centre stage B cells (Gaidano et al., 1999; reviewed in Boshoff and Weiss, 2001). PEL cells lack many adhesion molecules present on other diffuse lymphomas which may contribute to their phenotype (Boshoff et al., 1998). The KSHV genome is present in PEL cells at a very high copy number compared with KS (Boshoff and Weiss, 2001).

It has been possible to establish KSHV positive cell lines from PEL and from the peripheral blood of PEL patients, the latter suggesting that malignant cells are not confined to the malignant effusions (Boshoff et al., 1998). These cell lines have proved invaluable in the study of KSHV gene expression as they express KSHV latent genes and can be induced into lytic replication.

Multicentric Castleman's Disease (MCD): MCD is a lymphoproliferative disorder associated with the development of secondary B cell lymphoma (reviewed in Boshoff and Chang, 2001). KSHV can be identified in >95% of AIDS-associated cases and in around 40% of cases in HIV-negative patients. KSHV-associated MCD is distinguished from other forms of the disease by the presence of plasmablasts of B cell lineage (Dupin and Calvez, 2000; Dupin et al., 1999).

It is possible, but unusual, for an individual to develop more than one KSHV associated tumour (Jones et al., 1998).

KSHV genome

The KSHV genome (see figure 1.4) is approximately 165kbp in length and consists of a long unique coding region of 140.5kbp flanked by variable numbers of 801bp repeats (Russo et al., 1996; Talbot and Whitby, 1999). Ninety ORFs have been identified though whether some encode exons or complete genes remains to be identified. Of these, sixty-six have homologues within HVS and the remainder, thought to be unique to KSHV, are numbered with the prefix "K". Subsequent to naming two of these, K8 and K13, have been found to have homologues in other viruses. KSHV is unusual in that it encodes a large number of proteins with cellular homologues which may contribute to the subversion of cellular pathways (Jenner and Boshoff, 2002).

Having entered the nucleus, the KSHV genome, in common with other herpesviruses, is transcribed in a controlled manner. Initial studies carried out on PEL- derived cell lines identified three classes of viral transcript based on the response to phorbol ester mediated induction of lytic replication (Sarid et al., 1998).

Class I genes comprise those transcripts that are constitutively transcribed under standard conditions, induction of lytic replication has very little effect on their levels and they are therefore considered to be true latent transcripts. Class II genes are transcribed in the absence of lytic replication, however, following induction of lytic replication using TPA, levels of these transcripts significantly increase. The final class, class III, includes those genes that are only transcribed following TPA treatment and contains mostly structural and replication proteins. Subsequently KSHV transcription in PEL- derived cell lines has been studied using microarray technology (Jenner et al., 2001; Paulose-Murphy et al., 2001). These studies confirm the previous data and provide more detailed information about the timing and coordination of gene expression. Clustering analysis allowed classification of the lytic transcripts into three classes namely primary, expression peaks within 10 hours post-induction; secondary, with a peak of expression between 10 and 24 hours; and tertiary, which are expressed predominantly between 48 and 72 hours (Jenner et al., 2001). It was observed that genes sharing similar functions were expressed at very similar times post-induction. For example, genes involved in virus gene regulation are all expressed similarly, as primary lytic genes, and genes encoding components of the virion are expressed much later on. Subsequently the transcription of KSHV genes in Kaposi's sarcoma lesions has been analysed by real-time quantitative RT PCR (Dittmer, 2003). In all 21 KS biopsies examined, LANA, vCyclin and vFLIP were found to be expressed indicating that they are latent transcripts in KS as well as PEL. It was found that transcription of some latent genes was dependent upon the nature of the KSHV-associated tumour i.e. K9/vIRF-1 was only detected in KS biopsies and LANA-2/vIRF-3 is transcribed only in B cell malignancies.

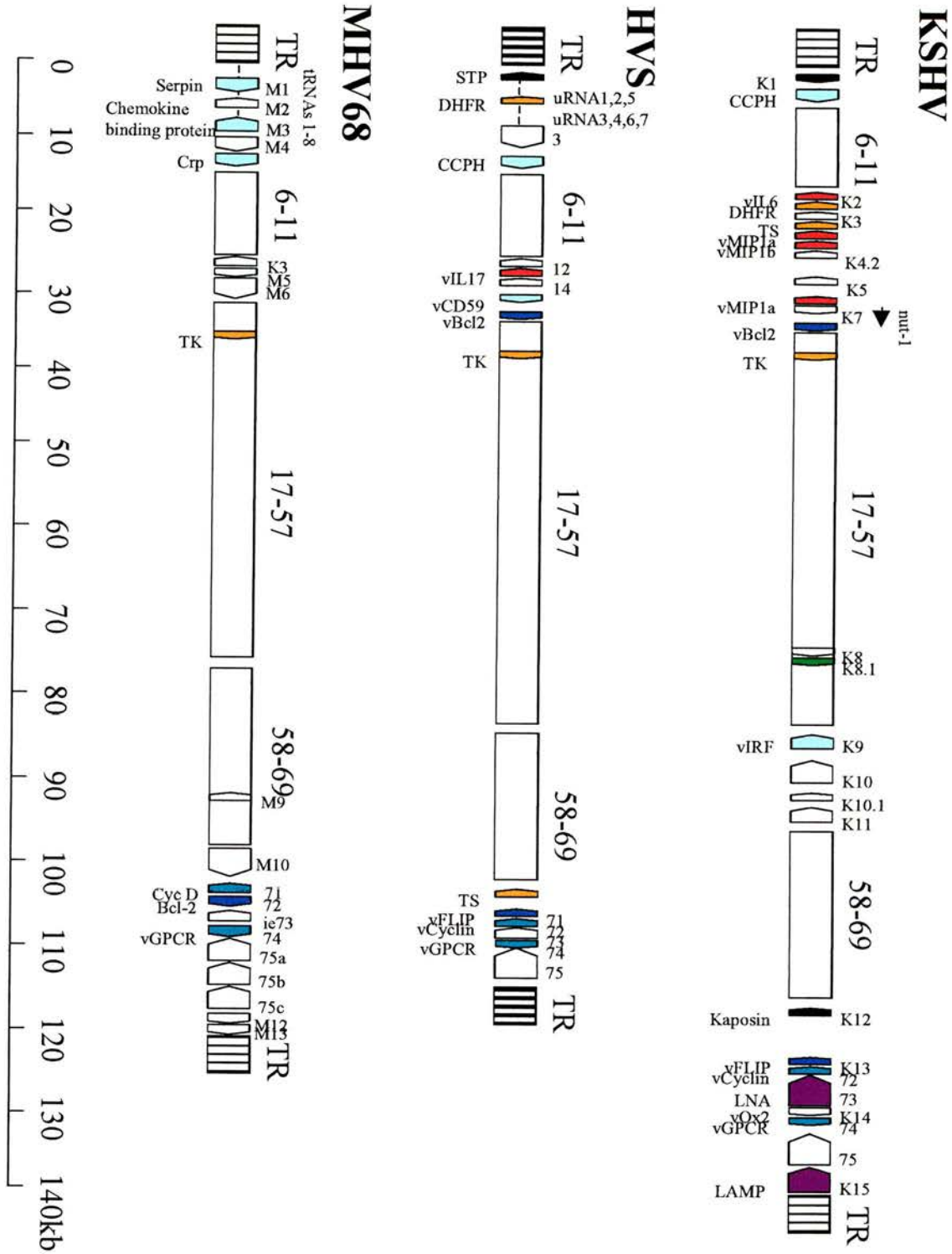

Figure 1.4 Representation of the genomes of three g-herpesviruses, KSHV, HVS and MHV-68. The large regions of homology are indicated by the un-shaded areas.

KSHV life cycle

In vivo KSHV DNA and transcripts have been found in B cells, macrophage, keratinocytes, endothelial and epithelial cells; *in vitro* KSHV has been shown to be able to infect a number of different cell types including B cells, endothelial, epithelial and fibroblast cells (Renne et al., 1998; Blackbourn et al., 2000). The initial interaction of KSHV with a host cell is mediated by the envelope glycoproteins gB and gpK8.1A which recognise heparan sulphate-like molecules on the cell surface (Akula et al., 2001; Wang et al., 2001; Birkmann et al., 2001). Additionally gB has been demonstrated to interact with cell surface alpha1beta3 integrin and expression of this molecule in CHO cells increased the infectivity of the virus (Akula et al., 2002). Interaction with integrin is dependent upon the RGD motif found within gB and independent of binding to heparan sulphate. Association of the viral gB with alpha1beta3 integrin activates focal adhesion kinase, this is the first step in a signalling cascade which results in cytoskeletal rearrangement and cell adhesion and thus, presumably, aids entry of the virus (Wang et al., 2003; Akula et al., 2002). Investigations utilising inhibitors of clathrin-mediated endocytosis imply that this may be the mechanism by which KSHV enters its target cells (Akula et al., 2003).

During latency the KSHV genome is maintained as an episome within the nucleus where it is tethered to chromosomes by the latently expressed protein LANA. In asymptomatic individuals latency is maintained primarily in $CD19^+$ B cells (Ambroziak et al., 1995). As KSHV- associated tumours affect other cell types, however, the virus must also be able to establish latency in a wider range of host cells e.g. cells of endothelial lineage found in KS lesions. Reactivation from latency into the lytic replication cycle is initiated by the replication and transcription

activator (RTA), the product of ORF 50. Expression of RTA was shown to interfere with the maintenance of latency in infected B cells (Lukac et al., 1998) and to upregulate the promoters of several KSHV (Lukac et al., 1999; Lukac et al., 2001) and cellular (Roan et al., 2002) genes. RTA has been demonstrated to bind directly to the promoters of the KSHV genes ORF57 and K-bZIP (Lukac et al., 2001) and to interact with A/T trinucleotide motifs within the promoter region (Liao et al., 2003a). Production of ORF50 itself appears to be under epigenetic control. It has been noted that activity of the ORF50 promoter is induced in response to demethylation (Chen et al., 2001) and expression of histone acetyltransferase (HAT) (Lu et al., 2003) which implies a role for chromatin remodelling of the promoter region in ORF50 transcription. RTA dependent gene expression is mediated through interactions of RTA with cellular proteins responsible for chromatin remodelling (the Brg1 subunit of SWI/SNF and the TRAP230 subunit of TRAP/Mediator) via a short acidic region within its C-terminus (Gwack et al., 2003). Additionally the RTA protein has been shown to interact directly with the product of ORF K8, a member of the basic domain leucine zipper family, both *in vitro* and *in vivo*. This interaction apparently serves to regulate the expression of K8 and other immediate early genes as the RTA-K8 complex represses transcription from RTA response element-containing promoters (Liao et al., 2003b).

Latency associated genes

As is the case for other herpesviruses, KSHV gene transcription during latency is very tightly regulated. Only two transcripts are truly type I, that is, induction of lytic transcription does not result in their up-regulation (Sarid et al., 1998).

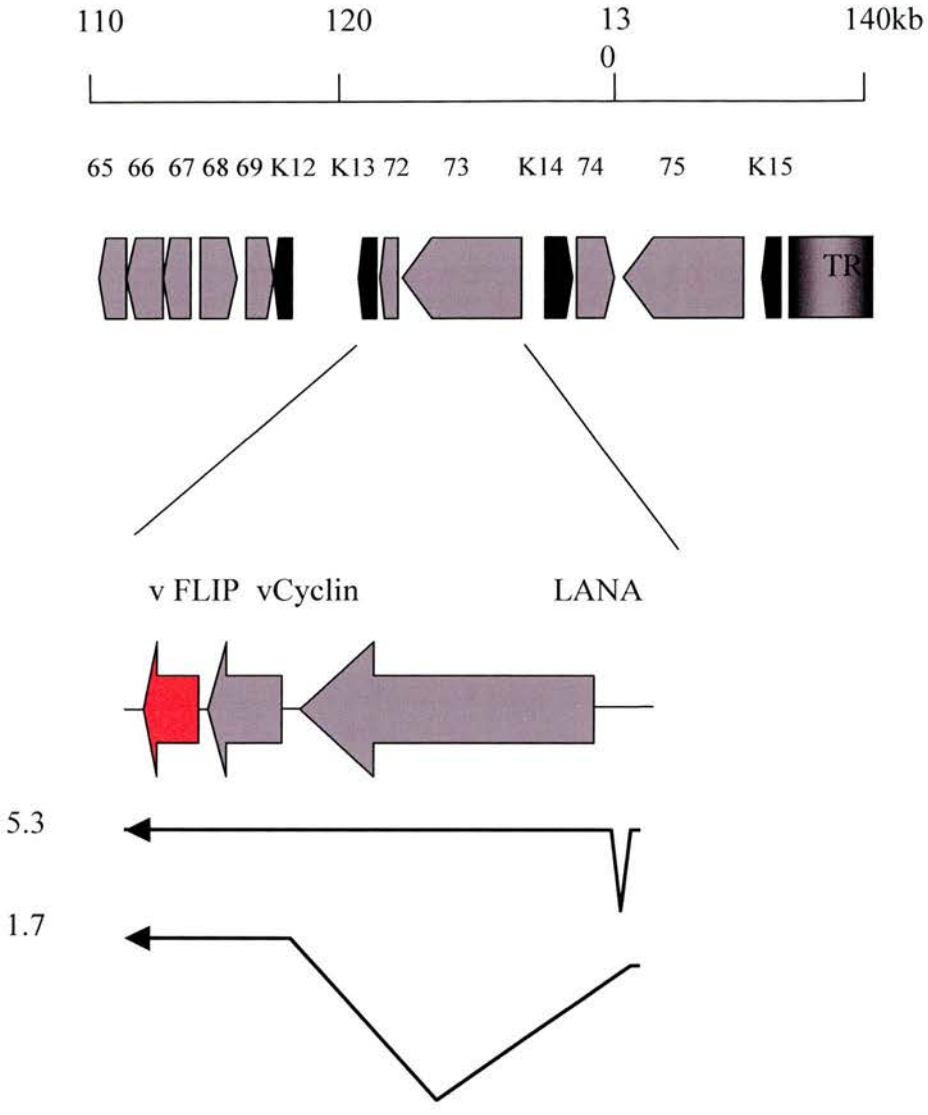

Figure 1.5 Schematic representation of the right-hand end of the KSHV genome showing the position and sizes of the latent transcripts. Adapted from Talbot *et al*, 1999.

Both transcripts are located at the right-hand end of the genome and are transcribed from a common start point, see figure 1.5. In fact, the smaller 1.7kb transcript results from splicing of the larger 5.32kb transcript (Talbot et al., 1999; Sarid et al., 1998). Northern blotting analysis indicated that the larger transcript encodes ORFs 71-73: vFLIP; vCyclin and LANA, whilst the smaller transcript encodes vCyclin and vFLIP only. A monocistronic transcript encoding vFLIP only has never been identified; it has since been demonstrated that there is an internal ribosome entry site (IRES) at the 3' end of the vCyclin coding sequence by which vFLIP may be translated (Bieleski and Talbot, 2001; Low et al., 2001b; Grundhoff and Ganem, 2001).

vFLIP: This protein was originally identified by database mining (Thome et al., 1997). Flice inhibitory proteins (FLIP) have been identified in a number of viruses and subsequently a cellular homologue has been discovered (Irmler et al., 1997). The KSHV vFLIP has been demonstrated to display anti-apoptotic behaviour *in vitro* (Djerbi et al., 1999) and to activate the NF-κB (Liu et al., 2002) and JNK/AP-1 (An et al., 2003) pathways *in vitro.*

vCyclin: KSHV encodes a type D cyclin (Chang et al., 1996) with 32% amino acid similarity to HVS vCyclin and 31% amino acid similarity to cellular cyclin D2 (Li et al., 1997). The synthesis and degradation of cyclins is fundamental to progression through the cell cycle; D-type cyclins are synthesised primarily during the G1 and S phases of the cell cycle and activate cyclin dependent kinases (cdk's) to phosphorylate target proteins including the tumour suppressor pRB1. KSHV vCyclin has specificity for cdk-6 and the cyclin-cdk-6 complex is able to phosphorylate pRB1 and histone H1 *in vitro* (Li et al., 1997; Godden-Kent et al., 1997) and the cdk inhibitor p27/Kip (Ellis et al., 1999). Phosphorylation of histone

H1 represents a change in substrate specificity of cdk6 in comparison to its activity following association with cellular cyclinD. Phosphorylation of pRB1 blocks its activity (including the repression of transcription factors involved in DNA synthesis) and drives transition of the cell cycle from G1 to S phase. Through its phosphorylation of p27, which results in destruction of the inhibitor, vCyclin also has a mechanism by which it can mediate escape from the normal controls of cdk activity. Together, these activities imply that vCyclin acts to drive progression of the cell cycle and it may, therefore, contribute towards cellular proliferation and oncogenesis (Moore and Chang, 2001). Additionally, expression of vCyclin in cells with a high level of cdk6 induces apoptosis independently of pRB1 and p53 (Ojala et al., 1999). KSHV vCyclin-driven apoptosis can be inhibited by the KSHV Bcl-2 homologue whereas the cellular Bcl-2 is ineffective (Ojala et al., 1999). This observation may be explained by the susceptibility of the two Bcl-2 proteins to phosphorylation by vCyclin. The vCyclin-cdk6 complex can phosphorylate and thus inactivate cellular Bcl-2 destroying its anti-apoptotic function. Investigation of a PEL-derived cell line in which lytic replication was induced showed that apoptotic cells contained phosphorylated cBcl-2 which was not detected in a KSHV-negative cell line (Ojala et al., 2000).

LANA: The product of ORF73 is an acidic nuclear protein which appears as a ~220kDa doublet following SDS-PAGE. Antibodies to LANA are used as the main serological evidence for KSHV infection and are found in almost all cases of KS (Dupin et al., 1999). LANA is a multi-functional protein with roles in the maintenance of the viral genome and in subversion of cellular processes. In a role analogous to that of EBV EBNA1, LANA tethers the KSHV episome to

chromosomes thus enabling maintenance of the viral DNA and probably aiding efficient segregation of the episome during cell division (Ballestas et al., 1999). Through co-localisation studies the association of LANA with chromosomes was seen to be maintained throughout interphase and mitosis (Ballestas et al., 1999). LANA binds to two nucleotide motifs within the terminal repeat region of the KSHV genome via a DNA-binding domain at its C-terminus (Garber et al., 2001; Ballestas and Kaye, 2001). Association of the LANA-episome complex with cell chromosomes involves two cellular proteins, MeCP2 and DEK. Following identification by yeast-2-hybrid screening and immunoprecipitation MeCP2 and DEK have been demonstrated to associate with the N and C terminus of LANA respectively. Their expression *in vitro* enables LANA to localise to mouse chromosomes (Krithivas et al., 2002). LANA is able to promote latent DNA replication via interactions with an origin of replication found within the terminal repeat sequence (Grundhoff and Ganem, 2003; Hu et al., 2002).

Analysis of the amino acid sequence of LANA revealed a putative Zinc finger DNA binding domain, a leucine zipper and a nuclear localisation signal making it a candidate for involvement in interactions influencing transcription. Subsequent studies revealed that it activates transcription from promoters including IL-6 (An et al., 2002), telomerase reverse transcriptase (Knight et al., 2001) and E2F regulated promoters (Radkov et al., 2000), and can also act to repress transcription (Krithivas et al., 2000; Garber et al., 2002). LANA's influence over transcriptional activity is mediated, at least in part, by its ability to affect the activity of cellular transcription factors. LANA binds to CBP, RING3, ATF/CREB2 and mSin3A all of which are cellular proteins involved in transcription regulation reviewed in (Verma and

Robertson, 2003). LANA is one of several potential oncogenes encoded by KSHV; mechanisms by which it may contribute to tumourigenesis continue to be proposed. It is known that LANA can interact with the tumour suppressors p53 and pRb. In co-transfection experiments using p53 and a reporter gene under the control of p53 response elements it was demonstrated that LANA substantially inhibited p53-dependent transcriptional activity (Friborg, Jr. et al., 1999). Direct interaction between p53 and LANA was demonstrated, as was LANA-mediated protection against apoptosis induced by over-expression of p53. Having demonstrated that LANA was able to act as a transcription co-factor for E2F-dependent transcription, Radkov *et al* (Radkov et al., 2000) aimed to identify which regulatory proteins were involved. Immunoprecipitation experiments showed that LANA was able to interact with pRb both *in vivo* and *in vitro.* Further evidence of LANA's potential role in tumourigenesis comes from the observation that primary REF cells co-transformed with LANA and the cellular oncogene HRAS formed foci of transformed cells greater than those observed when transfected with HRAS alone (Radkov et al., 2000). The most recently proposed mechanism by which KSHV may promote tumourigenesis is through subversion of the Wnt-β–catenin pathway (Fujimuro et al., 2003; Boshoff, 2003). High levels of β–catenin are observed in PEL and KS cells and can be induced in Vero cells following the transfection of a LANA-encoding plasmid (Fujimuro et al., 2003). β–catenin enters the nucleus, where it activates genes involved in cell proliferation via association with cellular transcription factors (Boshoff, 2003). A yeast-2-hybrid screen revealed that LANA is able to associate with Glycogen Synthase Kinase-3β (GSK-3β), which is part of a complex required for phosphorylation, subsequent ubiquitination, and degradation of β–catenin

(Fujimuro et al., 2003). LANA appears to sequester GSK-3β and redistribute it to the nucleus; this was also observed in a PEL-derived cell line. Co-transfection of LANA with GSK-3β significantly reduced β–catenin turnover and resulted in an accumulation of β–catenin within the cell (Fujimuro and Hayward, 2003). The accumulation of β–catenin is observed in several cancers (Polakis, 2000) further supporting the hypothesis that LANA-mediated down-regulation of GSK-3β activity may contribute to viral transformation (Fujimuro and Hayward, 2003; Boshoff, 2003).

Immune evasion and tumourigenesis

Besides the latent genes, vFLIP, vCyclin and LANA, a number of other KSHV proteins are potentially able to subvert the host immune response and/or contribute to tumourigenesis. These include a Bcl-2 homologue (Sarid et al., 1997) and the product of ORF K7 (Wang et al., 2002; Feng et al., 2002) both of which are anti-apoptotic. Neither protein is significantly expressed in KS lesions or latently infected cells, however, they may help to prevent apoptosis of cells harbouring lytic virus thus aiding the spread and persistence of the infection. KSHV is able to subvert the host interferon response through the product of ORF K9, viral Interferon Regulatory Factor (vIRF) (reviewed in Moore and Chang, 2001). vIRF inhibits interferon (IFN) activated signalling pathways within the cell through binding of transcriptional co-adaptors. The result is a repression of transcription from the majority of IFN-responsive promoters and an activation of promoters that are normally repressed by IFN signalling e.g. c-myc. Consequently vIRF is able to drive infected cells through the cell cycle and thus contribute toward cellular proliferation.

KSHV ORF K2 encodes an interleukin 6 (IL-6) homologue with 25% identity and 62% similarity to cellular IL-6 (Moore et al., 1996). vIL-6 is expressed at very low levels in KSHV positive tumours and PEL-derived cell lines. Following induction of lytic replication vIL-6 is abundantly expressed (Moore et al., 1996). KSHV vIL-6 is implicated in tumourigenesis as an autocrine growth factor, inducing B cell proliferation and preventing apoptosis (Burger et al., 1998; Moore et al., 1996), and as an antagonist of IFN signalling, blocking IFN-mediated cell cycle arrest and growth inhibition (Chatterjee et al., 2002). In contrast to cIL-6, vIL-6 requires only one of the two receptor subunits, gp130, for its activity (Wan et al., 1999). This suggests that it may have a broader range of target cells than its cellular homologue. Additionally, expression of IFNα down-regulates the gp80 component of the receptor, which is required for cIL-6 binding, but has no effect on gp130, allowing vIL-6 to overcome this regulation (Chatterjee et al., 2002). Interestingly, it has recently been shown that KSHV vFLIP is able to induce expression of cellular IL-6 (An et al., 2003) suggesting a possible mechanism by which growth signals can be supplied to lesions in which the virus is latent. Another viral gene with host cell origins is the G protein-coupled receptor homologue, vGPCR. The receptor has homology to the cellular CXCR1 and CXCR2 receptors (Cesarman et al., 1996). In contrast to its cellular counterparts, the KSHV protein is constitutively active once it has been expressed and is bound by an unusually wide range of ligands (Arvanitakis et al., 1997). The vGPCR is able to activate a number of signalling pathways within the cell, these include activation of the transcription factors AP-1 and NF-κB, with resultant induction of cytokines and chemokines (Schwarz and Murphy, 2001). Signalling of the vGPCR in NIH 3T3 cells results in tumour formation, following

injection into nude mice, and expression of vascular endothelial growth factor (VEGF) which contributes toward angiogenesis (Arvanitakis et al., 1997; Bais et al., 1998). Despite being expressed in only a fraction of cells within a tumour, vGPCR has been shown, in one mouse model, to be capable of inducing tumours with resemblance to KS and to promote tumour formation by latently infected cells (Montaner et al., 2003). ORF K1, at the far left hand side of the genome, can transform fibroblast cells (Lee et al., 1998b) and contains a functional immunoreceptor tyrosine activation motif (ITAM) (Lee et al., 1998a). The ITAM domain has constitutive signalling activity and is able to transduce cellular signalling pathways (Lee et al., 1998a; Lagunoff et al., 1999). A further strategy by which KSHV acts to dampen the immune response is through down-regulation of MHC class I molecules from the surface of infected cells. Two lytic proteins, K3 and K5, reduce the cell surface expression of MHC class I through promotion of endocytosis (Coscoy and Ganem, 2000). It has been suggested that this mechanism of immune evasion is also employed during latent infection as expression of MHC class I is also reduced on cells harbouring latent virus (Tomescu et al., 2003). In addition to its ability to down-regulate MHC class I expression, K5 is also able to inhibit natural killer (NK) cell activity through down-regulation of the ligands for NK cell-mediated cytotoxicity receptors, ICAM-1 and B7-2 (Ishido et al., 2000).

1.2.2.2 Murine Gammaherpesviruses: MHV-68 and MHV-76

Isolation

During field studies in Slovakia five novel herpesviruses were isolated from murid hosts; MHV-60, -68 and -72 from the bank vole (*Clethrionomys glareolus*) and MHV-76 and -78 from the yellow-necked wood mouse (*Apodemus flavicollis*) (Blaskovic et al., 1980). Subsequent analysis revealed that MHV-68 was a member of the genus *Rhadinovirus* (Efstathiou et al., 1990b; Efstathiou et al., 1990a).

Genome

The MHV-68 genome consists of 118kbp of unique DNA which is flanked at either end by variable numbers of 1.23kbp terminal repeat regions. It encodes 73 ORFs and 8 tRNA-like molecules (Virgin et al., 1997; Nash et al., 2001). Investigation of MHV-76 revealed its genome to be identical to that of MHV-68, with the exception of a 9,538bp deletion at the left-hand end of the genome resulting in the loss of 4 MHV-68 specific ORFs, M1-M4, and the tRNA-like molecules (Macrae et al., 2001). Both MHV-68 and -76 share large blocks of homology with other gamma herpesviruses (see figure 1.4).

As is the case for other gamma herpesviruses, MHV-68 and -76 appear to have carried out extensive piracy from their host's genome during their evolution; they encode a number of homologues of cellular genes including Bcl-2, cyclin D and G protein coupled receptor.

Pathogenesis

The natural route by which infection is spread is unknown, however, analogy with other animal gamma herpesviruses suggests that it is likely to be via the respiratory tract. Intranasal infection of 3-6 week old laboratory mice with MHV-68 results in a productive infection in the epithelial cells of the lung accompanied by bronchiolitis which is resolved by the second week following infection. The virus leaves the lung, via the mediastinal lymph node, where dendritic cells, macrophage and B cells become infected. These cells transport the virus to the draining lymph node where they seed B cells. Following infection in the lymph node there is a rapid expansion of latently infected B cells which traffic to the spleen and other lymphoid tissues. Once in the spleen splenomegaly occurs due to a rapid increase in the number of latently infected B cells present; this is resolved 3-4 weeks after initial infection. Thereafter a constant number of latently infected spleen cells (approx. $5x10^5$) are maintained throughout the life of an infected animal (Nash et al., 2001). It has been suggested that long term latency requires the CD40 dependent development of memory B cells (Kim et al., 2003). Whilst splenic B cells constitute the major reservoir of MHV-68 latency, the virus has also been reported to persist in splenic macrophage and dendritic cells (Flano et al., 2003) and in lung epithelial cells (Stewart et al., 1998).

Long term infection of BALB/c mice (>9 months) with MHV-68 results in the development of lymphoma in approximately 10% of animals (Sunil-Chandra et al., 1994). The frequency of tumour development increased to >50% following treatment with immunosuppressive agents.

As MHV-76 was isolated from a different murid species investigations were carried out to determine whether it had any different characteristics to MHV-68 (Macrae et al., 2001). Comparison of the *in vitro* growth characteristics of MHV-68 and -76 showed no significant difference in their replication. *In vivo* analysis, however, has shown that MHV-76 has a more attenuated pathology than MHV-68. Levels of infectious MHV-76 in the lung peak earlier and at a lower titre than does MHV-68 indicating more rapid clearance from the site of primary infection. The initial inflammatory response to MHV-76 in the lung is more severe than that caused as a response to MHV-68 infection although by day 8 post infection the response to both viruses is similar. In contrast to MHV-68, MHV-76 induces significantly less splenomegaly and establishes much lower levels of latency in the spleen although the virus is found in the same cell subsets as MHV-68. Both viruses maintain long term persistence in the spleen but, in contrast to MHV-68, MHV-76 does not appear to persist efficiently in the lung. The differences between the two viruses suggest roles for the genes M1-M4 and 8 tRNAs in pathogenecity though they appear not to be necessary for lytic replication or the establishment of latency.

Use as a model

The study of gamma herpesviruses, particularly KSHV and EBV, is limited by the lack of cell lines that support permissive replication *in vitro*. The fact that MHV-68 and -76 will readily infect fibroblast and epithelial cell lines from a number of species makes them an ideal system for the study of gamma herpesvirus replication (Simas and Efstathiou, 1998). Additionally, MHV-68 will establish lytic and latent infection in laboratory mice (Sunil-Chandra et al., 1992) making it an ideal system in

which to study pathogenesis and virus-host interactions. Finally, it is possible to study the function of individual viral genes because it is possible to manipulate the viral genome permitting the creation of knock-out or knock-in viruses.

Latency associated genes

During latency viral gene expression is very tightly regulated. Transcription of viral genes in a latently infected cell line S11, derived from a B cell lymphoma in a MHV-68 infected mouse, was investigated by microarray (Martinez-Guzman et al., 2003). The data confirmed previous reports that M2, M11, ORF73 and ORF74 were transcribed during latency (Virgin et al., 1999) and additionally identified ORFs 75a, 75b and 75c as candidate latency-associated genes. A brief description of each follows;

M2: The M2 gene is located in the unique left hand region of MHV-68. It encodes a 30kDa protein the expression of which appears to be restricted to splenic B-cells. Analysis of MHV-68 in which M2 translation was prematurely terminated showed that the increase in splenic infective centres following infection was inhibited (Macrae et al., 2003).

M11: M11 encodes a viral Bcl-2 homologue that has been shown to inhibit both CD95 and TNF induced apoptosis (Roy et al., 2000; Wang et al., 1999). Use of mutant MHV-68 in which M11 is not translated has shown that M11 is not necessary for lytic replication or the establishment of latency; however, it is needed for efficient reactivation of latent virus (Gangappa et al., 2002). The authors speculate that M11 protects cells in which viral replication is occurring from apoptosis induced by either viral or cellular products (Gangappa et al., 2002).

ORF73: MHV-68 ORF73 encodes a homologue of KSHV LANA. It was found to be the most abundantly expressed viral transcript in latently infected S11 cells (Martinez-Guzman et al., 2003). *In vivo* analysis, using a mutant MHV-68 in which ORF73 is not translated, shows a role for ORF73 in the establishment of splenic latency (Moorman et al., 2003); this result is supported by studies utilising an ORF73 knockout virus (Fowler et al., 2003). This would be consistent with a proposed role for LANA in the replication of the latent viral episome indicated by studies on the KSHV and HVS homologues.

ORF74: MHV-68 ORF74 encodes a G protein-coupled receptor homologue of the cellular CXCR2 chemokine receptor (Virgin et al., 1997). Homologues are also present in other herpesviruses including all rhadinoviruses that have been sequenced. ORF74 transcripts were detected, by RT-PCR, in the spleen and lung of persistently infected mice (Wakeling et al., 2001). The MHV-68 GPCR was shown to have transforming activity (Wakeling et al., 2001) and to mediate chemokine-dependent enhancement of viral replication (Lee et al., 2003) *in vitro.* Furthermore, a mutant MHV-68 unable to express ORF74, showed significantly less ability to reactivate from latently infected murine lymphocytes *in vitro* (Lee et al., 2003).

K3: Latency associated expression of K3 was not detected by microarray analysis of S11 cells (Martinez-Guzman et al., 2003). K3 was, however, identified as a latency transcript by RNase protection assay on material from infected spleens (Rochford et al., 2001). The K3 protein has been shown to down regulate MHC I on mice and hamster cells (Stevenson et al., 2000). In comparison to wild type virus, MHV-68 in which K3 is disrupted shows no differences in lytic replication in the lung or entry into latency. It appears that K3 acts to prevent CTL recognition of infected cells as

the normal expansion of latently infected B cells was inhibited; this phenotype was reversed following depletion of the $CD8^+$ T cells (Stevenson et al., 2002). Proteins homologous to K3 are found in some other rhadinoviruses including KSHV and HVS.

ORF75: ORF75 is a tegument protein of unknown function.

1.2.2.3 Herpesvirus Saimiri

Herpesvirus Saimiri (HVS) is the prototype rhadinovirus having significant homology to KSHV and MHV-68 as well as to the lymphocryptovirus EBV (figure 1.4). Its natural host is the squirrel monkey (Saimiri sciureus) which is native to South American rainforests. In its host HVS establishes an asymptomatic infection; however, within two months of injection into other new world primates it induces acute peripheral T- cell lymphoma (Fickenscher and Fleckenstein, 2001).

The HVS genome is approximately 140kbp in size and contains up to 77 ORFs (Albrecht et al., 1992). Different strains tend to show considerable variation only in their left-hand region; it is this variation upon which classification is based (Medveczky et al., 1984). Depending on their sequence and pathogenic properties HVS strains are subdivided into three groups, A, B and C. Of these, subgroup C strains are the most oncogenic; strain C488 causes a T-cell lymphoma in cynomolgus monkeys with a histopathology very similar to EBV-induced PTLD (Knappe et al., 2000) and they are able to transform human T-cell lines *in vitro* (Biesinger et al., 1992). The transforming activity of HVS has been attributed to sequences within this variable left-hand end of the genome. Subgroup C strains encode two genes with limited homology to cellular genes, StpC (a form of the STP oncogene) and Tip

(tyrosine kinase interacting protein), which are required for T-cell transformation and pathogenecity (Duboise et al., 1998). Subgroup A strains have a single gene at the homologous position; StpA has limited homology to StpC and is required for transformation.

In common with other gammaherpesviruses HVS has acquired several cell-homologous genes, the majority of which are expressed during lytic replication. They include genes involved in nucleotide metabolism, cell cycle regulation, complement system regulation, apoptosis inhibition and the cytokine network (Fickenscher and Fleckenstein, 2001). Additionally HVS, like KSHV, encodes a latently expressed polycistronic mRNA encompassing ORFs 71-73 (which are homologous to their KSHV counterparts) (Hall et al., 2000).

1.3 Apoptosis

The phenomenon of cell death has been documented for over a century; the first description, noting the disappearance of some cells during normal toad development, was made in 1842 (reviewed in Hacker, 2000). The term apoptosis was proposed by Kerr, Wyllie and Currie in 1972 to describe "a hitherto little recognised mechanism of controlled cell deletion, which appears to play a complementary but opposite role to mitosis in the control of animal cell populations" (Kerr et al., 1972). Originally described in morphological terms it is now appreciated that that the changes observed result from the activation of an intracellular signal transduction pathway. It is probable that the sole function of the pathway is to bring about cell death and subsequent disposal of the cell body.

1.3.1 The morphology of apoptosis

In most situations cells dying by apoptosis display very similar morphology, independent of the mechanism by which apoptosis was instigated. Exceptions do occur, however, including differing "degrees" of morphology in the same cell line, *in vitro*, depending upon the agent used to induce cell death. Differences may be explained by the limited opportunity for observation *in vivo*, artificial apoptotic inducers affecting more than just the apoptotic pathways or differing protein expression within a cell at the time of apoptosis induction (Hacker, 2000).

Morphological events occurring as a result of apoptosis are often categorised into events necessary for death of the cell and those that are dispensable "post-mortem" events. Post-mortem events include nuclear changes which, although very useful in the identification of apoptotic cells, are not required for cell death to occur. It is difficult to study morphology *in vivo* because apoptotic cells are swiftly engulfed by their neighbours. Consequently the majority of studies have been carried out using *in vitro* systems identifying changes using specific dyes or microscopy. Briefly, early events include the severing of attachments to other cells and the extracellular matrix, rounding up of cells and the appearance of protrusions from the plasma membrane. Subsequently nuclear chromatin begins to condense along the perimeter of the nucleus. This is followed by complete nuclear condensation and fragmentation, dilation of the endoplasmic reticulum and formation of cytoplasmic vacuoles. Finally, the entire cell condenses and is re-organised into apoptotic bodies, a term coined by Kerr *et al* in 1972, to describe membrane bound vesicles of differing size and composition which contain the entire contents of the cell. These

apoptotic bodies are taken up by other cells and digested via the lysosomal pathway. These morphological events occur in the same sequence in all cases and take between thirty minutes and an hour to complete (reviewed in Hacker, 2000).

1.3.2 Caspases

Apoptosis is an active form of cell death which is executed by specialised cellular machinery. The morphological changes seen are the direct result of the action of a family of cysteine proteases, the caspases.

Studies on *C.elegans* led to the recognition that the pathway to developmental cell death in the nematode was regulated by the same principles as apoptotic cell death in mammalian cells. A homologue of Ced-3, a product required for nematode cell death, was cloned in mammals and identified as interleukin-1β-converting enzyme, or caspase 1 (Yuan et al., 1993). This was the first of more than a dozen mammalian caspases, all of which are similar in terms of sequence, structure and substrates, to be identified (reviewed in Nicholson and Thornberry, 1997). Caspases function both to disassemble the cell and also further upstream in the initiation of disassembly in response to pro-apoptotic signals.

Caspases are all expressed as pro-enzymes containing three separate domains; an NH_2 terminal domain, a large (~20kD) and a small (~10kD) subunit. The caspase becomes activated via proteolytic processing between the domains which is followed by association of the large and small subunits to form a heterodimer. Two heterodimers then associate, forming a tetramer, which has two independent active sites containing catalytic residues from both subunits (Walker et al., 1994). Caspases are very specific proteases with an absolute requirement for cleavage after an

aspartic acid, consistent with the fact that proteolytic cleavage during apoptosis is not indiscriminate but is coordinated (Thornberry and Lazebnik, 1998).

1.3.3 Apoptotic pathways

In mammalian cells there are two major pathways by which apoptosis can be triggered; through death receptors, in response to external stimuli, or via the mitochondria, in response to external signals and intracellular damage.

Death receptors are members of the tumour necrosis factor receptor (TNF-R) gene superfamily. They are present on the cell surface and contain a cytoplasmic "death domain" which enables the receptor to engage the cell's apoptotic machinery (Tartaglia et al., 1993). The receptors are activated by their natural ligands, which are type II transmembrane proteins (of the TNF family) of which a soluble form can be generated by proteolysis (reviewed in Smith et al., 1994). The best characterised death receptor is CD95 (also called Fas or Apo1). Amongst other roles CD95 signalling is important in the killing of virus-infected or cancer cells by cytotoxic T cells and natural killer cells (Sayers et al., 1998). Cross-linking of CD95, following association with its natural ligand, or anti-CD95 antibody, results in receptor oligomerisation, probably trimerisation. The death domains of the receptors are consequently brought together into a conformation which allows association with the adaptor molecule Fas- associated death domain (FADD). As well as a death domain, through which it interacts with CD95, FADD also contains a death effector domain (DED) which binds to a homologous region of the pro-caspase 8. This complex of proteins is termed the death-inducing signalling complex (DISC). The resulting high concentration of pro-caspase 8 at the DISC allows the low intrinsic protease activity

of pro-caspase 8 to autocatalytically cleave, and activate, itself and subsequently downstream effector caspases (figure 1.6) (Muzio et al., 1998).

A large number of apoptotic signals, both extra- and intracellular, converge at the mitochondria where, in a process regulated by members of the Bcl-2 family, they result in changes to the permeability of the mitochondrial membranes. Pro-apoptotic signalling leads to an increase in mitochondrial membrane permeability and the subsequent release of soluble inter-membrane proteins, including cytochrome c and Smac/DIABLO, into the cytosol. As a consequence pro-caspase-3 is cleaved and activated (reviewed in Hengartner, 2000).

The death receptor and mitochondrial pathways converge at caspase-3 and downstream apoptotic events are independent of the pathway by which they were initiated. In some cells, termed type I, large amounts of caspase 8 are activated at the DISC resulting in rapid downstream caspase activation. In other, type II, cells the amount of caspase 8 activated at the DISC is much reduced; the apoptotic signal is amplified by the mitochondria which are activated by caspase 8 cleavage of a Bcl-2 family member, Bid. In type I cells mitochondrial activation is not necessary for cell death and anti-apoptotic Bcl-2 proteins cannot inhibit apoptosis. In type II cells the apoptotic signal initiated at the death receptor can be inhibited by proteins acting at the mitochondria (Krammer, 2000).

1.3.4 Viruses and apoptosis

Upon viral infection many cells undergo apoptosis so as to prevent viral replication and release of progeny. In response, many viruses have acquired mechanisms by which they can subvert the apoptotic process. Viral modulation of apoptosis was

first studied in adenoviruses; strains lacking a functional E1B 19kDa gene led to a greatly enhanced cytopathic effect following infection (Ezoe et al., 1981) and the E1A oncogene dependent transformation was dependent upon co-expression of E1B 19kDa. Analysis of E1B 19kDa showed it to contain a region of sequence homology to the Bcl-2 protein which was essential for its anti-apoptotic function (Chiou et al., 1994). Subsequently Bcl-2 homologues have been detected in other virus families including the herpesviruses. EBV encodes BHRF1 which has limited homology to cellular Bcl-2 and is able to enhance the survival of latently infected B cells when they are challenged with apoptotic stimuli (Henderson et al., 1993a) and a second Bcl-2 homologue that interacts with cellular family members, Bax and Bak, to inhibit apoptosis (Marshall et al., 1999). Both HVS and KSHV also encode Bcl-2 homologues; the KSHV vBcl-2 is lytically expressed and, like BHRF1, is thought to aid the release of progeny virus (Sarid et al., 1998).

Several viruses also target p53, an essential tumour suppressor gene that induces cell cycle arrest or apoptosis in response to a number of stimuli (reviewed in Fridman and Lowe, 2003). Small DNA tumour viruses, such as adenovirus and SV40, activate genes necessary for cell cycle progression by releasing the E2F transcription factors; however, this also results in p53 activation so these viruses also encode products that disrupt p53 activity. An example is the SV40 large T antigen which sequesters p53 (Yanai and Obinata, 1994). KSHV LANA has also been demonstrated to interact with p53 and reduce its transcriptional and cell death inducing activity (Friborg, Jr. et al., 1999).

As previously mentioned, the inhibition of mitochondrially initiated apoptosis cannot prevent cell death in type I cells. To overcome this problem some viruses have yet

another mechanism by which they can subvert apoptosis; disruption of the DISC by viral FLICE inhibitory proteins or vFLIPs (see section 1.4). These proteins prevent association of FADD with pro-caspase 8 and have been shown to confer resistance to CD95- mediated apoptosis and apoptosis initiated from some other death receptors (Irmler et al., 1997; Thome et al., 1997). All viruses encoding a vFLIP protein are associated with tumour formation e.g. HVS, EHV2 and KSHV. In addition, they all encode Bcl-2 homologues and therefore can potentially inhibit apoptosis in type I and type II cells. Pro-apoptotic CD95 signalling is manipulated in different ways by other viruses; mechanisms include the internalisation and degradation of the receptor by adenoviruses (Elsing and Burgert, 1998) and interactions between components of the CD95 signalling pathway and HIV gene products (Geleziunas et al., 2001).

1.4 FLICE inhibitory proteins

1.4.1 The discovery of vFLIPs

Using the knowledge that deletion mutants of FADD or caspase 8 (FLICE) lacking the DED domain, could inhibit death receptor mediated apoptosis, protein databases were screened using a generalised profile of DEDs for potential inhibitors of apoptosis. This approach led to the initial identification of the EHV-2 E8 and MCV MC159 proteins, both of which contained two DED motifs, and subsequently similar proteins were found in the genomes of BHV-4, HVS and KSHV (Thome et al., 1997; Hu et al., 1997; Bertin et al., 1997). They were named, amongst other things, vFLIPs (viral FLICE inhibitory proteins) (Thome et al., 1997) and this is how they are now most commonly referred to. The homology of the viral DED domains with those of

caspase-8 and FADD led to the hypothesis that vFLIPs may bind to the adaptor molecule FADD and somehow interfere with death receptor signalling at the level of FADD-caspase 8 association. The proposed interaction between EHV-2 vFLIP and FADD was confirmed by co-immunoprecipitation experiments which also indicated that the CD95-FADD interaction could still occur in the presence of vFLIP (Thome et al., 1997). It was also demonstrated that expression of EHV-2 vFLIP inhibited recruitment and activation of caspase-8 and conferred considerably decreased susceptibility to CD95 mediated apoptosis in a B cell line; apoptosis induced by alternative means was unaffected (Thome et al., 1997).

1.4.2 Identification of cFLIPs

Soon after the discovery of viral FLIP proteins a cellular homologue was identified by several groups and named cFLIP (Irmler et al., 1997). cFLIP was identified through database searching using a consensus FLIP sequence, derived from the viral proteins previously identified, and subsequent screening of a cDNA library with the corresponding EST. There have been two variants of cFLIP protein identified to date ($cFLIP_s$ and $cFLIP_L$); both contain two DEDs and the longer version ($cFLIP_L$) additionally contains an inactive caspase like domain (Irmler et al., 1997). An anti-apoptotic role for both forms of cFLIP was indicated by experiments in which stably transfected BJAB cell lines expressing high levels of cFLIP protein were challenged with CD95L and found to be resistant to apoptosis (Krueger et al., 2001). The mechanisms by which cFLIP functions have not, as yet, been elucidated, however, it has been demonstrated that both forms of cFLIP are recruited to the DISC (Scaffidi et al., 1999) where they may prevent autocatalytic activation and processing of

caspase 8. The role of $cFLIP_S$ as an apoptosis inhibitor is now well established, however, there is more controversy surrounding $cFLIP_L$. It has been demonstrated that the long form, $cFLIP_L$, can act in a pro-apoptotic manner (Chang et al., 2002). $cFLIP_L^{-/-}$ knockout mice expressed a phenotype very similar to caspase 8 or FADD knockouts (Yeh et al., 2000). The pro-apoptotic function is dependent on the protease domain which heterodimerises with caspase 8, at the DISC, raising concentrations of caspase 8 and resulting in its auto-catalytic activation. At higher levels of expression $cFLIP_L$ was found to inhibit apoptosis, as demonstrated by Krueger *et al,* (Chang et al., 2002). It now appears that $cFLIP_L$ is a regulator of apoptosis and that whether it acts in a stimulatory or inhibitory manner is dependent upon the levels of its expression. cFLIP expression has been implicated in immune escape and resistance to apoptosis in a number of tumours (in which $cFLIP_L$ levels are probably enhanced) (Medema et al., 1999; Okano et al., 2003; Ryu et al., 2001). Additionally, up-regulation of cFLIP has been suggested as a possible mechanism of EBV tumourigenesis (Tepper and Seldin, 1999).

1.4.3 KSHV vFLIP

KSHV vFLIP is expressed during latency

As previously described, analysis of KSHV gene transcription in PEL cell lines showed that vFLIP (ORF 71) is latently expressed. It is transcribed from the same promoter as vCyclin and LANA (ORFs 72 and 73) as a ~6kB polycistronic transcript which is subsequently cleaved to produce a ~2kB transcript encoding vFLIP and vCyclin (figure 1.5). Induction of lytic replication using TPA does not cause an

increase in total levels of the transcripts. A vFLIP only transcript has never been seen (Sarid et al., 1999; Talbot et al., 1999).

In situ hybridisation studies have suggested that vFLIP expression increases from early to late stage KS lesions and that this is accompanied by a drop in the number of apoptotic cells within the lesion (Sturzl et al., 1999). However, this study quantified vFLIP transcripts and does not indicate whether an increased rate of transcription is accompanied by increased levels of translation.

Translation of KSHV vFLIP

The failure to detect a monocistronic vFLIP transcript led to investigation of the mechanism by which vFLIP was translated and identification of an internal ribosome entry site (IRES) at the 3' end of ORF72 (Bieleski and Talbot, 2001; Low et al., 2001b; Grundhoff and Ganem, 2001). A 233bp sequence (nucleotides 123206 to 122973; GeneBank accession number U75698) was able to direct translation of downstream sequences in KSHV positive, but not negative, cell lines perhaps reflecting a requirement for virally expressed, or induced, interacting factors (Bieleski and Talbot, 2001).

Roles of KSHV vFLIP

1) Resistance to death receptor mediated apoptosis

Transduction of the B lymphoma cell line, A20, with a retroviral vector expressing KSHV vFLIP, and subsequent challenge with CD95L, demonstrated that KSHV vFLIP was able to confer resistance to CD95 mediated apoptosis. The cleavage of fluorescent caspase -8, -3 and -9 substrates was almost completely blocked in vFLIP

expressing cells indicating that the anti-apoptotic activity of vFLIP is due to its prevention of caspase activation (Djerbi et al., 1999). Expression of KSHV vFLIP permitted the clonal outgrowth of A20 cells which were continually exposed to death receptor stimuli and was, therefore, implicated in tumour establishment and progression *in vivo* (Djerbi et al., 1999). vFLIP is expected to act as $cFLIP_S$ and inhibit the autocatalytic processing of pro-caspase 8 at the DISC (Belanger et al., 2001; figure 1.6).

2) Activation of cellular transcription

In addition to its anti-apoptotic role KSHV vFLIP has recently been shown to be able to activate the transcription factor NF-κB. NF-κB binding sites have been identified in more than 150 cellular genes; initially described as a central regulator of the innate and adaptive immune response, it has since been demonstrated to be important in the control of cell proliferation and survival (reviewed in Santoro et al., 2003). NF-κB is activated in response to a large number of stimuli via multiple signalling pathways. Most pathways converge on the IKK signalsome complex, a multi-subunit complex with kinase activity that phosphorylates, and thus causes the degradation of, proteins that normally keep NF-κB sequestered in the cytoplasm and inactive. KSHV vFLIP has been demonstrated to bind to the IKK signalsome complex, via the regulatory subunit IKKγ (Field et al., 2003). When all IKK subunits are present vFLIP-mediated NF-κB activation can occur (Matta et al., 2003).

Transient expression of vFLIP *in vitro* has been shown to induce NF-κB activation (Liu et al., 2002) and provide protection against growth factor withdrawal-induced apoptosis, through NF-κB activation; a possible mechanism through which vFLIP may contribute to lymphoproliferative disorders (Sun et al., 2003a).

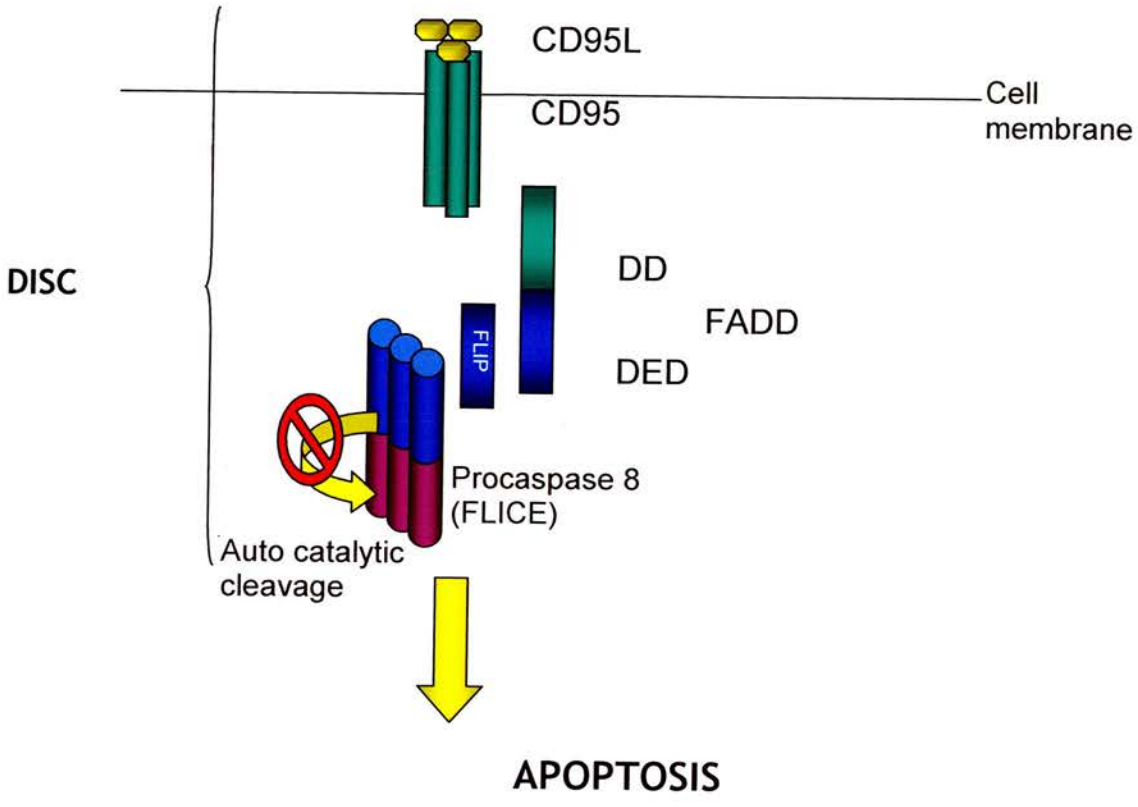

Figure 1.6 Schematic representation of CD95-mediated induction of apoptosis and the predicted anti-apoptotic activity of KSHV vFLIP. Trimerisation of CD95 following binding of its ligand results in association of the adaptor protein FADD with the C-terminus of the receptor via interaction between there homologous death domains (DD). FADD also contains a death effector domain (DED) through which it associates with pro-caspase 8. The resulting high local concentration of pro-caspase 8 enables auto-catalytic cleavage, and thus activation, to take place thereby beginning the caspase cascade that ultimately results in apoptosis. KSHV vFLIP is believed to prevent incorporation of sufficient quantities of pro-caspase 8 into the death inducing signalling complex (DISC), preventing its auto-catalytic activation.

In contrast to the EHV-2 and MCV vFLIPs, KSHV vFLIP is able to transform cells *in vitro* and promote tumour development *in vivo*. Rat-1 cells stably expressing KSHV vFLIP showed greater proliferation, loss of contact inhibition and anchorage-independent growth, additionally their injection into nude mice gave rise to tumours. This *in vitro* phenotype was accompanied by an increase in NF–κB activity and could be reversed by application of NF-κB inhibitors (Sun et al., 2003b). Moreover, the constitutive expression of activated NF-κB is essential for the survival of PEL cells (Keller et al., 2000) and this expression has been attributed to vFLIP (Guasparri et al., 2004). Besides anti-apoptotic factors and growth factors, it is possible that NF-κB activation is needed to promote the expression of viral and/ or cellular genes necessary for the production of infectious virions (Sgarbanti et al., 2004). It was demonstrated that virions produced from BCBL-1 cells which stably expressed a repressor of NF-κB activation were unable to initiate *de novo* infection of an endothelial cell line. Interestingly, the ability to activate NF-κB signalling appears to be a common feature of gamma-herpesviruses; the Tip and Stp proteins of HVS and LMP-1 of EBV activate NF-κB via both the canonical and non-canonical pathways (Atkinson et al., 2003; Herrero et al., 1995; Merlo and Tsygankov, 2001; Sorokina et al., 2004).

In addition to activation of NF-κB, KSHV vFLIP has been shown to activate a second signalling pathway, the JNK/AP1 pathway, resulting in activation of the cIL-6 promoter (which is also activated by NF-κB). All KSHV neoplasms employ IL-6 as a growth factor so this may be another mechanism by which vFLIP contributes towards the transforming capacity of the virus (An et al., 2003).

1.5 Internal Ribosome Entry Sites

In both prokaryotes and eukaryotes the translation of an mRNA, to produce protein, proceeds through three phases; initiation, elongation and termination. Translation is dependent upon aminoacyl-tRNAs, single-stranded RNA molecules of about 80 nucleotides with a specific three-dimensional structure and covalently attached amino acid. Base pair interactions, between the anticodon of the tRNA and the codon of the mRNA, enable transfer of the genetic data into protein. The processes, through which tRNAs are aligned on the mRNA and peptide bonds are formed between amino acids are mediated by ribosomes, large RNA-protein complexes consisting of a large and a small subunit.

In all cases the first codon translated is AUG, which encodes methionine. Throughout a messenger RNA there will typically be several AUG codons, however, only one of these will normally be utilised as a start codon. During eukaryotic post-transcriptional modification of the mRNA, in the nucleus, a 7-methylguanosine cap structure is added to the 5' end and a poly-adenosine tail to the 3'end. The 5'cap is essential for translation initiation as it allows the ribosome to locate the correct AUG codon to commence synthesis. The small ribosomal subunit recognises the cap structure, by means of a complex of proteins, and then proceeds to scan along the mRNA until it reaches an AUG codon from where translation commences. It is usually the first AUG encountered that is used as the start codon, however, the nucleotides surrounding the AUG influence the efficiency of recognition. If recognition is poor the small subunit will move on until it reaches a suitable AUG codon. This "leaky scanning" can be used to produce two or more proteins from the

same mRNA. The initiation process is complicated, involving several steps catalysed by initiation factors (eIF) (Alberts et al., 1994).

1.5.1 5'cap-dependent initiation of translation in eukaryotic cells

Cap-dependent translation is a complex process, see figure 1.7. Initiation requires assembly of a multi-protein translation initiation complex on the mRNA. The 5'cap, a methylated guanine, is recognised by the eIF4F complex. The eIF4F complex consists of eIF4G, which acts as a scaffold; eIF4E, which binds to the cap and eIF4G, and eIF4A, an ATP-dependent RNA helicase which is also associated with eIF4G. This complex binds to the 5'end of the mRNA and removes any secondary structure present. The small ribosomal subunit, associated with eIF2-GTP-met tRNA and eIF3, is then brought to the complex through interactions of eIF3 with the ribosomal subunit and eIF4G. Additionally the mRNA is circularised as the polyA-binding protein (PABP) binds the 3'polyA tail and eIF4G simultaneously. Following phosphorylation of eIF4E, by protein kinases associated with the C-terminus of eIF4G, the complex scans the mRNA until it identifies the start AUG codon. The large ribosomal subunit then joins with the small subunit allowing translation to commence (reviewed in Schneider et al., 2001).

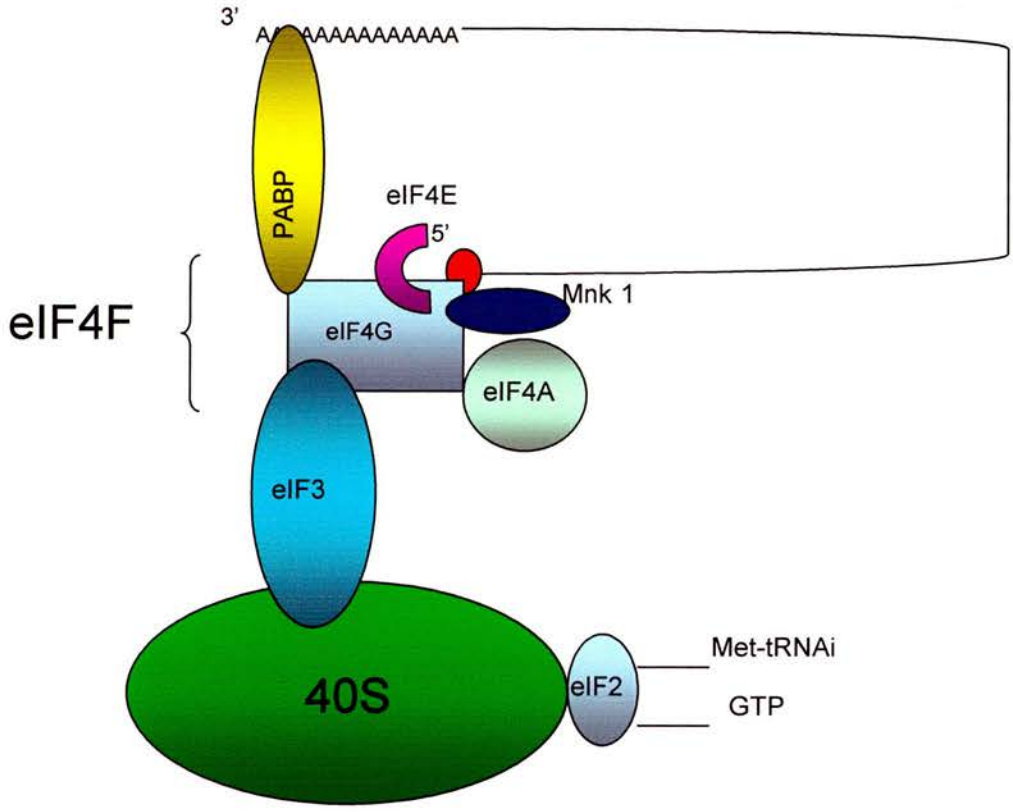

Figure 1.7: The eukaryotic translation initiation complex. The complex assembles on the mRNA following recognition of the 5'cap structure by eIF4E. Subsequent protein-protein interactions result in circularisation of the mRNA and recruitment of the small ribosomal subunit (40S). This complex scans the mRNA until a suitable start codon is located at which point the large ribosomal subunit joins and translation commences.

1.5.2 Identification of internal ribosome entry sites

Whilst 5'cap dependent scanning is the most common mechanism by which eukaryotic ribosomes locate the AUG start codon, translation can also be initiated in a cap-independent manner. This process utilises a different method of recruitment of the small ribosomal subunit to the mRNA, mediated by Internal Ribosome Entry Sites (IRES).

Since the 1970s it has been recognised that the rate of protein synthesis within a eukaryotic cell is cell-cycle dependent. Cells arrested at the G2/M phase, or that are undergoing mitosis carry out translation at only 25% the rate of interphase (G1, S, G2) cells. This down-regulation is partly due to inhibition of the translation initiation step as a consequence of reduced cap binding (reviewed in Sachs, 2000). Despite this general reduction in protein synthesis the production of some viral and cellular proteins is unaffected indicating an alternative, cap independent, mechanism of translation initiation. The internal entry of ribosomes was discovered through investigation of picornaviral mRNAs which, despite being uncapped and containing complex features at their 5' end which would be expected to impede ribosome scanning, efficiently recruit the ribosome (Pelletier et al., 1988; Jang et al., 1988; Jackson, 1988). Internal ribosome entry sites (IRES) have subsequently been identified in many viral RNAs and an increasing number of cellular mRNAs. The principle assay used to define a section of RNA as an IRES is a bicistronic reporter system. In these assays the levels of expression of a reporter gene translated via conventional 5' cap dependent translation is compared to that of a reporter gene under the control of the suspected IRES. Under conditions refractory for cap-dependent translation the IRES-dependent reporter gene should continue to be

translated (Vagner et al., 2001). The nature of the RNA transcript must also be investigated as the possibility that translation results from aberrant splicing events producing monocistronic transcripts in transfected cells must be ruled out.

The majority of IRES elements require protein co-factors for their activity, these proteins are termed IRES transactivating factors (ITAFs).

1.5.3 Viral IRESs

IRES elements were first identified in picornaviruses in 1988 (Jang et al., 1988; Jackson, 1988; Pelletier et al., 1988) and since then internal initiation of translation has been demonstrated in a number of different RNA viruses including members of the pestivirus, hepacivirus and retrovirus families and in some gamma-herpesviruses, which have DNA genomes. Some examples of viral IRESs include;

Picornaviruses: It was initially observed that infection of cultured cells with poliovirus results in a general shut down of cellular protein synthesis whilst viral proteins continue to be translated (Holland and Peterson, 1964; reviewed in Bushell and Sarnow, 2002). It subsequently became clear that this is true of the majority of picornaviral infections which result in cleavage of the translation initiation factor eIF4G, resulting in inhibition of cap-dependent translation. Investigation of the mechanism by which viral proteins could continue to be translated despite eIF4G cleavage resulted in identification of IRES elements (Pelletier and Sonenberg, 1988) Picornavirus IRESs are categorised into three types according to their sequence and structure. Enteroviruses and rhinoviruses have type I structures; aphthoviruses, cardioviruses and parechoviruses are type II; the hepatitis C virus IRES is distinct from the other picornaviral IRES elements. The different IRES groups differ in their

ITAF requirements and therefore influence viral host range; mutations in the IRES sequence can affect the virulence of the virus (Shiroki et al., 1997).

Cricket Paralysis Virus: An unusual IRES has been discovered in the family of cricket paralysis virus (CrPV)-like viruses (Wilson et al., 2000b) which, in at least two members of the family, has been shown to initiate translation at a non-methionine codon (Sasaki and Nakashima, 1999; Wilson et al., 2000a) and to function independently of any initiation factors (Wilson et al., 2000a). The CrPV are positive strand RNA viruses similar to mammalian picornaviruses. They encode two open reading frames both of which are translated by internal ribosome entry (Wilson et al., 2000a).

Flaviviruses: The HCV IRES was first identified in 1993 (Wang et al., 1993). The minimal functional IRES is approximately 330bp long and is highly conserved. The IRES binds directly to the 40S ribosomal subunit and eIF3 independently of any other translation initiation factors (Pestova et al., 1998) and through these interactions other factors such as eIF2 and initiator tRNA are recruited (Kieft et al., 2001). An IRES sequence has also been identified in classical swine fever virus (CSFV) at the 5' end of the genome (Rijnbrand et al., 1997).

Lentiviruses: Internal ribosome entry has been described for a number of members of the lentivirus family. These include SIV (Ohlmann et al., 2000), which encodes an IRES at the 5' end of its genomic mRNA, and HIV-1 which has an IRES within the *gag* ORF (Buck et al., 2001) and within the 5' leader sequence of its genomic mRNA (Brasey et al., 2003). It is proposed that, as the IRES is functional during the G_2/M phase of the cell cycle, it may play a role in virus replication during virus-induced cell cycle arrest (Brasey et al., 2003).

Gamma-herpesviruses: As mentioned previously, an IRES has been identified within the vCyclin mRNA of KSHV that controls the expression of the downstream ORF, vFLIP (Bieleski and Talbot, 2001; Grundhoff and Ganem, 2001; Low et al., 2001b). More recently an IRES has been identified within the 5' untranslated region (UTR) of EBV nuclear antigen 1 (EBNA1), the only protein absolutely required to maintain EBV latency (Isaksson et al., 2003). EBNA1 expression is controlled at multiple levels including the use of four alternative transcription start sites depending upon whether the virus is lytic or latent and the stage of latency. Transcription from each of the four start sites results in a 5'UTR of differing lengths, however, the U leader exon is common to all four transcripts. Using a bicistronic reporter system an IRES was identified in the 5'UTR which was most efficient in EBV-positive Burkitt's Lymphoma cell lines. Experiments using fragments of the 5'UTR, to identify the minimal sequences necessary for activity, identified sequences with both a positive and negative effect on translation. The IRES was found to be highly conserved between different EBV strains. It is proposed that the IRES provides a mechanism by which protein levels can be maintained independent of the stage of the cell cycle, throughout which mRNA levels fluctuate. In addition to EBV and KSHV, an IRES has recently been identified in MHV-68. Following the observation that the latently expressed protein K3 was encoded by a bicistronic transcript (Coleman et al., 2003) investigations were undertaken to determine the mechanism by which K3 is produced. An IRES was subsequently identified within the intergenic region of the transcript. The K3 protein is involved in evasion of the T cell response (Stevenson et al., 2000) a role also attributed to KSHV vFLIP (Djerbi et al., 1999). In light of this similarity it is striking that the translation of both proteins is achieved via an IRES.

1.5.4 Cellular IRES elements

Whilst the majority of cellular mRNAs are translated in a cap-dependent manner an increasing number of cellular transcripts are being identified which are able to support cap-independent translation. The majority of mRNAs exhibiting such properties encode proteins involved in gene expression, apoptosis and cell signalling. These include c-myc (Nanbru et al., 1997), x linked inhibitor of apoptosis (XIAP) (Holcik and Korneluk, 2000), apoptotic protease-activating factor (Apaf-1) (Coldwell et al., 2000) and fibroblast growth factor 2 (FGF-2) (Vagner et al., 1995). Several IRES elements have been demonstrated to operate in a cell cycle specific manner. Through the synchronisation of cultured cells and subsequent study of protein expression it has been demonstrated that ornithine decarboxylase (ODC) (Pyronnet et al., 2000), $p58^{PITSLRE}$ (Cornelis et al., 2000) and La (Qin and Sarnow, 2004) are preferentially translated at specific points of the cell cycle, namely G2 and/or mitosis. It seems likely that IRES mediated translation enables expression of specific proteins to be maintained whilst general protein synthesis levels are decreased.

1.5.5 IRES structure

Whilst there is very little conservation of primary sequence between IRES elements encoded by viruses of the same family, the secondary structure adopted by the RNA is phylogenetically conserved (Stoneley and Willis, 2004). Mutations in the IRES primary sequence, with implications for the secondary structure, have been observed to affect the virulence of poliovirus (Shiroki et al., 1997) and cellular tropism of HCV (Lerat et al., 2000). Additionally, studies of naturally occurring genetic drift in

virus sequence show that, in the vast majority of instances, any substitutions that do occur result in compensatory changes in IRES secondary structure (Martinez-Salas et al., 2002). These findings imply that the secondary structure of the viral IRES is fundamental to its successful interaction with the translational machinery. In contrast, cellular IRES elements display very little similarity in secondary structure even when they are located in the mRNA of similar genes (Le Quesne et al., 2001; Jopling et al., 2004; reviewed in Stoneley and Willis, 2004).

1.5.6 IRES transactivating factors (ITAFs)

Translation from IRES elements is, obviously, independent of the 5'cap-associated translation initiation complex; however, in the vast majority of cases additional factors are required to assist ribosomal assembly on the mRNA. At present the only IRES elements capable of mediating formation of the complete ribosome independently of additional factors are those encoded by cricket paralysis virus-like viruses (Wilson et al., 2000a). To date all other IRES elements that have been investigated have a requirement for additional host proteins. With the exception of CrPV-like viruses all viral IRES elements, for which essential interacting factors have been identified, interact with one or more eukaryotic initiation factors (eIFs). The specific requirements vary, for example EMCV and FMDV require eIF4A, eIF3, eIF2 and the C-terminus of eIF4G (Pestova et al., 1996; Kolupaeva et al., 1998; Lopez et al., 2001; Lopez and Martinez-Salas, 2000) whilst the HCV and CSFV IRESes require only eIF2 and eIF3 (Pestova et al., 1998). A number of non-canonical factors have also been demonstrated to be necessary for the activity of certain viral and cellular IRES elements. These include the polypyrimidine tract

binding protein (Mitchell et al., 2003; Kaminski and Jackson, 1998; Kaminski et al., 1995; Hunt and Jackson, 1999), upstream of N-ras (Mitchell et al., 2003; Hunt et al., 1999) and La (Holcik and Korneluk, 2000). Research in the area of cap-independent translation is fast moving; novel IRES elements are identified on a regular basis and it therefore seems likely that the range of ITAFs will extend as further studies are conducted.

1.5.7 The KSHV IRES

As mentioned above, the KSHV IRES, located in the 3' coding sequence of the vCyclin mRNA (Bieleski and Talbot, 2001; Grundhoff and Ganem, 2001; Low et al., 2001a) is responsible for the translation of vFLIP. This was the first example of an IRES element to be identified in a DNA virus. The predicted secondary structure is shown in figure 1.8. Biophysical analysis of its structure by electron microscopy supports the predicted structure and reveals that the KSHV IRES is similar to the HCV IRES (Beales et al., 2003), having two stem-loops and a flexible hinge region between. Using a bicistronic reporter assay the activity of the KSHV IRES was estimated to be approximately one third that of the EMCV IRES, the most efficient element identified to date (Bieleski and Talbot, 2001).

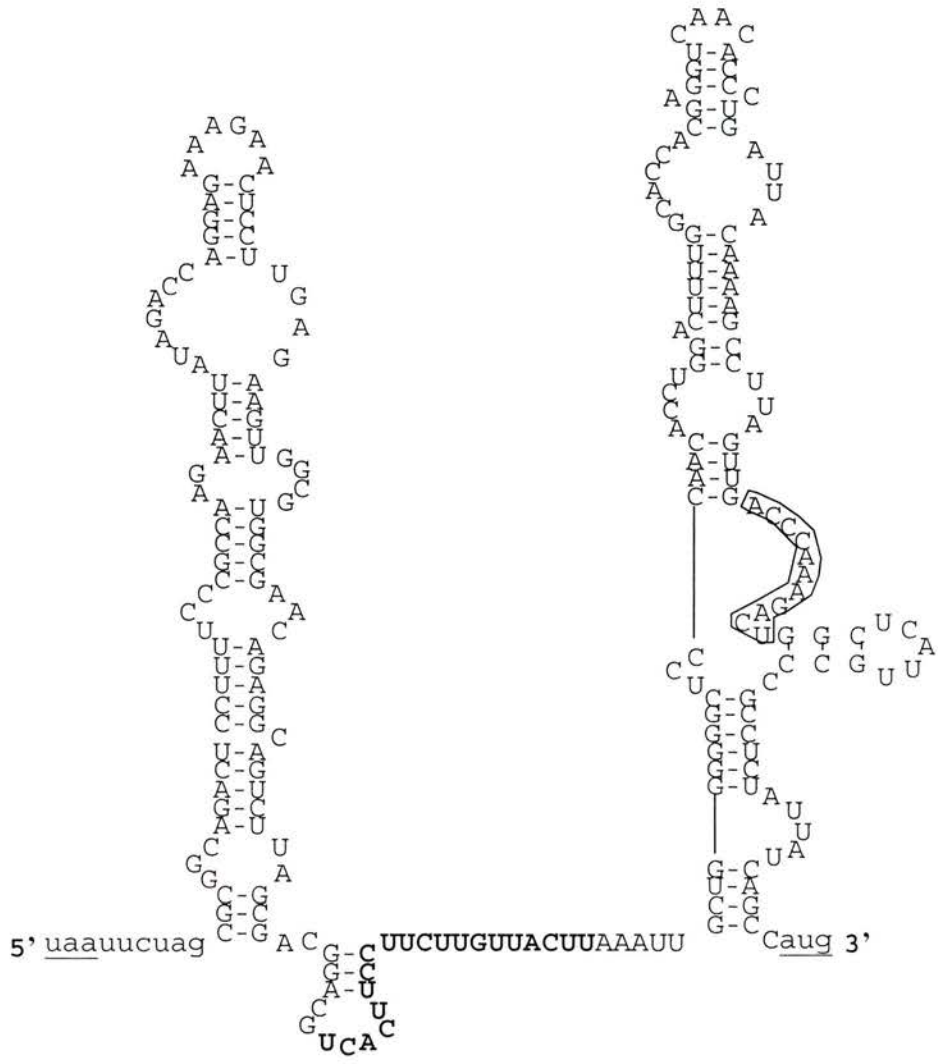

Figure 1.8 Predicted secondary structure of the KSHV IRES generated using RNA mfold version 3.0. Shown in upper case are the nucleotides 123206- 122973. The polyprimidine tract is highlighted in bold type and the 11 nucleotide sequence complementary to 18s rRNA is boxed. Taken from Bieleski and Talbot, 2001.

1.6 Project Aims

This thesis aimed to investigate two separate aspects of KSHV vFLIP biology. The first aim was to further understanding of the contribution of vFLIP towards viral pathogenesis through the use of recombinant MHV-76 viruses. As KSHV is a human virus it is very difficult to study the *in vivo* contribution of individual viral gene products towards pathogenesis. We hypothesised that expression of KSHV vFLIP in the closely related MHV-76 would enable comparison of a vFLIP expressing virus with viruses lacking vFLIP to determine any changes in virus replication or disease outcome that may be attributable to vFLIP.

Secondly, I aimed to continue investigations, already underway in the lab, into the mechanisms by which vFLIP translation is achieved. The cell type specificity of the IRES activity, and past precedent of other IRES systems, mean that it is unlikely that translation of vFLIP is achieved without ITAF involvement. Several methods were utilised in order to investigate the identity of these ITAFs.

Chapter 2 Materials and Methods

2.1 Materials

2.1.1 General solutions

TE buffer	10mM Tris-HCl pH 8 1mM EDTA
PBS pH 7.4	137mM NaCl 2.7mM KCl 4.3mM Na_2HPO_4 1.4mM KH_2PO_4
TBE buffer pH 8.3	0.44M Tris 0.44M Boric acid 12mM EDTA
Luria-Bertani (LB) broth	10g/l bactotryptone 5g/l bacto yeast extract 10g/l NaCl
LB agar	LB broth plus 15g/l bacto-agar
SOC medium	LB broth 10mM glucose 10mM $MgSO_4$ 20mM $MgCl_2$
Versene pH 7.2	200μg/ml EDTA 1% phenol red PBS

2.1.2 Commercial cloning vectors

pCR2.1 TOPO	Invitrogen
pGEX4T-1	Amersham
pTrcHis2A	Invitrogen
pRL-TK	Promega
pSP64polyA	Promega

Plasmid maps can be seen in appendix 1.

2.2 Molecular Cloning

2.2.1 Restriction digests

Restriction enzymes were purchased from either NEB or Roche. All were used as instructed by the manufacturer, typically 1 unit per μg DNA, in the supplied reaction buffer, in a total volume ranging from 10-40μl. Incubation at the appropriate temperature (usually 37°C) was typically for 2 hours.

2.2.2 Dephosphorylation

The 5' phosphate groups of linearised DNA were removed using Shrimp Alkaline Phosphatase (Roche). 1μl (10 units) was added to restriction digests and incubated at 37°C for 20 minutes. The enzyme was inactivated by incubation at 70°C for 10 minutes.

2.2.3 Blunt ending

DNA fragments were treated with DNA polymerase I, large (klenow) fragment (NEB), to remove 3' overhangs and fill in 5' overhangs. The DNA was dissolved either in 1x restriction enzyme buffer or 1x EcoPol reaction buffer (NEB) supplemented with 20μM of each dNTP (Amersham). Generally 1μl (10 units) of enzyme was added per reaction. Following 15 minutes incubation at 25°C the enzyme was inactivated by addition of EDTA to 10mM and incubation at 75°C for 20 minutes.

2.2.4 Annealing oligonucleotides

5pmoles of each oligonucleotide were mixed together in a total volume of 10µl. The mixture was heated to 95°C for 90 seconds then allowed to cool to room temperature. 2µl of 10x restriction buffer (NEB) were added to provide salts necessary for annealing and the mixture cooled to 4°C.

2.2.5 Gel purification

DNA was run on a 0.8-2% high-grade agarose gel and, using UV to visualise, the desired fragment was cut from the gel. DNA was then extracted from the agarose using the QIAquick gel extraction kit (Qiagen). Briefly, the gel slice was weighed and then solubilised in 3 volumes buffer QG by incubation at 50°C and occasional vortexing. Once the gel had dissolved 1 volume isopropanol (Sigma) was added, mixed and the mixture transferred to a QIAquick column, containing a silica-gel membrane to which the DNA binds. The column was washed with 0.75ml buffer PE, containing ethanol, by centrifugation and the DNA was eluted in 30- 50µl buffer EB (10mM Tris-HCl, pH 8.5).

2.2.6 Site directed mutagenesis

Site directed mutagenesis was carried out using the QuikChange XL Site-Directed Mutagenesis Kit (Stratagene). Primers containing the desired mutation were designed to comply with the manufacturers recommendations. The sample reaction was set up to contain 10ng template DNA; 125ng primer 1; 125ng primer 2; 5µl 10x reaction buffer (100mM KCl; 100mM $(NH_4)_2SO_4$; 200mM Tris-HCl, pH8.8; 20mM $MgSO_4$; 1% (v/v) Triton X-100; 1% (w/v) nuclease free BSA); 1µl dNTP mix and 3µl QuikSolution in a total volume of 50µl. Following addition of 2.5U *PfuTurbo*

the reaction mix was heated to 95°C for 1 minute then subjected to 18 rounds of the following reaction cycle before a final elongation step of 7 minutes at 68°C;

95°C 50 seconds

60°C 50 seconds

68°C 2 minutes per Kb plasmid.

Following cycling the reaction was cooled to 37°C and 10U *DpnI* restriction enzyme was added to each reaction. The reactions were then incubated at 37°C for 1 hour to digest the parental, methylated and unmutated, plasmid.

45µl XL 10-Gold competent cells were transformed with 2µl of the *DpnI* treated DNA by heat-shock. Transformation reactions were plated onto LB-agar plates containing the appropriate selection agent and incubated overnight at 37°C. Typically 10 colonies per plate were then picked, overnight cultures grown and plasmid minipreps carried out. Restriction digests and DNA sequencing were used to confirm that the mutagenesis had been successful.

2.2.7 Ligation

The insert was incubated with the digested vector (at a ratio varying from 1:1 to 5:1) and 1- 2U T4 DNA ligase (Roche) in 2x ligation buffer (Roche) for either 5 minutes, for sticky ended ligations, or 15 minutes, for blunt ended ligations. Ligation was carried out at room temperature. Aliquots of the ligation mixture, typically 2µl, were then used to transform competent cells by heat shock.

2.2.8 Transformation of competent cells with plasmid DNA

Approximately 0.1-50μg plasmid DNA was incubated with 20μl TOP10 competent cells (Invitrogen) on ice for 30 minutes. Cells were heat shocked at 42°C for 30 seconds then returned to ice for 5 minutes. 200μl SOC medium (Gibco) was then added to the cells and they were incubated, with shaking, at 37°C for 1 hour. Up to 100μl of cells were then plated onto LB-agar plates containing the appropriate selective medium and incubated overnight at 37°C to allow colony formation.

2.2.9 Agarose gel electrophoresis

The concentration of the agarose gel used to analyse nucleic acids was dependent upon the predicted fragment size; gels were typically in the range of 0.8- 2% (w/v). Agarose was dissolved in the appropriate volume of 0.5x TBE by heating in a microwave. Ethidium bromide, ~10μg per 100ml, was added whilst the gel was molten to allow later visualisation of the nucleic acid. The appropriate volume of 10x loading buffer (100mM EDTA pH8, 60% (w/v) sucrose, 0.1% (w/v) bromophenol blue, 0.1% (w/v) xylene cyanol) was added to nucleic acid samples which were then loaded into the set gel. Agarose gels were typically run at 100-150V in TBE buffer. The bands of nucleic acid were visualised using a UV transilluminator (UVP).

2.2.10 DNA sequencing

DNA was sequenced using the BigDye Terminator Cycle Sequencing system (Applied Biosystems). 200ng of the PCR product to be sequenced was made up to a total volume of 5μl with nuclease-free water. 4μl Big Dye reaction mix and 1μl primer (1.6pmoles) were added. DNA was amplified using the following cycle;

95°C 30 seconds

50°C 20 seconds

60°C 4 minutes

The cycle was repeated 25 times.

Amplified DNA was ethanol precipitated and sent to Jill Lovell at I.C.A.P.B., University of Edinburgh, for sequencing using an ABI sequencer (Applied Biosystems).

2.3 DNA Extraction

2.3.1. Plasmid minipreps

Single colonies of transformed bacteria were inoculated into 4ml LB broth, containing the appropriate selection agent, and grown overnight, shaking at 37°C. The bacteria were pelleted by centrifugation, 8,000g, 4 minutes, and plasmid was DNA extracted using a Rapid Plasmid Miniprep System (Marligen Bioscience Inc). Briefly, cells were resuspended in 250µl buffer G1 (50mM Tris-HCl, pH 8; 10mM EDTA; RNase A 0.1mg/ml) by vortexing and then lysed by addition of 250µl buffer G2 (200mM NaOH; 1% (w/v) SDS) and incubation at room temperature for 5 minutes. Following lysis 350µl buffer M3 (containing acetate and guanidine hydrochloride) was added, the mixture was inverted several times to mix and then centrifuged at 12,000g for 10 minutes. The supernatant was added to a spin cartridge which was subsequently centrifuged at 12,000g for 1 minute. The cartridge was washed with 700µl buffer G4 (containing NaCl; EDTA; Tris-HCl, pH 8; ethanol) by centrifugation. Finally, the plasmid DNA was eluted by addition of 75µl TE to the

cartridge, incubation at room temperature for 1 minute and centrifugation at 12,000g for 2 minutes. Plasmid DNA was stored at either 4°C or -20°C.

2.3.2 Plasmid midi and maxipreps

Larger quantities of plasmid DNA were prepared using QIAfilter plasmid Midi or Maxi kits (Qiagen). Briefly, competent bacteria transformed with the required plasmid DNA were grown overnight in LB broth, containing the appropriate selection agent, in a volume of 25-100ml and 100-200ml (Midi and Maxi kits respectively, volumes were dependant upon whether the plasmid was high or low copy number). The cells were pelleted by centrifugation at 6,000g for 15 minutes at 4°C. The pellet was resuspended in buffer P1 (50mM TrisHCl, pH8, 10mM EDTA, RNase A (0.1mg/ml)) by vortexing. Buffer P2 (200mM NaOH, 1% (w/v) SDS) was added to lyse the cells. Following a 5 minute incubation at room temperature genomic DNA and cell debris was precipitated by addition of chilled buffer P3 (3M potassium acetate, pH 5.5). The lysate was poured into a QIAfilter cartridge and incubated at room temperature for 10 minutes during which the precipitate floated to the top. The lysate was then filtered into equilibrated QIAGEN-tips (containing an anion-exchange resin to which plasmid DNA binds in low salt and pH conditions) and allowed to filter through under gravity flow. The tips were washed with buffer QC (1M NaCl; 50mM MOPS, pH7; 15% (v/v) isopropanol) to remove RNA, proteins and other low Mr impurities (by raising the salt concentration and pH). Plasmid DNA was eluted by addition of buffer QF (1.6M NaCl; 50mM MOPS, pH7; 15% (v/v) isopropanol) and concentrated and desalted by isopropanol precipitation

and washing in 70% (v/v) ethanol. DNA was air-dried prior to resuspension in approximately 100- 200µl water or TE and storage at 4°C or -20°C.

2.3.3 Phenol: chloroform extraction

1 volume of phenol: chloroform: isoamyl alcohol (25:24:1 ratio) (Sigma) was added to the DNA, which was then shaken and centrifuged at 13,000g for 1 minute. The aqueous layer, containing the DNA, was removed to a clean tube and the procedure repeated until no protein remained at the interface. 1 volume of chloroform was then added, mixed and centrifuged as before. The aqueous layer, containing DNA, was removed to a clean tube and the DNA extracted by ethanol precipitation.

2.3.4 Ethanol precipitation

0.1 volumes of 3M NaOAc (Sigma), pH 4.6, and 2.5 volumes 95% (v/v) ethanol (Sigma) were added. The mixture was vortexed and incubated, on ice, for 20 minutes then centrifuged at 13,000g, 4°C for 30 minutes. The pellet was rinsed in 70% (v/v) ethanol and centrifuged at 13,000g, 4°C for 15 minutes. The supernatant was removed and the DNA pellets air dried before resuspension in either TE or dH_2O and storage at 4°C or -20°C.

2.3.5 Determination of DNA concentration

The concentration of DNA solutions was estimated using a GeneQuant II spectrophotomer (Pharmacia Biotech). The buffer in which the DNA was dissolved was used to zero the machine. The OD_{260} of the DNA was measured and the concentration estimated using the following formula:

DNA concentration (μg/ml) = OD_{260} x dilution factor x 50

2.4 Polymerase Chain Reaction (PCR)

PCR reactions were carried out using Taq DNA polymerase in storage buffer A (Promega). In a typical reaction mix 100ng- 1μg of a DNA template was added to 10pmoles primer 1; 10pmoles primer 2; 20mM dNTPs (each dNTP at 20mM; Amersham); 5mM Mg^{2+} (Promega); 5μl 10x PCR reaction buffer (500mM KCl; 100mM Tris pH 9; 1% Triton X-100. Promega) and 2.5 units Taq in a total volume of 50μl.

Cycling was performed using a Biometra thermocycler. A typical reaction consisted of an initial denaturation at 94°C for 2 minutes followed by 25- 30 cycles of denaturation (94°C), annealing (variable depending on the primers in use) and elongation (72°C, 1 minute per kb). A final elongation step of 10 minutes was followed by cooling to 4°C before analysis of the products by agarose gel electrophoresis.

2.5 Southern Blotting

2.5.1 DNA digests and gel electrophoresis

Approximately 5μg DNA was digested with 10 units of restriction enzyme (NEB), in the correct restriction buffer, in a total reaction volume of 20μl. Digestion was carried out overnight. The entire digest was run on a 0.8% (w/v) agarose gel at 75V for 6 hours.

2.5.2 Blotting to nylon membrane

The gel was briefly rinsed in distilled water to remove any residual TBE. The gel was then denatured by incubation, with gentle agitation, in 1.5M NaCl; 0.5M NaOH for 30 minutes at room temperature. Following a brief rinse in water, the gel was neutralised by incubation in 1.5M NaCl; 0.5M Tris-HCl pH 7.2; 1mM EDTA for 30 minutes at room temperature. To transfer the DNA to nylon membrane a large tray was filled with 10x SSC and a plastic plate was placed over the tray. A piece of 3MM paper was soaked in SSC and placed over the plate so that each end rested in the SSC in the tray. The gel then was placed onto the 3MM paper and a piece of nylon membrane was positioned on top of the gel. More pre-soaked 3MM paper and paper towels were piled on top of the membrane and weighed down. Following overnight incubation, during which the DNA transferred to the membrane by capillary action, the membrane was rinsed briefly in 2x SSC and the DNA was cross-linked to the membrane using a UV Stratalinker 2400 (Stratgene).

2.5.3 Preparation of probe

The DNA fragments to be used as probes were cut using the appropriate restriction enzymes and gel purified. 10µl DNA and 6µl water were heated to 100°C for 10 minutes. 4µl DIG High Probe reagent (Roche) was added and the mixture was incubated at 37°C overnight. The enzymatic reaction was inactivated by the addition of 2µl 0.2M EDTA and incubation at 65°C for 10 minutes. Immediately prior to use probes were denatured by incubation at 100°C for 5 minutes.

2.5.4 Hybridisation of probe to membrane and detection

The membrane was incubated in 20ml of pre-warmed prehybridisation buffer (DIG Easy Hyb (Roche)) for at least 30 minutes at 50°C with gentle agitation. The buffer was discarded and replaced with 3.5ml pre-warmed DIG Easy Hyb containing 2µl DIG-labelled probe. The membrane and probe were incubated together, with gentle agitation, at 50°C overnight. The membrane was then washed twice with 2x SSC; 0.1% (w/v) SDS at room temperature and briefly rinsed in 100ml washing buffer (0.1M Maleic acid; 0.15M NaCl; 0.3% (v/v) Tween 20 pH 7.5). Blocking was carried out at room temperature using 100ml blocking buffer (Blocking solution (Roche) in 0.1M Maleic acid, 0.15M NaCl pH 7.5) for 30 minutes with constant agitation. The membrane was then incubated in 20ml antibody solution (anti-DIG-AP conjugate diluted 1:10,000 in blocking solution) for 30 minutes at room temperature. Following two 15 minute washes in washing buffer the membrane was transferred to a hybridisation bag and equilibrated for 5 minutes in 20ml detection buffer (0.1M Tris-HCl; 0.1M NaCl pH 9.5). The equilibration buffer was discarded and replaced with 2ml CSPD (Disodium 3-(4-metho xyspiro {1,2-dioxetane-3,2-(5-chloro)tricyclo [3.3.1.1^{3},7]decan}-4-yl)phenyl phosphate), a chemiluminescent substrate of alkaline phosphatase (Roche), diluted 1 in 100 in detection buffer. The membrane was incubated with the CSPD for 5 minutes after which it was rinsed in detection buffer, sealed in a hybridisation bag and incubated for 10 minutes at 37°C. The membrane was then exposed to Lumi-Film chemiluminescent Detection film (Roche) at room temperature.

2.5.5 Stripping blots

In order to remove the labelled probe and allow hybridisation of a second probe to the same blot the membrane was rinsed thoroughly in distilled water; washed twice in 0.2M NaOH, 0.1% (w/v) SDS for 15 minutes at 37°C and rinsed twice in 2x SSC.

2.6 Tissue Culture Techniques

2.6.1 Maintenance of cell lines

2.6.1.1 Tissue culture media

Cell lines were maintained at 37°C, 5% CO_2 in the appropriate medium as indicated below;

Cell Line	Medium	Supplements
BHK-21	Glasgows	10% NBCS 2mM L-glutamine 60µg/ml pen/strep 50ml tryptose phosphate broth
BCBL-1	RPMI	20% FBS 2mM L-glutamine 60µg/ml pen/strep
BCP-1	RPMI	As BCBL-1
NS0	RPMI	As BCBL-1
C127	DMEM	10% FBS 2mM L-glutamine 60µg/ml pen/strep

HEK 293	DMEM	10% FBS 2mM L-glutamine 60μg/ml pen/strep

2.6.1.2 Passaging adherent cell lines

The medium was removed from cell monolayers. The cells were then washed with versene prior to incubation in a small volume of trypsin-EDTA (0.05% v/v; Gibco) at 37°C until the cells became detached from the plastic. Fresh medium was added, to neutralise the trypsin-EDTA, and the cells were transferred to a 50ml falcon tube. The cells were pelleted by centrifugation at 1,000g for 7 minutes; the supernatant was removed and the cells were resuspended in fresh growth medium. An appropriate dilution of cells was then used to seed a new tissue culture flask.

2.6.1.3 Removal of dead cells by Histopaque-1077 separation

Dead cells were removed from cultures of suspension cells by Ficoll separation. Cells were layered onto approximately 10ml Histopaque-1077 (Sigma) in 50ml falcon tubes. Following centrifugation at 1,500g for 20 minutes dead cells are pelleted and viable cells remain at the Histopaque/ medium interface. Viable cells were transferred to a clean universal and 10ml SPBS was added to dilute the Histopaque. The cells were pelleted by centrifugation at 1,000g for 7 minutes; resuspended in an appropriate volume of medium and transferred to a new tissue culture flask.

2.6.2 Transfection of tissue culture cell lines

2.6.2.1 Effectene

BHK cells were transfected with plasmid DNA using Effectene Transfection reagent (Qiagen). Cells were seeded (typically $4x10^5$ cells/well in a 6 well plate) the day before transfection to reach approximately 70% confluence. 1μg DNA per well was made up to 150μl total volume with buffer EC (DNA condensation buffer). Following addition of 8μl Enhancer, the mixture was vortexed briefly and incubated at room temperature for 5 minutes. 25μl of Effectene reagent were then added to the DNA mix and vortexed for 10 seconds. The samples were incubated at room temperature for 10 minutes. During incubation the cells to be transfected were washed in SPBS and 4ml fresh medium was added. 1ml medium was added to the Effectene-DNA complexes, mixed by pipetting and added to the cells drop-wise. Cells were then incubated at 37°C, 5% CO_2.

2.6.2.2 Electroporation

BHK cells were trypsinised, washed and resuspended in PBS at a concentration of $1x10^7$ cells/ml. A 200μl aliquot (i.e. $2x10^6$ cells) was placed in a 4mm electroporation cuvette (Biorad). 10μg plasmid DNA was added to the cells and mixed gently. Following a brief incubation on ice the cells were electroporated using an Equibio Easyject Plus electroporator;

Pulse 1 600V, 25μF, 99Ω

Pulse 2 250V, 1050μF, 99Ω

0.1 second delay between pulses.

Cells were then added to 10ml of fresh medium in a universal and seeded into a 6 well plate at 5ml/well. Cells were incubated at 37°C, 5% CO_2.

2.6.3 Preparation of S10 cytoplasmic protein extract

BCP-1 or BCBL-1 cells were counted in a haemocytometer and 10^8 cells were pelleted by centrifugation at 1,200rpm for 7 minutes. Cells were then washed 3 times in isotonic buffer (35mM Hepes pH 7.4; 146mM NaCl; 11mM glucose) by resuspension and centrifugation. The cell pellet was then resuspended in 2 volumes hypotonic buffer (20mM Hepes pH 7.4; 10mM KCl; 1.5mM Mg Acetate; 1mM DTT) and incubated on ice for 10 minutes. Cells were broken open by 25 strokes of dounce homogenisation on ice. Subsequently 0.1 volumes of 10x buffer (0.2M Hepes pH 7.4; 1.2M K Acetate; 40mM Mg Acetate; 50mM DTT) were added and the nuclei removed by centrifugation at 2,000rpm for 10 minutes at 4°C. The supernatant was removed and centrifuged at 10,000rpm for 15 minutes at 4°C. The supernatant was removed and 0.01 volumes 100mM $CaCl_2$ and 75U/ml S7 nuclease (Roche) were added. Following 15 minutes incubation at 20°C the nuclease was inactivated by addition of EGTA to a final concentration of 2mM. The S10 supernatant was then centrifuged at 10,000rpm for 15 minutes at 4°C and small aliquots stored at -80°C.

2.6.4 Preparation of nuclear protein extract

$1x10^7$ cells were harvested by centrifugation and resuspended in 1ml PBS. Following transfer to a 1.5ml eppendorf the cells were pelleted by centrifugation at 500g, 4°C for 5 minutes. The S/N was removed and the cells were washed in 100µl sucrose buffer (0.32M sucrose; 10mM Tris HCl pH 8.0; 3mM $CaCl_2$; 2mM MgOAc; 0.1mM EDTA; 0.5% (v/v) NP-40; 1mM DTT and 0.5mM mammalian protease inhibitors were added immediately prior to use) by gentle resuspension followed by

centrifugation at 500g, 4°C for 5 minutes. The supernatant, containing the cytoplasmic protein fraction, was removed. The remaining nuclear pellet was washed in 1ml sucrose buffer (as above, without NP-40) by resuspension followed by centrifugation as before. The wash buffer was removed and the cell nuclei were resuspended in 30µl low salt buffer (20mM HEPES pH 7.9; 1.5mM $MgCl_2$; 20mM KCl; 0.2mM EDTA; 25% (v/v) glycerol; 0.5mM DTT and 0.5mM protease inhibitors were added immediately prior to use) by gentle flicking of the tube. An equal volume of high salt buffer (20mM HEPES pH 7.9; 1.5mM $MgCl_2$; 800mM KCl; 0.2mM EDTA; 25% (v/v) glycerol; 1% (v/v) NP-40; 0.5mM DTT and 0.5mM protease inhibitors added immediately prior to use) was then added very slowly whilst constantly agitating the tube. The samples were incubated for 40 minutes on a rotating wheel at 4°C and then the debris was pelleted by centrifugation at 14,000g for 15 minutes at 4°C. The nuclear protein extract was stored at -80°C.

2.6.5 Preparation of cytospins

Cells were counted and resuspended in PBS at a concentration of $1x10^6$ cells/ml. 50µl aliquots were spun onto poly-lysine coated microscope slides (BDH) at 1,000g for 3 minutes. Cells were then fixed by incubation in 4% paraformaldehyde in PBS for 30 minutes at room temperature and stained as appropriate.

2.7 Recombinant Virus Techniques

2.7.1 Purification of recombinant virus

A total of $1.25x10^6$ BHK cells were transfected with 10-20μg linearised plasmid DNA and ~5μg MHV-76 DNA by electroporation. The cells were added to 10ml of fresh medium and plated into 6 well plates at 5ml/ well. The plates were incubated at 37°C, 5% CO_2, and monitored for plaque formation and, if appropriate, GFP expression. Once obvious plaques had formed, generally after 4-5 days, 4ml of medium was removed from each well and discarded. The cells were then scraped into the remaining medium and transferred to a 1.5ml eppendorf. Following three freeze-thaw cycles the cell debris was pelleted by centrifugation and the supernatant, containing the virus, was stored in cryovials at -80°C.

Recombinant viruses were then purified by plaque purification in 96 well plates. BHKs were seeded at $5x10^3$ cells per well and incubated overnight. Dilutions of the virus stock were made in Glasgows medium and 10μl added per well. After 1 hour incubation at 37°C 200μl of medium, containing 100μg/ml hygromycin if appropriate, were added to each well. The plates were incubated for 4-5 days or until plaques had formed. The lowest dilution yielding plaques was harvested by scraping the cells into the medium. A 100μl aliquot was subjected to three rounds of freeze-thawing to give a virus stock. Viral DNA was prepared from the remainder; the samples were pelleted, the supernatant was removed and the pellet was resuspended in 50μl TE (20mM Tris, pH 8; 1mM EDTA). One freeze-thaw cycle was then carried out. 1μl (0.05U) Proteinase K (Roche) was added to the samples which were then incubated at 55°C overnight. The Proteinase K was inactivated by heating to 90°C. The extracted DNA was subsequently used in PCR reactions to screen for presence of the insert and wild type virus. Plaque purification was continued until there appeared to be no wild type virus in the samples.

2.7.2 Preparation of virus stock

BHK cells were resuspended in Glasgows medium at 10^7/ml and infected with virus at a multiplicity of infection (moi) of 0.001. Cells were incubated, with shaking, at 37°C for 1 hour then seeded into 175cm^2 tissue culture flasks at $3x10^6$ cells/ flask. The flasks were checked daily until C.P.E. was reached. Any cells still attached to the flask were scraped into the medium, which was then dispensed into 50ml falcon tubes. The cells were pelleted by centrifugation at 2,500rpm, 4°C, for 20 minutes and the pellet was resuspended in the smallest possible volume of SPBS. The pellet was homogenised by 30 strokes with a Dounce. Following transfer to a glass universal the cells were sonicated in an ice bath for 15 minutes. The resulting suspension was centrifuged at 2,500rpm, 4°C for 20 minutes and the supernatant was stored on ice. The pellet was resuspended in 1ml SPBS and another 30 strokes of the Dounce were carried out. This suspension underwent centrifugation at 2,500rpm, 4°C for 20 minutes after which the two supernatants were pooled. Aliquots were stored at -80°C.

2.7.3 Virus DNA preparation

BHK cells were resuspended in Glasgows medium at 10^7 cells/ml and infected with virus at an moi of 0.1 pfu/cell. Cells were incubated, with shaking, at 37°C for 1 hour and seeded into 175cm^2 tissue culture flasks at $5x10^6$ cells/ flask. Flasks were incubated at 37°C, 5% CO_2 until complete C.P.E. was reached. Cells were scraped into the medium, which was then decanted into 50ml falcon tubes. The cells were pelleted by centrifugation at 2,500rpm, 4°C for 20 minutes and resuspended in at total volume of 1ml SPBS. The pellet was homogenised by 30 strokes with a dounce

and transferred to a universal. Following centrifugation at 2,500rpm, 4°C, for 30 minutes the supernatant was removed and stored on ice and the pellet was resuspended in 1ml SPBS. The pellet was re-homogenised and centrifuged as before. The two supernatants were pooled and 1µl RNase A (1mg/ml) was added. The supernatants were incubated at 37°C for 1 hour. An equal volume of High Molecular Weight DNA extraction buffer (0.1M EDTA; 0.5% (w/v) SDS; 0.2M TRIS pH 8; 100µg/ml proteinase k (Roche)) was added and the supernatant was incubated overnight at 55°C. The supernatant was transferred to a 15ml falcon tube and the DNA extracted twice with phenol: chloroform: isoamyl alcohol (25:24:1 ratio) (Sigma) and twice with chloroform (Sigma). The viral DNA was precipitated by addition of 0.3 volumes 7.5M ammonium acetate and 2.5 volumes 96% (v/v) ethanol and centrifugation for 30 minutes at 8,000rpm, 4°C. The DNA pellet was rinsed in 70% (v/v) ethanol and resuspended in TE pH8.

2.7.4 Virus titration

Virus samples were thawed at 37°C and 10 fold dilutions were made in Glasgows medium each with a volume of 4ml. $2x10^6$ BHK cells were added to each dilution. Following incubation for 1 hour at 37°C, with shaking, each dilution was plated into two 60mm Petri dishes containing 3ml Glasgows medium i.e. 2ml dilution/ dish. Cells were incubated at 37°C, 5% CO_2 for 4 days and then fixed in 4% (w/v) neutral buffered formal saline. Plates were stained with 0.1% (w/v) toluidine blue. Plaques were counted and the titre calculated as follows;

$$\text{Titre} = \frac{\text{no.of plaques x dilution}}{\text{volume of sample}}$$

2.7.5 One-step growth curve

$5x10^6$ BHK cells were infected with virus at an m.o.i. of 5 pfu per cell in a total volume of 25ml Glasgow's by shaking at 37°C for 1 hour. Following adsorption the cells were washed three times with 15ml Glasgow's by centrifugation and then resuspended to a final volume of 25ml. Cells were aliquoted into a 24 well plate at $2x10^5$ cells per well (i.e. 1ml). Samples were harvested at the appropriate time points, typically 0, 4, 8, 12, 18, 24, 30, 36, 48, 60 and 72 hours post infection, by scraping the cells into the medium with a 1000µl Gilson tip and storing them at -80°C. Once all time points were complete virus was released from the cells by freeze-thawing three times. Samples were titrated as described elsewhere.

2.7.6 Multi-step growth curve

The multistep growth curve carried out to assess cell-to-cell spread of the virus was carried out mainly as described above with the exception that $1x10^5$ BHK cells per well were infected at a m.o.i. of 0.01 pfu/cell. Typical time points at which cells were harvested were 0, 12, 24, 36, 48, 72, 96, 120 and 144 hours post infection.

2.7.7 Infection of mice

All procedures were carried out in the Summerhall animal unit under the home office project licence 60/2429 and personal licence 60/8831.

Mice were anaesthetised with halothane and infected intranasally with $4x10^5$ pfu virus diluted in 40µl SPBS. At appropriate time points, mice were euthanised by CO_2 inhalation.

2.7.8 Infective centre assay

Spleens were removed from mice and placed into 5ml of RPMI supplemented with 10% (v/v) FBS; 2mM L-glutamine; 60μg/ml pen/strep; fungizone; β-mercaptoethanol; 25mM Hepes, in a Petri dish. The end of the spleen was cut with a scalpel and the spleen cells gently squeezed out. The contents of the Petri dish were transferred to a universal. 5ml medium was added to the Petri dish, to rinse off the remaining spleen cells, and this was then added to the universal. The cells were centrifuged at 1,800rpm for 5minutes at 4°C. The supernatant was removed and the pellet was resuspended by tapping. 1ml of sterile water was added to the cells followed immediately by 8ml SPBS. Having allowed the red cell ghosts to settle the remaining cells were transferred to a clean universal and centrifuged at 1,800rpm for 5 minutes at 4°C. The supernatant was removed and the cells resuspended in 5ml medium. Cells were counted using a heamocytometer.

60mm Petri dishes were prepared containing 5ml medium and $2x10^6$ BHK cells. Spleen cells were added to the dishes at 10^{-1}, 10^{-2} and 10^{-3} dilutions (i.e. 500μl, 50μl, 5μl). Petri dishes were then incubated at 37°C, 5% CO_2 for 5 days. Following incubation the medium was removed and the cells were fixed with 4% (w/v) neutral buffered saline and stained with 0.1% (w/v) toluidine blue. Plaques were counted and the number of infectious centres was calculated per 10^7 spleen cells.

2.7.9 Virus titration of lung homogenate

Lungs were removed from mice and stored at -80°C, in cryovials, until titrations were carried out.

Lungs were homogenised in 1ml Glasgow's and the resulting suspension was placed in a cryovial. The remaining lung was re-homogenised in 0.8ml Glasgow's and then

pooled with the first suspension. The suspension was then frozen at -80°C for at least 1 hour. The lung homogenate was thawed and centrifuged at 3,000rpm for 5minutes at 4°C to sediment cellular debris. The supernatant was serially diluted to give a range of 10^{-1} to 10^{-6} each in a total volume of 4ml Glasgows. $2x10^6$ BHK cells were added to each dilution and the samples were then incubated, with shaking, at 37°C for 1 hour. 2ml of each dilution was added to two 60mm Petri dishes containing 3ml Glasgows. Following incubation at 37°C, 5% CO_2 for 4 days the cells were fixed with 4% (w/v) neutral buffered saline and stained with 0.1% (w/v) toluidine blue. The plaques were counted and the titre of each sample determined.

2.7.10 DNA extraction from snap-frozen tissue

Tissues were removed from mice, placed in cryovials and snap-frozen in liquid nitrogen. DNA was extracted from tissue samples using the QIAamp DNA Mini Kit (Qiagen) as described by the manufacturer. Briefly, tissue samples were thawed to room temperature and a section of <25mg (<10mg spleen) removed. This section was cut into small pieces, with a clean scalpel, and placed into a 1.5ml microcentrifuge tube. 180µl buffer ATL and 20µl Proteinase K (600U/ml) were added. Samples were incubated overnight at 56°C, with occasional vortexing, to allow complete lysing of the tissue. 200µl buffer AL were added to each sample and mixed by vortexing followed by 10 minutes incubation at 70°C. 200µl high-grade ethanol was added to each sample and mixed by vortexing. The mixture was then added to a QIAamp spin column which was subsequently centrifuged at 6, 000g for 1 minute. 500µl Buffer AW1 was added and the column was centrifuged again. 500µl Buffer AW2 was added to the column which was then centrifuged at 20, 000g for 3 minutes. The column was placed in a clean 1.5ml microcentrifuge tube and the DNA

eluted in 200µl Buffer AE by centrifugation at 6, 000g for 1 minute. The elution step was then repeated. DNA concentrations were determined by spectrometry.

2.7.11 NS0 growth curve

NS0 cells were infected at an m.o.i. of 5 pfu/cell by shaking at 37°C for 2 hours. Cells were then aliquoted into 24 well plates at $1x10^5$ cells/ well. Plates were incubated at 37°C, 5% CO_2. Throughout the course of the assay cells were monitored and fed as necessary. At each time point the cell proliferation, lytic virus titre, cell-associated virus titre and latent titre was assessed. The levels of virus within the supernatant were assayed by titrating the S/N from 1ml of cells. To assay cell-associated virus titre 1ml cells were pelleted and washed x3 with SPBS. The cells were resuspended in 1ml SPBS and titrated on BHK cells. Latent virus titre was calculated by lysing washed cells through repeated freeze-thaw cycles, and titration of the resultant lysate to calculate the amount of infectious virus that has remained cell-associated. This figure was then subtracted from the infectious centre titre to give the latent virus titre. In all cases plates were incubated for 5 days prior to being fixed in 4% (w/v) neutral buffered formal saline and stained with 0.1% (w/v) toluidine blue.

Plaques were then counted and the viral titre per 10^5 cells calculated.

2.8 Northern Blotting

All procedures were carried out using RNase free solutions (prepared by addition of 1ml diethyl pyrocarbonate per litre of solution, overnight incubation with stirring at room temperature and deactivation by autoclaving) and equipment, which had been

cleaned of contaminating RNase by treatment with either 5M NaOH or RNaseZap (Ambion).

2.8.1 RNA extraction from virus infected cells

$2x10^6$ C127 cells were infected at an m.o.i. of 5 with virus, seeded into T75 tissue culture flasks (Nunc) and incubated at 37°C, 5% CO_2 until CPE was reached (usually 3 days p.i.). Cells were then scraped into the medium, decanted into universals and pelleted by centrifugation at 1,000g for 7 minutes. Total RNA was extracted from the cells using the RNeasy Mini Kit (Qiagen). Briefly, cells were disrupted by addition of 600µl buffer RLT (containing guanidinium thiocyanate; 1% (v/v) β–mercaptoethanol) and vortexing. The sample was then homogenised using a QIAshredder spin column (Qiagen). 600µl 70% (v/v) ethanol was added to the homogenised sample and mixed thoroughly prior to application to an RNeasy mini column. Following centrifugation at 10,000g for 15 seconds, 700µl buffer RW1 (containing guanidinium thiocyanate and ethanol) was added and the column was centrifuged again. The column was washed twice with 500µl buffer RPE (containing 80% (v/v) ethanol) by centrifugation. RNA was eluted from the column with 50µl RNase free H_2O.

2.8.2 Estimation of RNA concentration

The concentration of RNA was quantified using a Genequant II spectrophotometer (Pharmacia Biotech). Water was used to zero the machine. The OD_{260} of the RNA was measured and the concentration estimated using the following formula:

RNA concentration (µg/ml) = OD_{260} x dilution factor x 40.

2.8.3 Denaturing RNA and electrophoresis

RNA samples were added to 5x RNA loading buffer (0.25% bromophenol blue; 4mM EDTA; 0.9M formaldehyde; 20% (v/v) glycerol; 30.1% (v/v) formamide; 80mM MOPS; 20mM Na acetate) at a 4:1 ratio. The RNA secondary structure was denatured by incubation at 65°C for 5 minutes followed by rapid cooling on ice. The RNA samples were loaded onto a formaldehyde agarose gel (1% (w/v) agarose in 20mM MOPS; 5mM Na acetate; 1mM EDTA; pH 7.0) to which 10μg ethidium bromide and 0.67% (v/v) formaldehyde were added once the gel had cooled to 65°C. Once the gel had set, the tank was filled with running buffer (20mM MOPS; 5mM Na acetate; 1mM EDTA; 2.5M Formaldehyde) and equilibrated by running at 100V for 30 minutes after which the samples were loaded. The gel was run overnight at 25V with the buffer being re-circulated through the apparatus continuously.

2.8.4 Blotting onto nylon membranes

The gel was washed in 200ml RNase free water for 10 minutes followed by 15 minutes incubation in 0.05M NaOH. The NaOH was then neutralised by a 10 minute incubation in 10x SSC. The gel was placed onto filter paper, laid over a glass plate, each end of which was immersed in a tank containing 20x SSC. A piece of nylon membrane (Amersham) and 2 pieces of 3MM paper pre-soaked in 20x SSC were placed on top of the gel followed by a stack of paper towels and finally a 1kg weight. The RNA was allowed to transfer to the membrane by capillary action overnight.

2.8.5 Preparation of probes

DNA complimentary to the RNA sequence to be detected was amplified by PCR. 50ng of probe DNA was made up to 45µl volume in TE buffer and denatured by incubating at 100°C for 2 minutes followed by immediate cooling on ice. The DNA was added to a Ready-to-Go DNA labelling bead (Amersham) and the bead was allowed to dissolve. Approximately 50µCi α-^{32}P dCTP were added and the DNA was incubated at 37°C for 25 minutes. The DNA was then denatured by incubation at 100°C for 2 minutes and unincorporated nucleotides were removed using a G-25 spin column (Amersham).

2.8.6 Hybridisation and detection

The blot was transferred to a hybridisation tube and incubated with 6ml Ultrahyb (Ambion), which had been warmed to 68°C, for 30 minutes at 42°C with constant gentle agitation. After 30 minutes approximately 1/3 of the labelled probe was added to the hybridisation tube and the blot was hybridised overnight at 42°C. Following hybridisation the Ultrahyb containing the probe was discarded and the blot was washed twice for 5 minutes in 2x SSC, 0.1% (w/v) SDS and then twice for 15 minutes in 0.1x SSC, 0.1% (w/v) SDS, all washes at 42°C. Blots were then covered in clingfilm and exposed to Lumi-Film Chemiluminescent Detection film (Roche).

2.8.7 Stripping blots

The blot was placed into a hybridisation tube to which boiling 0.1% (w/v) SDS was added. Once cooled, the blot was washed with 2x SSC.

2.9 Protein Techniques

2.9.1 Protein purification

2.9.1.1 Purification of GST fusion protein

An overnight culture of bacteria transformed with pGEX4T-1 vFLIP was diluted 1 in 50 into 200ml LB-carb and incubated, shaking at 37°C, until the OD_{600} reached 0.6. IPTG was then added to a final concentration of 0.1mM and the bacteria incubated for a further 2- 4 hours. Cells were pelleted by centrifugation at 5,000g for 15 minutes. The supernatant was removed and the pellet resuspended in 10ml ice-cold SPBS to which protease inhibitor cocktail set 2 (1:100 dilution; Sigma) had been added. The cells were lysed by sonication on ice. Triton X-100 was then added to a final concentration of 1% (v/v) and the extract was mixed for 30 minutes at 4°C followed by centrifugation at 12,000g for 10 minutes at 4°C. The supernatant was stored at 4°C.

100µl Glutathione Sepharose 4B (Pharmacia Biotech) was washed twice with 1ml PBS, by centrifugation at 500g, then diluted 1:1 in PBS to give a 50% slurry. The slurry was added to the sonicate prepared previously and incubated, with mixing, at 4°C overnight. Following incubation the slurry, with bound fusion protein, was washed three times in 1ml PBS by centrifugation at 500g. vFLIP was removed from the column by thrombin cleavage, leaving the GST moiety bound to the sepharose. 1µl thrombin solution (1 cleavage unit) was added to 95µl PBS and the sepharose was then incubated in this solution overnight, with gentle mixing, at room temperature. The sepharose was pelleted by centrifugation at 500g for 5 minutes and the eluate, containing vFLIP, was removed and stored at -20°C. GST was removed from the sepharose by elution with 100µl glutathione elution buffer (10mM reduced glutathione; 50mM Tris-HCl, pH8; Pharmacia Biotech).

2.9.1.2 Purification of Histidine-tagged protein

An overnight culture of *E.coli* transformed with pTrc His vFLIP was diluted 1 in 50 into 200ml LB-carbenicillin (100μg/ml) and incubated with shaking at 37°C, until the OD_{600} reached 0.6 at which point IPTG was added to a final concentration of 0.1mM. The culture was incubated for a further 2 hours before being dispensed into 50ml aliquots. Each aliquot was pelleted by centrifugation at 5,000g for 10 minutes, the supernatant removed and the pellet stored at -20°C.

Prior to purification the bacterial pellet was thawed and lysed by incubation with 1.25ml BugBuster Protein Extraction Reagent (Novagen) supplemented with 25 units Benzonase Nuclease; 1kU recombinant lysozyme (Novagen) and 12.5μl EDTA-free protease inhibitor cocktail set III (Calbiochem). Following 15 minutes incubation at room temperature the mixture was centrifuged at 10,000g for 20 minutes at 4°C and the soluble protein extract decanted to a clean tube.

1ml HIS-Select HC Nickel Affinity Gel (Sigma) was aliquoted into a falcon tube and centrifuged at 5,000g for 3 minutes to pellet the gel. The supernatant was discarded and the gel was washed twice in 10ml de-ionised water and three times in 10ml equilibration buffer (50mM sodium phosphate, pH 8.0; 0.3M sodium chloride) by resuspension and centrifugation. After the final wash the solubilised protein extract, prepared previously, was added to the pelleted affinity gel and this was then mixed gently at room temperature for 30 minutes. The affinity gel was pelleted by centrifugation and the supernatant, containing unbound protein, was removed. The affinity gel was washed three times with 10ml equilibration buffer. The bound protein was eluted from the gel by the addition of 2 gel volumes elution buffer (50mM sodium phosphate, pH 8.0; 0.3M sodium chloride; 250mM imidazole),

incubation, with gentle mixing, for 15 minutes at room temperature and pelleting of the affinity gel. The supernatant, containing the eluted protein was removed and stored at -20°C.

2.9.2 Concentrating proteins

2.9.2.1 Protein precipitation

Following elution from the Ni- agarose, proteins were concentrated by precipitation. 0.1 volumes of 1% (w/v) sodium deoxycholate (Sigma) solution were added to the eluted protein and mixed thoroughly by pipetting. Following 15 minutes incubation, at room temperature, 0.22 volumes of 50% (w/v) trichloroacetic acid (BDH) solution was added and mixed by pipetting. The mixture was incubated, rotating, for 2 hours at 4°C. The mixture was centrifuged at 20,000g for 20 minutes at 4°C and the supernatant carefully removed. 500µl of ice-cold acetone (BDH) were added to the pellet, which was resuspended by gentle pipetting. Following incubation at -20°C for 30 minutes the sample was centrifuged as before. The supernatant was removed carefully and the pellet allowed to air dry before being resuspended in SPBS.

2.9.2.2 Spin columns

Purified protein was concentrated using VIVASPIN columns with a 10,000 Molecular weight cut-off membrane (Vivascience). Samples to be concentrated (2-4ml volume) were loaded into the column, which was then centrifuged at 5,000g, 20°C for 7 minutes. Concentrated samples were stored at -20°C prior to analysis by western blot or silver stain.

2.9.3 SDS-PAGE

Proteins were separated by SDS-PAGE prior to visualisation by either Western blotting or direct protein staining. Both self-poured and pre-cast gels were used with the particular percentage being dependent upon the size of the protein of interest.

In the case of self-poured gels, protein samples were made up to a total volume of 20µl with 5x loading buffer (50% (v/v) glycerol; 1% (v/v) SDS; 20mM Tris pH 6.8; 0.5% (w/v) bromophenol blue. 35µl/ml β-mercaptoethanol were added immediately prior to use). Samples were boiled for 5 minutes before loading onto the gel (resolving gel: *x*ml 40% acrlamide/bisacrylamide; 0.5M Tris pH 8.8; 0.2% (v/v) SDS; 0.1% (w/v) ammonium persulphate (APS); 0.01% (v/v) TEMED. Stacking gel: 3.2% (v/v) acrylamide/bisacrylamide; 80mM Tris pH 6.8; 0.2% (v/v) SDS; 0.1% (w/v) APS; 0.015% (v/v) TEMED). Gels were run at 300mA each in running buffer (25mM Tris; 192mM glycine; 0.1% (v/v) SDS).

Pre-cast gels were obtained from Invitrogen and used as instructed by the manufacturer.

2.9.4 Coomassie staining

Gels were incubated in Brilliant Blue R concentrate (Sigma: 0.25% (w/v) Brilliant Blue R; 40% (v/v) methanol; 7% (v/v) acetic acid) with shaking for at least 1 hour. After a brief rinse with de-stain (50% (v/v) methanol; 10% (v/v) acetic acid) gels were incubated in de-stain until bands were clear.

2.9.5 Silver staining

Gels were fixed in 45% (v/v) ethanol, 35% (v/v) glacial acetic acid for 20 minutes followed by a 10 minute wash in 10% (v/v) ethanol. Following three 10 minute washes in de-ionised water gels were incubated in Farmers reagent reducer (0.3% (w/v) sodium thiosulphate; 0.15% (w/v) potassium ferricyanide; 0.05% (w/v) sodium carbonate) for 1 minute. Gels were washed three times in de-ionised water and incubated in 0.1% (w/v) $AgNO_3$ for 30 minutes. After a brief rinse in de-ionised water, gels were developed in 2.5% (w/v) Na_2CO_3, 0.05% (v/v) formaldehyde until bands were of the desired intensity. Gels were stored in 30% (v/v) methanol, 10% (v/v) glacial acetic acid.

2.9.6 Western blotting

Generally, proteins were transferred to nitrocellulose membrane in transfer buffer (25mM Tris; 192mM glycine; 20% (v/v) methanol) at 30mA for at least 1 hour. The membrane was air dried and then incubated in blocking buffer (1xPBS; 1% (w/v) BSA; 0.05% (v/v) Tween 20) for 30 minutes at room temperature. The primary antibody was diluted appropriately in blocking buffer and incubated with the membrane for at least 1 hour at room temperature with gentle agitation. The membrane was rinsed three times with PBS. Alkaline Phosphatase conjugated secondary antibody (Sigma) was diluted 1/ 2,500 in blocking buffer and incubated with the membrane for 1 hour at room temperature with gentle agitation. The membrane was rinsed three times in PBS and allowed to dry. A NBT/BCIP tablet (Roche) was dissolved in 10ml water and poured onto the membrane. Once bands had reached the desired intensity the membrane was rinsed with distilled water and allowed to dry.

2.9.7 Pull down assay

The pull down assay was adapted from that described by Stassinopoulos and Belsham (Stassinopoulos and Belsham, 2001). The probe sequence was cloned into a pSP64 polyA vector (Promega). 1μg of the plasmid was linearised by *EcoR*I digestion and purified by ethanol precipitation. RNA was transcribed using the SP6 Megascript kit (Ambion) as instructed, briefly, the DNA template was added to 2μl each of ATP, CTP, GTP and UTP (all at 50mM), 2μl 10x reaction buffer and 2μl SP6 polymerase (40U) in a total volume of 20μl RNase free water. The reaction was incubated overnight at 37°C after which the RNA was purified by phenol:chloroform extraction and isopropanol precipitation and resuspended in 10μl RNase free water.

0.5ml Oligo dT Dynabeads (Dynal) were washed twice in 0.5x SSC and once in binding buffer (10mM Tris pH 7.5; 100mM KCl; 2mM $MgCl_2$). The beads were resuspended in 50μl binding buffer and the RNA transcripts added; this was incubated on a rotating wheel for 30 minutes at 4°C. The beads were captured with a magnet and the supernatant removed. Following two washes with 200μl binding buffer the beads were incubated with 20μl S10 extract on a rotating wheel for 60 minutes at 4°C. The beads were captured as before, washed twice in 200μl binding buffer and bound proteins eluted by incubation in 20μl SDS loading buffer for 10 minutes at 4°C.

2.9.8 Electrophoretic mobility shift assay (EMSA)

2.9.8.1 EMSA for the detection of RNA binding proteins

The plasmid DNA template was linearised by restriction digest and ethanol precipitated. RNA was transcribed using the SP6 Megascript kit (Ambion) and

labelled internally with ^{32}P-UTP. The reaction was set up as follows: 0.5µl ATP (50mM); 0.5µl CTP (50mM); 0.5µl GTP (50mM); 25µCi ^{32}P-UTP; 0.5µl RNaseOUT (Invitrogen); 2.5µl 10x reaction buffer; 2µl (40U) SP6 RNA polymerase; H_2O to 25µl. Following overnight incubation at 37°C the RNA was treated with 1U DNase for 10 minutes at 37°C and unincorporated nucleotides were removed using a G-25 spin column (Amersham). The binding reaction was set up as follows: 25,000cpm RNA were incubated with ~6µg BCBL-1 S10 extract, 1U RNaseOUT (Invitrogen) and 0.05µg poly(dI-dT) in a total volume of 20µl binding buffer (20mM HEPES/KOH pH 7.5; 50mM KCl; 10mM $MgCl_2$, 0.1% (v/v) NP40; 5% (v/v) glycerol). Following 20 minutes incubation at room temperature the samples were loaded onto a 5% (w/v) polyacrylamide gel containing 0.5x TBE. The gel was run in 0.5x TBE for 1 hour at 30mA prior to exposure to autoradiography film (Roche) at -80°C.

2.9.8.2 EMSA for the detection of nuclear NF-κB

Oligonucleotides encoding repeats of the NF-κB response element, NFkBfor and NFkBrev, were separately labelled with ^{32}P by the following reaction: 100ng DNA was incubated with 5 units T4 polynucleotide kinase (NEB) and 1.5µl γ-^{32}P-ATP (10mCi/ml stock; Amersham) in a total volume of 20µl, made up with PNK reaction buffer (NEB), for 1 hour at 37°C. Unincorporated nucleotides were removed by passage through G-25 columns (Amersham). The sense and anti-sense oligos were then mixed together and allowed to anneal at room temperature for 10 minutes. Probe was either used immediately or stored at -20°C.

Binding reactions were set up, on ice, as follows: 5μg nuclear protein extract, 2μl 5x binding buffer (50mM Tris pH 8.0; 750mM KCl; 2.5mM EDTA; 0.5% (v/v) Triton-X 100; 62.5% (v/v) glycerol; 1mM DTT), 1μg poly dI-dT and 1μl labelled probe (1:10 dilution). Once all components were added the reaction was incubated at room temperature for 30 minutes. Samples were then loaded onto a 5% (w/v) polyacrylamide gel, containing 0.5x TBE, which was then run at 200V for 90 minutes. Once electrophoresis was complete, the gel was wrapped in Saranwrap and exposed to autoradiography film (Roche) at -20^{0}C.

2.9.9 Isolation of protein from polyacrylamide gel

Reactions were performed as described by Heaton *et al* (Heaton et al., 2001). The binding reaction was carried out as described for EMSA but on a larger scale i.e. 1ml total volume, and using a non-radiolabelled probe. A radiolabelled reaction was used as a marker. Unlabelled complexes were excised at positions indicated by the labelled complexes. Proteins were eluted from the gel by overnight incubation in protein elution buffer (50mM Tris pH 7.9; 0.1mM EDTA, 5mM DTT; 150mM NaCl; 0.1% (v/v) SDS) at room temperature with gentle agitation. Proteins were concentrated using Vivaspin columns.

2.9.10 Raising antiserum against KSHV vFLIP

Following purification and concentration of vFLIP aliquots of protein were sent to Diagnostics Scotland (Edinburgh, EH17 7QT). There a rabbit was immunised and boosted every four weeks for a total of 12 weeks with 100μl (150μg) of vFLIP. The rabbit was bled before immunisation and at monthly intervals before final

exsanguination. Serum samples were dispensed into 1ml aliquots and stored at -20°C.

2.10 Dual Luciferase Reporter Assay

Either $1x10^5$ BCP-1 or $5x10^4$ HEK 293 cells were seeded in 24 well plates overnight. Cells were washed with OptiMEM medium (GibcoBRL) prior to infection at 5pfu/cell in 200µl OptiMEM with vTF7-3 (Fuerst et al., 1986), a recombinant vaccinia virus expressing T7 RNA polymerase, for 1 hour at 37°C. The cells were then washed twice with OptiMEM prior to transfection with 0.5µg of linearised plasmid DNA and 1.5µg Transfast reagent (Promega) according to the manufacturers instructions. The DNA and Transfast reagent were added to 200µl OptiMEM and vortexed rapidly. After a 20 minute incubation at room temperature the transfection mix was added to the cells. 1ml complete medium was added after 1 hour incubation at 37°C, 5% CO_2 and the cells were incubated overnight. The transfected cells were washed twice in SPBS prior to lysis in 200µl Passive Lysis Buffer (Promega). After incubation at room temperature for 15 minutes the lysates were transferred to Eppendorf tubes and snap-frozen on dry ice. The lysates were then thawed and vortexed for 1 minute prior to centrifugation at 10,000g for 1 minute to sediment cell debris. The activities of the *Renilla* and firefly luciferases were assayed using the dual luciferase reporter assay (Promega) according to the manufacturer's instructions. Luciferase activities were determined using a Labsystems benchtop luminometer.

Chapter 3 Construction and utilisation of recombinant MHV-76 expressing KSHV vFLIP to investigate the contribution of vFLIP toward viral pathogenesis *in vivo*

Construction and utilisation of recombinant MHV-76 expressing KSHV vFLIP to investigate the contribution of vFLIP towards viral pathogenesis *in vivo*

The narrow host range of gamma herpesviruses means that assessing the contribution of individual KSHV genes towards viral pathogenesis *in vivo* is difficult. The murine gamma herpesviruses, MHV-68 and MHV-76, represent a potential model system whereby pathogenesis can be investigated and related to specific gene products. As mentioned previously it is possible to manipulate the MHV-68 and -76 genomes. This property has been exploited by a number of groups to create both knock-in and deletion mutants of MHV-68, analysis of which has contributed toward elucidation of the function of a number of MHV-68 genes including M2 (Macrae et al., 2003), M4 (Townsley et al., 2004) and ORF73 (Fowler et al., 2003). The genomes of MHV-76 and KSHV are very similar containing many homologous gene products; however, KSHV possesses some genes which are not represented within MHV-76. It was hypothesised that generation of recombinant MHV-76 viruses that express the unique KSHV genes may provide insights into the *in vivo* function of these genes. MHV-76 does not encode either a vFLIP or an anti-apoptotic product targeting caspase-8 activation. Consequently, recombinant viruses expressing KSHV vFLIP were constructed. It was believed that the degree of homology between the murine and human components of pathways influenced by vFLIP is such as to allow any specific interactions to occur.

3.1 Recombinant virus construction using the CMV IE promoter

The first recombinants to be constructed expressed vFLIP, EGFP and hygromycin resistance (see figure 3.1); their expression was driven by the CMV IE promoter, which is a strong promoter and thus should drive expression of the inserted sequences at a high level. Translation of vFLIP is dependent upon the EMCV IRES; EMCV is a picornavirus and its IRES element is one of the most efficient to be discovered so far. This IRES element has been demonstrated to function efficiently in murine cells (Kim et al., 1992).

KSHV vFLIP was inserted at the left-hand end (LHE) of the MHV-76 genome by homologous recombination. A pure virus population was then isolated by plaque purification and confirmed by PCR and Southern blotting.

The plasmids pAB13 and pAB14 had been constructed previously (Appendix 1b; Brass, 2004). The vOx2 gene was removed by digestion with *Asc*I and *Fse*I followed by gel purification of the vector backbone; this was then S.A.P. treated. KSHV vFLIP was amplified by PCR from BCP-1 DNA using the primers FLIP 76-1 and FLIP 76-2. The resulting product was gel purified, digested with *Asc*I and *Fse*I, and ligated into the vector. Correct insertion of vFLIP was confirmed by restriction digest. The resulting plasmids are termed pFL1 and pFL2. Confirmation that the CMV IE promoter was active was achieved by transfection of 293 cells with both plasmids; high EGFP expression was observed from both plasmids.

The plasmids were linearised by digestion with *Eco*RV and *Pvu*II, which cuts the inserted sequences and MHV-76 LHE from the vector backbone. BHK-21 cells were transfected with linearised plasmid and MHV-76 DNA by electroporation. The cells were divided between two wells of a 6 well plate and incubated for 72 hours.

Subsequent examination of the cells revealed the formation of plaques some of which expressed EGFP. A virus stock was then prepared by freeze-thaw and used to infect BHK-21 cells previously seeded in 96 well plates. Recombinant MHV-76 containing the insert was purified from wild-type virus by four rounds of plaque purification and an agarose overlay. After each round of purification the presence of vFLIP in the viral DNA was confirmed by PCR. Once all plaques expressed EGFP a masterstock of each virus, named FL1 and FL2, was made and viral DNA was prepared. Southern blotting was carried out to confirm that the recombinant viruses contained the insert in the correct location and orientation and were free of wild-type contamination.

3.1.1 Southern blotting

DNA extracted from both recombinant viruses and wild type MHV-76 was subjected to either *Mfe*I or *Nhe*I digestion followed by Southern blotting with two different probes. The expected hybridisation patterns are shown in figure 3.1 and table 3.1. The resulting Southern blots (figures 3.2 and 3.3) confirmed the presence of the inserts, in the correct orientation, and the absence of contaminating wild-type MHV-76. As a further confirmation of purity PCR was carried out for wild-type virus using primers M4B and Trepeat (figure 3.4); this was only positive in the MHV-76 sample.

Virus stocks were made, titred and stored at -80°C.

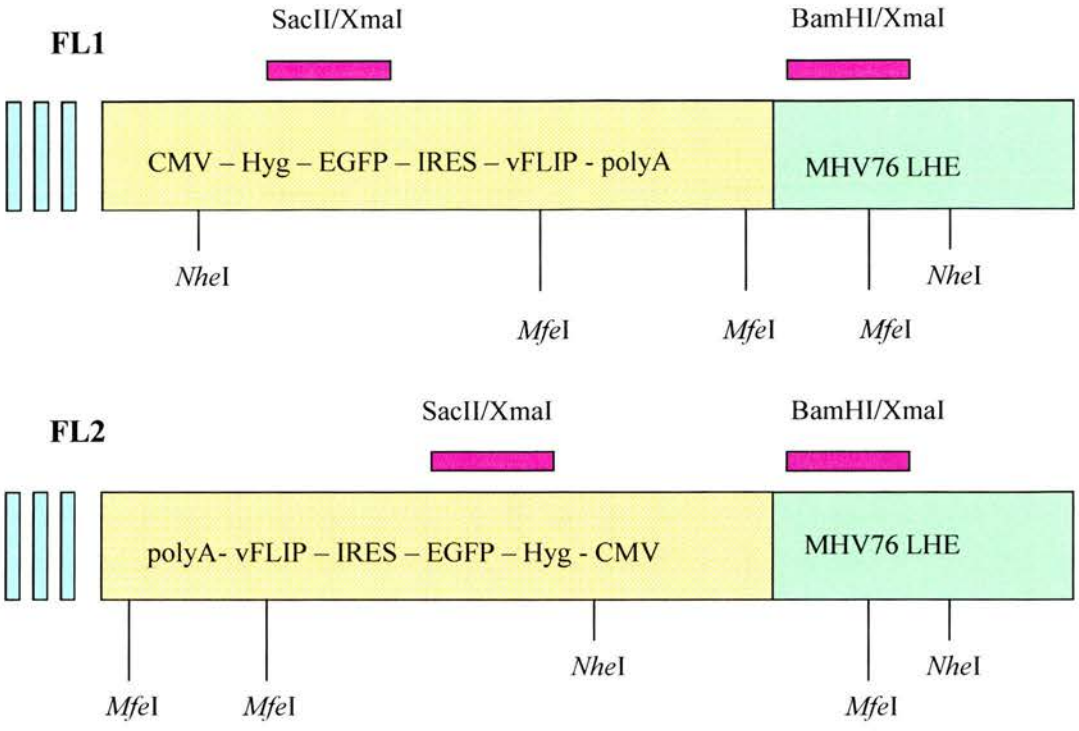

Figure 3.1 Schematic representations of the left hand end sequences of the recombinant viruses FL1 and FL2. The restriction sites used for Southern blot digestions and probe hybridisation locations are indicated.

	FL1		FL2		MHV-76	
	*Nhe*I	*Mfe*I	*Nhe*I	*Mfe*I	*Nhe*I	*Mfe*I
GFP probe	6.17kb	laddering	laddering	4.75kb	-	-
LHE probe	6.17kb	1.15kb	3.9kb	4.75kb	laddering	laddering

Table 3.1 The expected band patterns for FL1 and FL2 Southern blots following either *Nhe*I or *Mfe*I digestion.

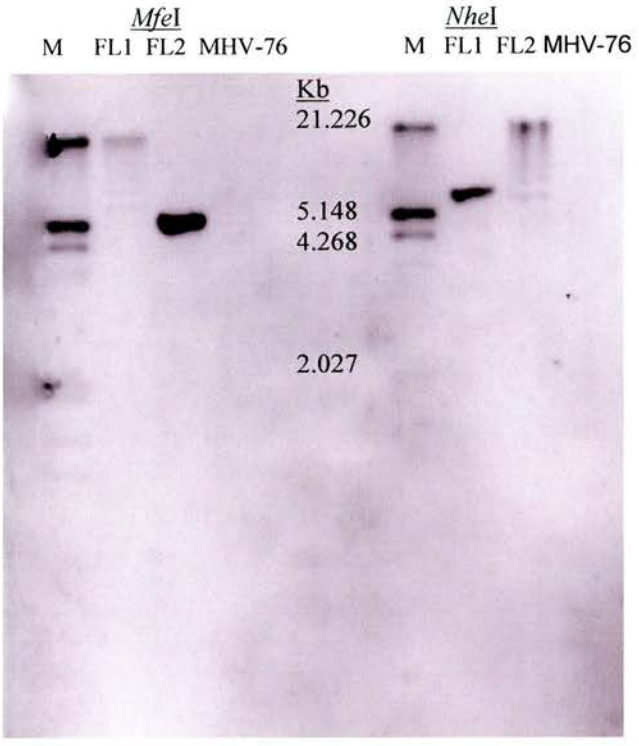

Figure 3.2 Southern blot of digested FL1, FL2 and wild-type MHV-76 DNA using GFP probe.

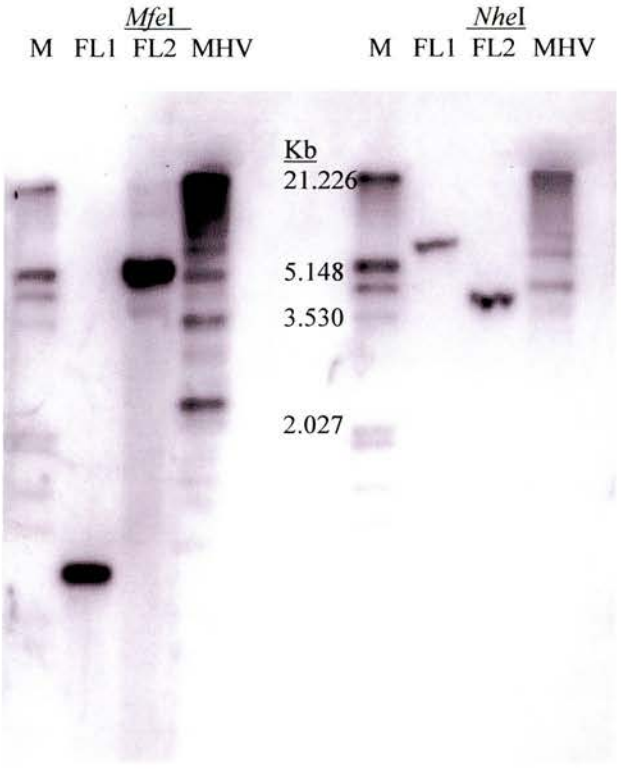

Figure 3.3 Southern blot of digested FL1, FL2 and wild-type MHV-76 DNA using LHE probe.

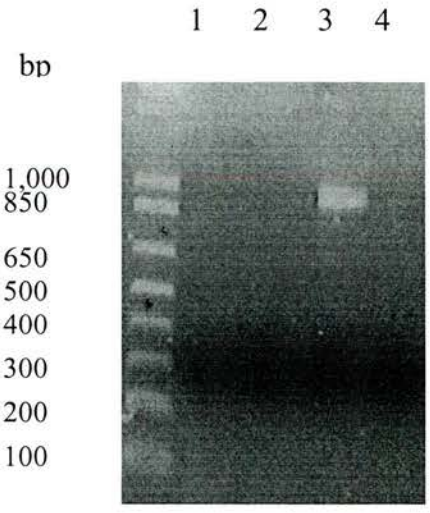

Figure 3.4 PCR for wild type virus. Lane 1: FL1; lane 2: FL2; lane 3: MHV-76 (positive control); lane 4: water (-negative control).

3.1.2 *In vitro* growth characteristics

A one-step growth curve was carried out to assess the kinetics of replication of the vFLIP expressing recombinant viruses in comparison to wild-type MHV-76. Also included is the IRES control recombinant virus (Brass, 2004). The IRES control contains the same inserted sequence as FL1 and FL2, in the FL1 orientation, with the exception of vFLIP.

Infection of BHK-21 cells was carried out in duplicate and samples were taken at intervals from 0 to 72 hours post infection. Samples were titrated on BHK-21 cells and the viral titre at each time point was calculated. The resulting growth curve can be seen in figure 3.5. The data indicate that the recombinant viruses all replicate with similar kinetics to MHV-76 during a single round of replication *in vitro*. The viral titre for all four viruses is indistinguishable up to 18 hours p.i. after which point MHV-76 and IRES reach a higher titre than FL1 and, particularly, FL2. At the final time point, 72 hours p.i., both vFLIP expressing recombinant viruses are at log lower titre than the wild-type and control viruses.

As all four viruses displayed similar kinetics and were clearly viable *in vitro,* further characterisation of their phenotype was undertaken using an *in vivo* system.

3.1.3 *In vivo* infection

Transcription of the KSHV vFLIP encoded by FL1 and FL2 is driven by the CMV IE promoter and subsequent translation of vFLIP is dependent upon the EMCV IRES. The expression of EGFP seen following infection of cells with pFL1 and pFL2 cannot, therefore, be taken as proof that vFLIP is expressed. However, northern blotting on total RNA extracted from C127 cells indicates that the insert is

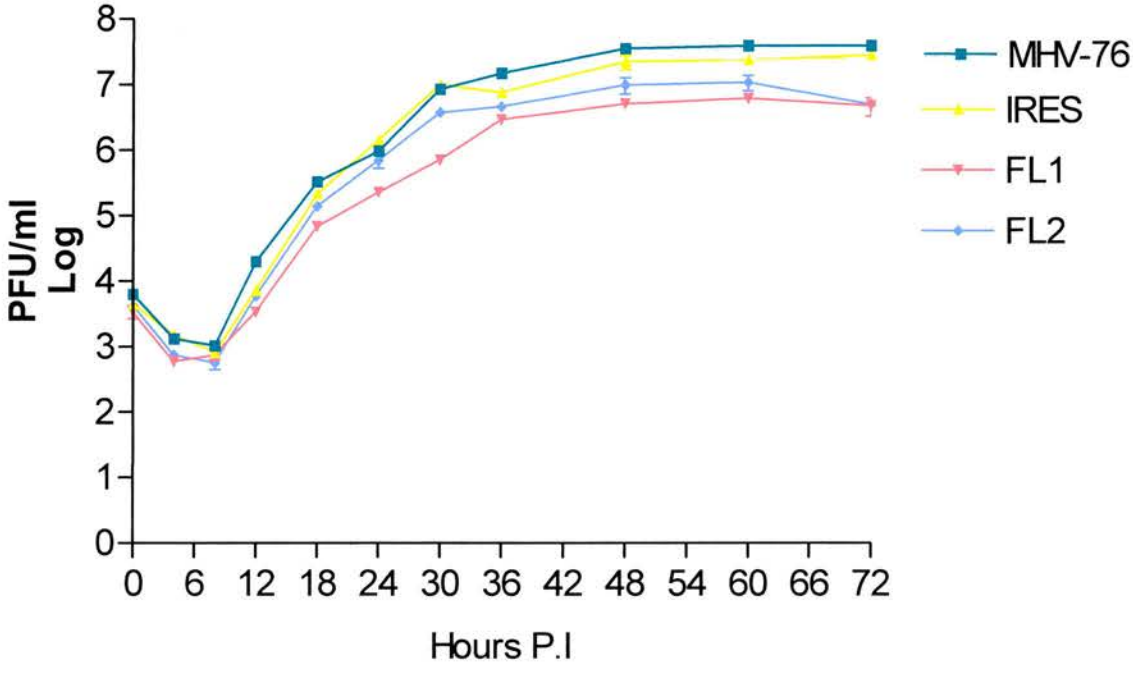

Figure 3.5 One step growth curve of recombinant viruses FL1, FL2, IRES control and wild-type MHV-76. The data represent the mean +/- the standard error of the mean with each time point assayed in duplicate.

transcribed; probing with a probe against vFLIP results in a band of ~4.2kb in both FL1 and 2 but not in wild-type MHV-76. A MHV-76 ORF50 probe was used as a control to confirm the presence of viral transcripts; all viruses produce the characteristic pattern of a strong band around 2Kb in size and further additional bands (Liu et al., 2000; figure 3.6). There is no commercially available antibody against vFLIP and attempts to raise antiserum proved unsuccessful (see section 3.5). This meant that expression of the protein could not be directly confirmed. However, the EMCV IRES has been demonstrated to mediate translation at approximately 30% the efficiency of cap-dependent translation *in vivo* (Bieleski and Talbot, 2001) and consequently we assume that some vFLIP is expressed. As vFLIP is not under the control of its own promoter (even if it could be, a KSHV promoter would not necessarily function correctly in a murine system) any expression will be at artificial levels and not necessarily representative of protein levels achieved during natural KSHV infection. Despite these limitations the opportunity to study the effect of a KSHV gene product in the context of an *in vivo* infection was deemed to be valuable.

Twenty 3-4 week old BALB/c female mice were infected with each virus. At each time point four mice per virus were euthanized and their organs harvested. The titres of lytic virus in the lung and cell-associated virus in the spleen were determined by plaque assay.

In comparison to MHV-68, MHV-76 is attenuated in lytic replication; it is rapidly cleared from the lung (Macrae et al., 2001). The lytic virus titres in the lung indicate that both FL1 and FL2 were cleared from the lung as rapidly as MHV-76 and the control recombinant virus (figure 3.7).

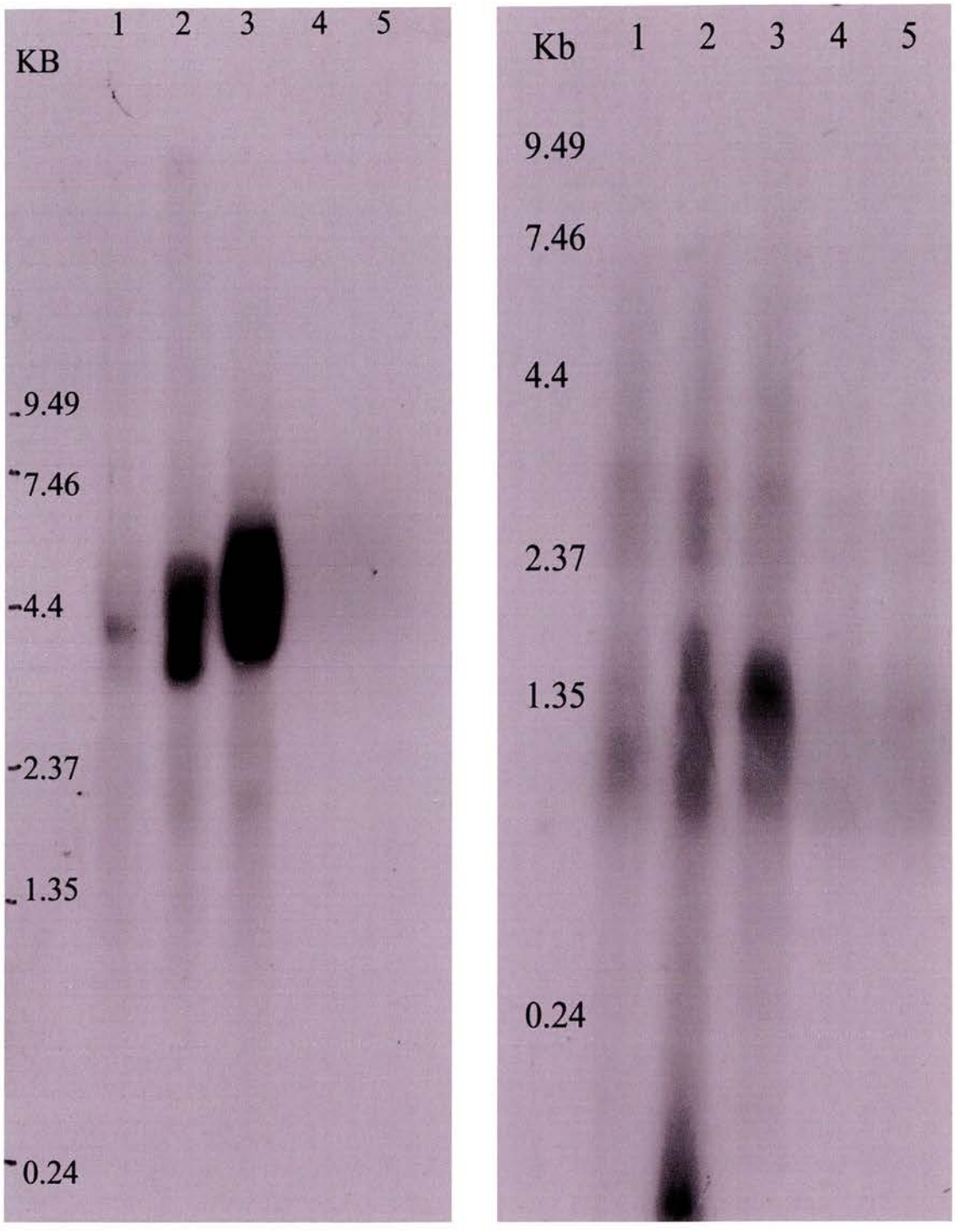

Figure 3.6 Northern blotting of total RNA extracted from virus infected C127 cells using probe for vFLIP (left hand image, expected size ~4.2 Kb) or ORF 50 (right hand image, expected size ~2Kb). Lane 1, FL3 (refer to section 3.2); lane 2, FL2; lane 3, FL1; lane 4 PGK-IRES; lane 5, MHV-76.

MHV-76 reaches peak titre in the lung at day 4 p.i. and is cleared by day 10 (Macrae et al., 2001). All three recombinant viruses appear to display similar kinetics *in vivo*. No virus could be detected in any animal by day 10 p.i. indicating that they were all cleared equally efficiently from the site of initial replication. Whilst the viruses all appear to be cleared at a similar rate the virus titres achieved show considerable variation. At day 5 p.i. both vFLIP expressing recombinant viruses were at a 2 log higher titre than MHV-76 and showed an even greater difference with respect to the control recombinant virus, IRES. It is clear that the difference is not due to outlying animals as in each group all four animals had very similar titres (figure 3.8). It seems that the IRES virus is attenuated in lytic replication in the lung; this has also been noted elsewhere (Brass, 2004).

The MHV-76 titres in the lung are much lower than would be expected from previous *in vivo* work carried out in the lab ((Macrae et al., 2001); B. Dutia; personal communication). The reason for this is unclear and it would seem presumptive to take this result as indicating that the vFLIP expressing viruses do attain a higher titre of lytic virus than MHV-76. This aside, both vFLIP expressing recombinant viruses attain a greater viral titre than the control, IRES, virus.

Turning to the spleen, titres of cell-associated recombinant virus were significantly lower than those achieved by the wild-type virus (figure 3.9). This pattern has been observed previously with other, similarly constructed, recombinant viruses (Douglas et al., 2004; Brass, 2004).

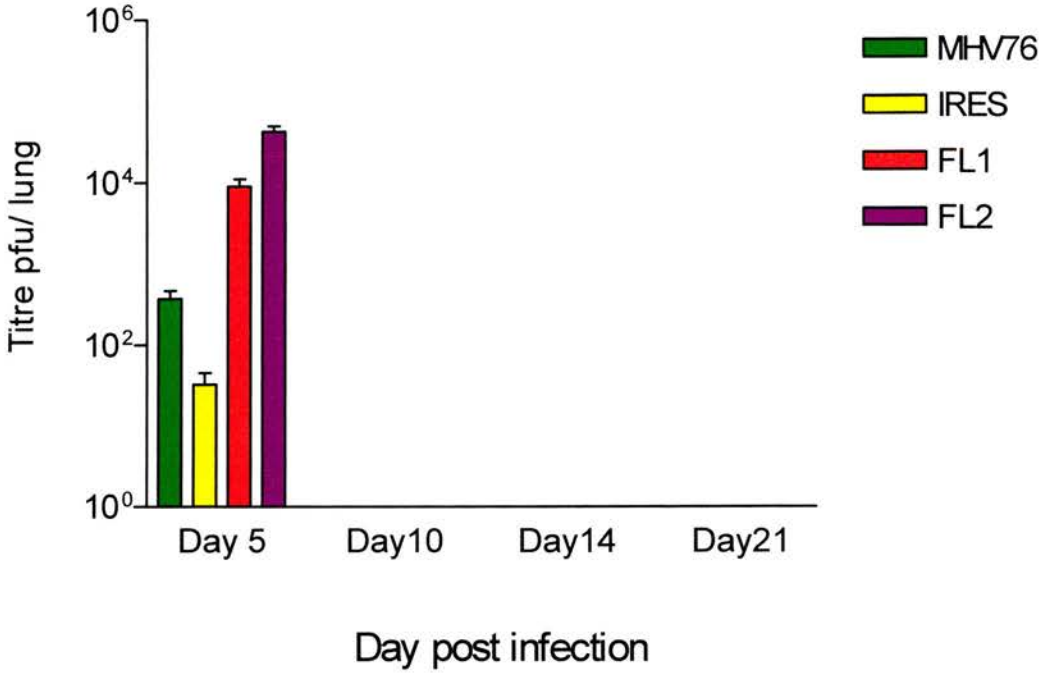

Figure 3.7 Infectious virus titres determined by plaque assay of lung homogenates from infected BALB/c mice. Data shown represents the mean of 4 animals +/- S.E.M.

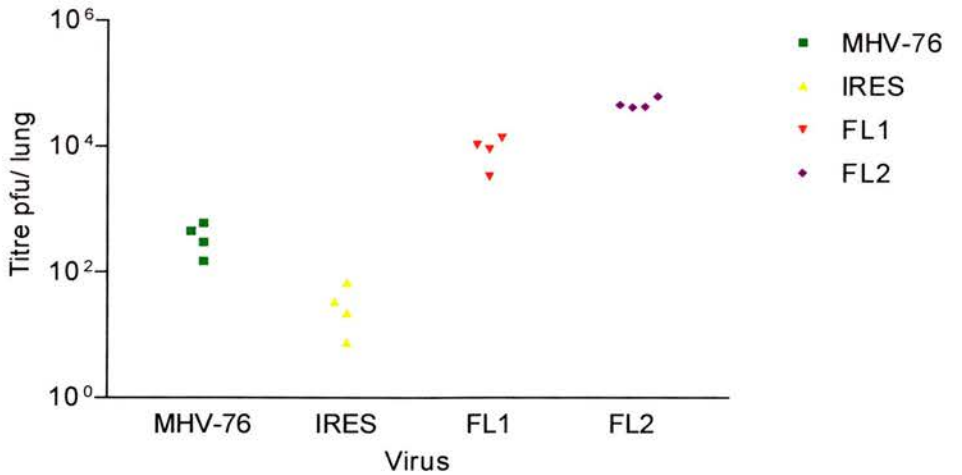

Figure 3.8 Day 5 lung infectious virus titres. Each point represents the viral titre in the lung of one BALB/c mouse.

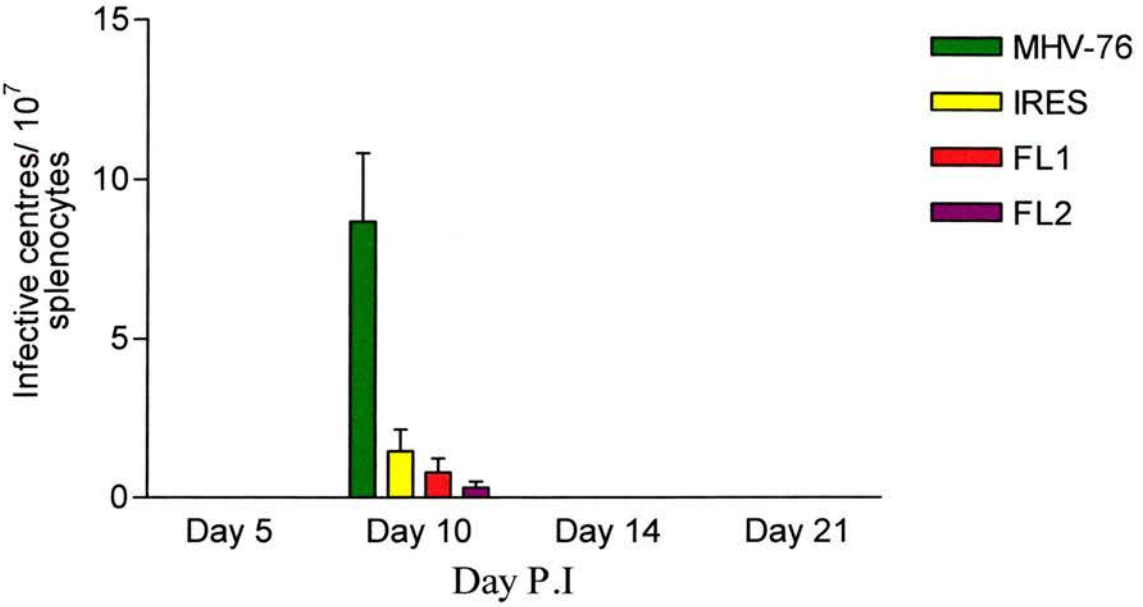

Figure 3.9 Spleen infective centres. Titres represent the amounts of cell-associated virus in the splenocytes of infected BALB/c mice. Values represent the mean titre from four animals +/- SEM.

In comparison to MHV-68, MHV-76 itself displays a significantly reduced splenic latent titre which peaks sooner post-infection (Macrae et al., 2001). The insertion of additional sequences at the LHE seems to compound this attenuation.

3.2 Recombinant virus construction using the PGK promoter

There are reports that the CMV IE promoter becomes silenced over time (Gerolami et al., 2000). As KSHV vFLIP is latently expressed it was decided that it would be best to construct recombinant viruses in which expression of the vFLIP gene is mediated by a promoter which would not undergo silencing.

The murine phosphoglycerate kinase (PGK) promoter was chosen as there is evidence that it is active in the majority of cell types and over an extended period of time (Gerolami et al., 2000). It was decided to make only one vFLIP expressing recombinant virus, with the insert in the same direction as FL1; there was no significant difference observed between FL1 and FL2 either *in vitro* or *in vivo*. Additionally, the control recombinant virus is constructed in this orientation.

Site directed mutagenesis, using oligos pJ27 BglII forward and pJ27 BglII reverse, was carried out on pAB13 to generate a *Bgl*II restriction site at the 5' end of the CMV IE promoter (giving pAB13-BglII). The promoter was then removed by sequential *Mlu*I digestion; blunt ending and *Bgl*II digestion. The PGK promoter plus intervening sequence (IVS) sequence was cut from the vector pPGK-EGFP (gift of Jim Mcwhir; University of Edinburgh) with *Bgl*II/ blunt ends and ligated into pFL1-BglII. Correct insertion was confirmed by *Eco*RI digestion. The vOx_2 coding sequence was cut from the vector by *Fse*I, *Asc*I digestion and replaced with, similarly

digested, vFLIP DNA resulting in plasmid pFL3. Correct insertion was confirmed by *Fse*I, *Asc*I digestion and PCR. The control recombinant virus, PGK-IRES, was constructed in a similar way i.e. the CMV IE promoter in the plasmid used to construct the IRES recombinant virus was replaced by the PGK-IVS sequence resulting in plasmid pPGK-IRES.

Recombinant viruses were constructed and purified in the same manner as previously described for FL1 and FL2. Briefly, pFL3 and pPGK-IRES were digested with *Eco*RV and *Pvu*II and co-transfected into BHK-21 cells with wild-type MHV-76 DNA. Transfection by electroporation was unsuccessful on several occasions: eventually transfection was achieved using Effectene reagent (Qiagen). Recombinant viruses were purified by four rounds of limiting dilution plaque purification during which selection was achieved via hygromycin resistance, EGFP expression and in the case of FL3, PCR for vFLIP. Following agarose overlay a masterstock of each virus and viral DNA were prepared. Southern blotting was carried out to confirm the presence of the correct insert and the absence of wild-type MHV-76 in each recombinant virus preparation.

3.2.1 Southern blotting

DNA was extracted from two different isolates of each of FL3 and PGK-IRES, and from MHV-76, subjected to either *Mfe*I or *Sph*I digestion and blotted with two different probes. Expected digestion patterns and band sizes are detailed in figure 3.10 and table 3.2. The resulting Southern blots had bands of the expected sizes and confirmed the absence of wild-type virus in all of the recombinant virus samples (figure 3.11 and 3.12).

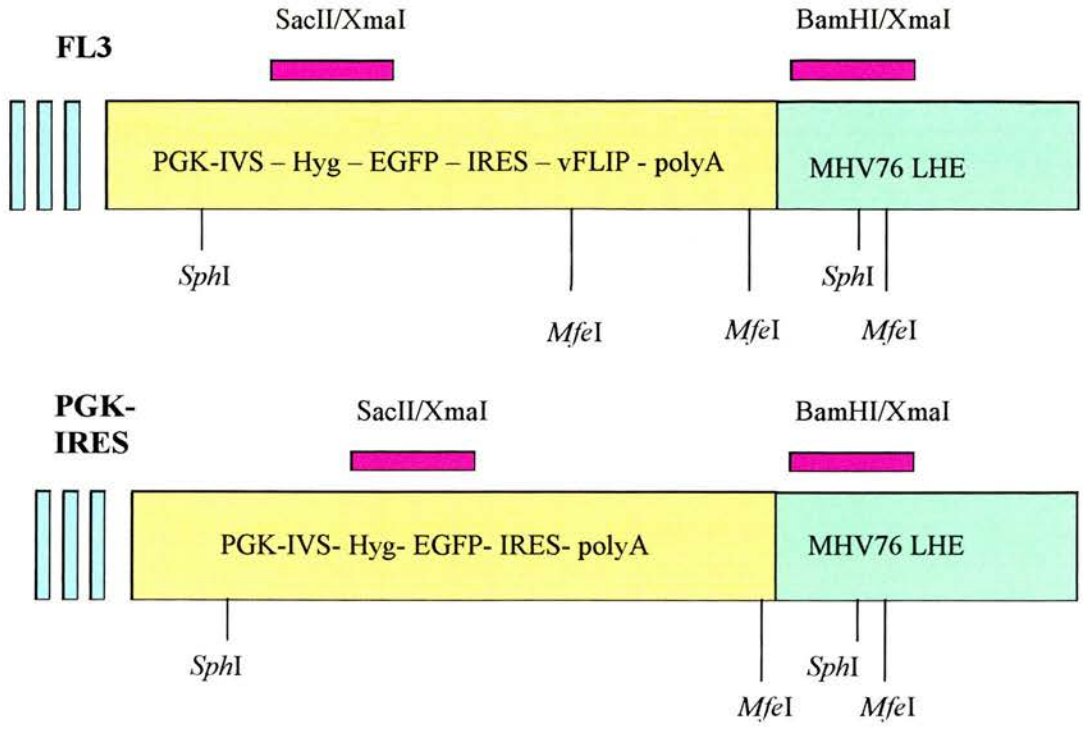

Figure 3.10 Schematic representations of the left hand end sequences of the recombinant viruses FL3 and PGK-IRES. The restriction sites used for Southern blot digestions and probe hybridisation locations are indicated.

	FL3		PGK-IRES		MHV-76	
	*Mfe*I	*Sph*I	*Mfe*I	*Sph*I	*Mfe*I	*Sph*I
GFP probe	laddering	~5kb	laddering	~4.4kb	-	-
LHE probe	1.15kb	~5kb	1.15kb	~4.4kb	laddering	laddering

Table 3.2 The expected band patterns for FL3 and PGK-IRES Southern blots following either *Nhe*I or *Mfe*I digestion.

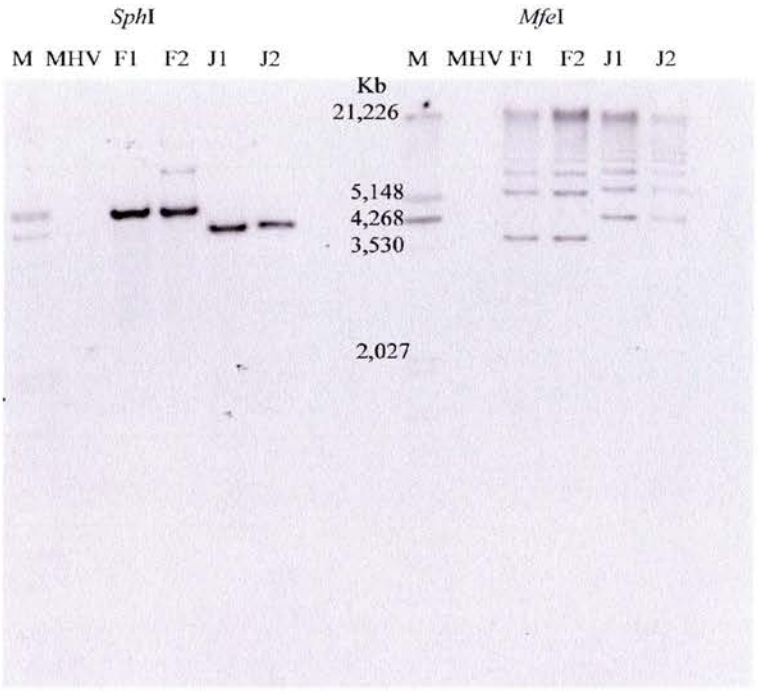

Figure 3.11 Southern blot of DNA of MHV-76 and two isolates each of FL3 (F1 and F2) and PGK-IRES (J1 and J2) using GFP probe.

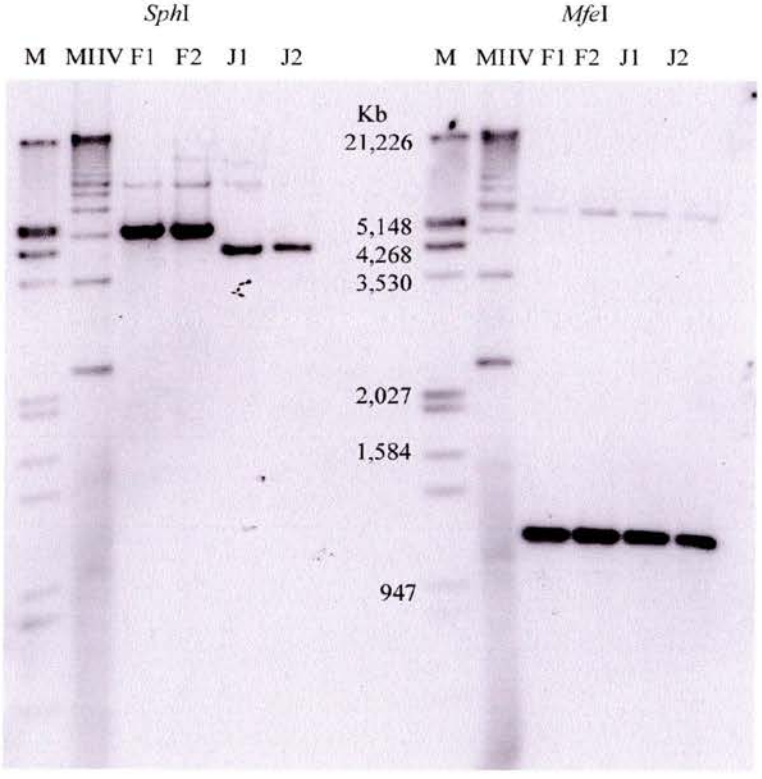

Figure 3.12 Southern blot of DNA from MHV-76 and two isolates each of FL3 (F1 and F2) and PGK-IRES (J1 and J2) using LHE probe.

There were some anomalous bands of higher molecular weight than expected; this phenomenon has been observed previously (Brass, 2004). As none of the additional bands corresponded to any in MHV-76 both recombinants were deemed to be pure. Virus stocks were made from FL3-1 and PGK-IRES-1, titred and stored at -80°C.

3.2.2 *In vitro* growth characteristics

A one-step growth curve was carried out to assess the kinetics of a single round of replication whilst a multi-step growth curve was used to compare the viruses over multiple rounds of replication. Infections of BHK-21 cells were carried out in duplicate and samples were taken at 0-72 hours for the one-step and 0-144 hours for the multi-step. Samples were subsequently titred on BHK-21 cells. The resulting curves can be seen in figures 3.13 and 3.14. Both growth curves indicate that the recombinant viruses replicate with almost identical kinetics to MHV-76.

In order to confirm that the inserted sequences were expressed, Northern blotting of RNA extracted from infected C127 cells was carried out. The C127 cell line was chosen as it is a murine cell line and expression in it is likely to correlate with expression *in vivo*. Total cellular RNA was extracted and probed for ORF 50 and KSHV vFLIP. The resulting blots (figure 3.6) confirmed the expression of viral transcripts (ORF 50) and, in the case of FL3, vFLIP. Again, this does not prove that vFLIP is being translated as this is under the control of the EMCV IRES and the presence of an mRNA transcript does not mean that protein is being made. As before, it must be assumed that there is some IRES activity and that some vFLIP will be produced.

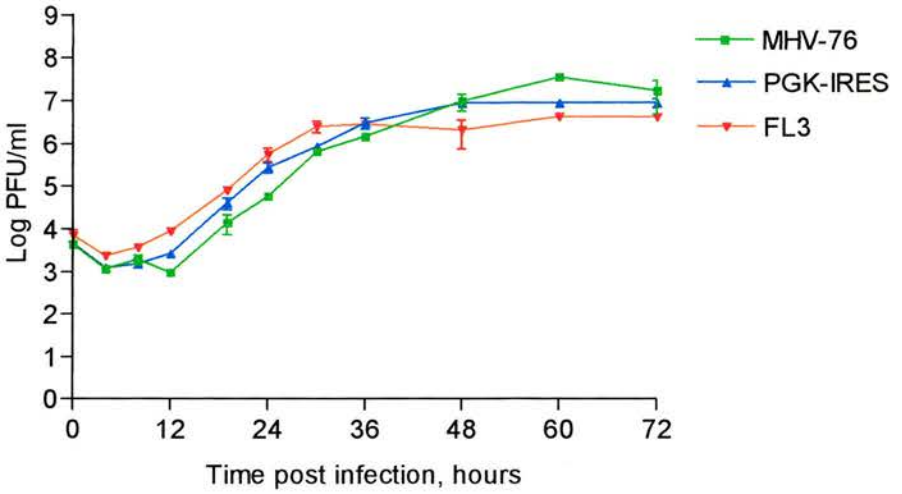

Figure 3.13 One step growth curve of recombinant viruses FL3 and PGK-IRES and wild-type MHV-76. The data represent the mean +/- the S.E.M., each time point was assayed in duplicate.

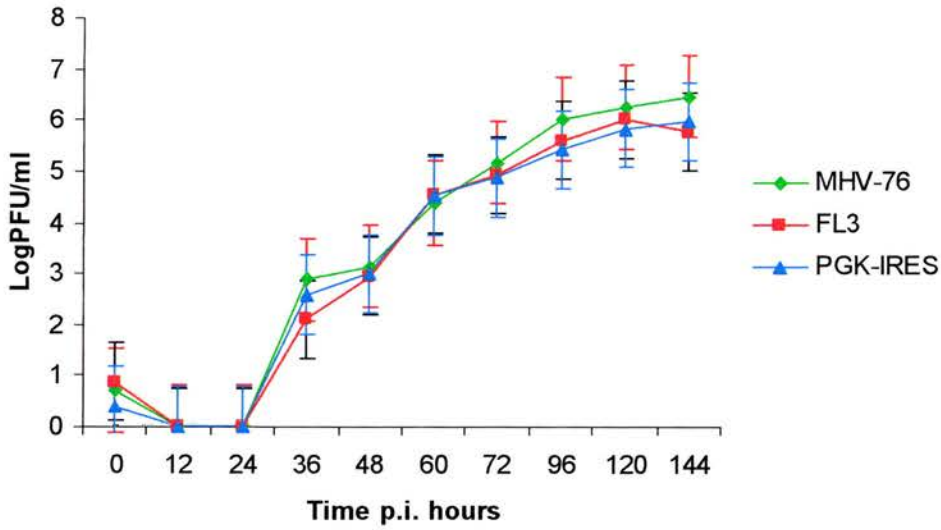

Figure 3.14 Multi-step growth curve of recombinant viruses FL3 and PGK-IRES and wild-type MHV-76. The data represent the mean +/- the S.E.M, each time point was assayed in duplicate.

3.2.3 *In vivo* infection

Thirty six 3-4 week old female BALB/c mice were infected with each virus. At each time point mice were euthanised and their organs harvested. An outline of the work undertaken is detailed in table 3.3.

Day p.i.	Mice	Lungs	Spleens
0 I/N Infection	36x FL3 36x PGK-IRES 36xMHV-76	-	-
3	6x FL3 6x PGK-IRES 6x MHV-76	Virus infected lungs split into two; 1/2- DNA extraction 1/2- virus titre	-
6	As day 3	As day 3	-
8	As day 3	As day 3	-
10	6x FL3 6x PGK-IRES 6x MHV-76	As day 3	5 per virus in RPMI 1 per virus in OCT
14	As day 10	2 per virus in N_2(l)	As day 10
21	As day 10	As day 14	As day 10

Table 3.3 Outline of PGK promoter viruses *in vivo* experiment

The titres of infectious virus in the lung and cell-associated virus in the spleen were determined as before. In contrast to the previous *in vivo* experiment, with the CMV IE promoter viruses, there was no difference in lung titres reached by the recombinant viruses and MHV-76 (figure 3.15). When the data is represented so as to show the titre from each mouse (figure 3.16) it is clear that the viral replication is similar and not skewed by the presence of outlying animals. Interestingly, the attenuation of the control recombinant virus seen previously (figure 3.7) is abolished in this experiment.

Each snap-frozen lung was sectioned and immunohistochemistry was carried out on the lung sections using a polyclonal antiserum, Rabbit B, raised against MHV-68. This serum is also able to recognise MHV-76. A FITC conjugated secondary antibody was used and the slides were mounted using mounting medium containing propidium iodide to allow visualisation of the cell nuclei. We had hoped that we would be able to see areas of apoptotic cells that corresponded with areas of infection and perhaps to see a reduction in apoptosis in animals infected with the vFLIP expressing recombinant virus. The resulting staining (figure 3.17) shows extensive infection of all three viruses at days 3, 6 and 8 p.i.: the most virus being present at day 6 p.i. which corresponds with the data obtained from the plaque assay. By day 10 p.i. the FITC staining has disappeared showing that the viruses have been cleared from the lungs.

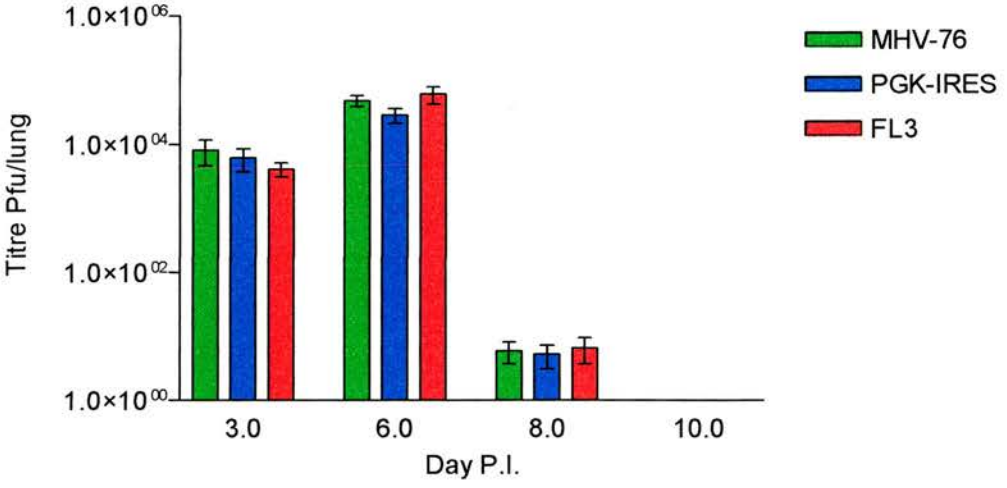

Figure 3.15 Titres of infectious virus in the lungs of infected BALB/c mice, values represent the mean titres from 6 mice per virus +/- the S.E.M.

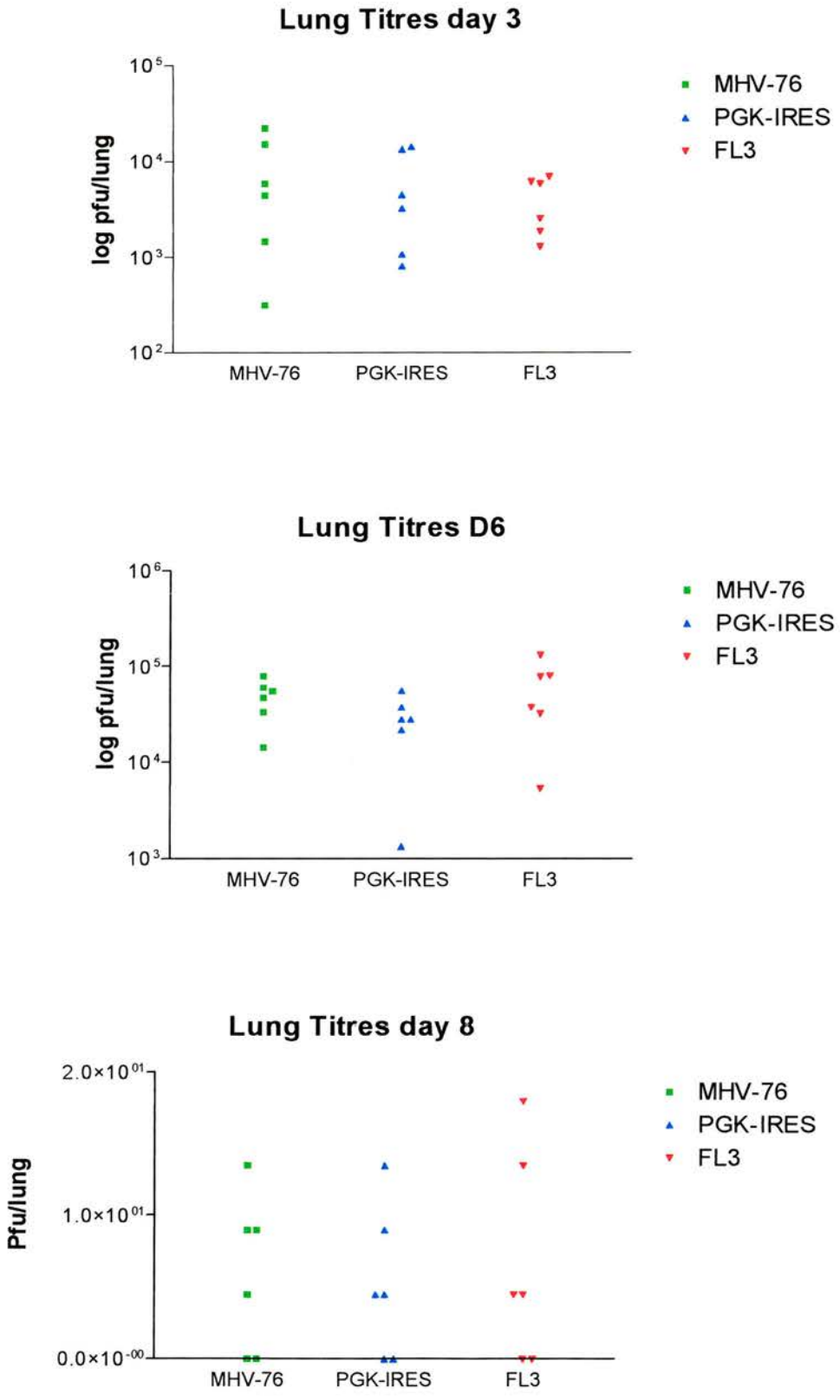

Figure 3.16 Infectious virus titres in the lungs of individual BALB/c mice. Note that the y axis scale varies.

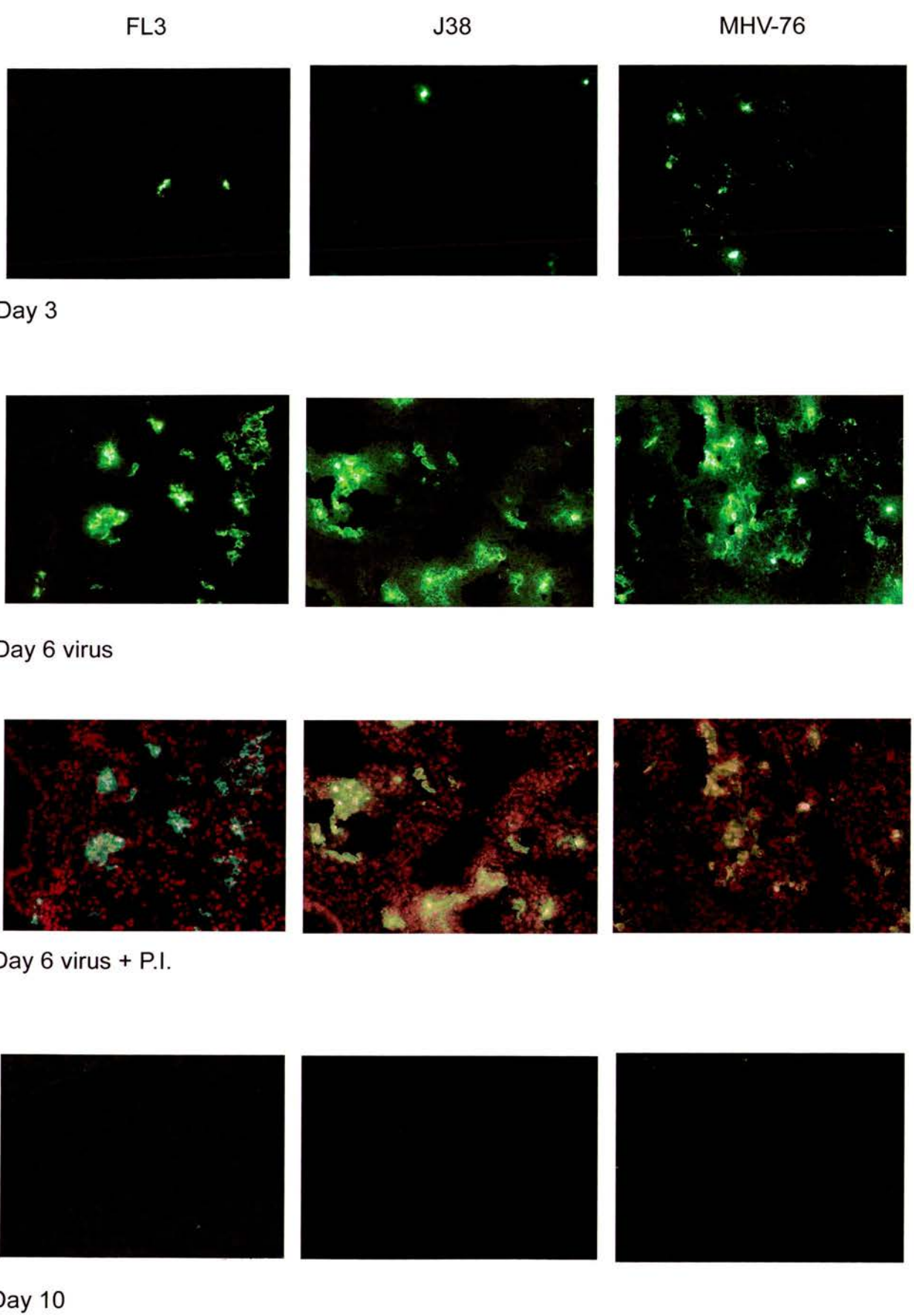

Figure 3.17 Immunostaining of snap-frozen lung sections using a polyclonal antiserum raised against MHV-68. The primary serum was used at 1/2000 dilution; the secondary goat anti-rabbit FITC was used at 1/500. Sections were mounted using propidium iodide containing mounting medium (vector labs). Images at 200x magnification.

The nuclear staining gives no indication of significant apoptosis occurring at any time point; no conclusions concerning that anti-apoptotic activity of vFLIP can be inferred from these sections.

In the spleen FL3 induces no splenomegaly in infected animals (figure 3.18) and infective centre levels attained by the recombinant viruses are greatly reduced in comparison to MHV-76 (figure 3.19). No cell associated FL3 or PGK-IRES virus was detectable from day 14 p.i. and at day 10 p.i. both viruses display severe attenuation similar to that observed previously for FL1, FL2 and the IRES control (figure 3.9).

3.2.4 Long term infection

All of the *in vivo* data presented above relates to the initial stages of infection. As gamma-herpesvirus infection persists for the life of the host there remained a possibility that any contribution of vFLIP towards viral pathogenesis is more pronounced at later time points. Mice from the first, FL1 and FL2, *in vivo* infection were euthanised approximately 1 year post-infection. The lungs, spleen, liver, kidney and salivary gland were removed and either snap frozen in liquid nitrogen for subsequent DNA extraction or preserved for sectioning. No mice displayed any obvious pathology in terms of tumour growth or sickness.

Following DNA extraction from all tissue samples a PCR for ORF50 was carried out to look for the presence of viral DNA. Following two rounds of 40 cycles, in which 2μl of the first round product was used as template for the second round, no viral DNA was detected in any tissue sample.

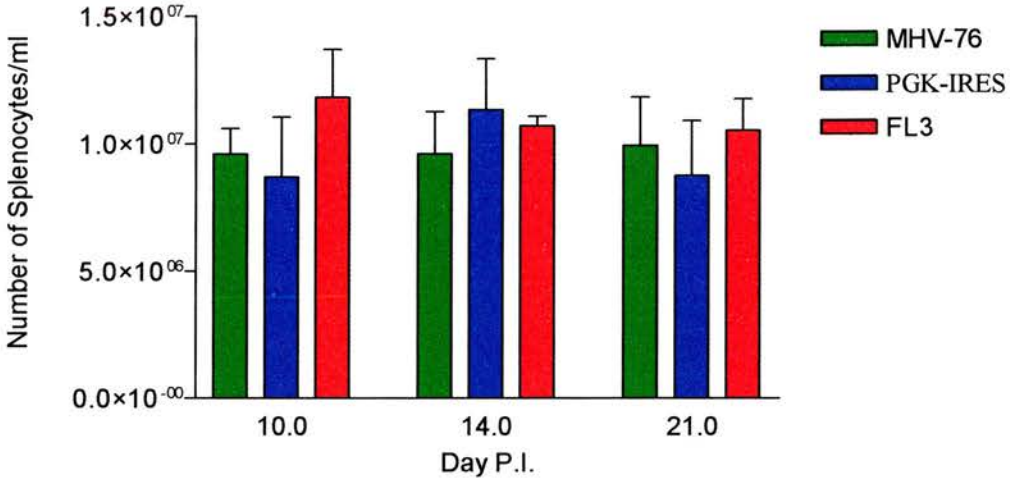

Figure 3.18 Total splenocytes per ml following extraction from the spleens of infected BALB/c mice. Data represent mean values from five animals +/- S.E.M.

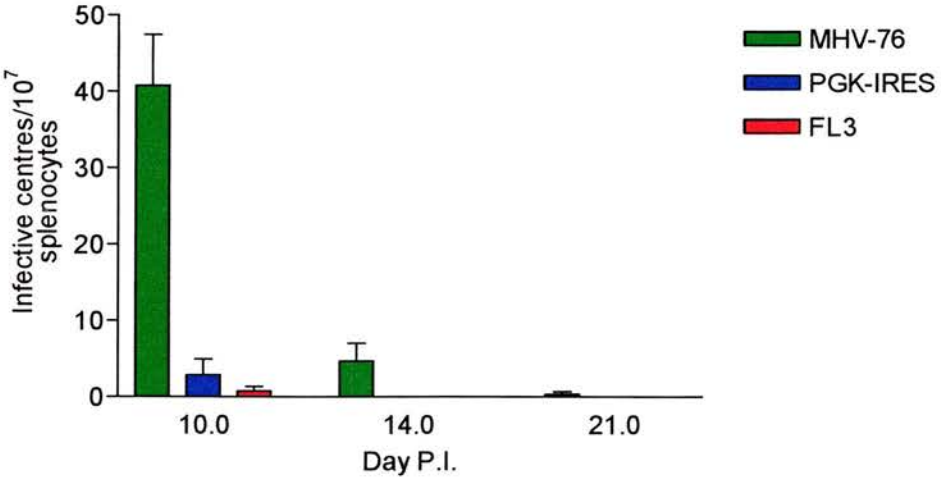

Figure 3.19 Spleen infective centre titres. Titres represent the amounts of cell-associated virus in the splenocytes of infected BALB/c mice. Values represent the mean titre from five animals +/- S.E.M.

This result implies that either the viruses had been completely cleared from the animals or that the levels of virus were so low as to be undetectable in this system. These results for FL1, FL2 and IRES are perhaps unsurprising given the severe attenuation seen in the infective centre assay (figure 3.9) which suggests that the recombinant viruses are unable either to establish a latent infection or to reactivate from latency.

3.3 Construction of recombinant viruses 76inFLIP and 76inEGFP

Concerns have previously been raised over the effects of large inserts on viral behaviour *in vivo*. It was demonstrated that whilst a BAC-derived MHV-68 replicated as wild-type virus *in vitro,* it was necessary to remove the BAC sequences to achieve wild-type *in vivo* properties (Adler et al., 2001). Similarly, MHV-68 mutants constructed through the insertion of a large DNA sequence, e.g. *lacZ*, to disrupt the gene of interest, show attenuation of the *in vivo* phenotype (Clambey et al., 2000).

As the recombinant viruses expressing EGFP and hygromycin resistance were unable to become latent *in vivo,* possibly because of an immune response to these inserts, efforts were made to construct recombinant viruses without these selection markers. Viruses similar to this had previously been successfully made, with MHV-68 genes inserted into the left-hand end of MHV-76 (Townsley et al., 2004). In this instance the gene of interest was inserted with its own promoter sequence driving expression. Obviously this would not be possible for KSHV vFLIP as it is expressed via an IRES element from a bicistronic transcript. Instead it was decided to try and insert vFLIP

under the control of the PGK promoter which would, hopefully, provide long-term expression of vFLIP. Additionally a second recombinant virus expressing EGFP from the PGK promoter would be constructed to act as a control.

3.3.1 Cloning strategy

Once again the construction of recombinant viruses was carried out by homologous recombination following transfection of BHK-21 cells with MHV-76 DNA and plasmid DNA encoding the sequence to be inserted adjacent to a 3kb section of the MHV-76 LHE. Two plasmids were prepared, one for each recombinant to be made. In both cases the plasmid pBS 76-LHE was used as the backbone. p76inPGK-EGFP was created by the insertion of the PGK-EGFP sequence from pEGFP-PGK into the vector using *Sac*I and *Not*I restriction sites. p76inFLIP was cloned sequentially: the PGK-IVS sequence was inserted first using the *Sac*I and *Bam*HI restriction sites; vFLIP, amplified from BCP-1 DNA using primers In flip forward and Flip polyA, was inserted into the pCR 2.1-TOPO cloning vector (Invitrogen), cut from this with *Bam*HI and inserted into p76-LHE PGK using the same enzyme. In both cases the vectors were checked by restriction digest to confirm insertion of the sequence in the correct orientation.

3.3.2 Purification of recombinant viruses

As the inserted sequence contained no selection markers generation of recombinant viruses was attempted purely by limiting dilution plaque purification. The presence of EGFP in 76inEGFP allowed for some degree of selection. Both plasmids had to be linearised prior to transfection to allow recombination to occur. The only suitable

restriction sites, *Eco*RV, resulted in a 10bp deletion from the 5' end of the PGK promoter sequence. Transfection of BHK-21 cells with *Eco*RV digested p76inPGK-EGFP resulted in strong EGFP expression indicating that the deletion did not have a detrimental effect on PGK activity.

Plasmid DNA, linearised by *Eco*RV digestion, and MHV-76 DNA were transfected into BHK cells using effectene transfection reagent (Qiagen). The cells were incubated and 5 days post transfection plaques had formed; in the case of 76inEGFP they were green. Purification was then attempted by plaque purification on BHK-21 cells in 96-well plates. After each round of purification the presence of the insert was confirmed either by PCR, in the case of 76inFLIP (using primers In flip forward and Flip polyA), or by EGFP expression. A PCR for wild-type MHV-76 using primers M4B and Trepeat was also performed. At all times plaque picks came up positive for wild-type virus and, as more rounds of purification were performed, the number of insert positive samples reduced. In an attempt to accelerate the process an agarose overlay was carried out. Again, all samples came up positive for wild-type virus and in the case of 76inFLIP none of the 24 plaques sampled were positive for vFLIP DNA.

Having failed once to purify 76inFLIP and 76inEGFP a second attempt was made. Transfection and plaque purification was carried out. Initial results were more promising as the insert was not lost as rapidly as previously seen and occasionally plaques were negative for wild-type virus by PCR. However, in all cases wild-type virus was again detected after a subsequent round of purification. This result suggests that either the insert was being lost from the recombinant viruses or that a

very low level of wild-type virus, below the limit of detection by PCR, was present and had a growth advantage over the recombinant viruses.

Despite the fact that these recombinant viruses would have been very beneficial to the project, efforts to purify them were halted as it became clear that the contaminating MHV-76 could not be removed.

3.4 Investigation as to whether an immune response against EGFP is responsible for the attenuation seen *in vivo*

Whilst the splenic attenuation of all of the recombinant viruses tested *in vivo* was extremely disappointing and frustrating it also raises the interesting question of what is causing it. There would seem to be two possibilities, firstly that the viruses are failing to establish latency in the first place and secondly that having established latency they are unable to reactivate and produce infectious virions. In order to address the hypothesis, forwarded above, that an immune response against EGFP results in clearance of the virus, mice tolerant to EGFP were infected and the spleen cell-associated virus titres at day 10 p.i. were determined.

The mice used were of the ROSA strain (Mao et al, 2001). They have EGFP inserted into their genome, the expression of which should be dependent on excision of a stop sequence, located between two *lox* sites, by cre recombinase. However, it has been discovered that there is some "leaky" expression of EGFP and we therefore assume that the mice are tolerant to its presence (B.Dutia; personal communication). The ROSA mice are on a L129 background and so different to BALB/c which were used in the previous experiments. Ideally the experiment would have been performed in

L129 and ROSA mice to determine that the behaviour of the viruses in the ROSA background was the same as that seen in BALB/c mice. Lack of availability of the L129 strain meant that this was not possible but MHV-68 is known to display similar behaviour in the ROSA mice as seen in BALB/c although the titres reached are lower (B.Dutia; personal communication). We made the assumption that MHV-76 would establish splenic latency at levels similar to infected BALB/c mice and that, as seen in BALB/c, the recombinant viruses would display attenuation in the spleen of the ROSA strain. It was hypothesised that if the attenuation was due to an immune response against EGFP this would be eradicated in these mice and thus the titres of the recombinant virus would rise to the levels of MHV-76.

Four mice per virus were infected intranasally with $4x10^5$ pfu of FL3, PGK-IRES and MHV-76. After 10 days, the point at which maximum splenic infective centre titres are achieved in BALB/c mice, the mice were euthanised and their spleens removed. The titres of cell-associated virus in the spleens were determined by infective centre assay. As previously there was no obvious splenomegaly induced by either recombinant virus; the splenocyte numbers are equivalent to those of the MHV-76 infected group (figure 3.20). Surprisingly it appears that not only the recombinant viruses but also MHV-76 are severely attenuated, with respect to the establishment of a latent infection of the spleen, in these mice (figure 3.21).

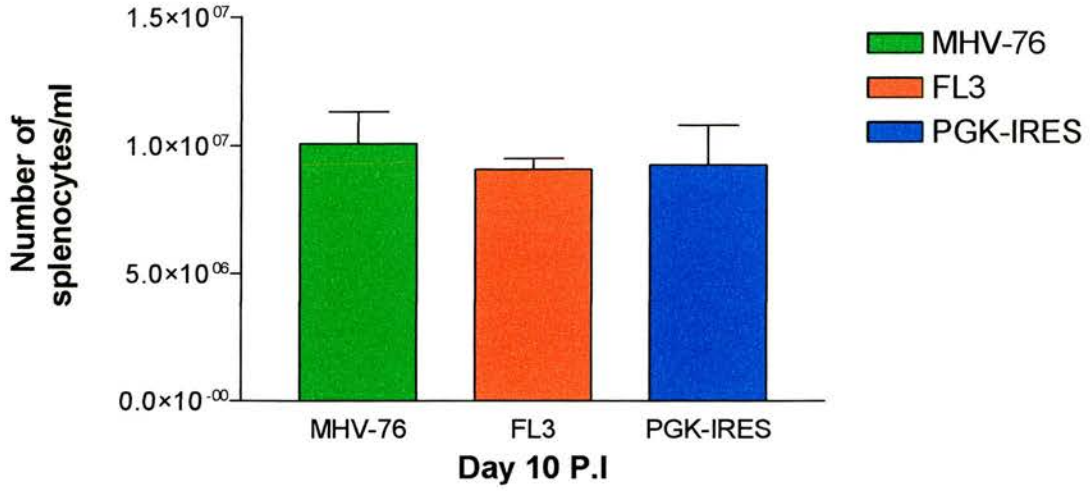

Figure 3.20 Total splenocytes per ml following extraction from the spleens of infected ROSA mice. Data represent mean values from four animals +/- S.E.M.

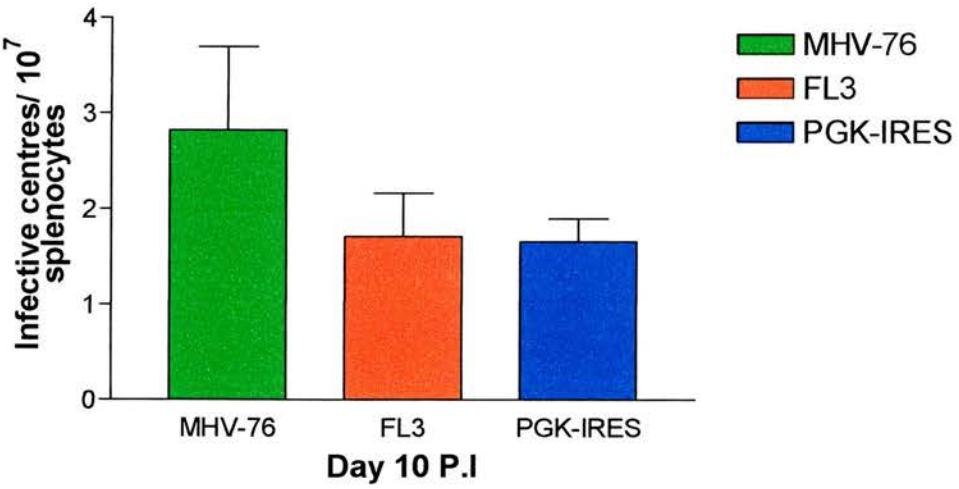

Figure 3.21 Spleen infective centre titres. Titres represent the amounts of cell-associated virus in the splenocytes of infected ROSA mice. Values represent the mean titre from five animals +/- S.E.M.

3.5 Purification of KSHV vFLIP protein and attempts to raise antiserum in rabbits

As vFLIP translation is under the control of an IRES element, both in its natural setting, KSHV, and in the recombinant viruses that have been constructed, the mere presence of an mRNA transcript (which is produced, see figure 3.6) does not equate with protein expression. In order to draw any absolute conclusions from work carried out using the vFLIP encoding viruses a method through which the presence of vFLIP protein can be verified must be in place. The obvious means by which the presence of a protein within a system can be proven is by immunostaining using an antibody raised against the protein in question. It would be most desirable to confirm the translation of vFLIP during the course of both of *in vivo* and *in vitro* experiments undertaken.

Additionally, an antibody would allow investigation of the levels of vFLIP expression in PEL derived cell lines. It would be fascinating to determine whether there was any change in translational activity throughout the course of the cell cycle. For instance, is there any decrease in cellular FLIP expression following inhibition of cap-dependent translation, at the entry to mitosis, and if so does a compensatory increase in IRES-mediated vFLIP translation take place? It would seem likely that the expression of vFLIP is closely linked to that of vCyclin as both proteins are encoded by the same transcript. Moreover, investigation of the kinetics and levels of expression of the two proteins relative to one another would perhaps give some indication as to whether a role of vFLIP is to protect virally infected cells as vCyclin

drives them through the cell cycle. If this is the case then vFLIP could be said to be acting as an indirect oncogene, protecting proliferating cells from apoptosis.

At present there are no commercially available antibodies against KSHV vFLIP, or indeed any other viral FLIP. I, therefore, carried out purification of vFLIP and attempted to raise antiserum by immunisation of rabbits with the resulting protein.

3.5.1 The Glutathione S-transferase (GST) Gene Fusion System

The first attempt to purify vFLIP utilised the GST Gene Fusion System (Amersham). In this system the protein to be purified is expressed in E.*coli* as a fusion with glutathione S-transferase (GST) from *Schistosoma japonicum*. The fusion proteins are expressed from an inducible promoter at high levels and can be purified from bacterial lysate by affinity chromatography using glutathione sepharose 4B; glutathione is bound by the GST moiety. Following washing steps, to remove non-specific binding, the fusion protein can be eluted from the glutathione sepharose or, alternatively, it can be treated with thrombin to cleave the target protein from the GST thus eluting vFLIP whilst GST remains bound to the sepharose. The purification process is monitored by Western blotting using a primary antibody against GST.

KSHV vFLIP was amplified from BCP-1 DNA by PCR using the primers FLIP GST-1 and FLIP GST-2 and sub-cloned into the *Eco*RI and *Xho*I sites of pGEX4T-1. This vector enables expression of the vFLIP from the IPTG responsive *tac* promoter and encodes a thrombin cleavage site immediately downstream of the MCS into which vFLIP is inserted. Correct insertion of vFLIP was confirmed by restriction digest and BigDye sequencing was also performed: the resulting sequences

confirmed that two of the clones, numbers 3 and 11, contained vFLIP that was correctly inserted with no deletions.

Protein purification was carried out according to the manufacturer's instructions. The purification process was monitored by Western blotting using an anti-GST antibody (Invitrogen). Cultures of E.*coli* transformed with pGEX4T1-vFLIP clone 3 were grown in 200ml volumes. Sonicate was prepared in a volume of 10ml and thrombin cleavage was carried out in a total volume of approximately 100µl. Despite extensive attempts to optimise the cleavage reaction in the majority of cases thrombin treatment resulted in disassociation of the GST-vFLIP fusion protein from the sepharose. In fact, successful cleavage, which released vFLIP whilst maintaining GST binding to the glutathione sepharose, was achieved only once (fig 3.22). The eluted vFLIP was run on a SDS-PAGE gel and coomassie stained. This showed a band at approximately 21kD, the correct size for vFLIP (gel shattered on drying).

A total of four, monthly, injections were made into a rabbit. The failure to purify vFLIP more than once meant that only the first two injections were of purified vFLIP; the final two were of vFLIP-GST fusion protein. The resulting serum was tested for reactivity against vFLIP by Western blot. Unfortunately the serum acted against the GST moiety; there was no band at 21kD. It was perhaps not unexpected that there would be an immune response directed toward GST, however, it is disappointing that there appears to have been no response against vFLIP.

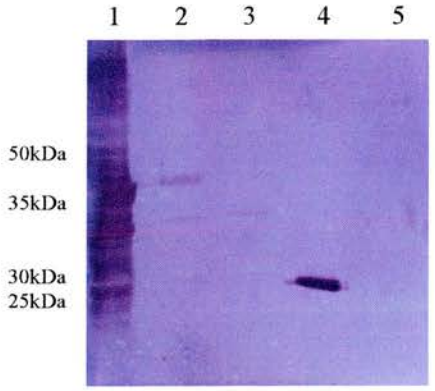

Figure 3.22 Western blot of vFLIP purification using the GST system. Lane 1, sonicated cells; lane 2, soluble protein; lane 3, supernatant following incubation with sepharose; lane 4, eluted GST; lane 5, supernatant following thrombin cleavage (vFLIP). The primary antibody, mouse anti-GST, was used at 1/1000 dilution, the secondary, goat anti-mouse alkaline phosphatase , was used at 1/ 2,500 dilution. The GST-vFLIP fusion protein is approximately 46kDa and can be seen in lane 2. This band is no longer seen following incubation with the sepharose indicating that the protein has bound successfully. Following thrombin cleavage no GST is seen in the supernatant (lane 5) whilst the fraction eluted from the sepharose contains only GST and no fusion protein (lane 4).

3.5.2 The pTrcHis expression system

A second attempt to purify vFLIP without any large additional tags was made using the pTrcHis expression system (Invitrogen). The protein of interest i.e. vFLIP, is expressed with both a His_6 and a myc tag at its C-terminus, which adds approximately 2.5kDa to the total size of the protein. The His_6 tag provides an efficient means of protein purification as it binds with high affinity and specificity to nickel. Consequently, His_6-tagged proteins can be separated from a mix of proteins by affinity chromatography. The myc epitope provides a means by which the purified protein can be detected, in both Western blotting and immunohistochemistry, as several companies supply monoclonal antibodies that recognise it. The vFLIP coding sequence was amplified by PCR from BCP-1 DNA, using the primers In flip forward and flip Myc His reverse which also add the *Hind*III and *Nco*I restriction sites and cloned into the corresponding sites of pTrcHis2A. Insertion of vFLIP was confirmed by restriction digest and PCR.

A pilot expression experiment was carried out to assess the kinetics of vFLIP expression following IPTG induction of *E.coli* transformed with pTrcHis2A-vFLIP. 1ml samples of the induced culture were pelleted and lysed in 100µl SDS PAGE loading buffer. A 10µl sample was then analysed by Western (fig 3.23). A protein of the correct size to be Myc-his tagged vFLIP is seen from 1 hour post induction. Having demonstrated that vFLIP was expressed in the system, larger scale purification was carried out and monitored by Western blotting (figure 3.24) and silver staining (figure 3.25). Lanes 3 and 4 of the western blot indicate that vFLIP is successfully eluted from the Nickel affinity gel; the silver stain shows that there are no higher molecular weight contaminants of the protein preparation.

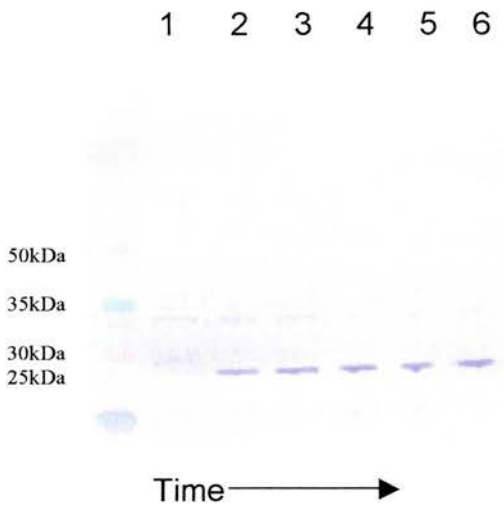

Figure 3.23 Western blot analysis of vFLIP expression following IPTG induction. Lane 1, 0 hours post induction; lane 2, 1 hour post induction; lane 3, 2 hours post induction; lane 4, 3 hours post induction; lane 5, 4 hours post induction; lane 6, 5 hours post induction. The primary antibody, mouse anti-Myc (Invitrogen), was used at 1/ 3,000 dilution. The secondary antibody, goat anti-mouse alkaline phosphatase, was used at 1/ 2,500 dilution. vFLIP protein is approximately 21kDa, the Myc-his tag adds approximately 2.5kDa.

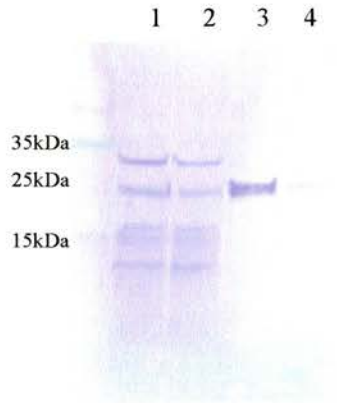

Figure 3.24 Western blot of vFLIP purification by nickel affinity. Lane 1, solubilised proteins; lane 2, unbound protein; lane 3, elute 1; lane 4, elute 2. The primary antibody, mouse anti-Myc (Invitrogen), was used at 1/ 3,000 dilution and the secondary antibody, goat anti-mouse alkaline phosphatase, at 1/ 2,500 dilution.

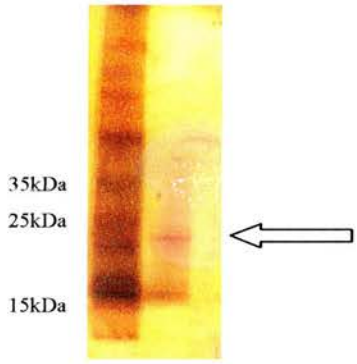

Figure 3.25. Silver stain of purified protein. A clear band is seen at approximately 21kD, the correct molecular weight to be vFLIP.

Once purified, vFLIP protein was concentrated using VIVASPIN columns and stored at -20°C. Four, monthly injections of 100µl (approx 150µg) vFLIP were made into a rabbit.

3.5.2.1 Testing the antiserum

The resulting antiserum was tested in both Western blotting, against purified vFLIP, and immunostaining, of BCP-1 cytospins, for its activity against vFLIP. Unfortunately the serum proved to be unreactive in both procedures

3.6 Conclusions

Through the generation of recombinant MHV-76 viruses expressing KSHV vFLIP we hoped to determine the effects of vFLIP expression on viral pathogenesis. The first viruses to be constructed utilised the CMV IE promoter to drive expression of the selection markers and, in the case of FL1 and FL2, vFLIP. *In vitro* characterisation by means of a one-step growth curve demonstrated that the three recombinant viruses replicated with similar kinetics to the wild-type MHV-76 (figure 3.5). However, the vFLIP expressing viruses lagged behind the wild-type and IRES control viruses in terms of the viral titre achieved at 72 hours p.i. Two possible explanations for this may be that either the expression of vFLIP is in some way reducing the lytic replication of the FL1 and FL2 viruses, or the virally infected cells are surviving longer and thereby increasing the time taken from infection to release of virus so the curve lags behind that of wild-type virus. Northern blotting of total RNA extracted from infected C127 cells indicated that transcription of viral genes

was taking place and that vFLIP transcripts were present in the FL1 and FL2 infected cells (figure 3.6). As mentioned, in the absence of an antiserum against vFLIP it is impossible to prove that vFLIP protein is being translated; we must assume that the strong EMCV IRES results in some protein production. It must be remembered that KSHV vFLIP is translated via an IRES element (Bieleski and Talbot, 2001) and therefore one can argue that its dependence upon an IRES for translation in this system is representative of the situation in KSHV infection.

Both FL1 and FL2, in which insert expression is driven by the CMV IE promoter, achieved significantly higher titres of infectious virus in the lungs of BALB/c mice at day 5 p.i. than did the control IRES virus (figure 3.7). They also reached titres approximately 2 log higher than MHV-76. It is worth noting that the lung titres observed following MHV-76 infection were lower than normal in this experiment and so great significance should not be given to this difference. That said the difference between the vFLIP expressing viruses and the IRES control is large and real. It may be inferred from this result that vFLIP provides some replicative advantage at the initial stages of infection. It is possible that use of the CMV IE promoter results in very high expression of EGFP resulting in a strong immune response to the recombinant viruses. The expression of vFLIP may delay cell death for long enough to allow greater levels of viral replication to take place in FL1 and FL2 infection.

As has previously been noted following infection of BALB/c mice with recombinant viruses of this type (Douglas et al., 2004; Brass, 2004) all three recombinant viruses were severely attenuated in terms of the cell-associated viral titre in the spleen (figure 3.9). The reasons for this are unclear. We hypothesised that the attenuation

was most likely due to either an enhanced immune response to the inserted sequences, perhaps EGFP, or a failure of the virus to reactivate from latency. I attempted to determine whether an immune response against EGFP was responsible through the infection of EGFP-expressing ROSA mice. Unfortunately determination of the infective centre titres in the spleens of these mice at day 10 p.i. revealed that not only the recombinant viruses but also MHV-76 were attenuated, reaching extremely low titres (figure 3.21). The levels of MHV-76 virus detected are at a similar level to that seen for the recombinant viruses in the BALB/c experiments (figures 3.9 and 3.19). Statistically speaking, the recombinant viruses and MHV-76 produce the same infective centre titres in ROSA mice i.e. the previously observed difference is abolished. One could interpret this as an abolition of the relative attenuation and therefore conclude that the previously seen deficiency of the recombinant viruses was due to their expression of EGFP. However, because the numbers are so small it is impossible to say conclusively. One would need to repeat the experiment in L129 mice to confirm that the recombinants reach a significantly lower infective centre titre than MHV-76 and if the numbers seen in this experiment are repeated this may well be impossible. The other possibility is that the viruses are unable to reactivate once they have established latency. Previous studies have indicated that viral DNA is present in the spleens of animals infected with recombinant viruses suggesting that there may be inefficient reactivation from latency (Brass, 2004). Unsurprisingly, given the extremely low recombinant virus titres in the spleen, no viral DNA was detectable in animals infected one year previously.

When it became apparent that the CMV IE driven viruses were attenuated in the spleen we decided to stop using them. At the time the focus of our experimental plans was driven by the fact that vFLIP is one of only three truly latent genes encoded by KSHV and we were therefore interested in looking for more long-term effects of vFLIP expression *in vivo*. However, vFLIP is also transcribed during lytic replication and thus may be important during this stage of the viral lifecycle. In hindsight the CMV viruses may have proved to be useful tools for investigating primary infection, especially now that it is clear that all recombinant viruses expressing EGFP and hygromycin resistance are attenuated.

As we were looking to elucidate the role of vFLIP over the long-term course of infection and because it has been reported that the CMV IE promoter is silenced over time (Gerolami et al., 2000) it was decided to construct new recombinant viruses in which expression of the inserted sequences would be driven by the PGK promoter. This is a murine promoter of a house-keeping gene and it is known to be active in most cell types and to be constitutively active (Gerolami et al., 2000). The vFLIP expressing virus, FL3, and control, PGK-IRES, were successfully constructed and purified. The replication of the viruses *in vitro* was investigated by means of a one-step and a multi-step growth curve: in both cases the recombinant viruses replicated with identical kinetics to MHV-76 and there was effectively no difference in the viral titres at any time point (figures 3.13 and 3.14 respectively). As previously, Northern blotting following infection of C127 cells with the two recombinant PGK driven viruses results in viral transcription and vFLIP transcription from FL3 (figure 3.6). Perhaps significantly the amount of vFLIP transcript present is greatly reduced in comparison to FL1 and FL2 infection: this demonstrates that the PGK promoter is

not as strong as the CMV IE promoter and implies that the level of vFLIP produced following *in vivo* infection will be lower than that resulting from FL1 and FL2 infection.

Determination of infectious virus titres in the lung shows that, in contrast to the CMV IE viruses, there is no difference in the replication of the control and vFLIP expressing viruses (figure 3.15). As PGK is not as strong a promoter as CMV IE, and consequently EGFP would not be expressed at such high levels, this gives weight to the theory that the reduced titre of the IRES control virus in the lung seen previously (figure 3.7) may be due to an immune response against EGFP. Perhaps when the levels of expression are reduced (because they are driven by the PGK promoter) the reaction to EGFP is not as severe and, therefore, the protective effect of vFLIP, which would be at a lower level itself, is not as apparent. The immunostaining carried out on frozen lung sections (figure 3.17) clearly shows the presence of virus in the lungs at early time points and its clearance by day 10. There was no distinct difference in the number or size of the foci of infection between all three viruses: this is not unexpected as the titres of all three viruses are very similar.

The PGK recombinant viruses were attenuated in the spleen in a similar manner to the CMV IE viruses (figure 3.19). The failure of the ROSA experiment to shed any light on the reason for the attenuation is frustrating; it remains unknown whether it is due to an immune response resulting in rapid clearance of the virus from the infected mice or because the viruses are unable to reactivate from latency. Whatever is the case it would seem that the attenuated phenotype is the result of the nature of the insertion into the LHE of MHV-76. These low infective centre titres in the spleen have been observed following infection of BALB/c mice with recombinant MHV-76

viruses expressing the KSHV genes vOx2 and K1 together with EGFP and hygromycin resistance (Douglas et al., 2004; Brass, 2004). In contrast, recombinant viruses in which the gene of interest was inserted into the LHE under the control of its own promoter and without selection markers are not attenuated in the splenocyte viral load (Townsley et al., 2004). Ultimately unsuccessful attempts to generate a recombinant virus in which vFLIP was inserted under the control of the PGK promoter and without selection markers were made. It seems that, for some reason, the PGK-vFLIP and PGK-EGFP sequences were not maintained within the viral genome. This phenomenon has been observed by others attempting to insert a similarly sized fragment into the LHE of MHV-76 (A.Cliffe; personal communication). It is possible that the small size of the insert results in a packaging deficiency for the virus: the addition of "stuffer DNA" sequences into the LHE may aid future attempts at generating recombinant MHV-76 viruses without EGFP and hygromycin resistance.

In an attempt to generate antiserum reactive against KSHV vFLIP two different protein purification systems were utilised. The first of these, glutathione affinity chromatography, which required vFLIP to be expressed as fusion protein with the GST moiety proved ultimately frustrating. With one exception all purification procedures resulted in vFLIP-GST fusion protein: the cleavage of GST from vFLIP by thrombin was in some way inhibited. Rabbits were injected with the fusion protein in the hope that there would be a reaction to vFLIP but the resulting serum was only reactive against a GST-sized protein (figure 3.23).

In terms of protein production, the second system, nickel affinity purification, was much more successful. Pure vFLIP protein was generated on all occasions.

However, injection of this vFLIP into rabbits failed to generate reactive antiserum. The reasons for this are unclear but one possibility may be that the level of homology between vFLIP and the rabbit $cFLIP_s$ was too great and that the KSHV protein was not recognised as being foreign.

Chapter 4 Utilisation of recombinant viruses to investigate establishment of latency i*n vitro*

Utilisation of recombinant viruses to investigate establishment of latency *in vitro*

4.1 Determination of the ability of recombinant and wild-type MHV-76 to infect NS0 cells

The inability of any of the recombinant viruses to establish a latent infection *in vivo* has meant that the mouse model could not be used to elucidate the long-term effects of vFLIP expression on the progression of disease. An alternative system by which viral latency could be investigated was therefore sought. It has previously been reported that MHV-68 can establish latency in the murine B cell line NS0 (Sunil-Chandra et al., 1993). If the same were true for MHV-76 and the MHV-76 recombinant viruses, NS0 cells may represent a useful system for studying latency *in vitro*. As mentioned previously none of the recombinant viruses were able to establish detectable latency *in vivo*; the reason for this is unknown but may be exacerbated by an immune response to EGFP.

NS0 cells are a myeloma cell line derived from the MOPC 21 BALB/c myeloma (Kohler and Milstein, 1976). Cells were infected at a M.O.I. of 5 and maintained at 37°C, 5% CO_2. Initially the cells were thought to be uninfected as there was no detectable EGFP expression. Nevertheless cellular DNA was extracted at 5 days p.i. and a PCR for MHV-76 ORF 50 was carried out using primers RTA3F and RTA3R. This proved positive in the case of all three viruses, although only weakly so for MHV-76, indicating that the cells were infected (figure 4.1).

Figure 4.1 PCR for MHV-76 ORF 50 carried out using DNA extracted from infected NS0 cells at 5 days p.i. Lanes 1-3, FL3 infected cells; lanes 4-6, PGK-IRES infected cells; lane 7, MHV-76 infected cells; lane 8, water.

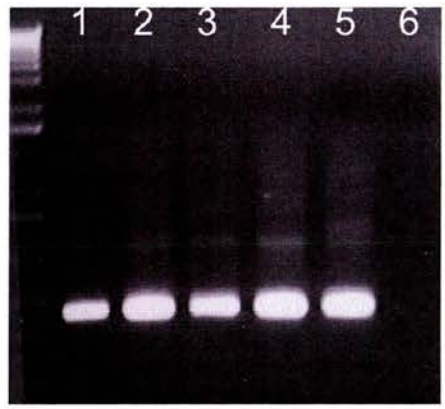

Figure 4.2 PCR for GAPDH carried out on cDNA from virally infected cells. Lanes 1-2, FL3 infected NS0 cells; lanes 3-4, PGK-IRES infected NS0 cells; lane 5, BCP-1 cells; lane 6, water.

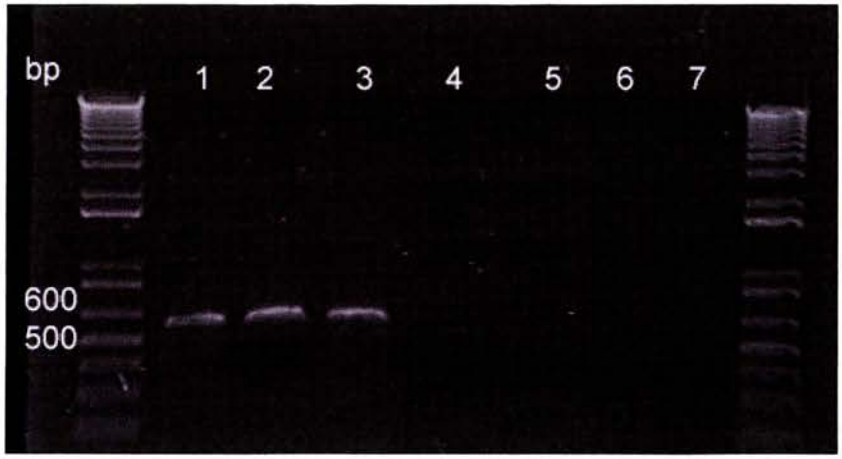

Figure 4.3 PCR for vFLIP carried out using cDNA generated from virally infected cells. Lanes 1 and 2, FL3 infected NS0 cells (2 separate cultures); lane 3, BCP-1 cells; lanes 4 and 5, FL3 infected NS0 cells –RT; lane 6, BCP-1 cells –RT; lane 7, water.

Subsequently mRNA was extracted from recombinant virus infected cells (4 days p.i.) and cDNA was generated. The quality of the cDNA was checked by PCR for GAPDH using primers GAPDH 1 and GAPDH 2 (figure 4.2). A PCR for vFLIP was then carried out using primers 76-1 and 76-2 (figure 4.3). This indicated that vFLIP was being actively transcribed in infected NS0 cells.

Having established that NS0 cells were permissive for infection with MHV-76 recombinant viruses and, therefore, presumably wild-type MHV-76, viral replication and its effects on cell proliferation were investigated.

4.2 Cell proliferation following infection

Infection of fibroblast cells lines e.g. BHK-21, with MHV-76 and the recombinant viruses results in rapid induction of cytopathic effects. In contrast, the majority of infected NS0 cells appear healthy. After infection at a M.O.I. of 5, measurements of viable cell numbers were taken over the next 21 days using trypan blue staining to distinguish viable from dead cells. The cell counts demonstrate that the cells continue to proliferate post infection (figure 4.4).

During the course of experimental infection dead cells were not removed by Histopaque-1077 separation in order to prevent loss of infectious virus in the supernatant. As a result, at later time points, the proportion of dead cells within the population was increased, however, viable cells remained in the majority at all times. The rate of cell proliferation is identical following infection with all three viruses which implies that the expression of vFLIP confers no growth advantage or disadvantage for the cells *in vitro*.

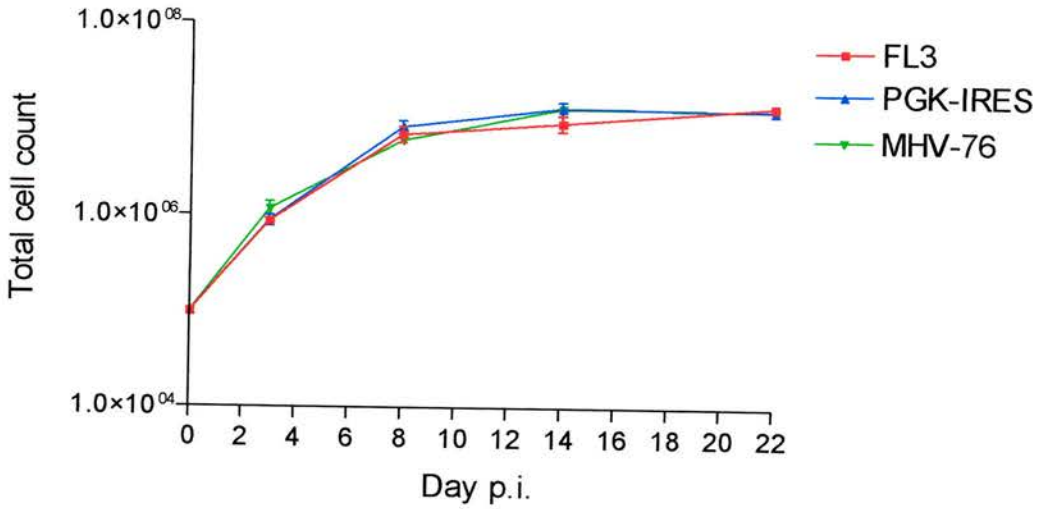

Figure 4.4 Total numbers of viable NS0 cells following infection with MHV-76, FL3 and PGK-IRES. Two infections with each virus were carried out in parallel; the data represents the mean value per virus at each time point.

4.3 Virus production and establishment of latency

The levels of virus in the supernatant were measured by plating dilutions of the supernatant, from a known number of NS0 cells, with BHK-21 cells. The supernatant viral titre was then calculated. This provides an indication of the amount of infectious virus being released by each cell line. The resulting data can be seen in figure 4.5. At all time points tested, and for all three viruses, there was infectious virus present in the supernatant. The titre of each virus decreased over the course of the experiment with FL3 titre decreasing most slowly. Throughout the course of the experiment there was more virus released from the FL3 infected cells than from either the PGK-IRES or MHV-76 infected cells. This could be because a greater proportion of the cells within the population were infected or because a larger burst size was achieved following FL3 infection.

Levels of cell-associated virus were assessed by standard infective centre assay, titrated on BHK-21 cells (figure 4.6). Again, there is no particular difference between the viruses in terms of the kinetics of the curves. The initial titres of FL3 and PGK-IRES are approximately one log greater than MHV-76. This may be partially due to an inaccuracy in dispensing the viruses, however, as the supernatant titres are almost identical at 0hrs it may be that the FL3 virus bound to the cells more efficiently. Whilst the infective centre assay allows calculation of the amount of cell-associated virus (both latent virus and infectious cell-associated virions) associated with the NS0 cells it gives no indication of the relative amounts of each. In order to distinguish between the two, the cells were subjected to freeze thaw treatment prior to titration of the resulting lysate (figure 4.7). Following this procedure only pre-formed virions will be capable of infecting cells resulting in plaque formation; no reactivation of latent virus will occur.

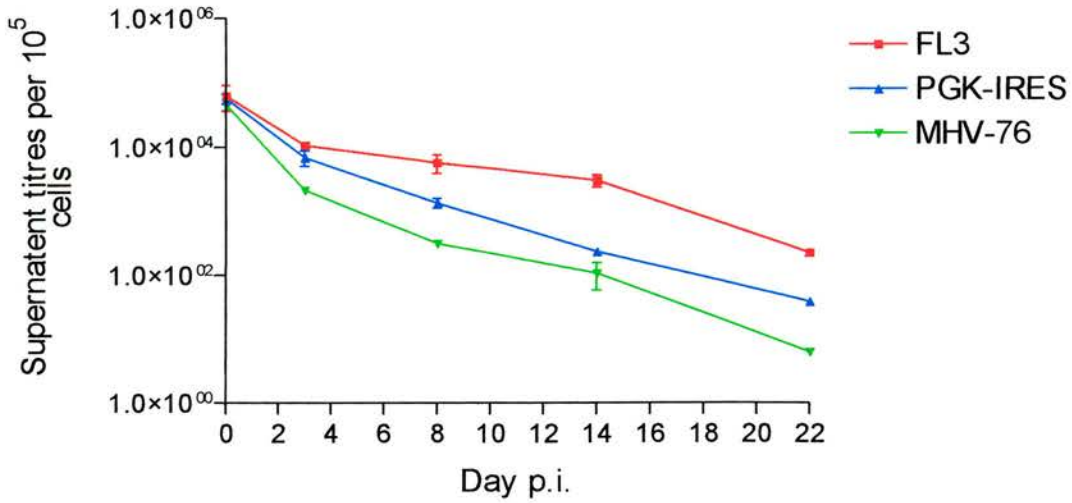

Figure 4.5 Infectious virus titre in the supernatant of infected NS0 cells. Data at each time point represent the mean of duplicate samples +/- S.E.M.

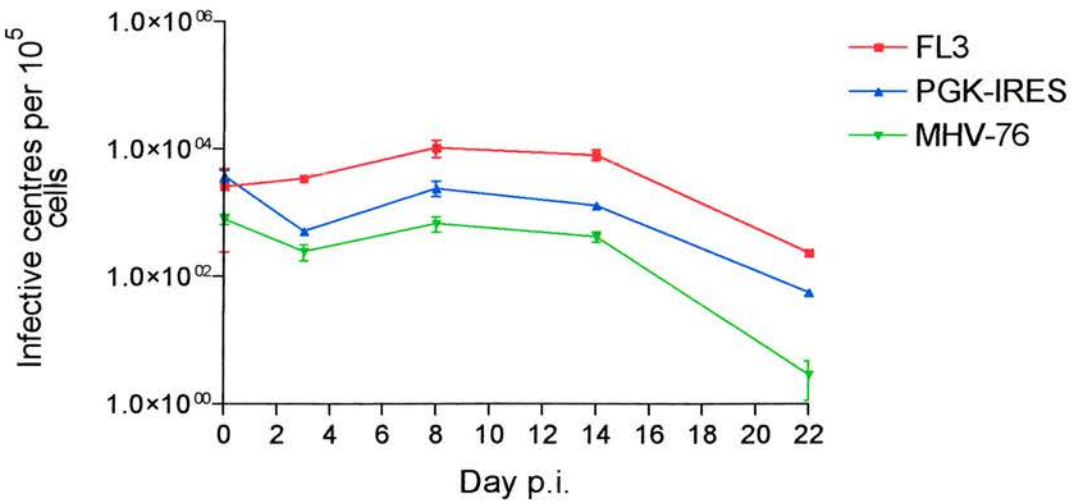

Figure 4.6 Infective centre titres of infected NSO cells.

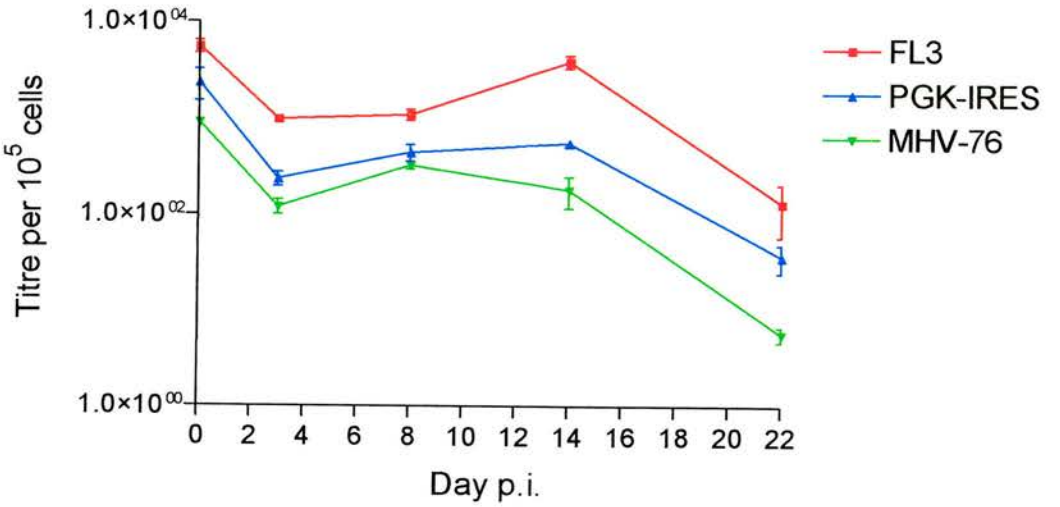

Figure 4.7: freeze thaw titres- indicating levels of cell-associated infectious virions.

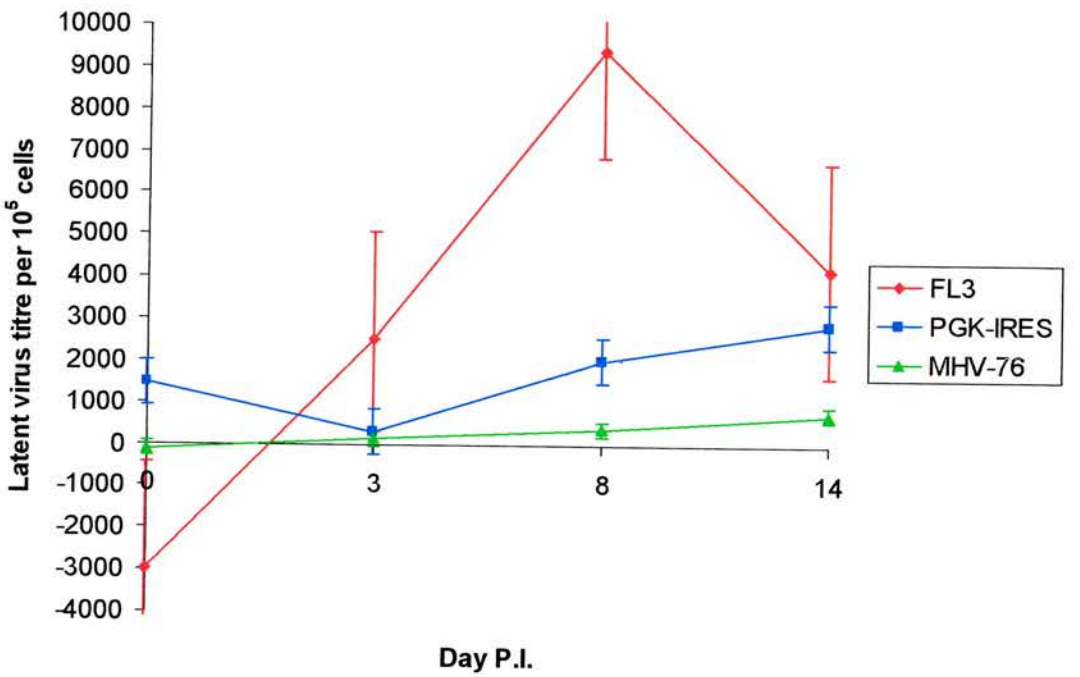

Figure 4.8 Latent virus titres of infected NS0 cells; calculated by subtracting freeze-thaw titres from infective centre titres.

Combining the data displayed in figures 4.6 and 4.7 enables the latent virus titre at each time point to be calculated (figure 4.8). The latent titres achieved following infection of NS0 cells with the three viruses vary considerably. FL3 establishes a much greater pool of latently infected cells than does PGK-IRES and MHV-76. This is most pronounced at day 8 p.i. at which point FL3 displays a 4-fold greater latent titre than PGK-IRES and a greater than 25-fold higher latent titre than wild-type MHV-76. These titres, calculated by subtracting the freeze-thaw titre from the cell-associated virus titre, may also prove to be an underestimate of the true extent of latency. Each plaque formed following titration of the cells following freeze-thaw treatment represents one infectious virus particle. However, each infected cell would most likely contain more than one infectious virion and consequently subtraction of these values will result in an underestimation of latent titre although this may be equal for all three viruses.

4.4 NF-kB activation following viral infection *in vitro*

Whilst working toward this thesis it was reported that the expression of KSHV vFLIP led to the activation of the cellular transcription factor NF-κB (Liu et al., 2002; Sun et al., 2003). NF-κB activation is important for the control of cell survival following a stress-inducing event. There are NF-κB response elements located in the promoters of more than 150 cellular genes (Pahl, 1999); these include pro-inflammatory cytokines and chemokines, immunoreceptors, anti-apoptotic proteins and factors involved in cell proliferation. Among the anti-apoptotic proteins induced by NF-κB, in conjunction with at least one other transcription factor, is cFLIP (Kreuz

et al., 2001). Thus, one result of vFLIP mediated NF-κB activation may be a general increase in FLIP activity in an infected cell; perhaps representing a kind of positive-feedback. Additionally, NF-κB activation has been implicated in the progression of cancers, toward which its anti-apoptotic and pro-inflammatory activity contribute (reviewed in (Karin et al., 2002; Pikarsky et al., 2004)): again, this may be a mechanism by which vFLIP can contribute toward the pathogenesis of KSHV. Finally, NF-κB activation has been shown to play an important role in the lifecycle of herpesviruses including HCMV, which requires functional IKK2, an NF-κB activator, to complete productive replication (Caposio et al., 2004) and EBV, which is dependent on NF-κB for LCL survival (Cahir-McFarland et al., 2004). Co-transfection of reporter plasmids under the control of gammaherpesvirus lytic promoters, together with their activators and increasing amounts of the transcriptionally active (p65) subunit of NF-κB, indicates that NF-κB is able to inhibit promoter activity in a dose dependant manner (Brown et al., 2003). As NF-κB appears to promote the survival of latently infected EBV positive cells and perhaps to inhibit reactivation, via its suppression of lytic promoters, the possibility that activation of NF-κB contributes toward the increase in numbers of latently infected NS0 cells following FL3 infection was investigated.

An electrophoretic mobility shift assay, using the NF-κB response element as the probe, was carried out in order to establish the kinetics of NF-κB activation following infection of NS0 cells with the recombinant viruses FL3 and PGK-IRES and the wild-type MHV-76. Cells were infected at a M.O.I. of 5 and subsequently maintained at 37°C, 5% CO_2. At each time point $1x10^7$ cells were harvested and nuclear extracts prepared. Uninfected NS0 cells were used as a negative control and

BCP-1 cells, which display constitutive activation of NF-κB (Cerimele et al., 2001), as a positive control. Samples were taken at days 1, 3, 5, 8 and 21 post infection. With the exception of the day 21 samples, dead cells were not removed by Histopaque-1077 separation; however, the cells were supplied with extra growth medium. EMSAs were carried out as described in Materials and Methods and can be seen in figures 4.9 to 4.13. At day 1 p.i. a shift can be seen in all lanes, except uninfected NS0, indicating that NF-κB was activated in all virally infected cells (figure 4.9). The shift observed using the BCP-1 nuclear extract is at a slightly different location to those observed using NS0 extracts: this is most likely to be due to the different amino acid composition and thus relative charge of the human and murine NF-κB subunits. These differences would be reflected in differences in mobility through the non-denaturing gel. In all three cases the activation of NF-κB was maintained throughout the time course of infection, up to day 8 p.i. The amount of protein used in each binding reaction was kept relatively constant through use of the same numbers of cells in each nuclear extract preparation and the same volume of extract in each reaction. By day 21 p.i. the shift in MHV-76 infected cells is much less intense than that in FL3 infected cells (figure 4.13), in fact it has almost disappeared. The intensity of the band in the PGK-IRES infected cells is less than that of the FL3 infected cells at day 21 p.i.: densitometry analysis (table 4.1) indicates that the PGK-IRES band is less than half as intense as the FL3 band suggesting that there is greater NF-κB activation in cells latently infected with FL3 than with the control.

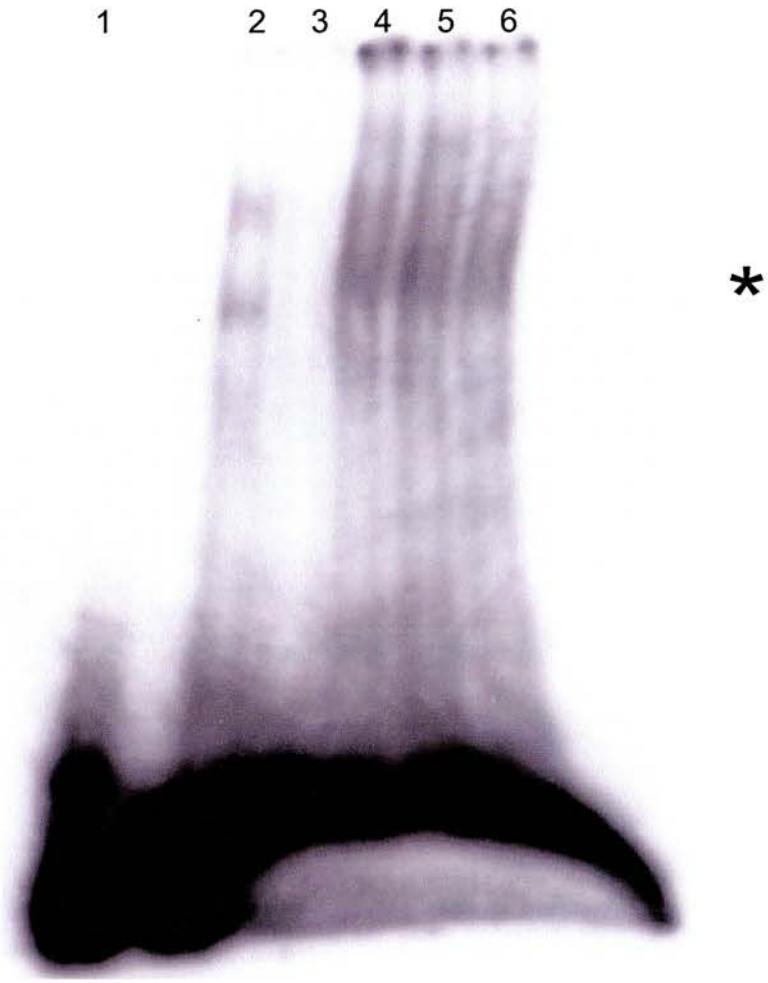

Figure 4.9 EMSA to show activated NF-κB in nuclear extracts of virally infected cells at day 1 post infection. Lane 1, probe only; lane 2, BCP-1; lane 3, NS0 only; lane 4, NS0 + FL3; lane 5, NS0 + PGK-IRES; lane 6, NS0 + MHV-76.

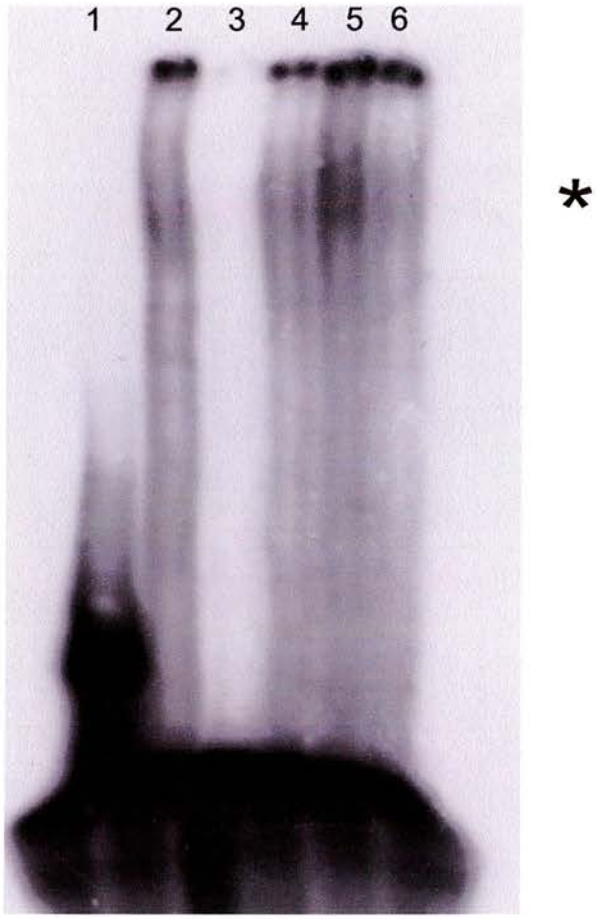

Figure 4.10 EMSA to show activated NF-κB in nuclear extracts of virally infected cells at day 3 post infection. Lane 1, probe only; lane 2, BCP-1; lane 3, NS0 only; lane 4, NS0 + FL3; lane 5, NS0 + PGK-IRES; lane 6, NS0 + MHV-76.

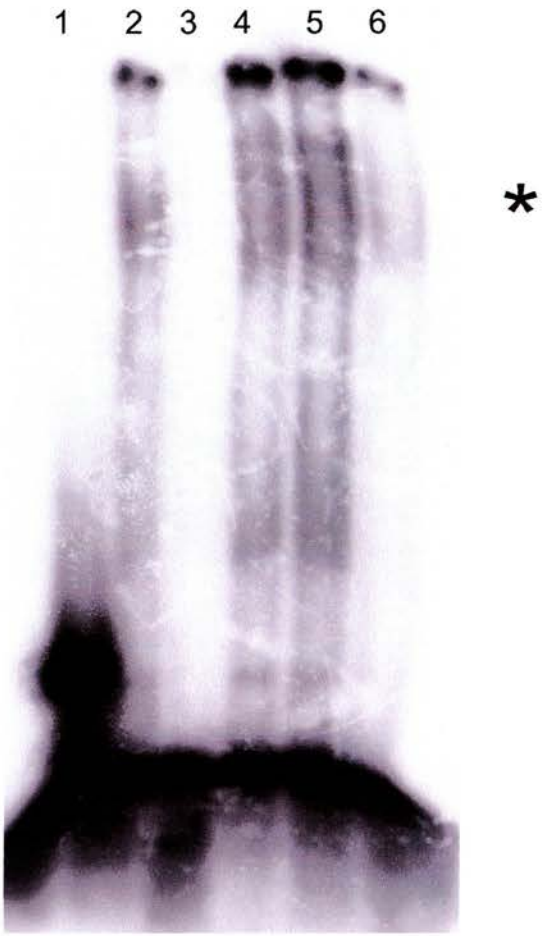

Figure 4.11 EMSA to show activated NF-κB in nuclear extracts of virally infected cells at day 5 post infection. Lane 1, probe only; lane 2, BCP-1; lane 3, NS0 only; lane 4, NS0 + FL3; lane 5, NS0 + PGK-IRES; lane 6, NS0 + MHV-76.

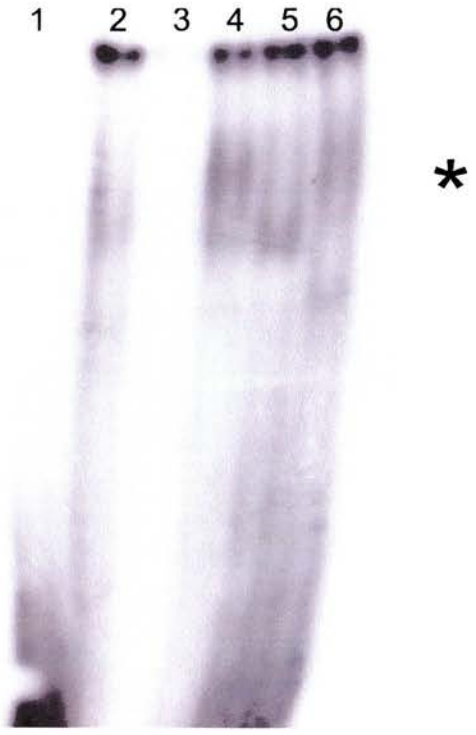

Figure 4.12 EMSA to show activated NF-κB in nuclear extracts of virally infected cells at day 8 post infection. Lane 1, probe only; lane 2, BCP-1; lane 3, NS0 only; lane 4, NS0 + FL3; lane 5, NS0 + PGK-IRES; lane 6, NS0 + MHV-76.

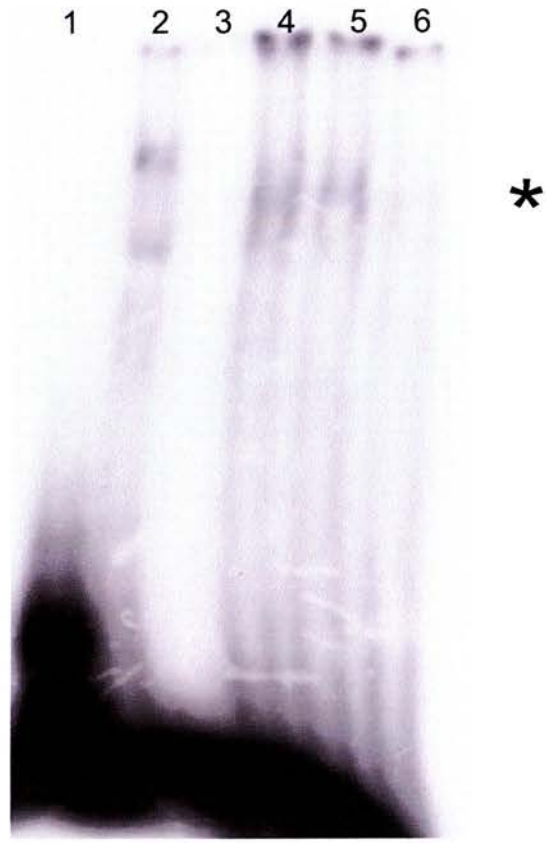

Figure 4.13 EMSA to show activated NF-κB in nuclear extracts of virally infected cells at day 21 post infection. Lane 1, probe only; lane 2, BCP-1; lane 3, NS0 only; lane 4, NS0 + FL3; lane 5, NS0 + PGK-IRES; lane 6, NS0 + MHV-76.

FL3	PGK-IRES	Ratio FL3: PGK-IRES
51.465	20.026	2.57: 1

Table 4.1 Table showing densitometry data from latent EMSA (figure 4.13). Readings are integrated optical density.

4.5 Conclusions

This work demonstrates that the recombinant viruses, FL3 and PGK-IRES, and wild-type MHV-76 are able to infect a B cell line, NS0, and establish a persistent, latent, infection of these cells. Cell-associated virus could be detected up to 35 days p.i. by infective centre assay (data not shown). This suggests that the inability of the recombinant viruses to establish latency *in vivo,* demonstrated in chapter 3, may be the result of some kind of immune response directed against one or more inserted products, most likely EGFP: such a response would be lacking *in vitro.* Consequently, it appears that any elucidation of the contribution of vFLIP towards long term *in vivo* pathogenesis would be impossible using these recombinant viruses. However, NS0 cells represent a system whereby some of the reported activities of vFLIP may be assessed in the context of a latent viral infection.

There is a marked difference between the *in vitro* phenotypes displayed following FL3 infection of NS0 cells when compared to infection with the control recombinant virus, PGK-IRES, and MHV-76. The amount of infectious virus produced by FL3 infected cells is greater than that released from PGK-IRES and MHV-76 infected cells (figure 4.5). Moreover, FL3 infection results in a greater cell-associated virus titre and higher titres of infectious virions per culture. Subtracting the cell-associated infectious virion titres (figure 4.7) from the infective centre titres (figure 4.6) allows calculation of the latent viral titre (figure 4.8). This demonstrates that FL3 initially establishes a greater degree of latency than do PGK-IRES and MHV-76. The difference is most distinct at day 8 p.i. after which the FL3 latent titre begins to fall. From this data it appears that vFLIP expression infers an advantage in the establishment of a latently infected pool of cells. This is particularly striking at

earlier time points: by day 8 post infection the FL3 infected cells display more than 4-fold greater latent titres than the PGK-IRES control and an even greater difference in titre when compared to wild type MHV-76 (approximately 25-fold). Thus, in this system, the expression of vFLIP confers an advantage to the virus through the establishment of a larger pool of latently infected cells than that established by the control recombinant virus or MHV-76. If such behaviour is indicative of its *in vivo* role this would imply that expression of vFLIP aids the initial viral infection and enhances the establishment of latency.

It would seem very unlikely that the differences observed in this system are a result of the directly anti-apoptotic activity of vFLIP i.e. its prevention of caspase-8 activation. This being so one must turn to vFLIPs other properties to determine how it elicits this effect. Over the last few years a second property of vFLIP has come to the fore namely its activation of the transcription factor NF-κB. This may be mediated by association of vFLIP with the IKK complex, via IKKγ (Field et al., 2003), resulting in constitutive phosphorylation of the IκBα subunit (Liu et al., 2002) and release of active NF-κB which is subsequently imported into the nucleus. The activation of NF-κB has been demonstrated to be necessary for the survival of KSHV infected PEL cells (Keller et al., 2000); vFLIP is responsible for maintaining constitutive NF-κB activity in these latently infected cells and vFLIP expression is essential for their survival (Guasparri et al., 2004).

In the light of this work the activation of NF-κB as a result of infection by the recombinant viruses, FL3 and PGK-IRES, was assessed and compared to the activation resulting from MHV-76 infection. This was done by EMSA using a ^{32}P-labelled NFκB binding site as the probe. Infection with all viruses resulted in

activation of NF-κB: this was expected as viral infection is one of the many events capable of activating NF-κB (reviewed in (Pahl, 1999)).

NF-κB remains activated in all virally infected cell cultures up to day 8 p.i. Once latency is established, assessed at day 21 p.i., there is almost no activated NF-κB in the MHV-76 infected cell culture. This is in contrast to the recombinant viruses. Whilst a quantitative measurement of NF-κB activation is difficult it is apparent that FL3 results in constitutive activation of NF-κB, but that this is not observed following MHV-76 infection. The day 21 data also seem to suggest that PGK-IRES infection results in the constitutive activation of NF-κB albeit at an apparently lower level than results from FL3 infection. If NF-κB activation is indeed responsible for the enhanced viral titres and establishment of latency observed in FL3 infection, the activated NF-κB in the PGK-IRES infected NS0 cultures explains why this recombinant virus displays a higher latent titre than the wild-type MHV-76 (figure 4.8). At this point one can only speculate as to the reason why PGK-IRES infection should result in long-term activation of NF-κB. It would seem very unlikely to be a result of EGFP-hyg expression; however, it is perhaps a possibility that the EMCV IRES in the inserted sequence at the LHE of PGK-IRES is able to drive expression from the first MHV-76 ORF in the virus. There is a short section of MHV-68 M4 sequence incorporated into pAB13 (Brass, 2004) and thus pFL3; this corresponds to the final 84 amino acids at the C-terminus of the M4 protein (56 of which follow the first methionine residue encoded). It has been suggested that M4 has a role in both the establishment of latency and in immunoregulation (Townsley et al., 2004). Consequently, if there is some leaky expression of a C-terminal fragment of M4 it is

a possibility that it is able to mediate NF-κB activation or to influence latency via some other mechanism.

I would hypothesise that FL3 infection results in a greater and longer lasting activation of NF-κB than either the control recombinant PGK-IRES or the wild type MHV-76 and that this is responsible for the greater latent viral titres seen following infection of NS0 cells *in vitro*.

It has previously been reported that vFLIP, through its activation of NF-κB, is essential for the survival of latently infected PEL cell lines (Guasparri et al., 2004). The data presented in this chapter indicates that this property of vFLIP also enhances the initial establishment of latency immediately following infection.

Chapter 5 Identification of IRES interacting factors

Identification of IRES interacting factors

Since the initial identification of internal ribosome entry as a mechanism of translation, the range of viral and cellular genes shown to be translated via an IRES has grown rapidly. The additional factors necessary for IRES function range from the 80s ribosomal subunits only (Wilson et al., 2000) to the canonical translation initiation factors together with several cis-acting factors. The KSHV IRES has previously been shown to be active only in KSHV positive cell lines (Bieleski and Talbot, 2001). This cell type specificity would make it unlikely that ribosome assembly occurs directly and raises the possibility that cis-acting factors are required. To date, only a limited number of IRES transactivating factors (ITAFs) have been identified. These include polypyrimidine tract binding protein (PTB), upstream of N-ras (unr) and members of the eIF4G family of translation initiation factors. Attempts were made to identify protein factors from PEL cell lines that are able to interact with the KSHV IRES.

Several different assays to determine RNA-protein interactions have been described. These include the yeast-3-hybrid system, cross-linking assays and pull down assays. Attempts to identify proteins capable of interacting with the KSHV IRES utilised a range of these techniques.

5.1 Yeast 3-hybrid assay

The aim behind conducting a yeast 3-hybrid screen was to carry out screening of all proteins expressed in a KSHV positive cell line; that is all the proteins present in a system in which the IRES is functional. It was hoped that proteins capable of interacting with the IRES sequence would be identified and that these could then be further characterised to establish whether they were necessary for translation initiation from the IRES.

The yeast 3-hybrid screen was developed to allow the detection of RNA-protein interactions independently of the biological role of the elements of interest (SenGupta et al., 1996). Based upon the yeast 2-hybrid system (Fields and Song, 1989; Chien et al., 1991), which is used to detect protein-protein interactions, the system enables analysis of large libraries of RNAs or proteins to identify specific interacting species. The basic principle by which the system works is illustrated in appendix 3. The intention was to utilise the system to screen a library of proteins derived from the KSHV-positive BCP-1 cell line for species that interacted specifically with the IRES RNA. A primary lambda phage library of BCP-1 cDNA in the HybriZAP vector (Stratagene) had previously been constructed. This was converted to a pAD-GAL4 phagemid library, by *in vivo* mass excision, and titred at $1.6x10^9$ colony forming units/ml. Plasmid DNA containing the DNA inserts was purified using a Qiagen maxiprep kit following incubation of the XLOLR bacterial host strain with the phagemid particles. The minimal IRES sequence was cloned into the vectors pIII/MS2-1 and pIII/MS2-2 (provided by Marvin Wickens, University of Wisconsin) by annealing the oligos 3 HYB IRES 3 and 3 HYB IRES 4 and ligating the annealed oligos into *Sma*I digested vectors. Sequencing confirmed the insertion

of the IRES in the correct orientation and without mutations. The yeast strain L40 coat (provided by M.Wickens) was successfully transformed with both plasmids, separately, with selection on medium lacking uracil. The next stage was to optimise the transformation of the yeast expressing the IRES sequence with the library plasmids. In order to ensure as complete representation of the library as possible it is necessary to achieve a 10-fold greater number of transfectants than there are cDNAs within the library. Despite carrying out the transformation on many separate occasions and changing a number of variables including: the order of transformation (i.e. IRES or library first or double transformation); amount of DNA; heat shock time; method of library DNA preparation (Qiagen kits and $CsCl_2$) and yeast strain, the efficiency with which the yeast could be transformed with the library was never great enough to allow screening to proceed.

5.2 Investigation of specific ITAFs

The failure of the yeast 3-hybrid screen was particularly disappointing as it would have allowed a global screening approach with all possible binding partners examined. The alternative strategies, whilst valid methods for the identification of interacting partners, were inferior, in that some idea as to the possible identity of the KSHV ITAFs was required. The decision was made to concentrate on factors already identified as ITAFs for other IRES elements and to investigate whether any of these could interact with the KSHV IRES.

Upon analysis of the IRES sequence the most striking feature to emerge is the presence of a polypyrimidine tract (PPT) (see figure 1.8). Using a number of

different bicistronic reporter constructs the minimum RNA sequence required for IRES activity has been determined; the PPT was shown to be fundamental (Bieleski et al., 2004). The polypyrimidine tract binding protein, PTB (hnRNP I), has been shown to associate with a number of different viral and cellular IRES elements. Viral IRES elements with which PTB interacts include FMDV (Luz and Beck, 1991; Luz and Beck, 1990), ECMV (Jang and Wimmer, 1990), poliovirus (Hellen et al., 1994) and hepatitis C virus (Ali and Siddiqui, 1995). Subsequent work has demonstrated that, in the majority of cases, PTB not only interacts with these IRESs but that this interaction is necessary for efficient cap-independent translation to occur. An example of this is the HCV IRES; the inhibition of PTB by the addition of an excess of its RNA binding site (Anwar et al., 2000) or by the expression of siRNA against PTB (Zhang et al., 2004) ablated IRES activity. In terms of cellular IRES elements, PTB associates with the Apaf-1 IRES and is proposed to be involved in altering the mRNA structure to allow interaction with the ribosome (Mitchell et al., 2003; Mitchell et al., 2001). In the light of its regular identification as an ITAF and the presence of the PPT within the KSHV IRES, PTB was investigated as a possible KSHV ITAF.

Whilst IRES mediated translation does not require the full translation initiation complex (eIF4F and associated factors) most cases investigated so far do not work independently of all eIFs. In particular, members of the eIF4G family have frequently been identified as being necessary for IRES activity. eIF4G itself, of which there are two functional homologues eIF4GI and eIF4GII (Gradi et al., 1998), can be regarded as a modular protein of at least 154kDa (Yan et al., 1992), consisting of three domains each of which interacts with different components of the

translational machinery. The N-terminus associates with the cap-binding protein eIF4E (Lamphear et al., 1995) and the polyA binding protein (PABP) (Le et al., 1997); the middle section contains binding sites for eIF4A, which unwinds the DNA, and eIF3 which recruits the 40S ribosomal subunit to the mRNA (Imataka and Sonenberg, 1997); the C-terminus interacts with eIF4A and the eIF4E kinase Mnk1 (Pyronnet et al., 1999). The hepatitis A virus (HAV) IRES requires full length eIF4G for its activity; the cleavage of eIF4G by FMDV Lb protease or rhinovirus 2A protease inhibits HAV IRES activity (Borman and Kean, 1997). This is in stark contrast to all other picornavirus IRES elements characterised to date, all of which display enhanced translational activity following cleavage of eIF4G. It has been appreciated for many years that picornavirus infection results in cleavage of eIF4G, down-regulation of cellular protein synthesis and preferential translation of viral proteins (reviewed in Belsham and Sonenberg, 1996). The altered translation pattern is the result of eIF4G cleavage mediated by viral proteases, for example the 2A protease of poliovirus (Etchison et al., 1982) and the Lb protease of FMDV (Devaney et al., 1988). The picornavirus proteases cleave eIF4G at specific sites within its protein sequence; 2A protease cuts between amino acids 486 and 487 (Lamphear et al., 1993) and Lb protease between amino acids 479 and 480 (Kirchweger et al., 1994). As a result, the eIF4E and eIF3 binding sites of eIF4G become dissociated (Lamphear et al., 1993) thus inhibiting 5' cap-dependent translation. In addition to its inhibitory effect on 5'cap- dependent translation, the picornavirus mediated cleavage of eIF4G results in protein fragments that are necessary for viral IRES function. It has been demonstrated that the EMCV IRES requires only the central, eIF4A-binding, domain of eIF4G for activity (Pestova et

al., 1996). Following picornavirus induced eIF4G cleavage the C-terminal fragment, which includes this central domain, is able to promote cap-independent translation (Ohlmann et al., 1996; Pestova et al., 1996; Borman et al., 1997). Whilst 2A protease can directly target eIF4G (Lamphear et al., 1993), cleavage has been reported to proceed very inefficiently (Bovee et al., 1998); however, there are more recent reports indicating that, *in vitro* at least, the reaction proceeds more efficiently than previously thought (Glaser and Skern, 2000). In any case, there is evidence that in addition to direct cleavage, 2A protease activates an as yet unidentified cellular protease which goes on to target eIF4G (Zamora et al., 2002; Bovee et al., 1998). Interestingly, eIF4G mRNA itself apparently contains an IRES (Gan et al., 1998) although the levels of activity are disputed (Han and Zhang, 2002). Besides eIF4GI and eIF4GII, another member of the same protein family, death associated protein 5 (DAP5/ p97/ NAT1) can act as an ITAF for some IRES elements (Henis-Korenblit et al., 2000; Henis-Korenblit et al., 2002; Nevins et al., 2003). DAP5 was identified independently through screens to identify genes of the eIF4G family (Imataka et al., 1997) and mediators of apoptosis (Levy-Strumpf et al., 1997). DAP5 shares homology with the central sections of eIF4GI and eIF4GII, which are responsible for eIF4A and eIF3 binding, and totally lacks the eIF4G N-terminal domain. DAP5 itself can be translated via an IRES and accumulates in apoptotic cells in which cap-dependent translation is compromised in a translation reaction dependent on complete DAP5 or a caspase-cleaved fragment, DAP5/p86 (Henis-Korenblit et al., 2000).

The cleavage of eIF4G can also be initiated through the action of caspases following the induction of apoptosis (Clemens et al., 1998). The fragments generated are

different from those resulting from poliovirus protease cleavage; three relatively long-lasting fragments termed C-FAG, M-FAG and N-FAG are produced (Bushell et al., 2000). It is proposed that the middle fragment, which maintains interactions with eIF3, eIF4A and the ribosome, is able to support limited levels of cap-independent translation (Bushell et al., 2000).

One hypothesis could be that following infection with KSHV members of the eIF4G family are cleaved, either as a result of apoptosis or activation of a cellular protease by a KSHV protein, and the resulting fragments may be able to promote vFLIP translation. Alternatively it is a possibility that the IRES may be more similar to HCV and require full length eIF4G. As they are frequently identified as being necessary for both viral and cellular IRES function, members of the eIF4G family were investigated as possible KSHV ITAFs.

5.2.1 Pull down assay using full-length IRES

A pull down assay was developed based on the method described by Stassinopoulos and Belsham (Stassinopoulos and Belsham, 2001). The premise of the assay is to use the IRES sequence as a probe to deplete a protein extract containing species suspected of being able to associate with the RNA sequence. In order to achieve this the sequence of interest is cloned into a vector from which it can be expressed with a polyA tail. Once mixed with magnetic beads with covalently attached poly dT sequences, the RNA associates with the beads through base pairing. The beads, with attached probe, are then incubated with the protein extract after which the beads can be separated from the mixture using a magnet. After washing steps, to remove non-

specifically bound proteins, any species that have associated with the probe sequence can be eluted with a denaturing buffer and subjected to further analysis.

In the following experiments the full length KSHV IRES sequence (233bp) was used as a probe. The IRES sequence was amplified from BCP-1 DNA using the primers IRES forward and IRES reverse, for the sense direction, and Anti-IRES forward and Anti-IRES reverse, for the antisense direction. Both PCR products and the vector pSP64poly(A) (Promega) were digested with *Hind*III and *Sac*I, gel purified and ligated together to give the contructs pSP64sense and pSP64antisense. Correct insertion was confirmed by *Aat*II digestion. These constructs were then used as templates in *in vitro* transcription reactions to produce the probes. The IRES inserted in the antisense direction serves as a control for the specificity of any interactions (the antisense IRES had no activity when tested in a bicistronic reporter assay; Bieleski and Talbot, 2001). Proteins that were eluted from the beads were subjected to Western blotting using primary antibodies against proteins suspected as possible ITAFs.

An initial experiment was carried out using rabbit reticulocyte lysate (Promega) as the protein extract. Whilst this will not contain any KSHV proteins it should contain the majority of cellular proteins and therefore most previously identified ITAFs. The captured proteins and depleted extract were run on a 12% SDS PAGE gel and subjected to Western blotting using an anti-PTB antiserum (a gift from R.J.Jackson, University of Cambridge; Hunt and Jackson, 1999). This first assay (figure 5.1) indicated that PTB was able to interact with the KSHV IRES sequence: no PTB was detected following incubation of the beads alone with RRL, however, a clear doublet at ~65kD can be seen in both the sense and antisense lane.

Having demonstrated that the pull-down assay was functional, using RRL as the source of proteins, it was decided to use a more physiologically relevant protein extract. To this end S10 extract was prepared from BCP-1 cells: the KSHV IRES is functional in these cells and therefore they contain all the factors necessary for its activity. The pull down assay and Western blot were repeated as before. The resulting Western blot (figure 5.2) again shows that PTB was captured by the IRES transcribed in the sense orientation. Using the BCP-1 S10 extract the interaction is specific for the IRES in the sense orientation only.

In addition to PTB, the possibility that some form of eIF4G was able to associate with the KSHV IRES was investigated. An antibody against the C-terminus of eIF4G (Santa Cruz Biotechnology) was used in Western blotting against proteins eluted from the beads and depleted extract. RRL was used as the source of proteins. The Western blot (figure 5.3) shows clear bands in the lanes containing protein eluted from both the sense and antisense orientation RNA. However, these bands are approximately 75kD in size, much smaller than the 154kD size of intact eIF4G. Bands of this size were consistently pulled down, by both probes, when the assay was repeated using RRL making it unlikely to be an artefact. The requirement for eIF4G as an ITAF for IRES activity was investigated by means of a dual luciferase reporter assay, see section 5.3.

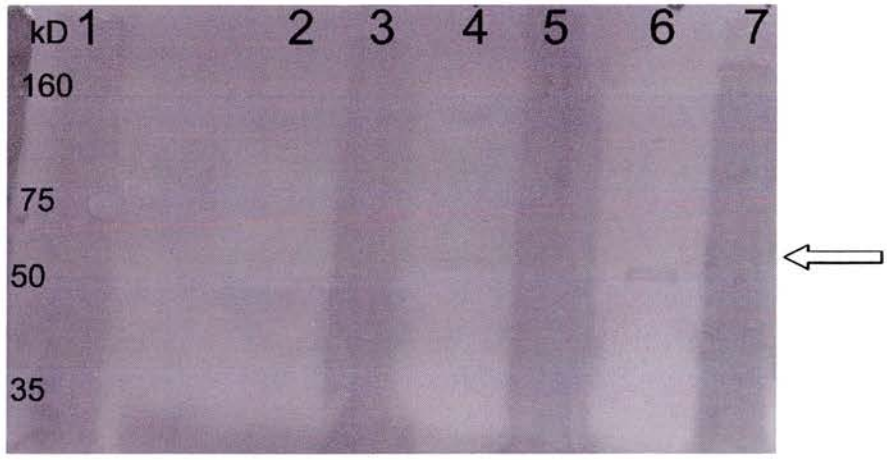

Figure 5.1 Western blot of pull down assay carried out using a 233bp IRES as probe and RRL. Lane 1, RRL proteins; lane 2, beads only captured protein; lane 3, beads only depleted extract; lane 4, sense RNA captured protein; lane 5, sense RNA depleted extract; lane 6, antisense RNA captured protein; lane 7, antisense RNA depleted extract. Primary antiserum, rabbit anti-PTB, used at 1/1000 dilution; secondary antibody, mouse anti-rabbit alkaline phosphatase, at 1/2,500 dilution.

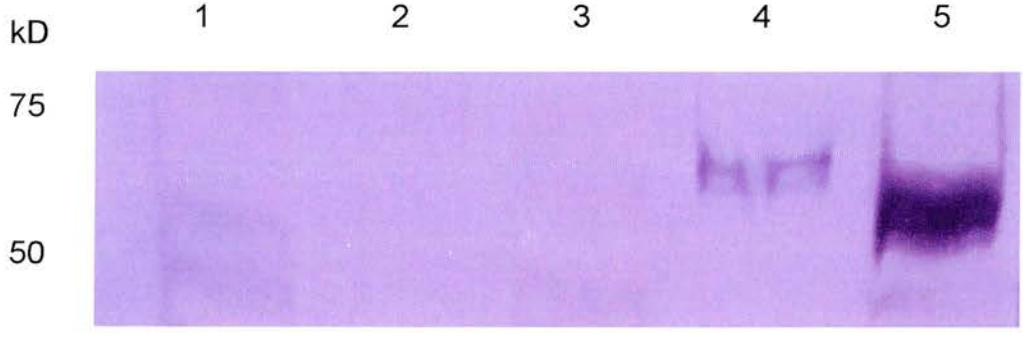

Figure 5.2. Western blot of pull-down assay using BCP-1 S10 extract. Lane 1, antisense RNA depleted extract; lane 2, antisense RNA captured protein; lane 3, sense RNA depleted extract; lane 4, sense RNA captured protein; lane 5; BCP-1 S10. Primary antiserum, rabbit anti-PTB, at 1/1000; secondary antiserum, mouse anti-rabbit alkaline phosphatase, at 1/2,500 dilution.

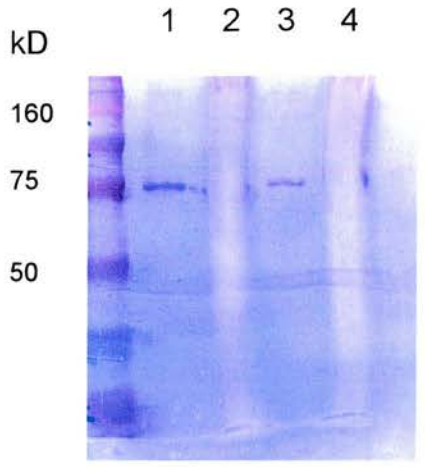

Figure 5.3 Western blot of pull down assay carried out using a 233bp IRES probe and RRL. Lane 1, sense orientation captured proteins; lane 2, sense orientation depleted extract; lane 3, antisense orientation captured proteins; lane 4, antisense orientation depleted extract. The primary antiserum was goat anti-eIF4G at 1/500 dilution; secondary antibody, mouse anti-goat alkaline phosphatase, at 1/2,500 dilution.

Western blotting of the captured proteins was also carried out using an antibody against DAP5 (Cell Signalling Technology) to address the possibility that the bands seen in figure 5.3 were due to cross-reactivity of the anti-eIF4G antibody with DAP5 or a cleavage product of DAP5. No bands were detected using this antibody.

5.2.2 Pull down assay using minimal functional IRES sequence

Since the initial characterisation of the KSHV IRES sequence (Bieleski and Talbot, 2001) further work has been able to demonstrate that the PPT is absolutely required for its activity and that this sequence alone is able to direct translation of a downstream cistron (Bieleski et al., 2004). We were interested to investigate the ITAFs able to interact with this "minimal" IRES sequence. To this end the oligos 3HYB IRES 3 and 3HYB IRES 4, which contain the PPT and produce a blunt ended fragment, were annealed together and ligated into the vector pSP64poly(A) which had been digested with *Sma*I. Insertion of the IRES sequence and the orientation in which it had been inserted were determined by *Aat*II digestion. The resulting plasmids were termed pSP64 60bp sense and pSP64 60bp antisense. These plasmids were used as templates in *in vitro* transcription reactions to produce probes for use in pull-down assays with BCP-1 S10 extract. Western blotting was carried out on captured proteins and depleted extract using the anti-PTB and anti-eIF4G antisera. On no occasion were bands observed in any of the captured protein lanes (data not shown).

5.3 Luciferase reporter assay to assess the impact of eIF4G cleavage on IRES activity

The size of the bands resulting from Western blotting of the captured RRL proteins with an antibody against eIF4G (figure 5.3) was reminiscent of the 76kD M-FAG fragment generated as a result of caspase cleavage (Bushell et al., 2000). As mentioned above this fragment is proposed to be able to support some cap-independent translation (Bushell et al., 2000). In an effort to investigate whether a cleavage product of eIF4G was necessary for activity of the KSHV IRES a dual luciferase reporter assay was utilised. This is the experimental system most commonly used to identify RNA sequences with IRES activity (Vagner et al., 2001). Following co-transfection of a dual luciferase reporter plasmid (figure 5.4), encoding the full-length KSHV IRES (pdLUC8; Bieleski and Talbot, 2001), and a plasmid encoding the rhinovirus 2A protease (pAΔ802; gift of L.Roberts, University of Surrey (Roberts et al., 1998)) the level of IRES activity was determined as described in section 2.9. Assays were performed initially in HEK 293 cells. The KSHV IRES is not functional in these cells (Bieleski and Talbot, 2001), however, it was hypothesised that if cleaved eIF4G is an ITAF some IRES activity may be restored when 2A protease is also present in the cell. As a control for transfection the plasmid pRL-TK (Promega) was used; the translation of Renilla luciferase (RL) transcribed from this plasmid is cap-dependent. The construct pdLUC-EMCV, containing the EMCV IRES sequence, (Bieleski and Talbot, 2001) was used as a control for IRES activity. The results following transfection of HEK 293 cells can be seen in table 5.1 and those for BCP-1 cells can be seen in table 5.2.

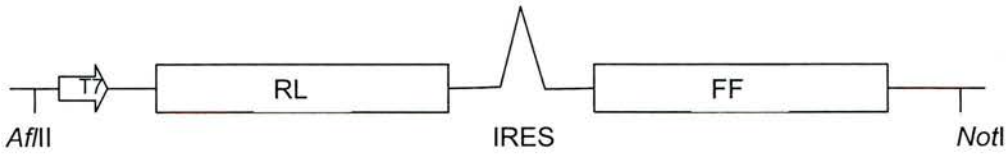

Figure 5.4 Schematic representation of pdLUC plasmid. The coding sequences of the *Renilla* and firefly luciferase enzymes are cloned downstream of the T7 RNA polymerase promoter. Ordinarily the FF would be inefficiently accessed by ribosomes which had completed translation of RL; insertion of an IRES sequence results in enhanced translation of the downstream cistron. pdLUC8= KSHV IRES; pdLUC-EMCV= EMCV IRES.

Plasmid	RL	FF
pRL-TK	1123	0.864
pRL-TK + pAΔ802	12.39	0.051
pdLUC8	8057	35.6
pdLUC8 + pAΔ802	5.483	0.00
pdLUC-EMCV	5051	2401
pdLUC-EMCV + pAΔ802	1.296	44.06

Table 5.1 The activities of the RL and FF enzymes (in relative light units) following transfection of HEK 293 cells. Data from a representative experiment is shown.

Plasmid	RL	FF
pRL-TK	>10,000	0.027
pRL-TK + pAΔ802	131.5	1.446
pdLUC8	5351	442.0
pdLUC8 + pAΔ802	1.005	0.305
pdLUC-EMCV	2157	873.9
pdLUC-EMCV + pAΔ802	0.311	4.782

Table 5.2 The activities of the RL and FF enzymes (in relative light units) following transfection of BCP-1 cells. Data from a representative experiment is shown.

The results show that, as previously observed, the KSHV IRES is not functional in HEK 293 cells. The cleavage of eIF4G by 2A protease did not restore any IRES activity in these cells: it is clear that the protease was active as the translation of RL, which is 5' cap dependent, has been inhibited. When the constructs are transfected into BCP-1 cells the KSHV IRES displays activity of translation at approximately 10% the efficiency of 5' cap dependent translation. This agrees with previously published data (Bieleski and Talbot, 2001). As observed previously, in HEK 293 cells, the co-transfection of pAΔ802 resulted in obliteration of RL translation. In these cells the KSHV IRES activity was not maintained following the cleavage of eIF4G by 2A protease. It must also be noted that the EMCV IRES activity was lost following 2A expression in BCP-1 cells; this contradicts previous findings that this IRES only requires the central third of eIF4G for its activity (Pestova et al., 1996). This suggests that the expression of 2A protease affects more than just eIF4G in these cells and, consequently, the obliteration of KSHV IRES activity cannot be definitively attributed to eIF4G cleavage.

5.4 Electrophoretic mobility shift assay

As an alternative method of investigating protein binding to the IRES an EMSA was employed. As mentioned previously the KSHV IRES activity is cell type dependent; there is very little or no activity in KSHV negative cell lines e.g. HEK 293 cells (Bieleski and Talbot, 2001). The radiolabelled IRES has been used as a probe in an EMSA. Specific protein complexes were formed when the probe was incubated with whole cell lysate from BCP-1 cells (a KSHV positive PEL cell line). These complexes were not formed following incubation with HEK 293 cell lysate and were

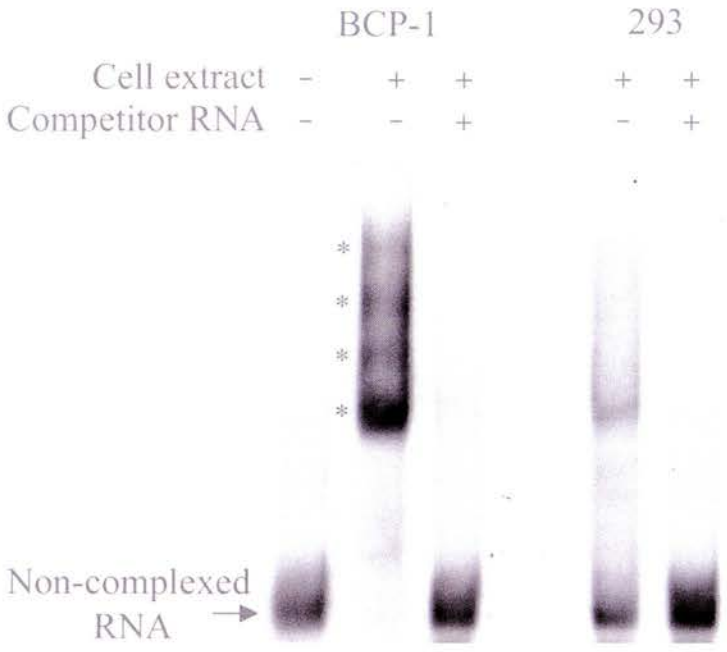

Figure 5.5 EMSA showing the formation of specific complexes between the KSHV IRES and components of BCP-1 S10 extract. These complexes are not replicated when HEK 293 cell extract is used and are specific as they are not formed in the presence of competitor, unlabelled, RNA. Taken from Bieleski *et al*, 2004.

competed out by an excess of unlabelled IRES indicating that they are specific (figure 5.5; Bieleski and Talbot, 2001).

The isolation of proteins from a polyacyrlamide gel, following gel shift, has been described previously (Heaton et al., 2001; Ranish and Hahn, 1991). The possibility of using this technique to isolate the components of the IRES-protein complexes was consequently investigated.

The probe was derived from the plasmid pSP64polyA sense, which was originally constructed for use in the pull-down assay. The plasmid DNA was linearised by *Sac*I digestion, which removes the polyA tail, prior to use as the template in an *in vitro* transcription reaction. Two transcription reactions were carried out; one with cold UTP and the second with ^{32}P-UTP. Following overnight transcription the template was removed by DNase treatment and unincorporated nucleotides were removed by passage through a G-25 column. The probes were then used in binding reactions with S10 extract from BCP-1 cells. The ^{32}P labelled reaction was as described in section 2.8.8.1. The cold reaction was performed on a larger scale; 200µl of S10 extract was used in a total volume of 1ml. Following 20 minutes incubation at room temperature the samples were run on a 5% polyacrylamide gel in 0.5x TBE running buffer. Once run, the gel was exposed to film at -20°C overnight prior to development to detect the position of the high molecular weight complexes. Using the labelled complexes as a guide the corresponding sections of the gel, where the unlabelled reaction was run, were excised and the proteins contained therein eluted.

The eluted proteins were concentrated using spin columns and 10µl of the resulting extract was run on a 12% SDS PAGE gel and subjected to silver staining (figure 5.6). Two bands can clearly be seen at approximately 75 and 100kD in size.

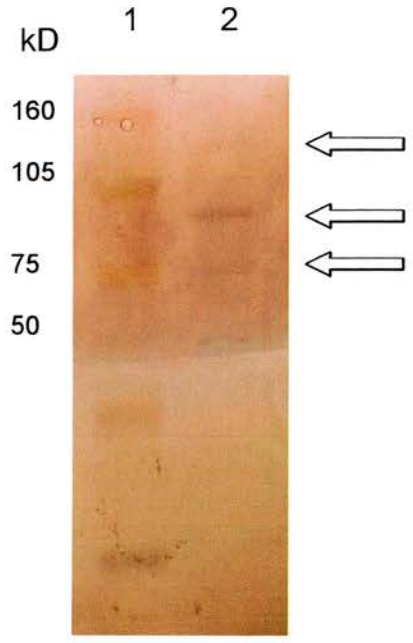

Figure 5.6 Silver staining of SDS PAGE gel of proteins eluted from EMSA. Lane 1, size markers; lane 2, eluted proteins. Two bands can clearly be seen in lane 2, one at approximately 100kD and the second at approximately 75kD; a third, weaker band is visible at approximately 150kD.

Western blotting was subsequently carried out using antisera against PTB, eIF4G and DAP5 but no bands were revealed in any blot.

As a final attempt to determine the identity of the proteins eluted from the EMSA the extract was run by SDS PAGE, stained using Sypro Ruby (Molecular Probes) and the individual bands cut from the gel. The band of approximately 100kD in size was subjected to MALDI-TOF mass spectrometry (carried out at the Edinburgh Protein Interaction Centre). This protein was identified as heat shock protein 90.

5.5 Conclusions

Unfortunately, attempts to carry out a large-scale yeast 3-hybrid screen for ITAFs proved unsuccessful. This would have been the ideal starting point in the search for viral and/ or cellular components of the vFLIP translation machinery as, theoretically, all possible interacting factors would have been represented. Despite trying a wide variety of different transformation conditions the efficiency with which the BCP-1 library DNA could be transformed into yeast remained too low for a screen to be carried out. This meant that efforts to identify any proteins that interact with the IRES sequence had to be carried out in a more focused manner; proteins previously identified as interacting with other IRES elements were investigated as possible ITAFs. The presence of a PPT within the minimal IRES sequence (Bieleski et al., 2004) and its frequent identification as an ITAF led to PTB being a strong candidate for a role in vFLIP translation. PTB was demonstrated to associate with the IRES by pull-down assay although it was not detectable by Western blotting following protein elution from an EMSA gel. There may be several reasons for this

apparent disparity, principal among which must be the possibility that the transcribed IRES does not fold correctly under one set of assay conditions.

Western blotting of proteins captured by the pull-down assay with an antibody against the C-terminus of eIF4GI revealed a band of approximately 76kDa associated with the IRES in both orientations (figure 5.3). This raised the possibility that a cleavage product of eIF4G was required for KSHV IRES function. In order to investigate this hypothesis a dual-reporter luciferase assay was employed and IRES function was assayed in HEK 293 and BCP-1 cells and in the presence of a protease that specifically cleaves eIF4G. The data obtained from these assays indicate that once cleaved eIF4G is not able to act as an ITAF. There was no enhancement of IRES activity in HEK 293 cells and in BCP-1 cells IRES activity was obliterated in the presence of the protease (tables 5.1 and 5.2). Correspondingly, the inhibition of KSHV IRES activity in BCP-1 cells following co-transfection of pAΔ802 suggests that full-length eIF4G may be required for translation to take place. There is a very faint band of approximately 150kD visible in the silver stain of proteins isolated following EMSA (figure 5.6); it is possible that this is eIF4G. One note of caution in relation to this must be the lack of EMCV IRES activity following 2A protease expression. Infection of cells with EMCV, unlike other picornaviruses, does not result in eIF4G cleavage. Instead, inhibition of cap-dependent translation is achieved through activation of the translational repressor 4E-BP (Gingras et al., 1996). However, it has been demonstrated that despite this lack of intrinsic cleavage, the EMCV IRES only requires the C-terminal fragment of eIF4G for its activity (Pestova et al., 1996) which is not reflected in the dual-luciferase assay data. Use of a stem-loop upstream of the RL coding sequence to inhibit cap-dependent translation,

through prevention of the assembled translation complex scanning along the mRNA to the start codon, has no effect upon levels of translation from the IRES (Bieleski and Talbot, 2001). Therefore, the inhibition of IRES activity following transfection of pAΔ802 suggests that the 2A protease has more effect upon the cell than merely cleavage of eIF4G. Consequently 2A protease may be responsible for the inhibition of IRES activity through secondary mechanisms. In light of this observation further studies must be carried out before one can conclude that full-length eIF4G is an ITAF for the KSHV IRES.

The abundant cellular protein Hsp90 was identified following mass spectrometry analysis of protein eluted from an EMSA gel using the full-length IRES sequence as a probe. Whilst this may well prove to be an artefact it is interesting to note that the same protein has been identified as a component of the IKK complex (Chen et al., 2002) with which vFLIP also interacts (Field et al., 2003). Addition of an inhibitor of Hsp90 resulted in inhibition of vFLIP induced NF-κB activation and led to the death of PEL cells (Field et al., 2003). If the interaction of Hsp90 with the IRES is real then this would also suggest a mechanism by which newly translated vFLIP could interact efficiently with the IKK complex.

Chapter 6 Discussion

Discussion

The work described in this thesis was performed to investigate two separate aspects of KSHV vFLIP biology, firstly its effect on viral pathogenesis and secondly the factors necessary for its translation. In this discussion I shall address each issue in turn.

6.1 The contribution of vFLIP toward viral pathogenesis

The relative ease with which the genome of the murine gammaherpesvirus MHV-76 can be manipulated was exploited to generate several recombinant viruses containing the selection markers EGFP and hygromycin resistance, and KSHV vFLIP at their LHE; FL1, FL2 and FL3. Expression of these genes was controlled by either the CMV IE or murine PGK promoter. Control recombinant viruses lacking vFLIP were also constructed; IRES and PGK-IRES. Southern blotting and PCR screening showed that the recombinant viruses contained the inserted sequences in the correct location and orientation and that there was no contamination of the viral stocks with wild-type MHV-76.

Following intranasal infection of BALB/c mice with $5x10^4$ pfu of virus, the titres of infectious virus in the lung and infective centres in the spleen were determined. In the lung the recombinant viruses displayed similar kinetics of infection to the wild-type virus; peak viral titres were achieved around day 5 p.i. and the viruses were completely cleared by day 10 p.i. When expression of the inserted sequences was driven by the strong CMV IE promoter the vFLIP expressing viruses, FL1 and FL2,

reached a higher titre at day 5 p.i. than the control, IRES, and wild-type viruses. Whilst the apparent attenuation of lytic replication of the IRES control virus has been noted elsewhere (Brass, 2004) it appears from these results that vFLIP provides a replicative advantage to the FL1 and FL2 viruses. This phenotype is not replicated following infection of BALB/c mice with recombinant viruses in which expression of the insert is driven by the PGK promoter i.e. FL3 and PGK-IRES. Following intranasal infection with these viruses there is no difference in the titres of infectious virus in the lung between the two recombinants and the wild-type virus at any time point. This result indicates that the attenuation of the IRES control is a result of CMV IE driven expression of the LHE. The CMV IE promoter is much stronger than the PGK promoter (Gerolami et al., 2000) and thus will result in higher levels of EGFP and vFLIP in infected cells. It is possible that the high concentration of EGFP in the lungs following infection of mice with FL1, FL2 and IRES elicits an immune response against the virally infected cells. In the case of IRES this results in clearance of the majority of virus from infected animals. KSHV vFLIP is known to have anti-apoptotic properties; it acts directly to inhibit activation of pro-caspase 8 at the DISC (Djerbi et al., 1999) and activates NF-κB (Liu et al., 2002) which mediates the transcription of many cellular genes including some involved in the prevention of apoptosis (Pahl, 1999). The expression of vFLIP, by FL1 and FL2, may provide protection for these virally infected cells against the immune response raised against EGFP and thus enable lytic replication to continue at a greater level than the control virus. When expression of the inserted sequences is driven by the weaker PGK promoter, i.e. following FL3 and PGK-IRES infection, the resulting concentrations of EGFP and vFLIP will be lower than in CMV IE virus infected cells. As a result,

one would expect the immune response against PGK-IRES to be much less significant than that against IRES and hence levels of viral replication to be maintained. This is seen to be the case as the previously observed attenuation of the control virus in the lung is obliterated when the PGK promoter is used to drive expression. Infection of mice with a vFLIP expressing virus, FL3, does not result in a greater viral titre than the control recombinant virus, PGK-IRES. There will be an immune response against these viruses, however, it is probably not exacerbated by EGFP and there is probably not enough vFLIP present in the system to provide a replicative advantage to FL3. In order to further clarify whether the expression of vFLIP by FL1 and FL2 does elicit a protective effect in the lungs of infected mice it will be necessary to establish that vFLIP is being expressed and determine the relative levels of vFLIP protein. Without an antibody against vFLIP this has not been possible. Antibody against KSHV vFLIP has been successfully produced (Low et al., 2001) and if it does become available to us it will be interesting to stain lung sections for vFLIP and correlate this with EGFP expression and viral titre. Such an antibody would also allow determination of the amount of vFLIP protein present following infection with FL3 and assessment of the efficiency of the EMCV IRES in this system.

No splenic infective centres were detected after day 10 p.i. following titration of splenocytes isolated from mice infected with any of the recombinant viruses. Thus, these viruses are either failing to establish latency in the spleen or, alternatively, they are attenuated in their reactivation from latency. An experiment using EGFP-expressing ROSA mice failed to elucidate whether an immune response against EGFP in infected BALB/c mice was responsible for this splenic attenuation.

The unsuitability of the recombinant viruses expressing EGFP for studies of latency *in vivo* and the inability to generate recombinant viruses without the selection markers (76inFLIP and 76inEGFP) meant that a different system had to be developed to study the establishment of latency. To this end NS0 cells were utilised. It was shown that these cells can be infected with MHV-76 and MHV-76 recombinant viruses and that the viruses can establish latency. Assays of infected cell cultures show that whilst the rate of cell proliferation is consistent, independent of the virus with which the cells have been infected, the viral titres achieved vary considerably. The expression of vFLIP results in higher titres of supernatant and cell-associated virus at all time points assayed. Moreover, at early time points there is a considerably larger pool of latently infected cells following FL3 infection in comparison to PGK-IRES and MHV-76. Thus it appears that vFLIP is able to enhance the initial establishment of latency. This effect may be mediated, at least in part, by vFLIP's ability to activate the transcription factor NF-κB. This property is known to be vital to the survival of KSHV infected cells once latency has been established (Guasparri et al., 2004) and it would follow that it may also aid the establishment of latency. Whilst NF-κB was activated in all samples immediately post infection the intensity of the gel shift decreased more quickly in the MHV-76 infected NS0 cells than in those infected with the recombinant viruses. Whilst the assay is not quantitative it is clear that activated NF-κB is lost from the cells fastest after infection with wild-type virus and that over time FL3 infection leads to a greater level of activation than does PGK-IRES infection. The reason that activated NF-κB is maintained in NS0 cells latently infected with PGK-IRES is unclear at present, one possible explanation may be the presence of a short C-terminal section

of the M4 gene from MHV-68 in the recombinant viruses. The relative levels of activated NF-κB observed correspond with the levels of virus produced in each infected culture: that is, higher viral titres are reached in those cultures containing the most activated NF-κB. In future it would be desirable to determine a quantitative readout of the activation of NF-κB by each of these viruses over the course of infection. Additionally, it would be interesting to investigate the establishment of latency of the recombinant viruses FL1, FL2 and IRES in NS0 cells and to assess the levels of NF-κB activated as a result of infection. Infection with both FL1 and FL2 should result in higher levels of vFLIP protein within the cells which may result in a greater activation of NF-κB. If this proves to be the case it would be fascinating to relate this to the viral titres achieved and determine whether increasing levels of activated NF-κB do indeed correspond to increased establishment of latency.

KSHV vFLIP has previously been attributed more than one function during the course of viral infection; protection of infected cells from death receptor mediated apoptosis and activation of NF-κB resulting in the maintenance of latency. The data presented here supports these roles for vFLIP and suggests that it may also play a part in the initial establishment of latency. The *in vivo* data from BALB/c mice infected with FL1 and FL2 implies that vFLIP has a protective effect during lytic replication of the virus, probably counteracting host attempts to initiate apoptosis via the death-receptor mediated pathway. The gammaherpesviruses encode a number of anti-apoptotic products that target various components of the apoptosis pathways, however, MHV-76 does not encode a direct inhibitor of pro-caspase 8 activation. The inclusion of vFLIP within the KSHV genome may reflect a difference in the

routes of infection or immune response mounted against KSHV infection as compared to MHV-76.

Alternatively, the possibility that the anti-apoptotic activity of vFLIP is secondary to its activation of NF-κB and that the rescue of the control, IRES, phenotype witnessed *in vivo* is an artefact of artificially high levels of vFLIP protein within the system must be considered. The recombinant viruses reflect the reality of KSHV infection in that the translation of vFLIP is mediated by an IRES element. As this is the case one would perhaps expect only low levels of vFLIP in KSHV positive cells. Having said this it should be noted that it has been demonstrated that, in PEL cells at least, this appears not to be the case as immunostaining using a monoclonal antibody against KSHV vFLIP demonstrates significant levels of protein in the cytoplasm of some of the cells (Low et al., 2001). Whilst acknowledging this observation it remains the case that the CMV IE promoter is very strong and the EMCV IRES also has high activity relative to other elements including the KSHV IRES (Bieleski and Talbot, 2001); together these factors may result in artificially high levels of vFLIP following infection with FL1 and FL2. If this is the case then FL3, with the much weaker PGK promoter, is probably more representative of KSHV infection. The data obtained using this virus do not show any difference in lung virus titres and indicate that the protective effect of vFLIP is minimal when it is present at lower concentrations. It therefore seems likely that the predominant role of vFLIP is its activation of NF−κB: these results suggest that its expression aids the establishment, as well as the maintenance, of latency most probably due to activation of NF-κB. The data gained during this study and others (Brass, 2004) indicates that recombinant viruses containing selection markers are unsuitable for addressing questions

regarding the establishment of latency in the mouse. Work carried out utilising recombinant MHV-76 in which a gene is inserted into the LHE without additional sequences show that such constructs can establish latency (Townsley et al., 2004). It would have been greatly beneficial to have successfully generated the viruses 76inFLIP and 76inEGFP and, in hindsight, efforts to construct such viruses should have been continued using "stuffer" DNA to increase the insert size and try to overcome any packaging problems. This work would be valuable in future and if successful it would allow investigation of the relevance of the NS0 data to the *in vivo* role of vFLIP.

In its activation of NF-κB the function of KSHV vFLIP resembles that of the EBV latent protein LMP-1 which is expressed during latency II and latency III and also activates NF-κB (Huen et al., 1995). Both viral proteins, vFLIP and LMP-1, are necessary for the growth of transformed cell lines, PEL and LCL respectively (Keller et al., 2000; Izumi et al., 1997), and they achieve this via NF-κB activation (Cahir-McFarland et al., 2004; Guasparri et al., 2004). KSHV vFLIP has been implicated as a viral oncogene (Djerbi et al., 1999) and its activation of NF-κB supports such a role. Recent work has implicated NF-κB as a component in the development of cancer and maintenance of malignant cells. The target genes of NF-κB constitute four broad categories: immunoregulatory and inflammatory; anti-apoptotic; positive regulators of cell proliferation and negative regulators of NF-κB, all of which can contribute toward tumourigenesis (reviewed in Karin et al., 2002). Generation of the recombinant viruses 76inFLIP and 76inGFP would also enable investigation of vFLIP as a mediator of oncogenesis. If the viruses were able to establish a latent infection, one could monitor the development of tumours in animals infected with

76inFLIP in comparison to those infected with 76inEGFP and the wild-type MHV-76.

6.2 Identification of ITAFs that interact with the KSHV IRES

A large scale screening programme, yeast 3-hybrid assay, for cellular proteins able to interact specifically with the KSHV IRES sequence proved impossible to carry out due to inefficient transformation of yeast with library DNA. In light of this a pull-down assay was utilised to investigate the ability of specific ITAFs to interact with the IRES. By means of this pull-down assay, in which the full-length IRES sequence was used to deplete a BCP-1 cell protein extract, the polypyrimidine tract binding protein (PTB) was shown to associate with the IRES in the sense orientation. This is perhaps unsurprising as the IRES contains a polypyrimidine tract and PTB has been identified as an ITAF for a large number of IRES elements including EMCV (Hellen et al., 1993), FMDV (Kolupaeva et al., 1996) and Apaf-1 (Mitchell et al., 2001). To date experiments have not been performed to assess the functional significance of the interaction between PTB and the IRES, and a supershift assay did not show complex formation using antiserum against PTB (data not shown). These are both issues that must be addressed before PTB can be classed as a true ITAF for the KSHV IRES. The failure of the supershift assay to confirm an interaction between the IRES and PTB may be attributable to any of a number of different reasons: the reaction conditions used may inhibit the interaction between either PTB and the IRES or PTB

and the antiserum; the IRES may not fold to its correct conformation or a secondary factor may be needed for the interaction to occur. This latter explanation is a possibility as it has been shown by Mitchell *et al* that PTB is only able to interact with the Apaf-1 IRES when the cellular protein upstream of N-ras (unr) is pre-bound to the RNA (Mitchell et al., 2003).

The translation initiation factor eIF4G has been identified as an ITAF for a number of IRES elements including those of EMCV (Pestova et al., 1996) and HAV (Borman and Kean, 1997). It was therefore investigated as a possible interacting partner of the KSHV IRES by means of the pull-down assay. Western blotting of proteins captured in a pull-down assay using RRL, with an antibody against the C-terminus of eIF4G identified a band of approximately 76kD. As this is the same size as the M-FAG fragment generated following caspase mediated cleavage of eIF4G (Bushell et al., 2000) the possibility that cleavage of eIF4G, resulting from KSHV infection, produced a fragment capable of promoting IRES activity was investigated. If a requirement for eIF4G cleavage was demonstrated this may explain the cell-type specificity of the KSHV IRES (Bieleski and Talbot, 2001) as viral infection would be required for its induction. It was hypothesised that any cleavage induced by KSHV infection would be as a result of caspase activation, in this investigation the picornavirus protease 2A was used to model eIF4G cleavage. IRES activity was determined by means of a dual-reporter luciferase assay. Two cell lines were used; one, HEK 293, in which the KSHV IRES is not normally functional and a second, BCP-1, in which IRES activity is seen. IRES activity was not restored in HEK 293 cells following eIF4G cleavage and neither was it maintained in BCP-1 cells. This implies that full-length eIF4G is needed for KSHV IRES function, analogous to the

HAV IRES (Borman and Kean, 1997). However, inhibition of the EMCV IRES was also seen following eIF4G cleavage which contradicts the published properties of this IRES (Pestova et al., 1996) and suggests that the 2A protease may have a more far-reaching effect than just cleavage of eIF4G. Further studies must be carried out to confirm whether full-length eIF4G interacts with the IRES; these could include UV cross-linking assays and identification of proteins that were shifted by EMSA. The luciferase assay results suggest that the band observed following Western blotting of captured RRL proteins with an antibody against the C-terminus of eIF4G may be either an artefact or it has no functional significance. If proved to be the case this will explain why a similar band was not observed following a pull-down assay using BCP-1 S10 extract (data not shown).

It should be noted that there has been increasing speculation about the validity of some reports of IRES activity, especially those pertaining to cellular IRES elements (Kozak, 2003; Van Eden et al., 2004; Han and Zhang, 2002). As KSHV is a DNA virus, and consequently its IRES sequence may share more features with cellular IRESs than those encoded by RNA viruses, the possibility that the identified IRES sequence is an artefact of aberrant splicing activity or contains a cryptic promoter must be considered. When the KSHV IRES was first identified the bicistronic reporter was transcribed from a T7 RNA polymerase promoter thus bypassing the necessity for nuclear transcription. Use of a stem-loop upstream of the RL coding sequence obliterated the activity of this luciferase whilst FF luciferase remained unaffected (Bieleski and Talbot, 2001). Additionally, Northern blotting, using the downstream cistron as the probe, was carried out to confirm that the bicistronic transcript was present and to demonstrate that a monocistronic transcript, which

would imply that splicing had taken place, was not (Bieleski and Talbot, 2001). The sensitivity of Northern blotting utilised in this manner has since been questioned (Van Eden et al., 2004). Van Eden *et al* used RT-PCR and RNAi technology to demonstrate that the XIAP 5'UTR (reported to contain an IRES; Holcik et al., 1999)) contains a splice acceptor site and that bicistronic transcripts containing the XIAP IRES actually underwent splicing events to produce monocistronic mRNAs that had not been detected by Northern blotting (Holcik et al., 2003). The authors conclude that the activity of the XIAP IRES is much weaker than that proposed by the researchers who identified the IRES (Van Eden et al., 2004).

With this in mind the possibility that the KSHV IRES activity is weaker than first proposed must be considered. In support of the presence of a functional IRES are the Northern blot data, stem-loop data, (Bieleski and Talbot, 2001) and the fact that a monocistronic vFLIP transcript has never been detected in KSHV positive cells.

It is clear from the EMSA data that there are proteins that interact specifically with the KSHV IRES sequence. PTB has been identified as being able to interact with the IRES sequence, although the inability to demonstrate this by supershift assays raises the possibility that either further ITAFs are required for the interaction or that it is not fundamental to IRES activity. Alternatively, one possibility is that PTB associates with the IRES sequence in its capacity as a mediator of splicing reactions. PTB was first identified as a result of its binding to the polypyrimidine tract which typically precedes the 3' splice site of eukaryotic introns (Garcia-Blanco et al., 1989). It was subsequently recognised to be a member of the hnRNP family of proteins that bind to nascent RNA, playing a number of roles in its processing, but that dissociate once splicing complexes assemble (Bennett et al., 1992). It was then

proposed that PTB plays a role in repression of splicing events (Mulligan et al., 1992); further evidence that PTB negatively regulates splicing has been forthcoming (reviewed in Valcarcel and Gebauer, 1997). Those that question the true nature of some IRES elements propose that PTB is found to be associated as a result of its role in splicing and that these IRESs probably contain splice sites (Van Eden et al., 2004). On the other hand, those that advocate its role as an ITAF postulate that PTB binding enables structural remodelling of the mRNA allowing access to the transcriptional machinery (Pickering et al., 2003). In either case it is clear that PTB can associate with the KSHV IRES. There is no splice acceptor site within a suitable distance from the PPT for splicing to occur (S.Talbot; personnal communication) and consequently, I believe that PTB is most likely to act as an ITAF and that it is highly unlikely that it binds to the sequence to repress an, as yet unknown, splice site within the putative IRES sequence.

Further work is needed to confirm the functional significance of the PTB and eIF4G interactions identified in this thesis and to determine the nature of any further ITAFs that are necessary for translation from the KSHV IRES. The most obvious conclusion to be drawn from the cell-type specificity of the IRES is that there is a viral determinant of its activity either directly, through expression of a KSHV protein, or indirectly, through virally induced modification of a host protein. If this is indeed the case and if full-length eIF4G is an ITAF then there is almost certainly at least one other ITAF still to be identified. Methods utilised to identify ITAFs could include: identifying the proteins isolated from shifted complexes following EMSAs; UV cross linking assays; further pull-down assays and Westerns for other possible ITAFs e.g. unr. Confirmation of the functional significance of any potential ITAFs

could be achieved by expression of identified proteins in non-permissive systems to assess whether they restore IRES function or by targeting the expression of the putative ITAF, for example by RNAi, and monitoring IRES activity in its absence.

References

Adler,H., Messerle,M., and Koszinowski,U.H. (2001). Virus reconstituted from infectious bacterial artificial chromosome (BAC)-cloned murine gammaherpesvirus 68 acquires wild-type properties in vivo only after excision of BAC vector sequences. J. Virol. *75*, 5692-5696.

Akula,S.M., Naranatt,P.P., Walia,N.S., Wang,F.Z., Fegley,B., and Chandran,B. (2003). Kaposi's sarcoma-associated herpesvirus (human herpesvirus 8) infection of human fibroblast cells occurs through endocytosis. J. Virol. *77*, 7978-7990.

Akula,S.M., Pramod,N.P., Wang,F.Z., and Chandran,B. (2001). Human herpesvirus 8 envelope-associated glycoprotein B interacts with heparan sulfate-like moieties. Virology *284*, 235-249.

Akula,S.M., Pramod,N.P., Wang,F.Z., and Chandran,B. (2002). Integrin alpha3beta1 (CD 49c/29) is a cellular receptor for Kaposi's sarcoma-associated herpesvirus (KSHV/HHV-8) entry into the target cells. Cell *108*, 407-419.

Alberts,B., Bray,D., Lewis,J., Raff,M., Roberts,K., and Watson,J.D. (1994). Control of Gene Expression. In Molecular Biology of the Cell, Garland), pp. 401-476.

Albrecht,J.C., Nicholas,J., Biller,D., Cameron,K.R., Biesinger,B., Newman,C., Wittmann,S., Craxton,M.A., Coleman,H., Fleckenstein,B., and . (1992). Primary structure of the herpesvirus saimiri genome. J. Virol. *66*, 5047-5058.

Ali,N. and Siddiqui,A. (1995). Interaction of polypyrimidine tract-binding protein with the 5' noncoding region of the hepatitis C virus RNA genome and its functional requirement in internal initiation of translation. J. Virol. *69*, 6367-6375.

Allan,G.J., Inman,G.J., Parker,B.D., Rowe,D.T., and Farrell,P.J. (1992). Cell growth effects of Epstein-Barr virus leader protein. J. Gen. Virol. *73 (Pt 6)*, 1547-1551.

Ambroziak,J.A., Blackbourn,D.J., Herndier,B.G., Glogau,R.G., Gullett,J.H., McDonald,A.R., Lennette,E.T., and Levy,J.A. (1995). Herpes-like sequences in HIV-infected and uninfected Kaposi's sarcoma patients. Science *268*, 582-583.

An,J., Lichtenstein,A.K., Brent,G., and Rettig,M.B. (2002). The Kaposi sarcoma-associated herpesvirus (KSHV) induces cellular interleukin 6 expression: role of the KSHV latency-associated nuclear antigen and the AP1 response element. Blood *99*, 649-654.

An,J., Sun,Y., Sun,R., and Rettig,M.B. (2003). Kaposi's sarcoma-associated herpesvirus encoded vFLIP induces cellular IL-6 expression: the role of the NF-kappaB and JNK/AP1 pathways. Oncogene *22*, 3371-3385.

Anwar,A., Ali,N., Tanveer,R., and Siddiqui,A. (2000). Demonstration of functional requirement of polypyrimidine tract-binding protein by SELEX RNA during

hepatitis C virus internal ribosome entry site-mediated translation initiation. J. Biol. Chem. *275*, 34231-34235.

Arvanitakis,L., Geras-Raaka,E., Varma,A., Gershengorn,M.C., and Cesarman,E. (1997). Human herpesvirus KSHV encodes a constitutively active G-protein-coupled receptor linked to cell proliferation. Nature *385*, 347-350.

Atkinson,P.G., Coope,H.J., Rowe,M., and Ley,S.C. (2003). Latent membrane protein 1 of Epstein-Barr virus stimulates processing of NF-kappa B2 p100 to p52. J. Biol. Chem. *278*, 51134-51142.

Bais,C., Santomasso,B., Coso,O., Arvanitakis,L., Raaka,E.G., Gutkind,J.S., Asch,A.S., Cesarman,E., Gershengorn,M.C., Mesri,E.A., and Gerhengorn,M.C. (1998). G-protein-coupled receptor of Kaposi's sarcoma-associated herpesvirus is a viral oncogene and angiogenesis activator. Nature *391*, 86-89.

Ballestas,M.E., Chatis,P.A., and Kaye,K.M. (1999). Efficient persistence of extrachromosomal KSHV DNA mediated by latency-associated nuclear antigen. Science *284*, 641-644.

Ballestas,M.E. and Kaye,K.M. (2001). Kaposi's sarcoma-associated herpesvirus latency-associated nuclear antigen 1 mediates episome persistence through cis-acting terminal repeat (TR) sequence and specifically binds TR DNA. J. Virol. *75*, 3250-3258.

Barozzi,P., Luppi,M., Facchetti,F., Mecucci,C., Alu,M., Sarid,R., Rasini,V., Ravazzini,L., Rossi,E., Festa,S., Crescenzi,B., Wolf,D.G., Schulz,T.F., and Torelli,G. (2003). Post-transplant Kaposi sarcoma originates from the seeding of donor-derived progenitors. Nat. Med. *9*, 554-561.

Beales,L.P., Holzenburg,A., and Rowlands,D.J. (2003). Viral internal ribosome entry site structures segregate into two distinct morphologies. J. Virol. *77*, 6574-6579.

Bejarano,M.T. and Masucci,M.G. (1998). Interleukin-10 abrogates the inhibition of Epstein-Barr virus-induced B-cell transformation by memory T-cell responses. Blood *92*, 4256-4262.

Belanger,C., Gravel,A., Tomoiu,A., Janelle,M.E., Gosselin,J., Tremblay,M.J., and Flamand,L. (2001). Human herpesvirus 8 viral FLICE-inhibitory protein inhibits Fas-mediated apoptosis through binding and prevention of procaspase-8 maturation. J. Hum. Virol. *4*, 62-73.

Belsham,G.J. and Sonenberg,N. (1996). RNA-protein interactions in regulation of picornavirus RNA translation. Microbiol. Rev. *60*, 499-511.

Bennett,M., Michaud,S., Kingston,J., and Reed,R. (1992). Protein components specifically associated with prespliceosome and spliceosome complexes. Genes Dev. *6*, 1986-2000.

Beral,V. (1991). Epidemiology of Kaposi's sarcoma. Cancer Surv. *10*, 5-22.

Bertin,J., Armstrong,R.C., Ottilie,S., Martin,D.A., Wang,Y., Banks,S., Wang,G.H., Senkevich,T.G., Alnemri,E.S., Moss,B., Lenardo,M.J., Tomaselli,K.J., and Cohen,J.I. (1997). Death effector domain-containing herpesvirus and poxvirus proteins inhibit both Fas- and TNFR1-induced apoptosis. Proc. Natl. Acad. Sci. U. S. A *94*, 1172-1176.

Bieleski,L., Hindley,C., and Talbot,S.J. (2004). A polypyrimidine tract facilitates the expression of Kaposi's sarcoma-associated herpesvirus vFLIP through an internal ribosome entry site. J. Gen. Virol. *85*, 615-620.

Bieleski,L. and Talbot,S.J. (2001). Kaposi's sarcoma-associated herpesvirus vCyclin open reading frame contains an internal ribosome entry site. J. Virol. *75*, 1864-1869.

Biesinger,B., Muller-Fleckenstein,I., Simmer,B., Lang,G., Wittmann,S., Platzer,E., Desrosiers,R.C., and Fleckenstein,B. (1992). Stable growth transformation of human T lymphocytes by herpesvirus saimiri. Proc. Natl. Acad. Sci. U. S. A *89*, 3116-3119.

Biggar,R.J., Whitby,D., Marshall,V., Linhares,A.C., and Black,F. (2000). Human herpesvirus 8 in Brazilian Amerindians: a hyperendemic population with a new subtype. J. Infect. Dis. *181*, 1562-1568.

Birkmann,A., Mahr,K., Ensser,A., Yaguboglu,S., Titgemeyer,F., Fleckenstein,B., and Neipel,F. (2001). Cell surface heparan sulfate is a receptor for human herpesvirus 8 and interacts with envelope glycoprotein K8.1. J. Virol. *75*, 11583-11593.

Blackbourn,D.J., Lennette,E., Klencke,B., Moses,A., Chandran,B., Weinstein,M., Glogau,R.G., Witte,M.H., Way,D.L., Kutzkey,T., Herndier,B., and Levy,J.A. (2000). The restricted cellular host range of human herpesvirus 8. AIDS *14*, 1123-1133.

Blaskovic,D., Stancekova,M., Svobodova,J., and Mistrikova,J. (1980). Isolation of five strains of herpesviruses from two species of free living small rodents. Acta Virol. *24*, 468.

Borman,A.M. and Kean,K.M. (1997). Intact eukaryotic initiation factor 4G is required for hepatitis A virus internal initiation of translation. Virology *237*, 129-136.

Borman,A.M., Kirchweger,R., Ziegler,E., Rhoads,R.E., Skern,T., and Kean,K.M. (1997). elF4G and its proteolytic cleavage products: effect on initiation of protein synthesis from capped, uncapped, and IRES-containing mRNAs. RNA. *3*, 186-196.

Boshoff,C. (2003). Kaposi virus scores cancer coup. Nat. Med. *9*, 261-262.

Boshoff,C. and Chang,Y. (2001). Kaposi's sarcoma-associated herpesvirus: a new DNA tumor virus. Annu. Rev. Med. *52*, 453-470.

Boshoff,C., Gao,S.J., Healy,L.E., Matthews,S., Thomas,A.J., Coignet,L., Warnke,R.A., Strauchen,J.A., Matutes,E., Kamel,O.W., Moore,P.S., Weiss,R.A., and

Chang,Y. (1998). Establishing a KSHV+ cell line (BCP-1) from peripheral blood and characterizing its growth in Nod/SCID mice. Blood *91*, 1671-1679.

Boshoff,C. and Weiss,R.A. (2001). Epidemiology and pathogenesis of Kaposi's sarcoma-associated herpesvirus. Philos. Trans. R. Soc. Lond B Biol. Sci. *356*, 517-534.

Bovee,M.L., Marissen,W.E., Zamora,M., and Lloyd,R.E. (1998). The predominant elF4G-specific cleavage activity in poliovirus-infected HeLa cells is distinct from 2A protease. Virology *245*, 229-240.

Brasey,A., Lopez-Lastra,M., Ohlmann,T., Beerens,N., Berkhout,B., Darlix,J.L., and Sonenberg,N. (2003). The leader of human immunodeficiency virus type 1 genomic RNA harbors an internal ribosome entry segment that is active during the G2/M phase of the cell cycle. J. Virol. *77*, 3939-3949.

Brass, A. vOx2-a potential immune regulatory protein involved in Kaposi's sarcoma-associated herpesvirus pathogenesis. 2004. Thesis. University of Edinburgh.

Brown,H.J., Song,M.J., Deng,H., Wu,T.T., Cheng,G., and Sun,R. (2003). NF-kappaB inhibits gammaherpesvirus lytic replication. J. Virol. *77*, 8532-8540.

Buck,C.B., Shen,X., Egan,M.A., Pierson,T.C., Walker,C.M., and Siliciano,R.F. (2001). The human immunodeficiency virus type 1 gag gene encodes an internal ribosome entry site. J. Virol. *75*, 181-191.

Burger,R., Neipel,F., Fleckenstein,B., Savino,R., Ciliberto,G., Kalden,J.R., and Gramatzki,M. (1998). Human herpesvirus type 8 interleukin-6 homologue is functionally active on human myeloma cells. Blood *91*, 1858-1863.

Bushell,M., Poncet,D., Marissen,W.E., Flotow,H., Lloyd,R.E., Clemens,M.J., and Morley,S.J. (2000). Cleavage of polypeptide chain initiation factor eIF4GI during apoptosis in lymphoma cells: characterisation of an internal fragment generated by caspase-3-mediated cleavage. Cell Death. Differ. *7*, 628-636.

Bushell,M. and Sarnow,P. (2002). Hijacking the translation apparatus by RNA viruses. J. Cell Biol. *158*, 395-399.

Cahir-McFarland,E.D., Carter,K., Rosenwald,A., Giltnane,J.M., Henrickson,S.E., Staudt,L.M., and Kieff,E. (2004). Role of NF-kappa B in cell survival and transcription of latent membrane protein 1-expressing or Epstein-Barr virus latency III-infected cells. J. Virol. *78*, 4108-4119.

Campbell,M.E., Palfreyman,J.W., and Preston,C.M. (1984). Identification of herpes simplex virus DNA sequences which encode a trans-acting polypeptide responsible for stimulation of immediate early transcription. J. Mol. Biol. *180*, 1-19.

Caposio,P., Dreano,M., Garotta,G., Gribaudo,G., and Landolfo,S. (2004). Human cytomegalovirus stimulates cellular IKK2 activity and requires the enzyme for productive replication. J. Virol. *78*, 3190-3195.

CDC (2004). Kaposi's sarcoma and Pneumocystis pneumonia among homosexual men - New York City and California. MMWR Weekly *30*, 305-308.

Cerimele,F., Curreli,F., Ely,S., Friedman-Kien,A.E., Cesarman,E., and Flore,O. (2001). Kaposi's sarcoma-associated herpesvirus can productively infect primary human keratinocytes and alter their growth properties. J. Virol. *75*, 2435-2443.

Cesarman,E., Chang,Y., Moore,P.S., Said,J.W., and Knowles,D.M. (1995). Kaposi's sarcoma-associated herpesvirus-like DNA sequences in AIDS-related body-cavity-based lymphomas. N. Engl. J. Med. *332*, 1186-1191.

Cesarman,E., Nador,R.G., Bai,F., Bohenzky,R.A., Russo,J.J., Moore,P.S., Chang,Y., and Knowles,D.M. (1996). Kaposi's sarcoma-associated herpesvirus contains G protein-coupled receptor and cyclin D homologs which are expressed in Kaposi's sarcoma and malignant lymphoma. J. Virol. *70*, 8218-8223.

Chang,D.W., Xing,Z., Pan,Y., Algeciras-Schimnich,A., Barnhart,B.C., Yaish-Ohad,S., Peter,M.E., and Yang,X. (2002). c-FLIP(L) is a dual function regulator for caspase-8 activation and CD95-mediated apoptosis. EMBO J. *21*, 3704-3714.

Chang,Y., Cesarman,E., Pessin,M.S., Lee,F., Culpepper,J., Knowles,D.M., and Moore,P.S. (1994). Identification of herpesvirus-like DNA sequences in AIDS-associated Kaposi's sarcoma. Science *266*, 1865-1869.

Chang,Y., Moore,P.S., Talbot,S.J., Boshoff,C.H., Zarkowska,T., Godden,K., Paterson,H., Weiss,R.A., and Mittnacht,S. (1996). Cyclin encoded by KS herpesvirus. Nature *382*, 410.

Chatterjee,M., Osborne,J., Bestetti,G., Chang,Y., and Moore,P.S. (2002). Viral IL-6-induced cell proliferation and immune evasion of interferon activity. Science *298*, 1432-1435.

Chen,G., Cao,P., and Goeddel,D.V. (2002). TNF-induced recruitment and activation of the IKK complex require cdc37 and Hsp90. Mol. Cell. *9*, 401-410.

Chen,J., Ueda,K., Sakakibara,S., Okuno,T., Parravicini,C., Corbellino,M., and Yamanishi,K. (2001). Activation of latent Kaposi's sarcoma-associated herpesvirus by demethylation of the promoter of the lytic transactivator. Proc. Natl. Acad. Sci. U. S. A *98*, 4119-4124.

Chevallier-Greco,A., Manet,E., Chavrier,P., Mosnier,C., Daillie,J., and Sergeant,A. (1986). Both Epstein-Barr virus (EBV)-encoded trans-acting factors, EB1 and EB2, are required to activate transcription from an EBV early promoter. EMBO J. *5*, 3243-3249.

Chien,C.T., Bartel,P.L., Sternglanz,R., and Fields,S. (1991). The two-hybrid system: a method to identify and clone genes for proteins that interact with a protein of interest. Proc. Natl. Acad. Sci. U. S. A *88*, 9578-9582.

Chiou,S.K., Tseng,C.C., Rao,L., and White,E. (1994). Functional complementation of the adenovirus E1B 19-kilodalton protein with Bcl-2 in the inhibition of apoptosis in infected cells. J. Virol. *68*, 6553-6566.

Clambey,E.T., Virgin,H.W., and Speck,S.H. (2000). Disruption of the murine gammaherpesvirus 68 M1 open reading frame leads to enhanced reactivation from latency. J. Virol. *74*, 1973-1984.

Clemens,M.J., Bushell,M., and Morley,S.J. (1998). Degradation of eukaryotic polypeptide chain initiation factor (eIF) 4G in response to induction of apoptosis in human lymphoma cell lines. Oncogene *17*, 2921-2931.

Clemens,M.J., Laing,K.G., Jeffrey,I.W., Schofield,A., Sharp,T.V., Elia,A., Matys,V., James,M.C., and Tilleray,V.J. (1994). Regulation of the interferon-inducible eIF-2 alpha protein kinase by small RNAs. Biochimie *76*, 770-778.

Cohen,J.I. and Lekstrom,K. (1999). Epstein-Barr virus BARF1 protein is dispensable for B-cell transformation and inhibits alpha interferon secretion from mononuclear cells. J. Virol. *73*, 7627-7632.

Coldwell,M.J., Mitchell,S.A., Stoneley,M., MacFarlane,M., and Willis,A.E. (2000). Initiation of Apaf-1 translation by internal ribosome entry. Oncogene *19*, 899-905.

Coleman,H.M., Brierley,I., and Stevenson,P.G. (2003). An internal ribosome entry site directs translation of the murine gammaherpesvirus 68 MK3 open reading frame. J. Virol. *77*, 13093-13105.

Cornelis,S., Bruynooghe,Y., Denecker,G., Van Huffel,S., Tinton,S., and Beyaert,R. (2000). Identification and characterization of a novel cell cycle-regulated internal ribosome entry site. Mol. Cell *5*, 597-605.

Coscoy,L. and Ganem,D. (2000). Kaposi's sarcoma-associated herpesvirus encodes two proteins that block cell surface display of MHC class I chains by enhancing their endocytosis. Proc. Natl. Acad. Sci. U. S. A *97*, 8051-8056.

Crawford,D.H. (2001). Biology and disease associations of Epstein-Barr virus. Philos. Trans. R. Soc. Lond B Biol. Sci. *356*, 461-473.

Dawson,C.W., Tramountanis,G., Eliopoulos,A.G., and Young,L.S. (2003). Epstein-Barr virus latent membrane protein 1 (LMP1) activates the phosphatidylinositol 3-kinase/Akt pathway to promote cell survival and induce actin filament remodeling. J. Biol. Chem. *278*, 3694-3704.

Dedicoat,M. and Newton,R. (2003). Review of the distribution of Kaposi's sarcoma-associated herpesvirus (KSHV) in Africa in relation to the incidence of Kaposi's sarcoma. Br. J. Cancer *88*, 1-3.

Devaney,M.A., Vakharia,V.N., Lloyd,R.E., Ehrenfeld,E., and Grubman,M.J. (1988). Leader protein of foot-and-mouth disease virus is required for cleavage of the p220 component of the cap-binding protein complex. J. Virol. *62*, 4407-4409.

Dittmer,D.P. (2003). Transcription profile of Kaposi's sarcoma-associated herpesvirus in primary Kaposi's sarcoma lesions as determined by real-time PCR arrays. Cancer Res. *63*, 2010-2015.

Djerbi,M., Screpanti,V., Catrina,A.I., Bogen,B., Biberfeld,P., and Grandien,A. (1999). The inhibitor of death receptor signaling, FLICE-inhibitory protein defines a new class of tumor progression factors. J. Exp. Med. *190*, 1025-1032.

Douglas,J., Dutia,B., Rhind,S., Stewart,J.P., and Talbot,S.J. (2004). Expression in a recombinant murid herpesvirus 4 reveals the in vivo transforming potential of the K1 open reading frame of Kaposi's sarcoma-associated herpesvirus. J. Virol. *78*, 8878-8884.

Duboise,S.M., Guo,J., Czajak,S., Desrosiers,R.C., and Jung,J.U. (1998). STP and Tip are essential for herpesvirus saimiri oncogenicity. J. Virol. *72*, 1308-1313.

Dupin,N. and Calvez,V. (2000). [HHV-8/KSHV. II--Associated diseases]. Ann. Dermatol. Venereol. *127*, 633-637.

Dupin,N., Fisher,C., Kellam,P., Ariad,S., Tulliez,M., Franck,N., van Marck,E., Salmon,D., Gorin,I., Escande,J.P., Weiss,R.A., Alitalo,K., and Boshoff,C. (1999). Distribution of human herpesvirus-8 latently infected cells in Kaposi's sarcoma, multicentric Castleman's disease, and primary effusion lymphoma. Proc. Natl. Acad. Sci. U. S. A *96*, 4546-4551.

Efstathiou,S., Ho,Y.M., Hall,S., Styles,C.J., Scott,S.D., and Gompels,U.A. (1990a). Murine herpesvirus 68 is genetically related to the gammaherpesviruses Epstein-Barr virus and herpesvirus saimiri. J. Gen. Virol. *71 (Pt 6)*, 1365-1372.

Efstathiou,S., Ho,Y.M., and Minson,A.C. (1990b). Cloning and molecular characterization of the murine herpesvirus 68 genome. J. Gen. Virol. *71 (Pt 6)*, 1355-1364.

Ellis,M., Chew,Y.P., Fallis,L., Freddersdorf,S., Boshoff,C., Weiss,R.A., Lu,X., and Mittnacht,S. (1999). Degradation of p27(Kip) cdk inhibitor triggered by Kaposi's sarcoma virus cyclin-cdk6 complex. EMBO J. *18*, 644-653.

Elsing,A. and Burgert,H.G. (1998). The adenovirus E3/10.4K-14.5K proteins down-modulate the apoptosis receptor Fas/Apo-1 by inducing its internalization. Proc. Natl. Acad. Sci. U. S. A *95*, 10072-10077.

Emery,V.C., Cope,A.V., Bowen,E.F., Gor,D., Griffiths,P.D. (1999). The dynamics of Human Cytomegalovirus Replication In Vivo. J. Exp. Med. *190 (Pt 2),* 177-182.

Epstein,M.A., Barr,Y.M., and Achong,B.G. (1965). Studies with Burkitt's lymphoma. Wistar. Inst. Symp. Monogr *4*, 69-82.

Etchison,D., Milburn,S.C., Edery,I., Sonenberg,N., and Hershey,J.W. (1982). Inhibition of HeLa cell protein synthesis following poliovirus infection correlates with the proteolysis of a 220,000-dalton polypeptide associated with eucaryotic

initiation factor 3 and a cap binding protein complex. J. Biol. Chem. *257*, 14806-14810.

Ezoe,H., Fatt,R.B., and Mak,S. (1981). Degradation of intracellular DNA in KB cells infected with cyt mutants of human adenovirus type 12. J. Virol. *40*, 20-27.

Feng,P., Park,J., Lee,B.S., Lee,S.H., Bram,R.J., and Jung,J.U. (2002). Kaposi's sarcoma-associated herpesvirus mitochondrial K7 protein targets a cellular calcium-modulating cyclophilin ligand to modulate intracellular calcium concentration and inhibit apoptosis. J. Virol. *76*, 11491-11504.

Fickenscher,H. and Fleckenstein,B. (2001). Herpesvirus saimiri. Philos. Trans. R. Soc. Lond B Biol. Sci. *356*, 545-567.

Field,N., Low,W., Daniels,M., Howell,S., Daviet,L., Boshoff,C., and Collins,M. (2003). KSHV vFLIP binds to IKK-gamma to activate IKK. J. Cell Sci. *116*, 3721-3728.

Fields,S. and Song,O. (1989). A novel genetic system to detect protein-protein interactions. Nature *340*, 245-246.

Flano,E., Kim,I.J., Moore,J., Woodland,D.L., and Blackman,M.A. (2003). Differential gamma-herpesvirus distribution in distinct anatomical locations and cell subsets during persistent infection in mice. J. Immunol. *170*, 3828-3834.

Fowler,P., Marques,S., Simas,J.P., and Efstathiou,S. (2003). ORF73 of murine herpesvirus-68 is critical for the establishment and maintenance of latency. J. Gen. Virol. *84*, 3405-3416.

Friborg,J., Jr., Kong,W., Hottiger,M.O., and Nabel,G.J. (1999). p53 inhibition by the LANA protein of KSHV protects against cell death. Nature *402*, 889-894.

Fridman,J.S. and Lowe,S.W. (2003). Control of apoptosis by p53. Oncogene *22*, 9030-9040.

Fuerst,T.R., Niles,E.G., Studier,F.W., and Moss,B. (1986). Eukaryotic transient-expression system based on recombinant vaccinia virus that synthesizes bacteriophage T7 RNA polymerase. Proc. Natl. Acad. Sci. U. S. A *83*, 8122-8126.

Fujimuro,M. and Hayward,S.D. (2003). The latency-associated nuclear antigen of Kaposi's sarcoma-associated herpesvirus manipulates the activity of glycogen synthase kinase-3beta. J. Virol. *77*, 8019-8030.

Fujimuro,M., Wu,F.Y., ApRhys,C., Kajumbula,H., Young,D.B., Hayward,G.S., and Hayward,S.D. (2003). A novel viral mechanism for dysregulation of beta-catenin in Kaposi's sarcoma-associated herpesvirus latency. Nat. Med. *9*, 300-306.

Gaidano,G., Capello,D., Cilia,A.M., Gloghini,A., Perin,T., Quattrone,S., Migliazza,A., Lo,C.F., Saglio,G., Ascoli,V., and Carbone,A. (1999). Genetic characterization of HHV-8/KSHV-positive primary effusion lymphoma reveals

frequent mutations of BCL6: implications for disease pathogenesis and histogenesis. Genes Chromosomes. Cancer *24*, 16-23.

Gan,W., LaCelle,M., and Rhoads,R.E. (1998). Functional characterization of the internal ribosome entry site of eIF4G mRNA. J. Biol. Chem. *273*, 5006-5012.

Gangappa,S., van Dyk,L.F., Jewett,T.J., Speck,S.H., and Virgin,H.W. (2002). Identification of the in vivo role of a viral bcl-2. J. Exp. Med. *195*, 931-940.

Garber,A.C., Shu,M.A., Hu,J., and Renne,R. (2001). DNA binding and modulation of gene expression by the latency-associated nuclear antigen of Kaposi's sarcoma-associated herpesvirus. J. Virol. *75*, 7882-7892.

Garcia-Blanco,M.A., Jamison,S.F., and Sharp,P.A. (1989). Identification and purification of a 62,000-dalton protein that binds specifically to the polypyrimidine tract of introns. Genes Dev. *3*, 1874-1886.

Geleziunas,R., Xu,W., Takeda,K., Ichijo,H., and Greene,W.C. (2001). HIV-1 Nef inhibits ASK1-dependent death signalling providing a potential mechanism for protecting the infected host cell. Nature *410*, 834-838.

Gerolami,R., Uch,R., Jordier,F., Chapel,S., Bagnis,C., Brechot,C., and Mannoni,P. (2000). Gene transfer to hepatocellular carcinoma: transduction efficacy and transgene expression kinetics by using retroviral and lentiviral vectors. Cancer Gene Ther. *7*, 1286-1292.

Gingras,A.C., Svitkin,Y., Belsham,G.J., Pause,A., and Sonenberg,N. (1996). Activation of the translational suppressor 4E-BP1 following infection with encephalomyocarditis virus and poliovirus. Proc. Natl. Acad. Sci. U. S. A *93*, 5578-5583.

Glaser,W. and Skern,T. (2000). Extremely efficient cleavage of eIF4G by picornaviral proteinases L and 2A in vitro. FEBS Lett. *480*, 151-155.

Godden-Kent,D., Talbot,S.J., Boshoff,C., Chang,Y., Moore,P., Weiss,R.A., and Mittnacht,S. (1997). The cyclin encoded by Kaposi's sarcoma-associated herpesvirus stimulates cdk6 to phosphorylate the retinoblastoma protein and histone H1. J. Virol. *71*, 4193-4198.

Gradi,A., Imataka,H., Svitkin,Y.V., Rom,E., Raught,B., Morino,S., and Sonenberg,N. (1998). A novel functional human eukaryotic translation initiation factor 4G. Mol. Cell Biol. *18*, 334-342.

Grogan,E., Jenson,H., Countryman,J., Heston,L., Gradoville,L., and Miller,G. (1987). Transfection of a rearranged viral DNA fragment, WZhet, stably converts latent Epstein-Barr viral infection to productive infection in lymphoid cells. Proc. Natl. Acad. Sci. U. S. A *84*, 1332-1336.

Grundhoff,A. and Ganem,D. (2001). Mechanisms governing expression of the v-FLIP gene of Kaposi's sarcoma-associated herpesvirus. J. Virol. *75*, 1857-1863.

Grundhoff,A. and Ganem,D. (2003). The latency-associated nuclear antigen of Kaposi's sarcoma-associated herpesvirus permits replication of terminal repeat-containing plasmids. J. Virol. *77*, 2779-2783.

Guasparri,I., Keller,S.A., and Cesarman,E. (2004). KSHV vFLIP Is Essential for the Survival of Infected Lymphoma Cells. J. Exp. Med. *199*, 993-1003.

Gwack,Y., Baek,H.J., Nakamura,H., Lee,S.H., Meisterernst,M., Roeder,R.G., and Jung,J.U. (2003). Principal role of TRAP/mediator and SWI/SNF complexes in Kaposi's sarcoma-associated herpesvirus RTA-mediated lytic reactivation. Mol. Cell Biol. *23*, 2055-2067.

Hacker,G. (2000). The morphology of apoptosis. Cell Tissue Res. *301*, 5-17.

Hall,K.T., Giles,M.S., Goodwin,D.J., Calderwood,M.A., Carr,I.M., Stevenson,A.J., Markham,A.F., and Whitehouse,A. (2000). Analysis of gene expression in a human cell line stably transduced with herpesvirus saimiri. J. Virol. *74*, 7331-7337.

Han,B. and Zhang,J.T. (2002). Regulation of gene expression by internal ribosome entry sites or cryptic promoters: the eIF4G story. Mol. Cell Biol. *22*, 7372-7384.

Haque,T., Thomas,J.A., Parratt,R., Hunt,B.J., Yacoub,M.H., and Crawford,D.H. (1997). A prospective study in heart and lung transplant recipients correlating persistent Epstein-Barr virus infection with clinical events. Transplantation *64*, 1028-1034.

Haque,T., Wilkie,G.M., Taylor,C., Amlot,P.L., Murad,P., Iley,A., Dombagoda,D., Britton,K.M., Swerdlow,A.J., and Crawford,D.H. (2002). Treatment of Epstein-Barr-virus-positive post-transplantation lymphoproliferative disease with partly HLA-matched allogeneic cytotoxic T cells. Lancet *360*, 436-442.

Hayward,G.S. (1999). KSHV strains: the origins and global spread of the virus. Semin. Cancer Biol. *9*, 187-199.

Heaton,J.H., Dlakic,W.M., Dlakic,M., and Gelehrter,T.D. (2001). Identification and cDNA cloning of a novel RNA-binding protein that interacts with the cyclic nucleotide-responsive sequence in the Type-1 plasminogen activator inhibitor mRNA. J. Biol. Chem. *276*, 3341-3347.

Hellen,C.U., Pestova,T.V., Litterst,M., and Wimmer,E. (1994). The cellular polypeptide p57 (pyrimidine tract-binding protein) binds to multiple sites in the poliovirus 5' nontranslated region. J. Virol. *68*, 941-950.

Hellen,C.U., Witherell,G.W., Schmid,M., Shin,S.H., Pestova,T.V., Gil,A., and Wimmer,E. (1993). A cytoplasmic 57-kDa protein that is required for translation of picornavirus RNA by internal ribosomal entry is identical to the nuclear pyrimidine tract-binding protein. Proc. Natl. Acad. Sci. U. S. A *90*, 7642-7646.

Henderson,S., Huen,D., Rowe,M., Dawson,C., Johnson,G., and Rickinson,A. (1993b). Epstein-Barr virus-coded BHRF1 protein, a viral homologue of Bcl-2,

protects human B cells from programmed cell death. Proc. Natl. Acad. Sci. U. S. A *90*, 8479-8483.

Henderson,S., Huen,D., Rowe,M., Dawson,C., Johnson,G., and Rickinson,A. (1993a). Epstein-Barr virus-coded BHRF1 protein, a viral homologue of Bcl-2, protects human B cells from programmed cell death. Proc. Natl. Acad. Sci. U. S. A *90*, 8479-8483.

Hengartner,M.O. (2000). The biochemistry of apoptosis. Nature *407*, 770-776.

Hengge,U.R., Ruzicka,T., Tyring,S.K., Stuschke,M., Roggendorf,M., Schwartz,R.A., and Seeber,S. (2002). Update on Kaposi's sarcoma and other HHV8 associated diseases. Part 1: epidemiology, environmental predispositions, clinical manifestations, and therapy. Lancet Infect. Dis. *2*, 281-292.

Henis-Korenblit,S., Shani,G., Sines,T., Marash,L., Shohat,G., and Kimchi,A. (2002). The caspase-cleaved DAP5 protein supports internal ribosome entry site-mediated translation of death proteins. Proc. Natl. Acad. Sci. U. S. A *99*, 5400-5405.

Henis-Korenblit,S., Strumpf,N.L., Goldstaub,D., and Kimchi,A. (2000). A novel form of DAP5 protein accumulates in apoptotic cells as a result of caspase cleavage and internal ribosome entry site-mediated translation. Mol. Cell Biol. *20*, 496-506.

Herrero,J.A., Mathew,P., and Paya,C.V. (1995). LMP-1 activates NF-kappa B by targeting the inhibitory molecule I kappa B alpha. J. Virol. *69*, 2168-2174.

Holcik,M., Gordon,B.W., and Korneluk,R.G. (2003). The internal ribosome entry site-mediated translation of antiapoptotic protein XIAP is modulated by the heterogeneous nuclear ribonucleoproteins C1 and C2. Mol. Cell Biol. *23*, 280-288.

Holcik,M. and Korneluk,R.G. (2000). Functional characterization of the X-linked inhibitor of apoptosis (XIAP) internal ribosome entry site element: role of La autoantigen in XIAP translation. Mol. Cell Biol. *20*, 4648-4657.

Holcik,M., Lefebvre,C., Yeh,C., Chow,T., and Korneluk,R.G. (1999). A new internal-ribosome-entry-site motif potentiates XIAP-mediated cytoprotection. Nat. Cell Biol. *1*, 190-192.

Holland,J.J. and Peterson,J.A. (1964). Nucleic acid and protein synthesis during poliovirus infection of human cells. J. Mol. Biol. *141*, 556-575.

Honess,R.W. and Roizman,B. (1974). Regulation of herpesvirus macromolecular synthesis. I. Cascade regulation of the synthesis of three groups of viral proteins. J. Virol. *14*, 8-19.

Hong,Y.K., Foreman,K., Shin,J.W., Hirakawa,S., Curry,C.L., Sage,D.R., Libermann,T., Dezube,B.J., Fingeroth,J.D., and Detmar,M. (2004). Lymphatic reprogramming of blood vascular endothelium by Kaposi sarcoma-associated herpesvirus. Nat. Genet. *36*, 683-685.

Hu,J., Garber,A.C., and Renne,R. (2002). The latency-associated nuclear antigen of Kaposi's sarcoma-associated herpesvirus supports latent DNA replication in dividing cells. J. Virol. *76*, 11677-11687.

Hu,S., Vincenz,C., Buller,M., and Dixit,V.M. (1997). A novel family of viral death effector domain-containing molecules that inhibit both CD-95- and tumor necrosis factor receptor-1-induced apoptosis. J. Biol. Chem. *272*, 9621-9624.

Huen,D.S., Henderson,S.A., Croom-Carter,D., and Rowe,M. (1995). The Epstein-Barr virus latent membrane protein-1 (LMP1) mediates activation of NF-kappa B and cell surface phenotype via two effector regions in its carboxy-terminal cytoplasmic domain. Oncogene *10*, 549-560.

Hunt,S.L., Hsuan,J.J., Totty,N., and Jackson,R.J. (1999). unr, a cellular cytoplasmic RNA-binding protein with five cold-shock domains, is required for internal initiation of translation of human rhinovirus RNA. Genes Dev. *13*, 437-448.

Hunt,S.L. and Jackson,R.J. (1999). Polypyrimidine-tract binding protein (PTB) is necessary, but not sufficient, for efficient internal initiation of translation of human rhinovirus-2 RNA. RNA. *5*, 344-359.

Imataka,H., Olsen,H.S., and Sonenberg,N. (1997). A new translational regulator with homology to eukaryotic translation initiation factor 4G. EMBO J. *16*, 817-825.

Imataka,H. and Sonenberg,N. (1997). Human eukaryotic translation initiation factor 4G (eIF4G) possesses two separate and independent binding sites for eIF4A. Mol. Cell Biol. *17*, 6940-6947.

Irmler,M., Thome,M., Hahne,M., Schneider,P., Hofmann,K., Steiner,V., Bodmer,J.L., Schroter,M., Burns,K., Mattmann,C., Rimoldi,D., French,L.E., and Tschopp,J. (1997). Inhibition of death receptor signals by cellular FLIP. Nature *388*, 190-195.

Isaksson,A., Berggren,M., and Ricksten,A. (2003). Epstein-Barr virus U leader exon contains an internal ribosome entry site. Oncogene *22*, 572-581.

Ishido,S., Choi,J.K., Lee,B.S., Wang,C., DeMaria,M., Johnson,R.P., Cohen,G.B., and Jung,J.U. (2000). Inhibition of natural killer cell-mediated cytotoxicity by Kaposi's sarcoma-associated herpesvirus K5 protein. Immunity. *13*, 365-374.

Izumi,K.M., Kaye,K.M., and Kieff,E.D. (1997). The Epstein-Barr virus LMP1 amino acid sequence that engages tumor necrosis factor receptor associated factors is critical for primary B lymphocyte growth transformation. Proc. Natl. Acad. Sci. U. S. A *94*, 1447-1452.

Jackson,R.J. (1988). RNA translation. Picornaviruses break the rules. Nature *334*, 292-293.

Jang,S.K., Krausslich,H.G., Nicklin,M.J., Duke,G.M., Palmenberg,A.C., and Wimmer,E. (1988). A segment of the 5' nontranslated region of

encephalomyocarditis virus RNA directs internal entry of ribosomes during in vitro translation. J. Virol. *62*, 2636-2643.

Jang,S.K. and Wimmer,E. (1990). Cap-independent translation of encephalomyocarditis virus RNA: structural elements of the internal ribosomal entry site and involvement of a cellular 57-kD RNA-binding protein. Genes Dev. *4*, 1560-1572.

Jenner,R.G., Alba,M.M., Boshoff,C., and Kellam,P. (2001). Kaposi's sarcoma-associated herpesvirus latent and lytic gene expression as revealed by DNA arrays. J. Virol. *75*, 891-902.

Jenner,R.G. and Boshoff,C. (2002). The molecular pathology of Kaposi's sarcoma-associated herpesvirus. Biochim. Biophys. Acta *1602*, 1-22.

Jones,D., Ballestas,M.E., Kaye,K.M., Gulizia,J.M., Winters,G.L., Fletcher,J., Scadden,D.T., and Aster,J.C. (1998). Primary-effusion lymphoma and Kaposi's sarcoma in a cardiac-transplant recipient. N. Engl. J. Med. *339*, 444-449.

Jopling,C.L., Spriggs,K.A., Mitchell,S.A., Stoneley,M., and Willis,A.E. (2004). L-Myc protein synthesis is initiated by internal ribosome entry. RNA. *10*, 287-298.

Jussila,L., Valtola,R., Partanen,T.A., Salven,P., Heikkila,P., Matikainen,M.T., Renkonen,R., Kaipainen,A., Detmar,M., Tschachler,E., Alitalo,R., and Alitalo,K. (1998). Lymphatic endothelium and Kaposi's sarcoma spindle cells detected by antibodies against the vascular endothelial growth factor receptor-3. Cancer Res. *58*, 1599-1604.

Kaiser,C., Laux,G., Eick,D., Jochner,N., Bornkamm,G.W., and Kempkes,B. (1999). The proto-oncogene c-myc is a direct target gene of Epstein-Barr virus nuclear antigen 2. J. Virol. *73*, 4481-4484.

Kallin,B., Sternas,L., Saemundssen,A.K., Luka,J., Jornvall,H., Eriksson,B., Tao,P.Z., Nilsson,M.T., and Klein,G. (1985). Purification of Epstein-Barr virus DNA polymerase from P3HR-1 cells. J. Virol. *54*, 561-568.

Kaminski,A., Hunt,S.L., Patton,J.G., and Jackson,R.J. (1995). Direct evidence that polypyrimidine tract binding protein (PTB) is essential for internal initiation of translation of encephalomyocarditis virus RNA. RNA. *1*, 924-938.

Kaminski,A. and Jackson,R.J. (1998). The polypyrimidine tract binding protein (PTB) requirement for internal initiation of translation of cardiovirus RNAs is conditional rather than absolute. RNA. *4*, 626-638.

Kaposi,M. (1872). Idiopathic multiple pigmented sarcoma of the skin. Arch. Dermatol. Syphil. *4*, 265-273.

Karin,M., Cao,Y., Greten,F.R., and Li,Z.W. (2002). NF-kappaB in cancer: from innocent bystander to major culprit. Nat. Rev. Cancer *2*, 301-310.

Kaye,K.M., Izumi,K.M., and Kieff,E. (1993). Epstein-Barr virus latent membrane protein 1 is essential for B-lymphocyte growth transformation. Proc. Natl. Acad. Sci. U. S. A *90*, 9150-9154.

Keller,S.A., Schattner,E.J., and Cesarman,E. (2000). Inhibition of NF-kappaB induces apoptosis of KSHV-infected primary effusion lymphoma cells. Blood *96*, 2537-2542.

Kerr,J.F., Wyllie,A.H., and Currie,A.R. (1972). Apoptosis: a basic biological phenomenon with wide-ranging implications in tissue kinetics. Br. J. Cancer *26*, 239-257.

Kieff,E. and Rickinson,A.B. (2001). Epstein-Barr Virus and Its Replication. In Fields Virology, D.M.Knipe and P.M.Howley, eds. Lippincott Williams and Wilkins), pp. 2511-2574.

Kieft,J.S., Zhou,K., Jubin,R., and Doudna,J.A. (2001). Mechanism of ribosome recruitment by hepatitis C IRES RNA. RNA. *7*, 194-206.

Kim,D.G., Kang,H.M., Jang,S.K., and Shin,H.S. (1992). Construction of a bifunctional mRNA in the mouse by using the internal ribosomal entry site of the encephalomyocarditis virus. Mol. Cell Biol. *12*, 3636-3643.

Kim,I.J., Flano,E., Woodland,D.L., Lund,F.E., Randall,T.D., and Blackman,M.A. (2003). Maintenance of long term gamma-herpesvirus B cell latency is dependent on CD40-mediated development of memory B cells. J. Immunol. *171*, 886-892.

Kirchweger,R., Ziegler,E., Lamphear,B.J., Waters,D., Liebig,H.D., Sommergruber,W., Sobrino,F., Hohenadl,C., Blaas,D., Rhoads,R.E., and . (1994). Foot-and-mouth disease virus leader proteinase: purification of the Lb form and determination of its cleavage site on eIF-4 gamma. J. Virol. *68*, 5677-5684.

Kitagawa,N., Goto,M., Kurozumi,K., Maruo,S., Fukayama,M., Naoe,T., Yasukawa,M., Hino,K., Suzuki,T., Todo,S., and Takada,K. (2000). Epstein-Barr virus-encoded poly(A)(-) RNA supports Burkitt's lymphoma growth through interleukin-10 induction. EMBO J. *19*, 6742-6750.

Knappe,A., Feldmann,G., Dittmer,U., Meinl,E., Nisslein,T., Wittmann,S., Matz-Rensing,K., Kirchner,T., Bodemer,W., and Fickenscher,H. (2000). Herpesvirus saimiri-transformed macaque T cells are tolerated and do not cause lymphoma after autologous reinfusion. Blood *95*, 3256-3261.

Knight,J.S., Cotter,M.A., and Robertson,E.S. (2001). The latency-associated nuclear antigen of Kaposi's sarcoma-associated herpesvirus transactivates the telomerase reverse transcriptase promoter. J. Biol. Chem. *276*, 22971-22978.

Kohler,G. and Milstein,C. (1976). Derivation of specific antibody-producing tissue culture and tumor lines by cell fusion. Eur. J. Immunol. *6*, 511-519.

Kolupaeva,V.G., Hellen,C.U., and Shatsky,I.N. (1996). Structural analysis of the interaction of the pyrimidine tract-binding protein with the internal ribosomal entry site of encephalomyocarditis virus and foot-and-mouth disease virus RNAs. RNA. *2*, 1199-1212.

Kolupaeva,V.G., Pestova,T.V., Hellen,C.U., and Shatsky,I.N. (1998). Translation eukaryotic initiation factor 4G recognizes a specific structural element within the internal ribosome entry site of encephalomyocarditis virus RNA. J. Biol. Chem. *273*, 18599-18604.

Komano,J., Maruo,S., Kurozumi,K., Oda,T., and Takada,K. (1999). Oncogenic role of Epstein-Barr virus-encoded RNAs in Burkitt's lymphoma cell line Akata. J. Virol. *73*, 9827-9831.

Kozak,M. (2003). Alternative ways to think about mRNA sequences and proteins that appear to promote internal initiation of translation. Gene *318*, 1-23.

Krammer,P.H. (2000). CD95's deadly mission in the immune system. Nature *407*, 789-795.

Kreuz,S., Siegmund,D., Scheurich,P., and Wajant,H. (2001). NF-kappaB inducers upregulate cFLIP, a cycloheximide-sensitive inhibitor of death receptor signaling. Mol. Cell Biol. *21*, 3964-3973.

Krithivas,A., Fujimuro,M., Weidner,M., Young,D.B., and Hayward,S.D. (2002). Protein interactions targeting the latency-associated nuclear antigen of Kaposi's sarcoma-associated herpesvirus to cell chromosomes. J. Virol. *76*, 11596-11604.

Krueger,A., Schmitz,I., Baumann,S., Krammer,P.H., and Kirchhoff,S. (2001). Cellular FLICE-inhibitory protein splice variants inhibit different steps of caspase-8 activation at the CD95 death-inducing signaling complex. J. Biol. Chem. *276*, 20633-20640.

Lagunoff,M., Majeti,R., Weiss,A., and Ganem,D. (1999). Deregulated signal transduction by the K1 gene product of Kaposi's sarcoma-associated herpesvirus. Proc. Natl. Acad. Sci. U. S. A *96*, 5704-5709.

Lamphear,B.J., Kirchweger,R., Skern,T., and Rhoads,R.E. (1995). Mapping of functional domains in eukaryotic protein synthesis initiation factor 4G (eIF4G) with picornaviral proteases. Implications for cap-dependent and cap-independent translational initiation. J. Biol. Chem. *270*, 21975-21983.

Lamphear,B.J., Yan,R., Yang,F., Waters,D., Liebig,H.D., Klump,H., Kuechler,E., Skern,T., and Rhoads,R.E. (1993). Mapping the cleavage site in protein synthesis initiation factor eIF-4 gamma of the 2A proteases from human Coxsackievirus and rhinovirus. J. Biol. Chem. *268*, 19200-19203.

Le Quesne,J.P., Stoneley,M., Fraser,G.A., and Willis,A.E. (2001). Derivation of a structural model for the c-myc IRES. J. Mol. Biol. *310*, 111-126.

Le,H., Tanguay,R.L., Balasta,M.L., Wei,C.C., Browning,K.S., Metz,A.M., Goss,D.J., and Gallie,D.R. (1997). Translation initiation factors eIF-iso4G and eIF-4B interact with the poly(A)-binding protein and increase its RNA binding activity. J. Biol. Chem. *272*, 16247-16255.

Lee,B.J., Koszinowski,U.H., Sarawar,S.R., and Adler,H. (2003). A gammaherpesvirus G protein-coupled receptor homologue is required for increased viral replication in response to chemokines and efficient reactivation from latency. J. Immunol. *170*, 243-251.

Lee,H., Guo,J., Li,M., Choi,J.K., DeMaria,M., Rosenzweig,M., and Jung,J.U. (1998a). Identification of an immunoreceptor tyrosine-based activation motif of K1 transforming protein of Kaposi's sarcoma-associated herpesvirus. Mol. Cell Biol. *18*, 5219-5228.

Lee,H., Veazey,R., Williams,K., Li,M., Guo,J., Neipel,F., Fleckenstein,B., Lackner,A., Desrosiers,R.C., and Jung,J.U. (1998b). Deregulation of cell growth by the K1 gene of Kaposi's sarcoma-associated herpesvirus. Nat. Med. *4*, 435-440.

Lerat,H., Shimizu,Y.K., and Lemon,S.M. (2000). Cell type-specific enhancement of hepatitis C virus internal ribosome entry site-directed translation due to 5' nontranslated region substitutions selected during passage of virus in lymphoblastoid cells. J. Virol. *74*, 7024-7031.

Lerner,M.R., Andrews,N.C., Miller,G., and Steitz,J.A. (1981). Two small RNAs encoded by Epstein-Barr virus and complexed with protein are precipitated by antibodies from patients with systemic lupus erythematosus. Proc. Natl. Acad. Sci. U. S. A *78*, 805-809.

Levy-Strumpf,N., Deiss,L.P., Berissi,H., and Kimchi,A. (1997). DAP-5, a novel homolog of eukaryotic translation initiation factor 4G isolated as a putative modulator of gamma interferon-induced programmed cell death. Mol. Cell Biol. *17*, 1615-1625.

Li,M., Lee,H., Yoon,D.W., Albrecht,J.C., Fleckenstein,B., Neipel,F., and Jung,J.U. (1997). Kaposi's sarcoma-associated herpesvirus encodes a functional cyclin. J. Virol. *71*, 1984-1991.

Liao,W., Tang,Y., Kuo,Y.L., Liu,B.Y., Xu,C.J., and Giam,C.Z. (2003a). Kaposi's sarcoma-associated herpesvirus/human herpesvirus 8 transcriptional activator Rta is an oligomeric DNA-binding protein that interacts with tandem arrays of phased A/T-trinucleotide motifs. J. Virol. *77*, 9399-9411.

Liao,W., Tang,Y., Lin,S.F., Kung,H.J., and Giam,C.Z. (2003b). K-bZIP of Kaposi's sarcoma-associated herpesvirus/human herpesvirus 8 (KSHV/HHV-8) binds KSHV/HHV-8 Rta and represses Rta-mediated transactivation. J. Virol. *77*, 3809-3815.

Liu,L., Eby,M.T., Rathore,N., Sinha,S.K., Kumar,A., and Chaudhary,P.M. (2002). The human herpes virus 8-encoded viral FLICE inhibitory protein physically associates with and persistently activates the Ikappa B kinase complex. J. Biol. Chem. *277*, 13745-13751.

Liu,S., Pavlova,I.V., Virgin,H.W., and Speck,S.H. (2000). Characterization of gammaherpesvirus 68 gene 50 transcription. J. Virol. *74*, 2029-2037.

Longnecker,R. (2000). Epstein-Barr virus latency: LMP2, a regulator or means for Epstein-Barr virus persistence? Adv. Cancer Res. *79*, 175-200.

Lopez,d.Q., Lafuente,E., and Martinez-Salas,E. (2001). IRES interaction with translation initiation factors: functional characterization of novel RNA contacts with eIF3, eIF4B, and eIF4GII. RNA. *7*, 1213-1226.

Lopez,d.Q. and Martinez-Salas,E. (2000). Interaction of the eIF4G initiation factor with the aphthovirus IRES is essential for internal translation initiation in vivo. RNA. *6*, 1380-1392.

Low,W., Harries,M., Ye,H., Du,M.Q., Boshoff,C., and Collins,M. (2001). Internal ribosome entry site regulates translation of Kaposi's sarcoma-associated herpesvirus FLICE inhibitory protein. J. Virol. *75*, 2938-2945.

Lu,F., Zhou,J., Wiedmer,A., Madden,K., Yuan,Y., and Lieberman,P.M. (2003). Chromatin remodeling of the Kaposi's sarcoma-associated herpesvirus ORF50 promoter correlates with reactivation from latency. J. Virol. *77*, 11425-11435.

Lukac,D.M., Garibyan,L., Kirshner,J.R., Palmeri,D., and Ganem,D. (2001). DNA binding by Kaposi's sarcoma-associated herpesvirus lytic switch protein is necessary for transcriptional activation of two viral delayed early promoters. J. Virol. *75*, 6786-6799.

Lukac,D.M., Kirshner,J.R., and Ganem,D. (1999). Transcriptional activation by the product of open reading frame 50 of Kaposi's sarcoma-associated herpesvirus is required for lytic viral reactivation in B cells. J. Virol. *73*, 9348-9361.

Lukac,D.M., Renne,R., Kirshner,J.R., and Ganem,D. (1998). Reactivation of Kaposi's sarcoma-associated herpesvirus infection from latency by expression of the ORF 50 transactivator, a homolog of the EBV R protein. Virology *252*, 304-312.

Luz,N. and Beck,E. (1990). A cellular 57 kDa protein binds to two regions of the internal translation initiation site of foot-and-mouth disease virus. FEBS Lett. *269*, 311-314.

Luz,N. and Beck,E. (1991). Interaction of a cellular 57-kilodalton protein with the internal translation initiation site of foot-and-mouth disease virus. J. Virol. *65*, 6486-6494.

Macrae,A.I., Dutia,B.M., Milligan,S., Brownstein,D.G., Allen,D.J., Mistrikova,J., Davison,A.J., Nash,A.A., and Stewart,J.P. (2001). Analysis of a novel strain of murine gammaherpesvirus reveals a genomic locus important for acute pathogenesis. J. Virol. *75*, 5315-5327.

Macrae,A.I., Usherwood,E.J., Husain,S.M., Flano,E., Kim,I.J., Woodland,D.L., Nash,A.A., Blackman,M.A., Sample,J.T., and Stewart,J.P. (2003). Murid herpesvirus 4 strain 68 M2 protein is a B-cell-associated antigen important for latency but not lymphocytosis. J. Virol. *77*, 9700-9709.

Macsween,K.F. and Crawford,D.H. (2003). Epstein-Barr virus-recent advances. Lancet Infect. Dis. *3*, 131-140.

Mao,X., Fujiwara,Y., Chapdelaine,A., Yang, H. and Orkin,S.H. (2001). Activation of EGFP expression by Cre-mediated excision in a new ROSA26 reporter mouse strain. Blood *97*, 324-326.

Marshall,W.L., Yim,C., Gustafson,E., Graf,T., Sage,D.R., Hanify,K., Williams,L., Fingeroth,J., and Finberg,R.W. (1999). Epstein-Barr virus encodes a novel homolog of the bcl-2 oncogene that inhibits apoptosis and associates with Bax and Bak. J. Virol. *73*, 5181-5185.

Martinez-Guzman,D., Rickabaugh,T., Wu,T.T., Brown,H., Cole,S., Song,M.J., Tong,L., and Sun,R. (2003). Transcription program of murine gammaherpesvirus 68. J. Virol. *77*, 10488-10503.

Martinez-Salas,E., Lopez,d.Q., Ramos,R., and Fernandez-Miragall,O. (2002). IRES elements: features of the RNA structure contributing to their activity. Biochimie *84*, 755-763.

Matta,H., Sun,Q., Moses,G., and Chaudhary,P.M. (2003). Molecular genetic analysis of human herpes virus 8-encoded viral FLICE inhibitory protein (vFLIP)-induced NF-kappa B activation. J. Biol. Chem.

McGeoch,D.J. and Davison,A.J. (1999). The descent of human herpesvirus 8. Semin. Cancer Biol. *9*, 201-209.

Medema,J.P., de Jong,J., van Hall,T., Melief,C.J., and Offringa,R. (1999). Immune escape of tumors in vivo by expression of cellular FLICE-inhibitory protein. J. Exp. Med. *190*, 1033-1038.

Medveczky,P., Szomolanyi,E., Desrosiers,R.C., and Mulder,C. (1984). Classification of herpesvirus saimiri into three groups based on extreme variation in a DNA region required for oncogenicity. J. Virol. *52*, 938-944.

Merlo,J.J. and Tsygankov,A.Y. (2001). Herpesvirus saimiri oncoproteins Tip and StpC synergistically stimulate NF-kappaB activity and interleukin-2 gene expression. Virology *279*, 325-338.

Mettenleiter,T.C. (2002). Herpesvirus assembly and egress. J. Virol. *76*, 1537-1547.

Mitchell,S.A., Brown,E.C., Coldwell,M.J., Jackson,R.J., and Willis,A.E. (2001). Protein factor requirements of the Apaf-1 internal ribosome entry segment: roles of polypyrimidine tract binding protein and upstream of N-ras. Mol. Cell Biol. *21*, 3364-3374.

Mitchell,S.A., Spriggs,K.A., Coldwell,M.J., Jackson,R.J., and Willis,A.E. (2003). The Apaf-1 internal ribosome entry segment attains the correct structural conformation for function via interactions with PTB and unr. Mol. Cell *11*, 757-771.

Montaner,S., Sodhi,A., Molinolo,A., Bugge,T.H., Sawai,E.T., He,Y., Li,Y., Ray,P.E., and Gutkind,J.S. (2003). Endothelial infection with KSHV genes in vivo reveals that vGPCR initiates Kaposi's sarcomagenesis and can promote the tumorigenic potential of viral latent genes. Cancer Cell *3*, 23-36.

Moore,P.S., Boshoff,C., Weiss,R.A., and Chang,Y. (1996). Molecular mimicry of human cytokine and cytokine response pathway genes by KSHV. Science *274*, 1739-1744.

Moore,P.S. and Chang,Y. (2001). Molecular virology of Kaposi's sarcoma-associated herpesvirus. Philos. Trans. R. Soc. Lond B Biol. Sci. *356*, 499-516.

Mulligan,G.J., Guo,W., Wormsley,S., and Helfman,D.M. (1992). Polypyrimidine tract binding protein interacts with sequences involved in alternative splicing of beta-tropomyosin pre-mRNA. J. Biol. Chem. *267*, 25480-25487.

Muzio,M., Stockwell,B.R., Stennicke,H.R., Salvesen,G.S., and Dixit,V.M. (1998). An induced proximity model for caspase-8 activation. J. Biol. Chem. *273*, 2926-2930.

Nanbru,C., Lafon,I., Audigier,S., Gensac,M.C., Vagner,S., Huez,G., and Prats,A.C. (1997). Alternative translation of the proto-oncogene c-myc by an internal ribosome entry site. J. Biol. Chem. *272*, 32061-32066.

Nash,A.A., Dutia,B.M., Stewart,J.P., and Davison,A.J. (2001). Natural history of murine gamma-herpesvirus infection. Philos. Trans. R. Soc. Lond B Biol. Sci. *356*, 569-579.

Nevins,T.A., Harder,Z.M., Korneluk,R.G., and Holcik,M. (2003). Distinct regulation of internal ribosome entry site-mediated translation following cellular stress is mediated by apoptotic fragments of eIF4G translation initiation factor family members eIF4GI and p97/DAP5/NAT1. J. Biol. Chem. *278*, 3572-3579.

Nicholson,D.W. and Thornberry,N.A. (1997). Caspases: killer proteases. Trends Biochem. Sci. *22*, 299-306.

Nonkwelo,C., Skinner,J., Bell,A., Rickinson,A., and Sample,J. (1996). Transcription start sites downstream of the Epstein-Barr virus (EBV) Fp promoter in early-passage Burkitt lymphoma cells define a fourth promoter for expression of the EBV EBNA-1 protein. J. Virol. *70*, 623-627.

Oguro,M.O., Shimizu,N., Ono,Y., and Takada,K. (1987). Both the rightward and the leftward open reading frames within the BamHI M DNA fragment of Epstein-Barr virus act as trans-activators of gene expression. J. Virol. *61*, 3310-3313.

Ohlmann,T., Lopez-Lastra,M., and Darlix,J.L. (2000). An internal ribosome entry segment promotes translation of the simian immunodeficiency virus genomic RNA. J. Biol. Chem. *275*, 11899-11906.

Ohlmann,T., Rau,M., Pain,V.M., and Morley,S.J. (1996). The C-terminal domain of eukaryotic protein synthesis initiation factor (eIF) 4G is sufficient to support cap-independent translation in the absence of eIF4E. EMBO J. *15*, 1371-1382.

Ojala,P.M., Tiainen,M., Salven,P., Veikkola,T., Castanos-Velez,E., Sarid,R., Biberfeld,P., and Makela,T.P. (1999). Kaposi's sarcoma-associated herpesvirus-encoded v-cyclin triggers apoptosis in cells with high levels of cyclin-dependent kinase 6. Cancer Res. *59*, 4984-4989.

Ojala,P.M., Yamamoto,K., Castanos-Velez,E., Biberfeld,P., Korsmeyer,S.J., and Makela,T.P. (2000). The apoptotic v-cyclin-CDK6 complex phosphorylates and inactivates Bcl-2. Nat. Cell Biol. *2*, 819-825.

Okano,H., Shiraki,K., Inoue,H., Kawakita,T., Yamanaka,T., Deguchi,M., Sugimoto,K., Sakai,T., Ohmori,S., Fujikawa,K., Murata,K., and Nakano,T. (2003). Cellular FLICE/caspase-8-inhibitory protein as a principal regulator of cell death and survival in human hepatocellular carcinoma. Lab Invest *83*, 1033-1043.

Pahl,H.L. (1999). Activators and target genes of Rel/NF-kappaB transcription factors. Oncogene *18*, 6853-6866.

Paulose-Murphy,M., Ha,N.K., Xiang,C., Chen,Y., Gillim,L., Yarchoan,R., Meltzer,P., Bittner,M., Trent,J., and Zeichner,S. (2001). Transcription program of human herpesvirus 8 (kaposi's sarcoma-associated herpesvirus). J. Virol. *75*, 4843-4853.

Pelletier,J., Kaplan,G., Racaniello,V.R., and Sonenberg,N. (1988). Cap-independent translation of poliovirus mRNA is conferred by sequence elements within the 5' noncoding region. Mol. Cell Biol. *8*, 1103-1112.

Pelletier,J. and Sonenberg,N. (1988). Internal initiation of translation of eukaryotic mRNA directed by a sequence derived from poliovirus RNA. Nature *334*, 320-325.

Pestova,T.V., Hellen,C.U., and Shatsky,I.N. (1996a). Canonical eukaryotic initiation factors determine initiation of translation by internal ribosomal entry. Mol. Cell Biol. *16*, 6859-6869.

Pestova,T.V., Shatsky,I.N., Fletcher,S.P., Jackson,R.J., and Hellen,C.U. (1998). A prokaryotic-like mode of cytoplasmic eukaryotic ribosome binding to the initiation codon during internal translation initiation of hepatitis C and classical swine fever virus RNAs. Genes Dev. *12*, 67-83.

Pestova,T.V., Shatsky,I.N., and Hellen,C.U. (1996b). Functional dissection of eukaryotic initiation factor 4F: the 4A subunit and the central domain of the 4G subunit are sufficient to mediate internal entry of 43S preinitiation complexes. Mol. Cell Biol. *16*, 6870-6878.

Pickering,B.M., Mitchell,S.A., Evans,J.R., and Willis,A.E. (2003). Polypyrimidine tract binding protein and poly r(C) binding protein 1 interact with the BAG-1 IRES and stimulate its activity in vitro and in vivo. Nucleic Acids Res. *31*, 639-646.

Pikarsky,E., Porat,R.M., Stein,I., Abramovitch,R., Amit,S., Kasem,S., Gutkovich-Pyest,E., Urieli-Shoval,S., Galun,E., and Ben Neriah,Y. (2004). NF-kappaB functions as a tumour promoter in inflammation-associated cancer. Nature *431*, 461-466.

Polakis,P. (2000). Wnt signaling and cancer. Genes Dev. *14*, 1837-1851.

Pyronnet,S., Imataka,H., Gingras,A.C., Fukunaga,R., Hunter,T., and Sonenberg,N. (1999). Human eukaryotic translation initiation factor 4G (eIF4G) recruits mnk1 to phosphorylate eIF4E. EMBO J. *18*, 270-279.

Pyronnet,S., Pradayrol,L., and Sonenberg,N. (2000). A cell cycle-dependent internal ribosome entry site. Mol. Cell *5*, 607-616.

Qin,X. and Sarnow,P. (2004). Preferential translation of IRES-containing mRNAs during the mitotic cycle in mammalian cells. J. Biol. Chem.

Radkov,S.A., Kellam,P., and Boshoff,C. (2000). The latent nuclear antigen of Kaposi sarcoma-associated herpesvirus targets the retinoblastoma-E2F pathway and with the oncogene Hras transforms primary rat cells. Nat. Med. *6*, 1121-1127.

Ranish,J.A. and Hahn,S. (1991). The yeast general transcription factor TFIIA is composed of two polypeptide subunits. J. Biol. Chem. *266*, 19320-19327.

Renne,R., Blackbourn,D., Whitby,D., Levy,J., and Ganem,D. (1998). Limited transmission of Kaposi's sarcoma-associated herpesvirus in cultured cells. J. Virol. *72*, 5182-5188.

Rickinson,A.B. and Kieff,E. (2001). Epstein-Barr Virus. In Fields Virology, D.M.Knipe and P.M.Howley, eds. Lippincott Williams and Wilkins), pp. 2575-2628.

Rijnbrand,R., van der,S.T., van Rijn,P.A., Spaan,W.J., and Bredenbeek,P.J. (1997). Internal entry of ribosomes is directed by the 5' noncoding region of classical swine fever virus and is dependent on the presence of an RNA pseudoknot upstream of the initiation codon. J. Virol. *71*, 451-457.

Roan,F., Inoue,N., and Offermann,M.K. (2002). Activation of cellular and heterologous promoters by the human herpesvirus 8 replication and transcription activator. Virology *301*, 293-304.

Roberts,L.O., Seamons,R.A., and Belsham,G.J. (1998). Recognition of picornavirus internal ribosome entry sites within cells; influence of cellular and viral proteins. RNA. *4*, 520-529.

Rochford,R., Lutzke,M.L., Alfinito,R.S., Clavo,A., and Cardin,R.D. (2001). Kinetics of murine gammaherpesvirus 68 gene expression following infection of murine cells in culture and in mice. J. Virol. *75*, 4955-4963.

Roizman,B. and Knipe,D.M. (2001). Herpes simplex Viruses and their replication. In Fields Virology, D.M.Knipe and P.M.Howley, eds. Lippincott Williams and Wilkins), pp. 2399-2460.

Roizman,B. and Pellet,P.E. (2001). The family *Herpesviridae*: A Brief Introduction. In Fields Virology, D.M.Knipe and P.M.Howley, eds. Lippincott Williams and Wilkins), pp. 2381-2398.

Rooney,C.M., Smith,C.A., Ng,C.Y., Loftin,S.K., Sixbey,J.W., Gan,Y., Srivastava,D.K., Bowman,L.C., Krance,R.A., Brenner,M.K., and Heslop,H.E. (1998). Infusion of cytotoxic T cells for the prevention and treatment of Epstein-Barr virus-induced lymphoma in allogeneic transplant recipients. Blood *92*, 1549-1555.

Roy,D.J., Ebrahimi,B.C., Dutia,B.M., Nash,A.A., and Stewart,J.P. (2000). Murine gammaherpesvirus M11 gene product inhibits apoptosis and is expressed during virus persistence. Arch. Virol. *145*, 2411-2420.

Russo,J.J., Bohenzky,R.A., Chien,M.C., Chen,J., Yan,M., Maddalena,D., Parry,J.P., Peruzzi,D., Edelman,I.S., Chang,Y., and Moore,P.S. (1996). Nucleotide sequence of the Kaposi sarcoma-associated herpesvirus (HHV8). Proc. Natl. Acad. Sci. U. S. A *93*, 14862-14867.

Ryu,B.K., Lee,M.G., Chi,S.G., Kim,Y.W., and Park,J.H. (2001). Increased expression of cFLIP(L) in colonic adenocarcinoma. J. Pathol. *194*, 15-19.

Sachs,A.B. (2000). Cell cycle-dependent translation initiation: IRES elements prevail. Cell *101*, 243-245.

Santoro,M.G., Rossi,A., and Amici,C. (2003). NF-kappaB and virus infection: who controls whom. EMBO J. *22*, 2552-2560.

Sarid,R., Flore,O., Bohenzky,R.A., Chang,Y., and Moore,P.S. (1998). Transcription mapping of the Kaposi's sarcoma-associated herpesvirus (human herpesvirus 8) genome in a body cavity-based lymphoma cell line (BC-1). J. Virol. *72*, 1005-1012.

Sarid,R., Sato,T., Bohenzky,R.A., Russo,J.J., and Chang,Y. (1997). Kaposi's sarcoma-associated herpesvirus encodes a functional bcl-2 homologue. Nat. Med. *3*, 293-298.

Sasaki,J. and Nakashima,N. (1999). Translation initiation at the CUU codon is mediated by the internal ribosome entry site of an insect picorna-like virus in vitro. J. Virol. *73*, 1219-1226.

Sayers,T.J., Brooks,A.D., Lee,J.K., Fenton,R.G., Komschlies,K.L., Wigginton,J.M., Winkler-Pickett,R., and Wiltrout,R.H. (1998). Molecular mechanisms of immune-mediated lysis of murine renal cancer: differential contributions of perforin-dependent versus Fas-mediated pathways in lysis by NK and T cells. J. Immunol. *161*, 3957-3965.

Scaffidi,C., Schmitz,I., Krammer,P.H., and Peter,M.E. (1999). The role of c-FLIP in modulation of CD95-induced apoptosis. J. Biol. Chem. *274*, 1541-1548.

Schneider,R., Agol,V.I., Andino,R., Bayard,F., Cavener,D.R., Chappell,S.A., Chen,J.J., Darlix,J.L., Dasgupta,A., Donze,O., Duncan,R., Elroy-Stein,O., Farabaugh,P.J., Filipowicz,W., Gale,M., Jr., Gehrke,L., Goldman,E., Groner,Y., Harford,J.B., Hatzglou,M., He,B., Hellen,C.U., Hentze,M.W., Hershey,J., Hershey,P., Hohn,T., Holcik,M., Hunter,C.P., Igarashi,K., Jackson,R., Jagus,R., Jefferson,L.S., Joshi,B., Kaempfer,R., Katze,M., Kaufman,R.J., Kiledjian,M., Kimball,S.R., Kimchi,A., Kirkegaard,K., Koromilas,A.E., Krug,R.M., Kruys,V., Lamphear,B.J., Lemon,S., Lloyd,R.E., Maquat,L.E., Martinez-Salas,E., Mathews,M.B., Mauro,V.P., Miyamoto,S., Mohr,I., Morris,D.R., Moss,E.G., Nakashima,N., Palmenberg,A., Parkin,N.T., Pe'ery,T., Pelletier,J., Peltz,S., Pestova,T.V., Pilipenko,E.V., Prats,A.C., Racaniello,V., Read,G.S., Rhoads,R.E., Richter,J.D., Rivera-Pomar,R., Rouault,T., Sachs,A., Sarnow,P., Scheper,G.C., Schiff,L., Schoenberg,D.R., Semler,B.L., Siddiqui,A., Skern,T., Sonenberg,N., Tahara,S.M., Thomas,A.A., Toulme,J.J., Wilusz,J., Wimmer,E., Witherell,G., and Wormington,M. (2001). New ways of initiating translation in eukaryotes. Mol. Cell Biol. *21*, 8238-8246.

Schwarz,M. and Murphy,P.M. (2001). Kaposi's sarcoma-associated herpesvirus G protein-coupled receptor constitutively activates NF-kappa B and induces proinflammatory cytokine and chemokine production via a C-terminal signaling determinant. J. Immunol. *167*, 505-513.

SenGupta,D.J., Zhang,B., Kraemer,B., Pochart,P., Fields,S., and Wickens,M. (1996). A three-hybrid system to detect RNA-protein interactions in vivo. Proc. Natl. Acad. Sci. U. S. A *93*, 8496-8501.

Serraino,D., Toma,L., Andreoni,M., Butto,S., Tchangmena,O., Sarmati,L., Monini,P., Franceschi,S., Ensoli,B., and Rezza,G. (2001). A seroprevalence study of human herpesvirus type 8 (HHV8) in eastern and Central Africa and in the Mediterranean area. Eur. J. Epidemiol. *17*, 871-876.

Sgarbanti,M., Arguello,M., TenOever,B.R., Battistini,A., Lin,R., and Hiscott,J. (2004). A requirement for NF-kappaB induction in the production of replication-competent HHV-8 virions. Oncogene.

Shiroki,K., Ishii,T., Aoki,T., Ota,Y., Yang,W.X., Komatsu,T., Ami,Y., Arita,M., Abe,S., Hashizume,S., and Nomoto,A. (1997). Host range phenotype induced by mutations in the internal ribosomal entry site of poliovirus RNA. J. Virol. *71*, 1-8.

Simas,J.P. and Efstathiou,S. (1998). Murine gammaherpesvirus 68: a model for the study of gammaherpesvirus pathogenesis. Trends Microbiol. *6*, 276-282.

Sitas,F. and Newton,R. (2001). Kaposi's sarcoma in South Africa. J. Natl. Cancer Inst. Monogr 1-4.

Smith,C.A., Farrah,T., and Goodwin,R.G. (1994). The TNF receptor superfamily of cellular and viral proteins: activation, costimulation, and death. Cell *76*, 959-962.

Sorokina,E.M., Merlo,J.J., Jr., and Tsygankov,A.Y. (2004). Molecular mechanisms of the effect of herpesvirus saimiri protein StpC on the signaling pathway leading to NF-kappaB activation. J. Biol. Chem. *279*, 13469-13477.

Spear,P.G., Eisenberg,R.J., and Cohen,G.H. (2000). Three classes of cell surface receptors for alphaherpesvirus entry. Virology *275*, 1-8.

Spear,P.G. and Longnecker,R. (2003). Herpesvirus entry: an update. J. Virol. *77*, 10179-10185.

Stassinopoulos,I.A. and Belsham,G.J. (2001). A novel protein-RNA binding assay: functional interactions of the foot-and-mouth disease virus internal ribosome entry site with cellular proteins. RNA. *7*, 114-122.

Stevenson,P.G., Efstathiou,S., Doherty,P.C., and Lehner,P.J. (2000). Inhibition of MHC class I-restricted antigen presentation by gamma 2-herpesviruses. Proc. Natl. Acad. Sci. U. S. A *97*, 8455-8460.

Stevenson,P.G., May,J.S., Smith,X.G., Marques,S., Adler,H., Koszinowski,U.H., Simas,J.P., and Efstathiou,S. (2002). K3-mediated evasion of CD8(+) T cells aids amplification of a latent gamma-herpesvirus. Nat. Immunol. *3*, 733-740.

Stewart,J.P., Usherwood,E.J., Ross,A., Dyson,H., and Nash,T. (1998). Lung epithelial cells are a major site of murine gammaherpesvirus persistence. J. Exp. Med. *187*, 1941-1951.

Stoneley,M. and Willis,A.E. (2004). Cellular internal ribosome entry segments: structures, trans-acting factors and regulation of gene expression. Oncogene *23*, 3200-3207.

Sturzl,M., Brandstetter,H., and Roth,W.K. (1992). Kaposi's sarcoma: a review of gene expression and ultrastructure of KS spindle cells in vivo. AIDS Res. Hum. Retroviruses *8*, 1753-1763.

Sturzl,M., Hohenadl,C., Zietz,C., Castanos-Velez,E., Wunderlich,A., Ascherl,G., Biberfeld,P., Monini,P., Browning,P.J., and Ensoli,B. (1999). Expression of K13/v-FLIP gene of human herpesvirus 8 and apoptosis in Kaposi's sarcoma spindle cells. J. Natl. Cancer Inst. *91*, 1725-1733.

Sun,Q., Matta,H., and Chaudhary,P.M. (2003a). The human herpes virus 8-encoded viral FLICE inhibitory protein protects against growth factor withdrawal-induced apoptosis via NF-kappa B activation. Blood *101*, 1956-1961.

Sun,Q., Zachariah,S., and Chaudhary,P.M. (2003b). The human herpes virus 8 encoded viral FLICE inhibitory protein (vFLIP) induces cellular transformation via NF-kappa B activation. J. Biol. Chem.

Sunil-Chandra,N.P., Arno,J., Fazakerley,J., and Nash,A.A. (1994). Lymphoproliferative disease in mice infected with murine gammaherpesvirus 68. Am. J. Pathol. *145*, 818-826.

Sunil-Chandra,N.P., Efstathiou,S., and Nash,A.A. (1992). Murine gammaherpesvirus 68 establishes a latent infection in mouse B lymphocytes in vivo. J. Gen. Virol. *73 (Pt 12)*, 3275-3279.

Sunil-Chandra,N.P., Efstathiou,S., and Nash,A.A. (1993). Interactions of murine gammaherpesvirus 68 with B and T cell lines. Virology *193*, 825-833.

Talbot,S. and Whitby,D. (1999). Kaposi's Sarcoma and Human Herpesvirus 8. In HIV and the New Viruses, A.Dalgleish and R.Weiss, eds. Academic Press), pp. 359-384.

Talbot,S.J., Weiss,R.A., Kellam,P., and Boshoff,C. (1999). Transcriptional analysis of human herpesvirus-8 open reading frames 71, 72, 73, K14, and 74 in a primary effusion lymphoma cell line. Virology *257*, 84-94.

Tartaglia,L.A., Ayres,T.M., Wong,G.H., and Goeddel,D.V. (1993). A novel domain within the 55 kd TNF receptor signals cell death. Cell *74*, 845-853.

Tepper,C.G. and Seldin,M.F. (1999). Modulation of caspase-8 and FLICE-inhibitory protein expression as a potential mechanism of Epstein-Barr virus tumorigenesis in Burkitt's lymphoma. Blood *94*, 1727-1737.

Thome,M., Schneider,P., Hofmann,K., Fickenscher,H., Meinl,E., Neipel,F., Mattmann,C., Burns,K., Bodmer,J.L., Schroter,M., Scaffidi,C., Krammer,P.H., Peter,M.E., and Tschopp,J. (1997). Viral FLICE-inhibitory proteins (FLIPs) prevent apoptosis induced by death receptors. Nature *386*, 517-521.

Thorley-Lawson,D.A and Gross,A. (2004). Persistence of the Epstein-Barr Virus and the Origins of Associated Lymphomas. N.Engl.J.Med. *350*, 1328-1337.

Thornberry,N.A. and Lazebnik,Y. (1998). Caspases: enemies within. Science *281*, 1312-1316.

Toczyski,D.P., Matera,A.G., Ward,D.C., and Steitz,J.A. (1994). The Epstein-Barr virus (EBV) small RNA EBER1 binds and relocalizes ribosomal protein L22 in EBV-infected human B lymphocytes. Proc. Natl. Acad. Sci. U. S. A *91*, 3463-3467.

Tomescu,C., Law,W.K., and Kedes,D.H. (2003). Surface downregulation of major histocompatibility complex class I, PE-CAM, and ICAM-1 following de novo infection of endothelial cells with Kaposi's sarcoma-associated herpesvirus. J. Virol. *77*, 9669-9684.

Tomkinson,B., Robertson,E., and Kieff,E. (1993). Epstein-Barr virus nuclear proteins EBNA-3A and EBNA-3C are essential for B-lymphocyte growth transformation. J. Virol. *67*, 2014-2025.

Townsley,A.C., Dutia,B.M., and Nash,A.A. (2004). The m4 gene of murine gammaherpesvirus modulates productive and latent infection in vivo. J. Virol. *78*, 758-767.

Uchida,J., Yasui,T., Takaoka-Shichijo,Y., Muraoka,M., Kulwichit,W., Raab-Traub,N., and Kikutani,H. (1999). Mimicry of CD40 signals by Epstein-Barr virus LMP1 in B lymphocyte responses. Science *286*, 300-303.

Vagner,S., Galy,B., and Pyronnet,S. (2001). Irresistible IRES. Attracting the translation machinery to internal ribosome entry sites. EMBO Rep. *2*, 893-898.

Vagner,S., Gensac,M.C., Maret,A., Bayard,F., Amalric,F., Prats,H., and Prats,A.C. (1995). Alternative translation of human fibroblast growth factor 2 mRNA occurs by internal entry of ribosomes. Mol. Cell Biol. *15*, 35-44.

Valcarcel,J. and Gebauer,F. (1997). Post-transcriptional regulation: the dawn of PTB. Curr. Biol. *7*, R705-R708.

Van Eden,M.E., Byrd,M.P., Sherrill,K.W., and Lloyd,R.E. (2004). Demonstrating internal ribosome entry sites in eukaryotic mRNAs using stringent RNA test procedures. RNA. *10*, 720-730.

Verma,S.C. and Robertson,E.S. (2003). Molecular biology and pathogenesis of Kaposi sarcoma-associated herpesvirus. FEMS Microbiol. Lett. *222*, 155-163.

Virgin,H.W., Latreille,P., Wamsley,P., Hallsworth,K., Weck,K.E., Dal Canto,A.J., and Speck,S.H. (1997). Complete sequence and genomic analysis of murine gammaherpesvirus 68. J. Virol. *71*, 5894-5904.

Virgin,H.W., Presti,R.M., Li,X.Y., Liu,C., and Speck,S.H. (1999). Three distinct regions of the murine gammaherpesvirus 68 genome are transcriptionally active in latently infected mice. J. Virol. *73*, 2321-2332.

Wabinga,H.R., Parkin,D.M., Wabwire-Mangen,F., and Mugerwa,J.W. (1993). Cancer in Kampala, Uganda, in 1989-91: changes in incidence in the era of AIDS. Int. J. Cancer *54*, 26-36.

Wabinga,H.R., Parkin,D.M., Wabwire-Mangen,F., and Nambooze,S. (2000). Trends in cancer incidence in Kyadondo County, Uganda, 1960-1997. Br. J. Cancer *82*, 1585-1592.

Wahman,A., Melnick,S.L., Rhame,F.S., and Potter,J.D. (1991). The epidemiology of classic, African, and immunosuppressed Kaposi's sarcoma. Epidemiol. Rev. *13*, 178-199.

Wakeling,M.N., Roy,D.J., Nash,A.A., and Stewart,J.P. (2001). Characterization of the murine gammaherpesvirus 68 ORF74 product: a novel oncogenic G protein-coupled receptor. J. Gen. Virol. *82*, 1187-1197.

Walker,N.P., Talanian,R.V., Brady,K.D., Dang,L.C., Bump,N.J., Ferenz,C.R., Franklin,S., Ghayur,T., Hackett,M.C., Hammill,L.D., and . (1994). Crystal structure of the cysteine protease interleukin-1 beta-converting enzyme: a (p20/p10)2 homodimer. Cell *78*, 343-352.

Wan,X., Wang,H., and Nicholas,J. (1999). Human herpesvirus 8 interleukin-6 (vIL-6) signals through gp130 but has structural and receptor-binding properties distinct from those of human IL-6. J. Virol. *73*, 8268-8278.

Wang,C., Sarnow,P., and Siddiqui,A. (1993). Translation of human hepatitis C virus RNA in cultured cells is mediated by an internal ribosome-binding mechanism. J. Virol. *67*, 3338-3344.

Wang,F.Z., Akula,S.M., Pramod,N.P., Zeng,L., and Chandran,B. (2001). Human herpesvirus 8 envelope glycoprotein K8.1A interaction with the target cells involves heparan sulfate. J. Virol. *75*, 7517-7527.

Wang,F.Z., Akula,S.M., Sharma-Walia,N., Zeng,L., and Chandran,B. (2003). Human herpesvirus 8 envelope glycoprotein B mediates cell adhesion via its RGD sequence. J. Virol. *77*, 3131-3147.

Wang,G.H., Garvey,T.L., and Cohen,J.I. (1999). The murine gammaherpesvirus-68 M11 protein inhibits Fas- and TNF-induced apoptosis. J. Gen. Virol. *80 (Pt 10)*, 2737-2740.

Wang,H.W., Sharp,T.V., Koumi,A., Koentges,G., and Boshoff,C. (2002). Characterization of an anti-apoptotic glycoprotein encoded by Kaposi's sarcoma-associated herpesvirus which resembles a spliced variant of human survivin. EMBO J. *21*, 2602-2615.

Wang,H.W., Trotter,M.W., Lagos,D., Bourboulia,D., Henderson,S., Makinen,T., Elliman,S., Flanagan,A.M., Alitalo,K., and Boshoff,C. (2004). Kaposi sarcoma herpesvirus-induced cellular reprogramming contributes to the lymphatic endothelial gene expression in Kaposi sarcoma. Nat. Genet. *36*, 687-693.

Wilson,J.B., Bell,J.L., and Levine,A.J. (1996). Expression of Epstein-Barr virus nuclear antigen-1 induces B cell neoplasia in transgenic mice. EMBO J. *15*, 3117-3126.

Wilson,J.E., Pestova,T.V., Hellen,C.U., and Sarnow,P. (2000a). Initiation of protein synthesis from the A site of the ribosome. Cell *102*, 511-520.

Wilson,J.E., Powell,M.J., Hoover,S.E., and Sarnow,P. (2000b). Naturally occurring dicistronic cricket paralysis virus RNA is regulated by two internal ribosome entry sites. Mol. Cell Biol. *20*, 4990-4999.

Yan,R., Rychlik,W., Etchison,D., and Rhoads,R.E. (1992). Amino acid sequence of the human protein synthesis initiation factor eIF-4 gamma. J. Biol. Chem. *267*, 23226-23231.

Yanai,N. and Obinata,M. (1994). Apoptosis is induced at nonpermissive temperature by a transient increase in p53 in cell lines immortalized with temperature-sensitive SV40 large T-antigen gene. Exp. Cell Res. *211*, 296-300.

Yeh,W.C., Itie,A., Elia,A.J., Ng,M., Shu,H.B., Wakeham,A., Mirtsos,C., Suzuki,N., Bonnard,M., Goeddel,D.V., and Mak,T.W. (2000). Requirement for Casper (c-FLIP) in regulation of death receptor-induced apoptosis and embryonic development. Immunity. *12*, 633-642.

Young,L.S., Dawson,C.W., and Eliopoulos,A.G. (2000). The expression and function of Epstein-Barr virus encoded latent genes. Mol. Pathol. *53*, 238-247.

Young,L.S. and Murray,P.G. (2003). Epstein-Barr virus and oncogenesis: from latent genes to tumours. Oncogene *22*, 5108-5121.

Yuan,J., Shaham,S., Ledoux,S., Ellis,H.M., and Horvitz,H.R. (1993). The C. elegans cell death gene ced-3 encodes a protein similar to mammalian interleukin-1 beta-converting enzyme. Cell *75*, 641-652.

Zamora,M., Marissen,W.E., and Lloyd,R.E. (2002). Multiple eIF4GI-specific protease activities present in uninfected and poliovirus-infected cells. J. Virol. *76*, 165-177.

Zhang,J., Yamada,O., Sakamoto,T., Yoshida,H., Iwai,T., Matsushita,Y., Shimamura,H., Araki,H., and Shimotohno,K. (2004). Down-regulation of viral replication by adenoviral-mediated expression of siRNA against cellular cofactors for hepatitis C virus. Virology *320*, 135-143.

Zong,J.C., Ciufo,D.M., Alcendor,D.J., Wan,X., Nicholas,J., Browning,P.J., Rady,P.L., Tyring,S.K., Orenstein,J.M., Rabkin,C.S., Su,I.J., Powell,K.F., Croxson,M., Foreman,K.E., Nickoloff,B.J., Alkan,S., and Hayward,G.S. (1999). High-level variability in the ORF-K1 membrane protein gene at the left end of the Kaposi's sarcoma-associated herpesvirus genome defines four major virus subtypes and multiple variants or clades in different human populations. J. Virol. *73*, 4156-4170.

Appendix 1: Commercial cloning vector maps

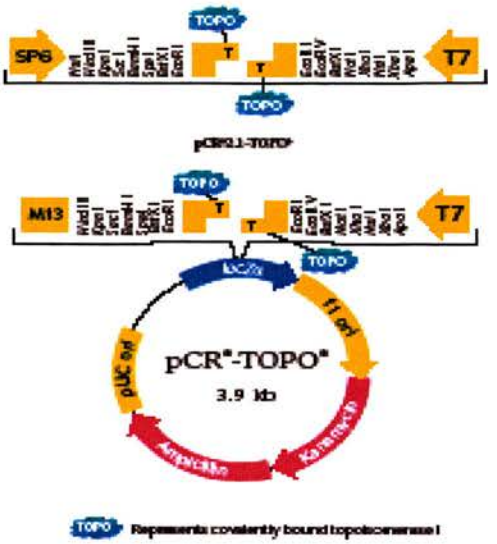

pCR-TOPO vector (Invitrogen)

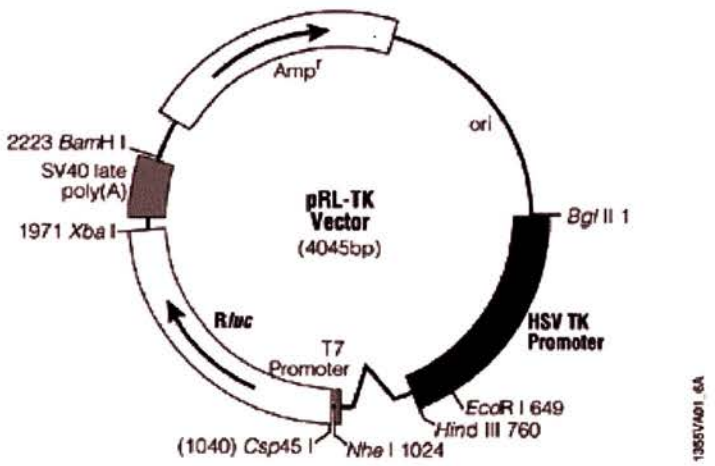

pRL-TK vector (Promega)

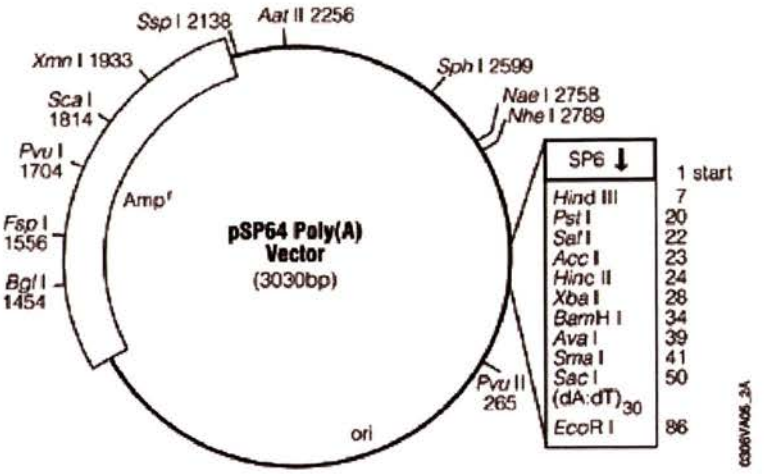

pSP64 Poly(A) vector (Promega)

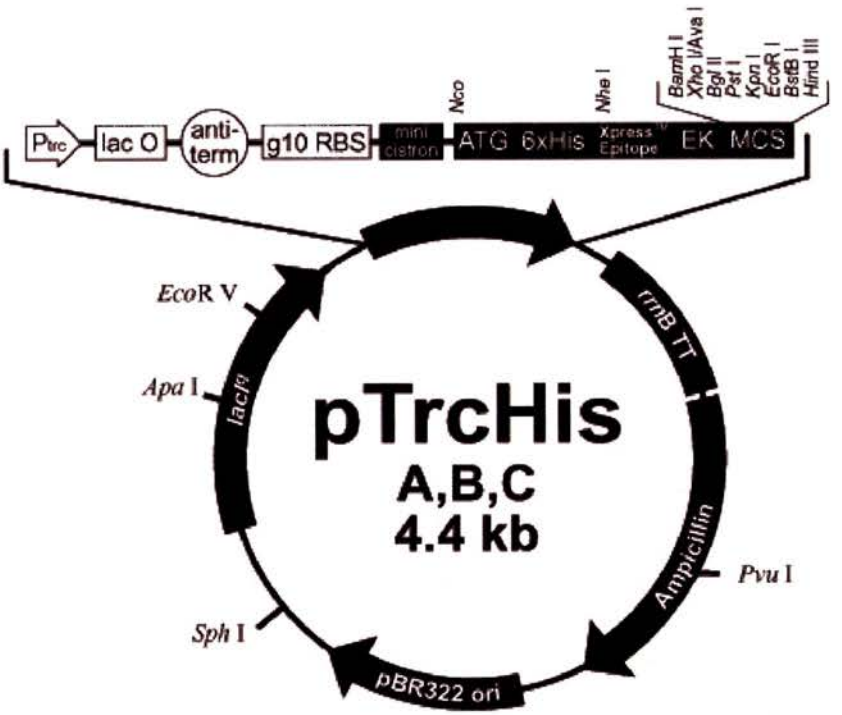

pTrcHis vector (Invitrogen).

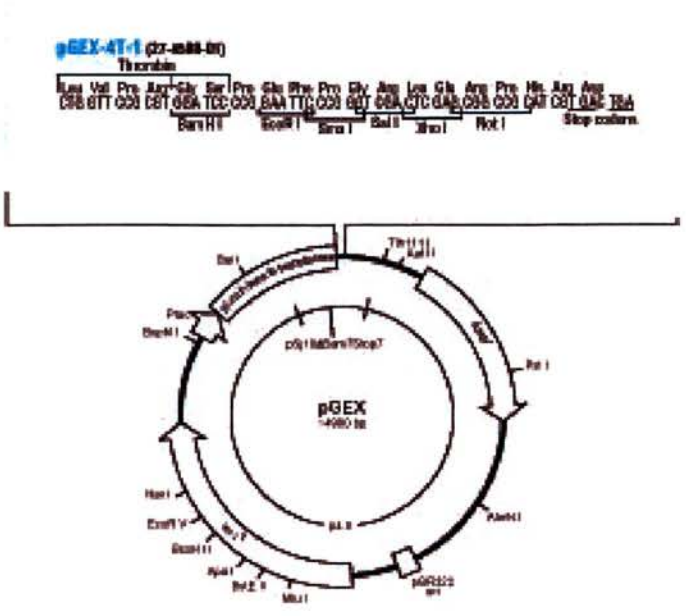

pGEX 4T-1 (Amersham biosciences)

Appendix 1b: pAB13 plasmid maps

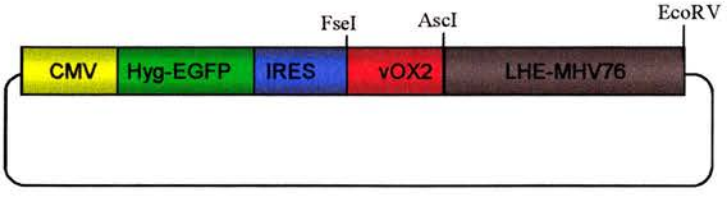

pAB13; vector was constructed as described in Brass; 2004 by subcloning of insert fragments into pBlueScriptIIKS-76LHE. The vector pAB14 is identical except that the insert CMV to vOX2 is in the reverse orientation.

Appendix 2 Oligonucleotide Sequences and appropriate PCR amplification conditions

RTA3F 5' GAC GGA TCC GGC ACA TTT GCT GCA GAA CCC 3'
RTA3R 5' TGC CTT AAG GAA CGG CGC CTG TGT ACT C 3'
94°C 30 sec; 60°C 45 sec; 72°C 30 sec. 30 cycles.

M4B 5' CGC GGA ATT CGG TTC TAG AAA GTC ATA AAT CTC AAT 3'
Trepeat 5' GCG CCA GGA GGA GCT AGG CCA CG 3'

94°C 45 sec; 55°C 45 sec; 72°C 1 min. 35 cycles.

FLIP GST-1 5' GCA TGA ATT CGC CAC TTA CGA GGT TCT CTG 3'
FLIP GST-2 5' GCA TCT CGA GCT ATG GTG TAT GGC GAT AGT G 3'

94°C 1 min; 55°C 1 min; 72°C 1 min. 30 cycles.

FLIP 76-1 5' GCA TGG CGC GCC ATG GCC ACT TAC GAG GTT CTC 3'
FLIP 76-2 5' GCA TGG CCG GCC CTA TGG TGT ATG GCG ATA GTG T 3'

94°C 1 min; 55°C 1 min; 72°C 1 min. 30 cycles.

In FLIP forward 5' GCA TGG ATC CAT GGC CAC TTA CGA GGT TC 3'
FLIP polyA 5' GCA TGG ATC CCA AAA CTT GTT AGT GTT TAT TAA ATC A

94°C 1 min; 55°C 1 min; 72°C 1 min. 30 cycles.

FLIP Myc HisA rev 5' GCA TAA GCT TTG GTG TAT GGC GAT AGT GTT GG

pJ27BglIIfor 5' GCCGCTCTAGAACTAGTAGATCTTCAATATTGGCC 3'
pJ27BglIIrev 5' GGCCAATATTGAAGATCTACTAGTTCTAGAGCGGC 3'

3HYB IRES 3 5' P- GAC GGA CGT CAC TTC CTT CTT GTT ACT TAA ATT GCT GGG GGG CTC CCA ACA CCT GGA C 3'
3HYB IRES 4 5' P- GTC CAG GTG TTG GGA GCC CCC CAG CAA TTT AAG TAA CAA GAA GGA AGT GAC GTC CGT C 3'

IRES forward 5' GTA CAA GCT TCC GCG GCA GAC TCC TTT TCC C 3'
IRES reverse 5' GTA CGA GCT CGC TGA TAA TAG AGG CGG GCA AT 3'

94°C 30 sec; 65°C 30 sec; 72°C 30 sec. 30 cycles.

Anti-IRES forward 5' GTA CGA GCT CCC GCG GCA GAC TCC TTT TCC C 3'
Anti-IRES reverse 5' GTA CAA GCT TGC TGA TAA TAG AGG CGG GCA AT 3
94°C 30 sec; 65°C 30 sec; 72°C 30 sec. 30 cycles.

PP1 5' TCG AGA CGG ACG TCA CTT CCT TCT TGT TAC TTA AAT TC 3'
PP2 5' CAT GGA ATT TAA GTA ACA AGA AGG AAG TGA CGT CCG TC 3'

94°C 1 min; 55°C 1 min; 72°C 1 min. 30 cycles

GAPDH 1 5'TGGATATTGTTGCCATCAATGACC
GAPDH 2 5'GATGGCATGGACTGTGGTCATG

94°C 30 sec; 58°C 30 sec; 72°C 30 sec. 30 cycles.

NFkBfor 5' GGGAATTTCCGGGAATTTCCGGGAATTTCCGGGAATTTCCCT ATAA 3'
NFkBrev 5' CTAGTTTTATAGGGAAATTCCCGGAAATTCCCGGAAATTCCC GGA 3'

Appendix 3 Yeast 3-hybrid scheme

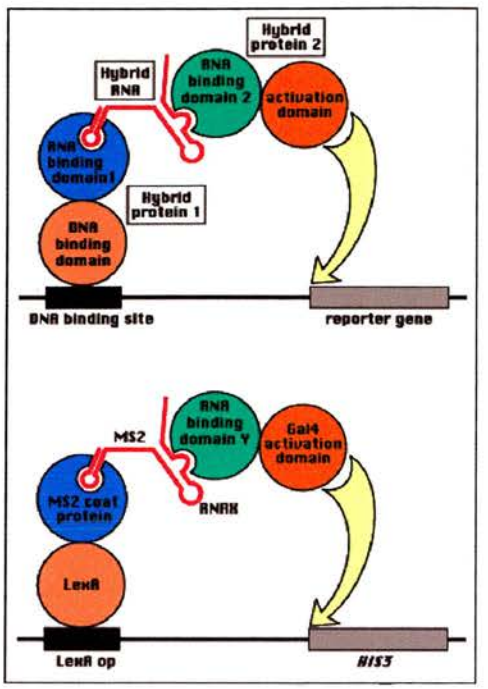

General 3-hybrid scheme

- 2 hybrid proteins are produced;
  .DNA binding domain +
  RNA binding domain

  .RNA binding domain +
  Activation domain

- The RNA sequence tethers the 2 proteins together bringing the activation domain into position so that it can initiate transcription of the reporter gene.

- RNA-protein interactions of sub-nM to μM affinities have been detected.

Generalised yeast 3-hybrid scheme (top) and protein and RNA domains utilised in this work (bottom), taken from SenGupta *et al*, 1996.

Journal of General Virology (2004), 85, 615–620 DOI 10.1099/vir.0.19733-0

A polypyrimidine tract facilitates the expression of Kaposi's sarcoma-associated herpesvirus vFLIP through an internal ribosome entry site

Lara Bieleski, Clemence Hindley and Simon J. Talbot

University of Edinburgh, Centre for Infectious Diseases, Summerhall, Edinburgh EH9 1QH, UK

Correspondence
Simon J. Talbot
stalbot@ed.ac.uk

We have identified a novel internal ribosome entry site (IRES) within a latently expressed Kaposi's sarcoma-associated herpesvirus (KSHV) gene (vCyclin) that controls the expression of a downstream open reading frame encoding an inhibitor of apoptosis (vFLIP). This IRES is the first such element to be identified in a DNA virus and may represent a novel mechanism through which this virus controls gene expression. We have used a dual luciferase reporter assay to identify important sequence elements essential for the activity of the IRES. A sequence of 32 nucleotides incorporating a polypyrimidine tract (PPT) was found to be required for the proper functioning of the IRES. We also show, using an electrophoretic mobility shift assay (EMSA), that proteins specific to a KSHV-infected cell line (BCP-1) but not a KSHV-negative cell line (HEK293) were able to form complexes with the IRES. By using an *in vitro* RNA binding assay, the cellular polypyrimidine tract binding protein (PTB, hnRNP-I) was found to bind to the IRES RNA. These results suggest that the interaction of PTB with the PPT may contribute to the correct functioning of the KSHV IRES in infected cells.

Received 20 October 2003
Accepted 5 December 2003

INTRODUCTION

Kaposi's sarcoma-associated herpesvirus (KSHV), also known as human herpesvirus-8 (HHV-8), is the most recently identified member of the herpesvirus family to infect humans (Chang *et al.*, 1994). KSHV, a gamma-2-herpesvirus, has been proposed as the aetiological agent for Kaposi's sarcoma as well as other malignancies such as primary effusion lymphoma (PEL) (Cesarman *et al.*, 1995) and multicentric Castleman's disease (MCD) (Soulier *et al.*, 1995).

KSHV is closely related to three other herpesviruses with oncogenic potential; herpesvirus saimiri (HVS), murine gammaherpesvirus (MHV-68) and, more distantly, to Epstein–Barr virus (EBV). The complete nucleotide sequence of KSHV DNA has revealed several genes which have probably been captured from the host cell during virus evolution, and whose products could also play a role in cellular transformation and tumour induction (Neipel *et al.*, 1997; Russo *et al.*, 1996). The three genes encoded by open reading frames (ORFs) K13, 72 and 73 [vFLIP (Fas-associated death domain-like IL-1β-converting enzyme-inhibitory protein) vCyclin and LANA] are transcribed from a common transcription start site in cell lines latently infected with KSHV. The resulting transcript is spliced to yield a 5·32 kb message encoding LANA, vCyclin, vFLIP and a 1·7 kb bicistronic message encoding vCyclin and vFLIP (Dittmer *et al.*, 1998; Talbot *et al.*, 1999).

The observation that a bicistronic transcript (Talbot *et al.*, 1999) encodes vCyclin and vFLIP led to the investigation of the mechanism of translation of the vFLIP ORF. We (Bieleski & Talbot, 2001) and others (Grundhoff & Ganem, 2001; Low *et al.*, 2001) were able to identify a novel internal ribosome entry site (IRES) within the latently expressed vCyclin gene that controls the expression of the downstream vFLIP ORF. This IRES is the first such element to be identified in a DNA virus. Recently, an IRES element has been described in the untranslated region of the Epstein–Barr nuclear antigen-1 (EBNA1) gene, which may contribute to the regulation of latent gene expression (Isaksson *et al.*, 2003).

IRES elements were first identified in the 5′ untranslated regions (UTR) of picornaviruses and are essential for the cap-independent translation of the viral polyprotein (Jang *et al.*, 1988; Pelletier & Sonenberg, 1988). More recently IRES elements have been characterized in several cellular genes which encode growth factors (FGF-2, VEGF) (Stein *et al.*, 1998; Vagner *et al.*, 1995), proto-oncogenes (c-*myc*) (Nanbru *et al.*, 1997) and an inhibitor of apoptosis (XIAP) (Holcik & Korneluk, 2000). IRES-dependent translation of these mRNAs may be essential for the survival and proliferation of cells under stressful conditions (Holcik *et al.*, 2000). IRES elements in two cellular mRNAs [encoding ornithine decarboxlyase (Cornelis *et al.*, 2000) and PITSLRE protein kinase (Pyronnet *et al.*, 2000)] have been identified, and are regulated in a cell cycle-dependent manner. These

data reveal a novel role for IRES elements in the translational regulation of protein expression during cell cycle progression. The IRES element that we have identified potentially controls the expression of a virus-encoded anti-apoptotic protein, vFLIP (Thome *et al.*, 1997), which is intimately linked to the expression of a cell growth promoting protein, vCyclin (Cesarman *et al.*, 1996; Godden-Kent *et al.*, 1997).

This paper investigates sequence elements within the KSHV IRES essential for efficient translation of the downstream ORF. In addition the cell type-specific activity of the IRES and cell-specific protein factors interacting with the IRES are investigated.

METHODS

Cells. The KSHV-positive primary effusion lymphoma (PEL) B-cell line, BCP-1 (Boshoff *et al.*, 1998), was grown in RPMI (Invitrogen) supplemented with 20% (v/v) fetal calf serum (FCS), 2 mM glutamine, 60 μg penicillin ml^{-1} and 100 μg streptomycin ml^{-1}. HEK293 cells (Graham *et al.*, 1977) were grown in DMEM (Invitrogen) supplemented with 10% (v/v) FCS, 2 mM glutamine, 60 μg penicillin ml^{-1} and 100 streptomycin μg ml^{-1}. Cells were incubated at 37 °C under 4% CO_2.

Plasmids. The plasmids pdLUC and pdLUC-SL were constructed as described previously (Bieleski & Talbot, 2001). The IRES sequence from encephalomyocarditis virus (EMCV) or fragments of KSHV vCyclin/vFLIP were cloned into the *Sma*I–*Nco*I or *Xho*I–*Nco*I sites of pdLUC (Fig. 1a). The following primers were used to PCR amplify specific IRES sequences:

Primer 1: GCATCTCGAGACGGACGTCACTTCCTTCTTG

Primer 2: GCATCTCGAGGCTGGGGGGCTCCCAAC

Primer 3: GCATCCATGGCAACTAAGGCTTTTGTAATCAG

Primer 4: GCATCCATGGAGTCTTTGGGTCAACTAAGGC

Complementary oligonucleotides (TCGAGACGGACGTCACTTCC-TTCTTGTTACTTAAATTC and CATGGAATTTAAGTAACAAGA-AGGAAGTGACGTCCGTC) were annealed and cloned directly in the *Xho*I–*Nco*I sites of pdLUC and pdLUC-SL to yield the PPT-encoding plasmid.

The KSHV IRES [nucleotides 123206–122973, GenBank accession no. U75698 (Russo *et al.*, 1996)] was cloned into the pSP64Poly(A) vector (Promega) for use in the pull-down assay. Primers GTACAAG-CTTCCGCGGCAGACTCCTTTTCCC and GTACGAGCTCGCTGA-TAATAGAGGCGGGCAAT (sense orientation) or GTACGAGCTC-CCGCGGCAGACTCCTTTTCCC and GTACAAGCTTGCTGATAA-TAGAGGCGGGCAAT (antisense orientation) were used to amplify the KSHV IRES by PCR. The DNA was then inserted into the *Hin*dIII–*Sac*I sites of the vector.

Transfection of cells. BCP-1 cells (1×10^5 cells per well), HEK293 (5×10^4 cells per well) were seeded in 24-well trays and incubated overnight. The cells were infected with vTF7-3 (Fuerst *et al.*, 1986), a recombinant vaccinia virus expressing T7 RNA polymerase, at 5 p.f.u. per cell in 200 μl serum free medium (OptiMEM; Gibco-BRL) for 60 min at 37 °C. The inoculum was removed and the cells washed once with OptiMEM. The cells were then transfected with 0·5 μg of linearized (*Afl*II and *Not*I) plasmid DNA and 1·5 μl Transfast transfection reagent per well according to the manufacturer's instructions (Promega). After incubation at 37 °C for 60 min, 1 ml of growth medium was added to the wells. The cells were assayed for luciferase activity 24 h later as described below.

Dual luciferase assays. Transfected cells were washed twice in PBS, and then lysed by addition of 200 μl of passive lysis buffer (PLB, Promega). After incubation for 15 min at room temperature the cell lysates were transferred to Eppendorf tubes and snap-frozen on dry ice. The lysates were then thawed, vortexed for 1 min and the cell debris removed by spinning at 10 000 r.p.m. for 1 min. The

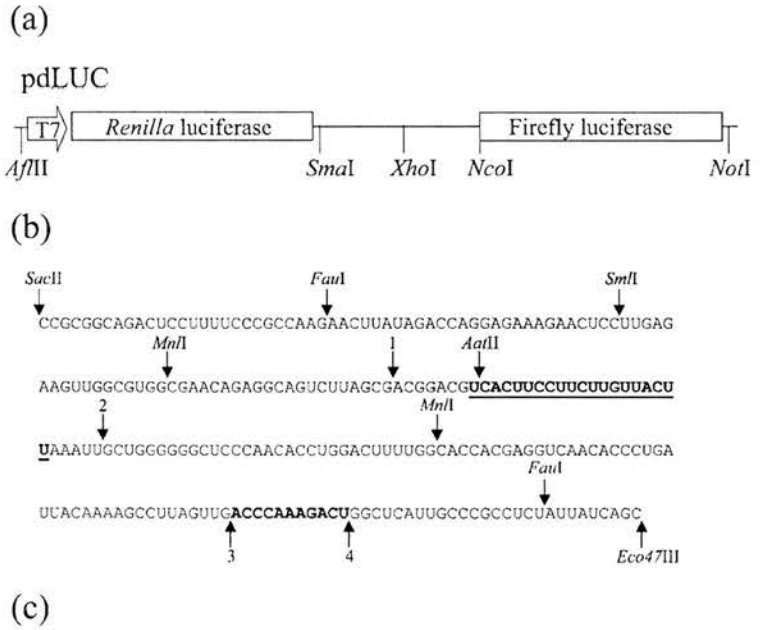

Fig. 1. (a) Schematic diagram of the plasmids pdLUC, showing the coding sequence for the *Renilla* and firefly luciferase enzymes cloned downstream of a T7 RNA polymerase promoter. (b) RNA sequence of vCyclin IRES. The sequence between the *Sac*II and *Eco47*III sites (nucleotides 123206–122973, Genebank accession no. U75698 (Russo *et al.*, 1996), and positions of restriction sites used in deletion analysis are shown. The 5′ ends of oligonucleotides (1, 2, 3 and 4; see Methods) used to PCR-amplify portions of the IRES are also indicated by arrows. The 11 nucleotide sequence complementary to 18S rRNA is shown in bold, and (c) the PPT is underlined and in bold.

activity of *Renilla* and firefly luciferase was assayed using the dual luciferase system as described by the manufacturer (Promega). Luciferase activities were measured using a Labsystems benchtop luminometer and the ratio of firefly luciferase to *Renilla* luciferase activity was calculated and used as a measure of IRES function.

Electrophoretic mobility shift assays (EMSAs). RNA was transcribed *in vitro* from 0·2 μg of linearized plasmid using T3 RNA polymerase and labelled internally with [α-^{32}P]UTP according to manufacturer's instructions (Life Science). Whole-cell lysate was prepared from BCP-1 or HEK293 cells by sonication for 15 min at 4 °C in binding buffer [20 mM HEPES/KOH pH 7·5, 50 mM KCl, 10 mM $MgCl_2$, 0·01 % (v/v) NP40, 5 % (v/v) glycerol], and the cellular debris was removed by centrifugation at 10 000 ***g*** for 5 min. The binding reaction was carried out in binding buffer containing 25 000 c.p.m. of labelled RNA, 6 μg protein, 1 unit RNasin, and 0·05 μg poly(dI–dT), in a total volume of 20 μl in the presence or absence of 10-fold excess of unlabelled competitor transcripts. After 15 min incubation at 20 °C, the samples were loaded on a 5 % (w/v) non-denaturing polyacrylamide gel containing 0·5× TBE. The gel was run in 0·5× TBE for 1 h at 30 mA before exposure to x-ray film (Hyperfilm) at −80 °C with an intensifying screen.

Preparation of S10 cell extract. Cells (1×10^8) were centrifuged and washed three times with isotonic buffer (35 mM HEPES pH 7·4, 146 mM NaCl, 11 mM glucose), resuspended in 2 vols of hypotonic buffer (20 mM HEPES pH 7·4, 10 mM KCl, 1·5 mM magnesium acetate, 1 mM DTT) and incubated on ice for 10 min. The cells were disrupted with 25 strokes of a Dounce homogenizer (on ice), before addition of 0·1 vols of 10× buffer (0·2 M HEPES pH 7·4, 1·2 M potassium acetate, 40 mM magnesium acetate, 50 mM DTT). The nuclei were removed by centrifugation at 2000 r.p.m. for 10 min at 4 °C, followed by addition of $CaCl_2$ (1 mM) and 75 units of S7 nuclease (Roche) per ml of supernatant. After incubation at 20 °C for 15 min the S7 nuclease was inactivated by adding EGTA to 2 mM. The S10 supernatant was centrifuged at 10 000 r.p.m. at 4 °C for 15 min before freezing in aliquots at −80 °C.

RNA–protein pull-down assays. Plasmids derived from the pSP64Poly(A) vector were linearized with *Eco*RI, and then used as templates for transcription reactions. RNA transcripts [containing a 3′ poly(A) tail of 30 residues] were produced and purified according to the manufacturer's instructions (Ambion; SP6 megascript). The KSHV vCyclin IRES RNA (sense or antisense) was captured onto oligo(dT) Dynabeads (Dynal, 0·5 ml) as described previously (Stassinopoulos & Belsham, 2001). The immobilized RNA transcripts were then incubated with BCP-1 cell S10 extract at 4 °C for 60 min on a rotating wheel. The magnetic beads were captured and the depleted S10 was removed. The beads–RNA–protein complex was washed twice in binding buffer, resuspended in SDS sample buffer, and incubated at 4 °C for 10 min. These samples were analysed by SDS-PAGE and Western blot analysis. The anti-PTB polyclonal antibody was a gift from R. J. Jackson (University of Cambridge, UK) (Hunt & Jackson, 1999; Mitchell *et al.*, 2001).

RESULTS

A polypyrimidine tract is essential for the activity of the vCyclin IRES

We have described previously a 233 nucleotide sequence within the vCyclin gene of KSHV that efficiently promotes the translation of the downstream vFLIP orf via internal ribosome entry (Bieleski & Talbot, 2001). We noted the presence of two sequence elements within the IRES that could potentially modulate its activity. The first was a pyrimidine-rich sequence and the second an 11 nucleotide sequence complementary to a sequence in 18s rRNA (Fig. 1b). We have used a combination of restriction enzyme-directed deletion and PCR to determine the minimal sequence necessary for the activity of the IRES. These sequences were cloned into the pdLUC plasmid as shown in Fig. 1(a). These plasmids were transfected into the BCP-1 cell line (latently infected with KSHV), which had been infected with vaccinia vTF7-3 (Fuerst *et al.*, 1986) at an m.o.i. of 5. The *Renilla* luciferase and firefly luciferase activities were measured in cell lysates 24 h post-transfection. The ratio of firefly luciferase to *Renilla* luciferase activity was calculated and used as a measure of IRES function. As shown in Table 1 we were able to delete the 18S rRNA sequence without significantly affecting IRES function, but deletion of the polypyrimidine tract (PPT) resulted in loss of IRES function. Two of these constructs (Primer 1&4 and 1&3) revealed a higher IRES activity than the other constructs and equivalent to the activity of the EMCV IRES. This may be due to the removal of inhibitory sequences or the presentation of the KSHV IRES in a more favourable structural conformation.

To confirm that the PPT was necessary and sufficient for IRES activity we cloned this sequence alone into the pdLUC plasmid using oligonucleotides encompassing the PPT (Fig. 1c). As seen in Table 1, the PPT alone was able to direct efficient expression of the downstream firefly luciferase. The cap-independent activity of this PPT sequence was confirmed using an equivalent reporter construct that contained an inverted repeat, with the potential to form a stable 28 bp stem–loop structure in the 5′ UTR immediately upstream from the *Renilla* luciferase start codon. Translation of the first cistron was efficiently inhibited by the presence of the stable stem–loop structure, whereas translation of the second cistron via the PPT sequence

Table 1. Activity of the vCyclin IRES and deletion derivatives in BCP-1 cells

Sequence	Activity of IRES [FF:RL (%)]*
EMCV IRES	12·3±1·1
*Sac*II–*Eco47*III	7·0±1·7
*Fau*I–*Fau*I	5·2±0·6
*Sml*I–*Eco47*III	5·1±1·3
*Mnl*I-*Mnl*I	5·1±0·5
*Aat*II–*Eco47*III	0·4±0·2
Primers 1 and 4	14·2±1·9
Primers 1 and 3	13·7±1·4
Primers 2 and 4	0·8±0·5
Primers 2 and 3	0·4±0·2
PPT†	6·9±0·7

*The ratio (%) of the firefly (FF) and *Renilla* (RL) luciferase activities are shown from an experiment performed in triplicate.
†PPT (polypyrimidine tract); see Fig. 1(c).

within the vCyclin gene was unaffected by the presence of the stem–loop (data not shown).

Cell-type specificity of KSHV IRES activity

We noted previously that the IRES activity was high in the PEL cell line BCP-1 (latently infected with KSHV) but that there was little or no activity in the cell lines HEK293, HeLa or KSIMM (Bieleski & Talbot, 2001). This suggests that cell-specific and/or KSHV-specific factors play an important role in the modulation of IRES activity. EMSA is a technique used to study the interaction of proteins with specific nucleic acid targets (DNA or RNA). Radiolabelled RNA encompassing the IRES was produced by *in vitro* transcription using T7 RNA polymerase mixed with protein (whole-cell lysate) and then electrophoresed through a non-denaturing polyacrylamide gel. Any RNA–protein complexes that are formed run with a slower mobility through the gel in comparison with non-complexed RNA. We have used this system to investigate the possibility of proteins interacting with the KSHV IRES. As shown in Fig. 2, several specific RNA–protein complexes (indicated by *) are formed when *in vitro*-transcribed IRES RNA is mixed with crude cell lysate from BCP-1 cells but not with cell lysate from HEK293 cells. The specificity of these RNA–protein interactions was confirmed by the fact that excess unlabelled IRES RNA successfully competed out these complexes. These data confirm the presence of specific protein factors present in the KSHV-positive BCP-1 cell line that may be essential for the activity of the IRES.

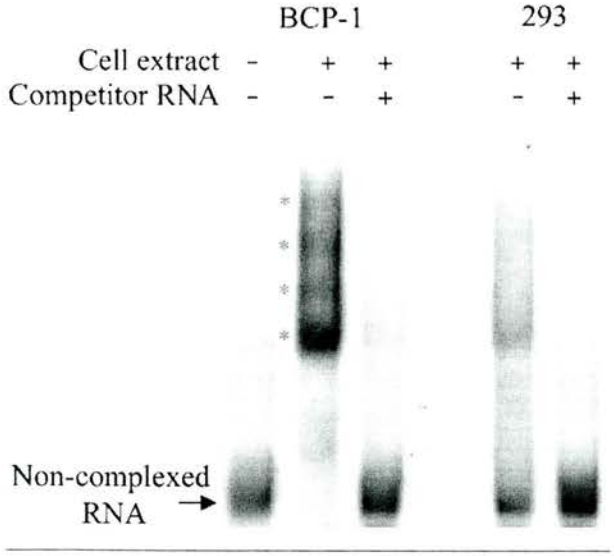

Fig. 2. EMSA showing the formation of complexes between the vCyclin IRES and whole-cell extract from BCP-1 cells, but not with cell extract from HEK293 cells. Approximately 6 μg of protein was mixed with 25 000 c.p.m. of *in vitro*-transcribed KSHV IRES RNA in the presence or absence of 10-fold excess of unlabelled KSHV IRES RNA. The positions of four RNA–protein complexes are indicated by *.

Specificity of proteins interacting with IRES

We have defined a minimal fragment of vCyclin coding sequence that is able to function as an IRES in our dual luciferase assay. The most striking feature of this sequence is a PPT, 17 nucleotides in length. The presence of a PPT has been noted in several other IRES elements in viruses and cellular mRNAs (Pyronnet *et al.*, 2000). Pyrimidine-rich sequences have been shown to interact with the PTB (hnRNP-I), and this protein is known to affect the function of certain IRES elements (Gosert *et al.*, 2000; Hunt & Jackson, 1999; Mitchell *et al.*, 2001). To test the possibility that PTB may bind to the KSHV IRES, we used an *in vitro* binding assay (Stassinopoulos & Belsham, 2001). The KSHV IRES (Fig. 1b; *Sac*II and *Eco*47III) was cloned in both the sense and antisense direction into the plasmid pSP64poly(A) allowing the production of RNA tailed with a 30 nucleotide poly(A) sequence. This RNA was bound to oligo(dT) Dynabeads and the complex incubated with S10 protein extract from BCP-1 cells. Proteins bound to the RNA were analysed by SDS-PAGE and Western blot. As shown in Fig. 3, PTB was found to bind specifically to the KSHV IRES in the sense but not the antisense orientation.

DISCUSSION

We have previously reported the presence of an IRES element within the coding region of the vCyclin ORF encoded by KSHV that directs the expression of the vFLIP ORF on a bicistronic message (Bieleski & Talbot, 2001). We determined that the sequence requirements for the correct functioning of the IRES fell within a 233 nucleotide fragment. We noted that there were two potentially interesting sequence motifs within the IRES that might contribute to its efficient functioning. These were an 11 nucleotide sequence complementary to a sequence in 18S rRNA, and a 20 nucleotide PPT. Deletion of the 18S rRNA sequence had no effect on the functioning of the IRES, whereas deletion of the PPT abolished IRES activity in a dual-luciferase reporter assay. To confirm the essential role for the PPT, we tested this sequence (32 nucleotides) in isolation for IRES activity and found that it efficiently directed expression of a downstream ORF on a bicistronic message. The presence of pyrimidine-rich sequences has

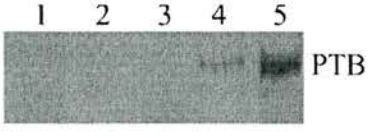

Fig. 3. *In vitro* RNA–protein binding assay showing the interaction of PTB (Hunt & Jackson, 1999; Mitchell *et al.*, 2001) with the vCyclin IRES. Lanes 1 and 2, antisense RNA; lanes 3 and 4, sense RNA; lane 5, BCP-1 S10 input. Lanes 1 and 3, unbound protein; lanes 2 and 4, bound protein eluted from beads. PTB runs as a dimer of approximately 60 kDa.

been noted in several other IRES elements in viruses and cellular mRNAs (Pyronnet *et al.*, 2000).

We have used an EMSA to define IRES–protein complexes within permissive (BCP-1) and non-permissive cells (HEK293). Four distinct IRES–protein complexes were observed with BCP-1 lysate, whereas no distinct species were identified in HEK293 cells. In order to identify potential interacting proteins we used an *in vitro* binding assay using poly(A)-tailed IRES RNA and oligo(dT) magnetic beads. Proteins interacting with the IRES RNA were enriched from BCP-1 S10 extract and analysed by SDS-PAGE and Western blot. Using this technique we were able to show that the cellular PTB (hnRNP-I) selectively bound to KSHV IRES RNA, but not to the antisense IRES RNA used as a control. Clearly, PTB is not the sole determinant of IRES activity since it is expressed in a wide variety of cell types including HEK293 cells in which the KSHV IRES is non-functional. The potential interaction of PTB with the PPT of the IRES may provide a framework for the binding of further cellular and/or viral factors. We tested whether the expression of PTB in an *in vitro* transcription/translation system (rabbit reticulocyte lysate) would enhance the activity of the IRES, but found that it had no effect (data not shown). This also supports the idea that multiple protein factors are required for efficient IRES activity.

Some viral IRESs, e.g. the EMCV IRES, do not appear to require proteins other than canonical translation initiation factors for function (Pestova *et al.*, 1996), while others require an additional complex set of factors for activity. Such factors include PTB, which binds specifically to several viral IRESs, although the absolute requirement of viral IRESs for this factor differs. For example, PTB stimulates the initiation of translation by internal ribosome entry from hepatitis C and A virus RNA *in vivo* (Gosert *et al.*, 2000) and from the human rhinovirus (HRV) and poliovirus IRESs *in vitro* (Hunt & Jackson, 1999) but is not necessary for the activity of wild-type EMCV (Kaminski & Jackson, 1998). PTB is a cellular protein known to be involved in splicing and branch point selection (Grossman *et al.*, 1998). It has been shown that the IRES element controlling the expression of the cellular gene Apaf-1, involved in the apoptotic cascade, requires both PTB and, upstream of N-*ras* (unr), two cellular RNA-binding proteins previously identified to be required for rhinovirus IRES activity (Mitchell *et al.*, 2001). This study showed that PTB binding to the Apaf-1 IRES occurred only if unr was present.

We have shown that a PPT is essential for the activity of the KSHV IRES and that PTB interacts with KSHV IRES RNA *in vitro*. Additional IRES RNA–protein complexes were observed using an EMSA that are yet to be identified. Further investigations will be required to determine other binding and regulatory components necessary for the correct functioning of the KSHV IRES.

ACKNOWLEDGEMENTS

We thank R. J. Jackson for providing PTB antisera. This work was supported by an MRC career establishment grant to S. J. T. and a BBSRC studentship to C. H.

REFERENCES

Bieleski, L. & Talbot, S. J. (2001). Kaposi's sarcoma-associated herpesvirus vCyclin open reading frame contains an internal ribosome entry site. *J Virol* **75**, 1864–1869.

Boshoff, C., Gao, S. J., Healy, L. E. & 10 other authors (1998). Establishing a KSHV+ cell line (BCP-1) from peripheral blood and characterizing its growth in Nod/SCID mice. *Blood* **91**, 1671–1679.

Cesarman, E., Chang, Y., Moore, P. S., Said, J. W. & Knowles, D. M. (1995). Kaposi's sarcoma-associated herpesvirus-like DNA sequences in AIDS-related body-cavity-based lymphomas. *N Engl J Med* **332**, 1186–1191.

Cesarman, E., Nador, R. G., Bai, F., Bohenzky, R. A., Russo, J. J., Moore, P. S., Chang, Y. & Knowles, D. M. (1996). Kaposi's sarcoma-associated herpesvirus contains G protein-coupled receptor and cyclin D homologs which are expressed in Kaposi's sarcoma and malignant lymphoma. *J Virol* **70**, 8218–8223.

Chang, Y., Cesarman, E., Pessin, M. S., Lee, F., Culpepper, J., Knowles, D. M. & Moore, P. S. (1994). Identification of herpesvirus-like DNA sequences in AIDS-associated Kaposi's sarcoma. *Science* **266**, 1865–1869.

Cornelis, S., Bruynooghe, Y., Denecker, G., Van Huffel, S., Tinton, S. & Beyaert, R. (2000). Identification and characterization of a novel cell cycle-regulated internal ribosome entry site. *Mol Cell* **5**, 597–605.

Dittmer, D., Lagunoff, M., Renne, R., Staskus, K., Haase, A. & Ganem, D. (1998). A cluster of latently expressed genes in Kaposi's sarcoma-associated herpesvirus. *J Virol* **72**, 8309–8315.

Fuerst, T. R., Niles, E. G., Studier, F. W. & Moss, B. (1986). Eukaryotic transient-expression system based on recombinant vaccinia virus that synthesizes bacteriophage T7 RNA polymerase. *Proc Natl Acad Sci U S A* **83**, 8122–8126.

Godden-Kent, D., Talbot, S. J., Boshoff, C., Chang, Y., Moore, P., Weiss, R. A. & Mittnacht, S. (1997). The cyclin encoded by Kaposi's sarcoma-associated herpesvirus stimulates cdk6 to phosphorylate the retinoblastoma protein and histone H1. *J Virol* **71**, 4193–4198.

Gosert, R., Chang, K. H., Rijnbrand, R., Yi, M., Sangar, D. V. & Lemon, S. M. (2000). Transient expression of cellular polypyrimidine-tract binding protein stimulates cap-independent translation directed by both picornaviral and flaviviral internal ribosome entry sites *in vivo*. *Mol Cell Biol* **20**, 1583–1595.

Graham, F. L., Smiley, J., Russell, W. C. & Nairn, R. (1977). Characteristics of a human cell line transformed by DNA from human adenovirus type 5. *J Gen Virol* **36**, 59–74.

Grossman, J. S., Meyer, M. I., Wang, Y. C., Mulligan, G. J., Kobayashi, R. & Helfman, D. M. (1998). The use of antibodies to the polypyrimidine tract binding protein (PTB) to analyze the protein components that assemble on alternatively spliced pre-mRNAs that use distant branch points. *RNA* **4**, 613–625.

Grundhoff, A. & Ganem, D. (2001). Mechanisms governing expression of the v-FLIP gene of Kaposi's sarcoma-associated herpesvirus. *J Virol* **75**, 1857–1863.

Holcik, M. & Korneluk, R. G. (2000). Functional characterization of the X-linked inhibitor of apoptosis (XIAP) internal ribosome entry site element: role of La autoantigen in XIAP translation. *Mol Cell Biol* **20**, 4648–4657.

Holcik, M., Sonenberg, N. & Korneluk, R. G. (2000). Internal ribosome initiation of translation and the control of cell death. *Trends Genet* **16**, 469–473.

Hunt, S. L. & Jackson, R. J. (1999). Polypyrimidine-tract binding protein (PTB) is necessary, but not sufficient, for efficient internal initiation of translation of human rhinovirus-2 RNA. *RNA* **5**, 344–359.

Isaksson, A., Berggren, M. & Ricksten, A. (2003). Epstein–Barr virus U leader exon contains an internal ribosome entry site. *Oncogene* **22**, 572–581.

Jang, S. K., Krausslich, H. G., Nicklin, M. J., Duke, G. M., Palmenberg, A. C. & Wimmer, E. (1988). A segment of the 5′ nontranslated region of encephalomyocarditis virus RNA directs internal entry of ribosomes during in vitro translation. *J Virol* **62**, 2636–2643.

Kaminski, A. & Jackson, R. J. (1998). The polypyrimidine tract binding protein (PTB) requirement for internal initiation of translation of cardiovirus RNAs is conditional rather than absolute. *RNA* **4**, 626–638.

Low, W., Harries, M., Ye, H., Du, M. Q., Boshoff, C. & Collins, M. (2001). Internal ribosome entry site regulates translation of Kaposi's sarcoma-associated herpesvirus FLICE inhibitory protein. *J Virol* **75**, 2938–2945.

Mitchell, S. A., Brown, E. C., Coldwell, M. J., Jackson, R. J. & Willis, A. E. (2001). Protein factor requirements of the Apaf-1 internal ribosome entry segment: roles of polypyrimidine tract binding protein and upstream of N-ras. *Mol Cell Biol* **21**, 3364–3374.

Nanbru, C., Lafon, I., Audigier, S., Gensac, M. C., Vagner, S., Huez, G. & Prats, A. C. (1997). Alternative translation of the proto-oncogene c-*myc* by an internal ribosome entry site. *J Biol Chem* **272**, 32061–32066.

Neipel, F., Albrecht, J. C. & Fleckenstein, B. (1997). Cell-homologous genes in the Kaposi's sarcoma-associated rhadinovirus human herpesvirus 8: determinants of its pathogenicity? *J Virol* **71**, 4187–4192.

Pelletier, J. & Sonenberg, N. (1988). Internal initiation of translation of eukaryotic mRNA directed by a sequence derived from poliovirus RNA. *Nature* **334**, 320–325.

Pestova, T. V., Shatsky, I. N. & Hellen, C. U. (1996). Functional dissection of eukaryotic initiation factor 4F: the 4A subunit and the central domain of the 4G subunit are sufficient to mediate internal entry of 43S preinitiation complexes. *Mol Cell Biol* **16**, 6870–6878.

Pyronnet, S., Pradayrol, L. & Sonenberg, N. (2000). A cell cycle-dependent internal ribosome entry site. *Mol Cell* **5**, 607–616.

Russo, J. J., Bohenzky, R. A., Chien, M. C. & 8 other authors (1996). Nucleotide sequence of the Kaposi sarcoma-associated herpesvirus (HHV8). *Proc Natl Acad Sci U S A* **93**, 14862–14867.

Soulier, J., Grollet, L., Oksenhendler, E. & 7 other authors (1995). Kaposi's sarcoma-associated herpesvirus-like DNA sequences in multicentric Castleman's disease. *Blood* **86**, 1276–1280.

Stassinopoulos, I. A. & Belsham, G. J. (2001). A novel protein-RNA binding assay: functional interactions of the foot-and-mouth disease virus internal ribosome entry site with cellular proteins. *RNA* **7**, 114–122.

Stein, I., Itin, A., Einat, P., Skaliter, R., Grossman, Z. & Keshet, E. (1998). Translation of vascular endothelial growth factor mRNA by internal ribosome entry: implications for translation under hypoxia. *Mol Cell Biol* **18**, 3112–3119.

Talbot, S. J., Weiss, R. A., Kellam, P. & Boshoff, C. (1999). Transcriptional analysis of human herpesvirus-8 open reading frames 71, 72, 73, K14, and 74 in a primary effusion lymphoma cell line. *Virology* **257**, 84–94.

Thome, M., Schneider, P., Hofmann, K. & 11 other authors (1997). Viral FLICE-inhibitory proteins (FLIPs) prevent apoptosis induced by death receptors. *Nature* **386**, 517–521.

Vagner, S., Gensac, M. C., Maret, A., Bayard, F., Amalric, F., Prats, H. & Prats, A. C. (1995). Alternative translation of human fibroblast growth factor 2 mRNA occurs by internal entry of ribosomes. *Mol Cell Biol* **15**, 35–44.